DESIGN OF MICROFLUIDIC MULTIPLEX CARTRIDGE FOR POINT OF CARE DIAGNOSTICS

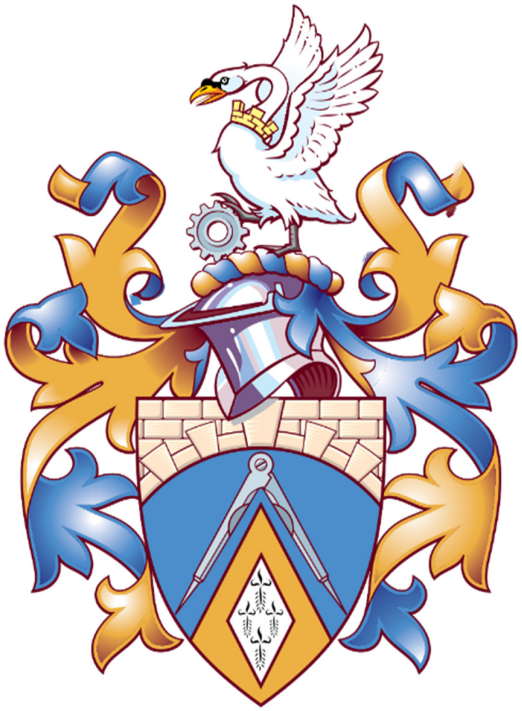

Ereku Luck TosanEreku Luck Tosan

College of Engineering, Design and Physical Sciences

Centre for Electronic Systems Research (CESR)

Department of Electronic and Computer Engineering

Brunel University London

This dissertation is submitted for the degree of Doctor of Philosophy

October 2017

DEDICATION

To God and Family.

DECLARATION

This dissertation is the result of my own work and includes nothing, which is the outcome of work done in collaboration except where specifically indicated in the text. It has not been previously submitted, in part or whole, to any university of institution for any degree, diploma, or other qualification.

Signed: ELT

Date: 10/04/2017

Ereku Luck TosanEreku Luck Tosan

ABSTRACT

A simple, but innovative microfluidic Lab-on-a-chip (LOC) device which is broadly applicable in point of care diagnostics of biological pathogens was designed, fabricated and assembled utilising explicit microfluidic techniques. The purpose of this design was to develop a cartridge with the capability to perform multiplex DNA amplification reactions on a single device. To achieve this outcome, conventional laboratory protocols for sample preparation; involving DNA extraction, purification and elution were miniaturized to suit this lab-on-a-chip device of 75mm X 50mm cross-sectional area. The extraction process was carried out in a uniquely designed microchamber embedded with chitosan membrane that binds DNA at pH 5.0 and elutes when a different solution at pH 9.0 flows through. Likewise, purification protocol that occurs in the designed waste reservoir is very significant in biomedical field because it is concerned with waste treatment and cartridge disposability, was performed with a super absorbent powder that converts liquid to a gel like substance. This powder is known as sodium polyacrylate, which is also they treated with anti-bacterial chemicals to prevent environmental contamination. Furthermore, this process also employed the use of a passive valve for a precise fluid handling operation involving flow regulation from extraction to waste reservoir. In order to achieve the intended multiplexing function a multiplexer was created to distribute flow simultaneously through a bifurcated network of channels connected to six similar amplification microchambers. Prior to fabrication, computational fluid dynamics (CFD) simulation was utilized at flowrates less than 10μL/s as the means to test the effectiveness of each design components and also to specifically deduct empirical values that can be analyzed to improve or understand the relationship between the fluid and geometrical constraints of the microfluidic modular elements. The device produced was a hybrid cartridge composed of PDMS and glass which is the most widely used materials microfluidics research due to their low cost and simplicity of fabrication by soft lithography technique. The choice of material also took into account the various physical and chemical properties advantages and disadvantages in their bio-medical applications. Such properties include but not limited to surface energy that determines the wetting fluid characteristics, biocompatibility, optical transparency. Subsequently, after a prototype cartridge was developed fluid flow experimentation using liquid coloured dye was used on the fully fabricated cartridge to test the efficacy of its microfluidic functionalities before expensive DNA amplification reagents were utilised at similar flowrates to the CFD simulations. This gave rise to

comparison between similar and dissimilar flow Peculiarities in the microfluidic circuit of both experiments.

The final experiment was performed with the aid of a recent molecular technique in DNA amplification known as of RPA kit (recombinase polymerase amplification reaction). It involved performing two main reaction experiments; first, was the positive experiment that bears the sample DNA and the latter, negative that served as the control without DNA. In the end, quantitative analysis of results was done using an agarose gel that showed 143 base pairs, for the positive samples, thus validating the amplification experiment.

ACKNOWLEDGEMENTS

Thanks to professor Wamadeva Balachandran and the two wonderful ladies, Ruth Mackay and Angel Naveenathayalan, without you guys this PHD programme would not be possible.

TABLE OF CONTENT

DEDICATION ..... **II**
DECLARATION ..... **III**
ABSTRACT ..... **IV**
ACKNOWLEDGEMENTS ..... **VI**
TABLE OF CONTENT ..... **VIII**
LIST OF FIGURES ..... **XII**
LIST OF TABLES ..... **XVII**
SYMBOLS, UNITS AND ACRONYMS ..... **XVIII**
1. INTRODUCTION **2-1**
1.1 MICROFLUIDICS TECHNOLOGY 2-1
1.2 POINT OF CARE DIAGNOSTIC 2-2
1.2.1 On-Chip Sample Preparation *2-4*
1.2.2 DNA Amplification *2-5*
1.2.3 DNA Detection *2-6*
1.3 OBJECTIVES OF RESEARCH 2-7
1.4 SUMMARY OF METHODOLOGY 2-9
1.5 CONTRIBUTION TO KNOWLEDGE 2-11
1.6 THESIS STRUCTURE 2-12
1.7 PAPERS PUBLISHED 2-13
2. LITERATURE REVIEW **2-14**
2.1 INTRODUCTION 2-14
2.2 MICROHYDRODYNAMICS 2-14
2.2.1 Viscosity effect *2-17*
2.2.2 Surface Tension Effect and Capillarity Phenomenon *2-17*
2.2.3 Pressure Driven Flow *2-19*
2.2.4 Electric Circuit Analogy Concept of Fluidic Resistance *2-20*
2.2.5 Multiphase flow *2-21*
2.3 MICROFLUIDIC LARGE SCALE INTEGRATION 2-24
2.3.1 Microfluidic Multiplexer *2-24*
2.3.2 Micromixer *2-24*
2.3.3 Micropumps *2-26*
2.3.4 Microwells *2-28*
2.3.5 Microvalves *2-28*
2.3.6 Magneto-hydrodynamics *2-30*
2.3.7 Dielectrophoresis *2-31*

2.4 MICROFLUIDIC MATERIALS 2-35
2.4.1 Required Properties *2-35*
2.4.2 Silicon *2-36*
2.4.3 GLASS *2-36*
2.4.4 FUSED SILICA QUARTZ *2-37*
2.4.5 Metals *2-38*
2.4.6 Paper *2-39*
2.4.7 POLYMER *2-39*
2.4.8 Material Bonding Properties *2-43*
2.4.9 Adhesive Bonding *2-43*
2.4.10 Thermal Fusion Bonding *2-44*
2.4.11 Solvent-Based Bonding *2-45*
2.4.12 Localized Welding *2-45*
2.4.13 Surface Treatment and Modification *2-45*
2.5 PROTOTYPE FABRICATION TECHNOLOGY 2-49
2.5.1 Material Depositing Technology *2-49*
2.5.2 3D Printing *2-49*
2.5.3 Stereolithography *2-49*
2.5.4 3D Inkjet Printing *2-50*
2.5.5 Binder jetting *2-50*
2.5.6 Material Extrusion *2-50*
2.5.7 Powder Bed *2-51*
2.5.8 Lithography *2-51*
2.5.9 Optical Lithography *2-51*
2.5.10 X-ray Lithography *2-52*
2.5.11 Material Removing Technology *2-53*
2.5.12 Etching *2-53*
2.5.13 Laser ablation *2-54*
2.5.14 Micromilling *2-54*
2.5.15 Micro Electrical Discharge Machining *2-55*
2.6 PROTOTYPE REPLICATION TECHNOLOGY 2-55
2.6.1 Injection molding *2-55*
2.6.2 Hot Embossing *2-56*
2.6.3 Soft lithography *2-56*
2.7 SUMMARY 2-57
3. DESIGN AND FABRICATION OF CARTRIDGE 3-59
3.1 INTRODUCTION 3-59
3.2 DESIGN OBJECTIVES: 3-59
3.3 DESIGN GEOMETRY OF FLUIDIC ELEMENTS 3-60
3.3.1 3D geometry Design of inlet and outlet ports *3-60*
3.3.2 3D geometry Design of Central Reaction Chamber *3-61*
3.3.3 3D geometry Design of Waste Reaction Chamber *3-61*

3.3.4 3D Design of a microfluidic Amplification chambers 3-62
3.4 3D DESIGN OF PASSIVE MICROVALVE 3-63
3.4.1 Multiphase Flow Simulation of Passive valve 3-65
3.4.2 Single Phase Flow Simulation of Passive valve 3-67
3.4.3 Simulation analysis of PAssive Valve 3-68
3.5 3D DESIGN OF A MICROFLUIDIC MULTIPLEXER 3-69
3.5.1 Multiphase Flow Simulation of Multiplexer 3-70
3.5.2 Single Phase Fluid Flow Simulation of Multiplexer 3-72
3.5.3 Simulation Analysis of Multiplexer 3-73
3.6 CARTRIDGE PROTOTYPE PRODUCTION 3-77
3.6.1 3D printing of Positive Mould 3-78
3.6.2 Soft Lithography PDMS Protocol 3-78
3.6.3 Production of Chitosan Membrane 3-79
3.6.4 Bonding and Sealing Technique 3-80
3.7 PDMS-GLASS CARTRIDGE CHARACTERISTICS 3-81
3.8 SUMARRY 3-82
4. EXPERIMENTAL VALIDATION OF CARTRIDGE 4-83
4.1 INTRODUCTION 4-83
4.2 OBJECTIVES OF EXPERIMENT: 4-84
4.3 VOLUMETRIC ANALYSIS 4-84
4.4 FLUIDIC EXPERIMENTAL MATERIALS 4-85
4.5 FLUIDIC EXPERIMENTAL PROTOCOL 4-86
4.5.1 flow conditions without chitosan 4-86
4.5.2 flow conditions with chitosan 4-87
4.6 EXPERIMENTAL RESULTS AND ANALYSIS WITHOUT CHITOSAN 4-87
4.7 EXPERIMENTAL RESULTS AND ANALYSIS WITH CHITOSAN 4-91
4.8 RPA DNA AMPLFICATION EXPERIMENT: 4-93
4.9 EXPERIMENTAL COMPLICATIONS 4-96
4.10 END POINT DETECTION ANALYSIS 4-96
4.11 SUMMARY 4-97
5. DESIGN AND FABRICATION OF AN ON-CHIP BLISTER 5-98
5.1 INTRODUCTION 5-98
5.2 BLISTER DESIGN OBJECTIVES 5-98
5.3 BLISTER GEOMETRY DESIGN 5-99
5.4 BLISTER FLOW CONTROL DESIGN 5-99
5.4.1 Flow Control with Magnetic Seal 5-100
5.4.2 Flow control with Rubber Seal 5-101
5.5 MATERIAL SELECTION OF BLISTER 5-101
5.6 MECHANICAL CHARACTERIZATION OF BLISTER 5-102
5.6.1 Results and Discussions 5-103
5.7 FINITE ELEMENT STRUCTURAL ANALYSIS 5-104
5.7.1 Useful volume Deformation 5-104

5.7.2 Finite Element analysis of Blister compression 5-105
5.8 BLISTER FABRICATION 5-106
5.9 ASSEMBLY OF FLUIDIC ELEMENTS ON CHIP 5-107
5.10 FLUID FLOW EXPERIMENTATION ON INTEGRATED CHIP 5-108
5.10.1 Experimental Results and Discussion 5-108
5.11 SUMMARY 5-111
6. CONCLUSIONS 6-112
7. RECOMMENDATIONS AND FUTURE WORKS 7-115
7.1 RECOMMENDATIONS 7-115
7.1.1 Passive valve: 7-115
7.1.2 Multiplexer: 7-115
7.1.3 Simulation Analysis 7-115
7.1.4 DNA Amplification Experiment: 7-116
7.2 FUTURE WORKS 7-116
7.2.1 Material selection: 7-116
7.2.2 DNA Detection on Cartridge : 7-116
7.2.3 Automation of Fluid Protocols on Cartridege 7-117
REFERENCES 118
APPENDIX 143

LIST OF FIGURES

FIGURE 1.1. ILLUSTRATION MINIATURIZATION OF CONVENTIONAL LABORATORY TO A CHIP 2-2
FIGURE 1.2. PICTURE OF A DISPOSABLE CHIP AND AUTOMATION CONTROL DEVICE. 2-3
FIGURE 1.3. PICTURE OF LAB-ON-A-CHIP WITH EXTERNAL AUTOMATION [11]. 2-3
FIGURE 1.4. DESIGN FLOW PROCESS FOR PDMS-GLASS CHIP FABRICATION 2-9
FIGURE 2.1. YOUNG EQUATION DEPICTION OF SOLID-LIQUID INTERACTION IN AMBIENCE AIR, THIS SCHEMATIC SHOWS THE SURFACE TENSION FORCES AT THE CONTACT LINE. (A) LIQUID DROPS PLACED ON A FLAT SURFACE TRY TO ADOPT SPHERICAL CAP SHAPE IN OTHER TO MINIMIZE THE SURFACE ENERGY. (B) THE SURFACE WETTABILITY IN RELATIONSHIP TO LIQUID-SURFACE ANGLE [79]. 2-18
FIGURE 2.2. SCHEMATIC REPRESENTATION OF THE PARABOLIC PATH WAY OF LIQUID IN A CYLINDRICAL CONDUIT [84] 2-19
FIGURE 2.3. SCHEMATIC REPRESENTATION OF EXTERNAL SYRINGE PUMP USED TO SUPPLY TYPICAL PRESSURE-DRIVEN MICROFLUIDIC PLATFORM FOR LIVING CELL ANALYSIS [90]. 2-20
FIGURE 2.4. THE GRAPHICAL ILLUSTRATION OF PHYSICAL SIMILARITIES BETWEEN THE FLOW OF FLUID AND FLOW OF ELECTRICITY. (A) POISEUILLE FLOWS IN A CIRCULAR CHANNEL. (B) THE HYDRAULIC RESISTANCE OF THE CIRCULAR CHANNEL $C_{GEOMETRY} = 8\Pi$ FOR THE CIRCULAR CHANNEL). (C) EQUIVALENT CIRCUIT SYMBOL OF A FLUIDIC RESISTOR FOR THE HYDRAULIC RESISTANCE AND HAGEN–POISEUILLE'S LAW ANALOGOUS TO A RESISTOR FOR THE ELECTRIC RESISTANCE AND OHM'S LAW [92]. 2-21
FIGURE 2.5. ILLUSTRATION OF GAS-LIQUID FLOW REGIMES IN HORIZONTAL PIPES [94]. 2-22
FIGURE 2.6. ILLUSTRATION OF VOLUME FRACTION OF AIR-WATER. 2-23
FIGURE 2.7. TIME-DEPENDENT FLOW MIXING BEHAVIOUR IN THREE DIFFERENT BEATING MODES (A) AND THE 2D GRAPHICAL CORRESPONDING MIXING PERFORMANCE (B) [118]. 2-25
FIGURE 2.8. A PICTURE OF A MICROFLUIDIC CHIP CONSISTING OF MICROFILTER, MICROMIXER AND MICROCHANNEL. (I–III) INLETS FOR ADDITIONAL SAMPLES, LYSIS BUFFER, WASHING AND ELUTION BUFFER. (IV) OUTLET FOR GATHERING OF THE EXTRACTED DNA [116]. 2-26
FIGURE 2.9. DISPOSABLE MICROFLUIDIC PUMP (BARTELS MIKROTECHNIK MP6 MICROPUMP) CAPABLE OF PUMPING BOTH AIR MAXIMUM FLOW: 18 ML/MIN (300 HZ) AND WATER MAXIMUM FLOW: 7 ML/MIN (100 HZ). IT IS MADE UP OF A HEAT AND CHEMICAL RESISTANT PLASTIC COVERING (30 X 15 X 3.8 MM^3), WEIGH 2GRAMS, 2 PIEZO ACTUATORS, 0 - 70 °C OPERATING TEMPERATURE AND AN ESTIMATED 5000 HOURS LIVE TIME [128]. 2-27
FIGURE 2.10. PASSIVE PUMPING MECHANISM OPERATED BY A WICKING PAD THAT REQUIRES PREREQUISITE PRIMING ACTION BY FINGER BELLOWS [9] 2-27
FIGURE 2.11. EXAMPLE OF BLISTER PACKAGING IN MICROFLUIDICS. (A) DEPOSABLE BLISTER DESIGN PACKS BY ACCEL BIOTECH, TAKEN FROM WWW.ACCELBIOTECH.COM (B) MINIFAB 3D PROTOTYPE BLISTER INTEGRATE MICROFLUIDIC CARTRIDGE, TAKEN FROM WWW.MINIFAB.COM.AU. 2-27

FIGURE 2.12. A GRAPHICAL DEPICTION OF POLY (ETHYLENE GLYCOL) (PEG) MICROWELLS INTEGRATED WITH PDMS FABRICATED MICROCHANNELS FOR PROTEIN, LIPID MEMBRANE AND CELL PATTERNING [131]. 2-28
FIGURE 2.13. A SCHEMATIC OF FLUID FLOW THROUGH AN ABRUPT JUNCTION PASSIVE MICROVALVE. 2-29
FIGURE 2.14. THE PASSIVE DESIGN IS BASED ON TWO EXTRUDED SYMMETRIC FLEXIBLE PDMS-BASED CANTILEVER BARS WHICH ACT AS VALVE FLAPS). THE DISTANCE OF THE VALVE FLAPS IS 20MM, THE HEIGHT OF THE VALVE FLAPS IS 70MM AND THE LENGTH OF THE VALVE FLAPS IS 300, 550, 700, AND 1000MM, RESPECTIVELY [150]. 2-30
FIGURE 2.15. THE PRINCIPLE OPERATION OF A CIRCULAR FERROFLUID PUMP USED TO MANIPULATE FLUIDS WITH FERROFLUID PLUGS IN CIRCULAR MICROCHANNELS [98]. 2-30
FIGURE 2.16. DIELECTROPHORETIC (DEP) SEPARATIONS CAN BE POSITIVE (PDEP) AS SHOWN IN (A) OR (B) NEGATIVE (NDEP) WHICH AFFECTS WHERE CELLS ARE POSITIONED WITHIN A FIELD. (C): GIVES A BASIC DEPICTION OF DEP BEEN UTILIZED IN DIFFERENT MICROFLUIDIC SYSTEMS [159]. 2-33
FIGURE 2.17. SEPARATION OF THE PARENTAL PLASMID, MINIPLASMID AND MINICIRCLE DNA. (A) COMBINATION OF THE FLUORESCENCE MICROSCOPY IMAGES. A MIXTURE OF THE PARENTAL PLASMID, MINIPLASMID AND MINICIRCLE DNA IS INSERTED TOWARDS THE RIDGES FROM A SIDE CHANNEL (EACH YELLOW SPOT REPRESENTS ONE DISTINCT DNA MOLECULE). AT THE FIRST RIDGE, THE MINICIRCLE DNA IS SEPARATED OUT OF THE MIXTURE AND DIRECTED INTO A SEPARATE CHANNEL. THE PARENTAL PLASMID AND MINIPLASMID DNA ARE DEFLECTED AND DRIFT TOWARDS THE SECOND RIDGE, WHERE ONLY THE PARENTAL PLASMID DNA IS DEFLECTED. THUS, ALL THREE SPECIES ARE RETRIEVED IN SEPARATE CHANNELS. (B) AND (C) FLUORESCENCE INTENSITIES UP- AND DOWNSTREAM OF THE TWO RIDGES. THE SCAN PATHS ARE PORTRAYED OVER THE GRAPHS. THE BLACK LINES SIGNIFY THE SCANS UPSTREAM OF THE RIDGE; THE DASHED LINES SYMBOLIZE THE SCANS DOWNSTREAM OF THE RIDGE. THE RED LINES ARE GAUSSIAN FITS. (B) AT THE FIRST RIDGE THE RESOLUTION WAS RES = 1.10. (C) AT THE SECOND RIDGE THE RESOLUTION WAS RES = 1.25. CONSEQUENTLY, A COMPLETE SEPARATION OF THE THREE SPECIES WAS ACHIEVED WITH VERY HIGH SEPARATION EFFICIENCY [104]. 2-34
FIGURE 2.18. CAPILLARITY-MEDIATED RESIN INTRODUCTION OF UV-CURABLE ADHESIVE [303]. COPYRIGHT WILEY-VCH VERLAG GMBH & CO. KGAA, COPIED WITH PERMISSION. 2-44
FIGURE 2.19. CROSS-SECTIONAL VIEWS OF ENCLOSED LASER MICROMACHINED PMMA CHANNELS, WITH INCREASING DEPTH FROM A–F, THERMALLY BONDED AT 18^0C, WELL ABOVE TG, USING A LOW BONDING PRESSURE BELOW 20 KPA [270]. 2-44
FIGURE 2.20. CORONA DISCHARGE USED TO BOND SURFACES OF PDMS TO GLASS. 2-46
FIGURE 3.1. PICTORIAL ILLUSTRATION OF MICROCHANNEL ASPECT RATIO OF (UNIT MM). 3-60
FIGURE 3.2. 3D GEOMETRICAL DESIGN OF INLET AND OUTLET (UNIT MM). 3-61
FIGURE 3.3. (A) 3D GEOMETRY DESIGN OF CENTRAL REACTION AND WASTE CHAMBERS. (B) CENTRAL REACTION CHAMBER WITH CHITOSAN. (C) WASTE REACTION CHAMBER WITH SODIUM POLYACRYLATE (SUPERABSORBENT POWDER). 3-62
FIGURE 3.4. (A) 2D SCHEMATIC DIAGRAM OF CENTRAL REACTION CHAMBER. (B) 2D SCHEMATIC DIAGRAM OF WASTE REACTION CHAMBER. 3-62
FIGURE 3.5. PREARRANGED DESIGN FORMATION OF AMPLIFICATION CHAMBERS (UNIT MM). 3-63
FIGURE 3.6. SEPARATION OF CHIP INTO TWO DISTINCT SECTIONS BY THE USE OF RED AND BLUE DOTTED LINES. 3-63

FIGURE 3.7. ILLUSTRATION SHOWING THE USE PASSIVE VALVE TO BRIDGE THE TWO MAIN SECTIONS OF THE MICROFLUIDIC CHIP 3-64
FIGURE 3.8. SCHEMATIC DIAGRAM OF THE DIFFERENT NARROW WIDTH THICKNESS OF THE PASSIVE VALVE TESTED BY SIMULATION. 3-64
FIGURE 3.9. FLUID FLOW OVERREACH IN THE MULTIPLEXER DURING THE WASTE CHAMBER FILLING PROCESS AS A RESULT OF THE ABSENCE OF A PASSIVE VALVE. 3-64
FIGURE 3.10. MULTIPHASE SIMULATION SHOWING FLOW REGULATION OF FLUID BY A PRESSURE SENSITIVE PASSIVE VALVE (300μM WIDTH) 3-66
FIGURE 3.11. DEPICTION OF PRESSURE VARIATION WITHIN THE VOLUME DOMAIN AS FLUID MOVE FROM CENTRAL CHAMBER TO THE WASTE CHAMBER AND ALSO THE PASSIVE VALVE (300μM WIDTH). 3-67
FIGURE 3.12. ILLUSTRATION OF FLOW VELOCITY VARIATION IN THE VOLUME DOMAIN AS FLOW MOVES WASTE CHANNEL AND PASSIVE VALVE (300μM WIDTH). THE FIRST LEGEND ON THE RIGHT-HAND SIDE INDICATES THE REYNOLDS NUMBER, WHILE THE SECOND LEGEND HIGHLIGHTS FLOW VELOCITY IN METRES PER SECONDS (M/S). 3-67
FIGURE 3.13. SCHEMATIC DIAGRAM SHOWING THE MEANS OF DERIVING THE PRESSURE DROP ALONG THE PASSIVE VALVE OF VARIOUS NARROW WIDTH THICKNESS (300μM, 400μM AND 500μM) AND CHANNEL WASTE CHAMBER OF VARIOUS BY A SINGLE PHASE CFD SIMULATION 3-68
FIGURE 3.14. LINE GRAPH SHOWING THE PRESSURE ALONG PASSIVE VALVES WIDTH (300μM, 400μM AND 500μM) IN COMPARISON WITH THE PRESSURE ALONG THE CHANNEL LEADING TO THE WASTE CHAMBER. 3-69
FIGURE 3.15. SPATIAL CONFIGURATION OF A 0.5MM ASPECT RATIO MULTIPLEXER MICROCHANNELS LINKED TO THE SIX AMPLIFICATION CHAMBERS 3-70
FIGURE 3.16. ILUSTRATION OF THE FILLING OF THE CRC BY GRADUAL DISPLACEMENT OF THE PREVALENT AIR BY THE INFLOW OF WATER. 3-71
FIGURE 3.17. ILLUSTRATION OF PRESSURE VARIATION WITHIN THE VOLUME DOMAIN AS FLUID MOVE FROM CENTRAL CHAMBER THROUGH THE PASSIVE VALVE (300μM WIDTH) TO THE MULTIPLEXER FOR DISTRIBUTION THE AMPLIFICATION RESERVOIRS. 3-72
FIGURE 3.18. DEPICTION OF FLOW VELOCITY VARIATION IN THE VOLUME DOMAIN WITH PASSIVE VALVE OF (300μM WIDTH) CONNECTED TO A MULTIPLEXER. THE FIRST LEGEND ON THE RIGHT-HAND SIDE INDICATES THE REYNOLDS NUMBER, WHILE THE SECOND LEGEND HIGHLIGHTS FLOW VELOCITY IN METRES PER SECONDS (M/S) 3-72
FIGURE 3.19. VEIN OUTLINE IN THE MULTIPLEXER TO INDICATE FLOW PATHWAY FROM DESIGNATED NODAL POINTS B AND C 3-73
FIGURE 3.20. SELECTED PRESSURE POINTS WHERE PRESSURE DROPS ARE MOST CRITICAL 3-73
FIGURE 3.21. REPRESENTATION OF CRITICAL PRESSURE POINTS IN FIGURE 3.18 AS ELECTRONIC RESISTORS ON A CONDUCTING WIRE. 3-74
FIGURE 3.22. GRAPHICAL ILLUSTRATION OF FLUIDIC RESISTANCE AT THE CRITICAL PRESSURE POINTS SHOWN IN FIGURE 3.20 3-74
FIGURE 3.23. (A) 2D ILLUSTRATION OF THE MULTIPLEXER CONNECTED TO SIX AMPLIFICATION CHAMBERS WITH PRESSURE LINES ALONG THEIR EXIT PORTS. (B) MAGNIFIED 3D DEPICTION OF THE PRESSURE LINES THE OUTLET PORTS THAT OFFER CHARACTERISTICS SIMILAR TO A PASSIVE VALVE DUE TO ITS GEOMETRIC FEATURES. 3-76

FIGURE 3.24. LINE GRAPH SHOWING THE PRESSURE ALONG ALL THE OUTLET PORT LINES OF THE AMPLIFICATION CHAMBERS.....3-77
FIGURE 3.25. 3D PRINTED POSITIVE MOULD USED FOR CREATING NEGATIVE PDMS MOULD. CREATED BY VIPER SI2 SLA PRINTER.....3-78
FIGURE 3.26. ENCASED 3D PRINTED MOULD IN A METAL FILLED WITH LIQUID PDMS. 3-79
FIGURE 3.27. CURED NEGATIVE PDMS MOULD STILL ATTACHED TO POSITIVE 3D PRINTED MOULD.....3-80
FIGURE 3.28. (A) BONDED PDMS-GLASS CHIP WITH CHITOSAN MEMBRANE IN THE CENTRAL REACTION CHAMBER. (B) BONDED PDMS-GLASS CHIP WITH NO CHITOSAN MEMBRANE 3-80
FIGURE 3.29. ILLUSTRATION OF A GLASS SEALED RECTANGULARLY SHAPED POLYDIMETHYLSILOXANE MICROCHANNEL STRUCTURE THAT IS EXEMPLARY OF GENERAL PDMS-GLASS CARTRIDGE. 3-81
FIGURE 4.1. (A) FLOW PROCESSES INVOLVING ONLY CENTRAL REACTION CHAMBER. (B) FLOW PROCESSES INVOLVING THE CENTRAL AND WASTE REACTION CHAMBER. (C) FLOW PROCESSES INVOLVING THE CENTRAL REACTION CHAMBER, MULTIPLEXER AND AMPLIFICATION REACTION CHAMBER. 4-85
FIGURE 4.2. PARTIAL FILLING OF THE CENTRAL REACTION CHAMBER WITH YELLOW DYE TO INDICATE DNA EXTRACTION 4-88
FIGURE 4.3. FLUSHING OF YELLOW DYE WITH AIR INTO THE WASTE REACTION CHAMBER TO REPRESENT DNA PURIFICATION 4-88
FIGURE 4.4. FILLING OF THE CENTRAL REACTION CHAMBER WITH BLUE DYE TO REPRESENT DNA ELUTION PROTOCOL 4-89
FIGURE 4.5. FILLING OF THE AMPLIFICATION REACTION CHAMBERS WITH BLUE DYE VIA THE MULTIPLEXER FOR DNA AMPLIFICATION REACTIONS. 4-89
FIGURE 4.6. ILLUSTRATION OF THE OUTLETS PORT OF THE AMPLIFICATION BEHAVING SIMILARLY TOO PASSIVE BY TEMPORALLY RESTRICTING FLOW. 4-90
FIGURE 4.7. FLOW PROCESS INVOLVING FILLING OF THE CENTRAL REACTION WITH YELLOW DYE AND ALSO WICKING OF THE DYE BY THE CHITOSAN MEMBRANE (DNA EXTRACTION). 4-91
FIGURE 4.8. FILING OF THE CENTRAL REACTION CHAMBER WITH BLUE DYE THAT MIXES WITH THE ABSORBED YELLOW DYE IN THE CHITOSAN TO FORM A GREEN COLOUR RESOLUTION (DNA ELUTION). 4-92
FIGURE 4.9. FLUSHING OF UNABSORBED THE YELLOW DYE BY THE CHITOSAN WITH AIR INTO THE WASTE REACTION CHAMBER (DNA PURIFICATION).....4-92
FIGURE 4.10. FILLING OF THE AMPLIFICATION REACTION CHAMBERS VIA MULTIPLEXER TO GIVE A GREENISH BLUE RESOLUTION (DNA AMPLIFICATION REACTIONS). 4-93
FIGURE 4.11. PDMS-GLASS MICROFLUIDIC CARTRIDGE WITH EMBEDDED CHITOSAN IN REACTION CHAMBER, SODIUM POLY ACRYLATE POWDER IN WASTE CHAMBER AND AIR-DRIED MAGNESIUM ACETATE IN SIX AMPLIFICATION CHAMBERS.....4-94
FIGURE 4.12. ILLUSTRATION OF AMPLIFICATION INCUBATION USING AN ELECTRIC HOT PLATE.....4-95
FIGURE 4.13. RPA AMPLICONS DETECTION BY AGAROSE GEL ELECTROPHORESIS USING A RED DNA-BINDING DYE. (A) EIGHT REACTION GEL RESULTS. (B) TWELVE REACTION GEL RESULTS 4-96
FIGURE 5.1. 3D SECTIONAL VIEW OF THE BLISTER MODEL SHOWING THE REGION WHERE FLUID IS RESERVED 5-99
FIGURE 5.2. FLUID FLOW MECHANISM USING A 3MM MAGNET LOCK 5-100
FIGURE 5.3. (A) BLISTER MAGNETIC SEAL RELEASE DEMONSTRATION. (B) BASE WASHER AND PINS 3D PRINTED FROM OBJET30 PRO (BEIGE) AND VIPER SI2 SLA SYSTEM (DARK GREY). (C) COMPLETE

BLISTER ASSEMBLY WITH FLOW CONTROL CONTRIVANCE. (D) MAGNET REQUIRED FOR SEALING FLUID IN THE BLISTER 5-100
FIGURE 5.4. ALTERNATE FLOW CONTROL MECHANISM WITH FRAGILE RUBBER SEAL 5-101
FIGURE 5.5. (A) SCHEMATIC DIAGRAM OF ASTM D412 DUMB BELL (B) SILICONE ELASTOMER LOADED ON A TENSILE GRIP. SAMPLE SHAPE. (C) GRAPHICAL ILLUSTRATION SHOWING LOAD VERSUS EXTENSION . 5-103
FIGURE 5.6. CROSS SECTION AL OF BLU-STUFF SILICONE ELASTOMER DUMB BELL MOULD. 5-103
FIGURE 5.7. STATIC ANALYSIS ON COMPLETE BLISTER ASSEMBLY SHOWING GRADUAL DECOMPRESSION OF BLISTER UNDER A RAMPED FORCED OF 10N. 5-105
FIGURE 5.8. ILLUSTRATION OF A FULLY DECOMPRESSED BLISTER WITH MINIMAL DEAD SPACE VOLUME..... 5-105
FIGURE 5.9. ILLUSTRATION OF THE PLUNGER AND A BASE MOULD DESIGN CONFIGURATION USED FOR MAKING BLISTERS 5-106
FIGURE 5.10. FABRICATION OF BLU-STUFF ELASTOMERIC BLISTER USING 3D PRINTED PLUNGER AND BASE MOULD 5-106
FIGURE 5.11. FABRICATED BLU-STUFF SILICONE ELASTIC BLISTER FOR MICROFLUIDIC CARTRIDGE 5-107
FIGURE 5.12. 3D DESIGN ASSEMBLY CONFIGURATION OF POSITIVE MOULD MICROFLUIDIC CARTRIDGE WITH A BLISTER AND ITS INTERNAL COMPONENTS 5-107
FIGURE 5.13. (A) FLUID FILLED BLISTER WITH POSITIVE MOULD CHIP IS INSTALLED IN A METAL JIG AND FILLED WITH LIQUID PDMS. (B) CURED PDMS NEGATIVE MOULD AND BLISTER STILL ATTACHED TO POSITIVE CHIP. (C) BONDED GLASS SLIDE WITH PDMS MOULD BEARING A BLISTER. 5-107
FIGURE 5.14. THE USE OF MAGNET TO RELEASE THE MINIATURE MAGNETIC VALVE FOR FLUID FLOW ACTIVATION 5-108
FIGURE 5.15. PSEUDO DNA ELUTION PROCESS THAT INVOLVED FILLING OF THE CENTRAL REACTION CHAMBER WITH BLUE DYE DISPENSED FROM THE BLISTER BY FINGER COMPRESSION. 5-109
FIGURE 5.16. EXTENDED FINGER COMPRESSION EXERCISE TO FILLING OF THE MULTIPLEXER AND AMPLIFICATION REACTION CHAMBERS BY FURTHER FINGER COMPRESSION. 5-110

LIST OF TABLES

TABLE 2.3. SYNOPSIS OF GENERAL BONDING TECHNIQUES FOR MICROFLUIDIC DEVICE [177]. 2-47
TABLE 3.1. DERIVATION OF FLUIDIC RESISTANCE FROM CRITICAL PRESSURE POINTS WITH REFERENCE TO DATUM PRESSURE 3-75
TABLE 5.1. COMPARISONS BETWEEN THE ORIGINAL TWISTDX CHEMICAL AND VOLUME COMPOSITIONS [368] WITH THE ALTERED VERSION USED FOR THE PDMS-GLASS CHIP FOR DNA AMPLIFICATION. 4-95
TABLE 6.6.1. PROVIDES A STANDARDISED TEST OF RATIO 10:1 (PART A: PART B) CURED AT VARIOUS TEMPERATURE 5-102
TABLE 6.2. MECHANICAL PROPERTIES OF BLU-STUFF SILICONE ELASTOMER 5-104

ACRONYMS

3D	*THREE DIMENSIONS*
ARC	*AMPLIFICATION REACTION CHAMBER*
ASTM	*AMERICAN SOCIETY FOR TESTING AND MATERIALS*
atm	*ATMOSPHERIC PRESSURE*
BIOMEMS	*BIOLOGICALMICRO-ELECTROMECHANICAL SYSTEMS*
Bp	*BASE PAIR*
CFD	*COMPUTATIONAL FLUDIC DYNAMICS*
CRC	*CENTRAL REACTION CHAMBER*
CPM	*CONTINUOUS PHASE MODEL*
COC	*CYCLIC OLEFIN COPOLYMER*
CNC	*COMPUTER NUMERICAL CONTROL*
CTE	*COEFFICIENT OF THERMAL EXPANSION*
DFR	*DRY FILM RESIST*
DNA	*DEOXYRIBONUCLEIC ACID*
dNTPs	*DEOXYNUCLEOTIDE TRIPHOSPHATES*
dsDNA	*DOUBLE STRANDED DEOXYRIBONUCLEIC ACID*
DPM	*DISCRETE PHASE MODEL*
HDA	*HELICASE-DEPENDENT AMPLIFICATION*
HDT	*HEAT OF DISTORTION TEMPERATURE*
GMR	*GIANT MAGNETO-RESISTANCE*
MEMS	*MICRO-ELECTROMECHANICAL SYSTEMS*
MES	*2-(N-MORPHOLINO) ETHANESULFONIC ACID*
NEAR	*NICKING ENZYME AMPLIFICATION REACTION*
NPT	*NEAR POINT TESTING*
N-S	*NAVIER STOKES*
LAMP	*LOOP-MEDIATED ISOTHERMAL AMPLIFICATION*
LOC	*LAB ON CHIP*
LOAC	*LAB ON A CHIP DEVICE*
PCR	*POLYMERASE CHAIN REACTION*
PDMS	*POLYDIMETHYLSILOXANE*
PMMA	*POLY (METHYL METHACRYLATE)*
POC	*POINT OF CARE*
POCT	*POINT OF CARE TESTING*
PTFE	*POLYTETRAFLUOROETHYLENE*

PCR	*POLYMERASE CHAIN REACTION*
RNA	*RIBONUCLEIC ACID*
SAP	*SUPERABSORBENT POLYMERS*
SDA	*STRAND DISPLACEMENT AMPLIFICATION*
SiO_2	*SILICON DIOXIDE*
SSB	*SINGLE-STRANDED BINDING PROTEIN*
ssDNA	*SINGLE STRAND DEOXYRIBONUCLEIC ACID*
STD	*POLY (METHYL METHACRYLATE)*
UV	*ULTRAVOLIET*
WRC	*WASTE REACTION CHAMBER*

SYMBOLS

μ-TAS	*MICRO TOTAL ANALYSIS SYSTEMS*
du/dy	*VELOCITY GRADIENT*
A	*CROSS SECTIONAL SURFACE AREA*
d	*DISTANCE*
D	*DIFFUSION COEFFICIENT*
h	*DEPTH*
VS	*SPECIFIC VOLUME*
VT	*TOTAL VOLUME*
VW	*WASTE CHAMBER VOLUME*
T	*TIME*
TD	*DECOMPOSITION TEMPERATURE*
Tg	*GLASS TRANSITION TEMPERATURE*
w	*WIDTH OF CHANNEL*

1. INTRODUCTION

1.1 MICROFLUIDICS TECHNOLOGY

In the latter period of the 20th Century, the interest in the innovative use of microfluidic technology for the expedient clinical application, especially in the case of "point-of-care" diagnosis of diseases, grew propitiously [1], [2]. This growing trend brought about the inception of the device known as "lab-on-a-chip" (LOAC).
This microfluidic device is a subset of micro-electromechanical systems (MEMS) for a biological application that is collectively known as (BioMEMS)[3]. MEMS technology involves the integration of electrical and mechanical components which is inclusive of microsensors, micropumps and microactuators on the same platform using standard fabrication techniques of the semiconductor industry with almost the same equipment and materials [4]. The technology involved in developing this device comes from a multidisciplinary field intersecting engineering, physics, chemistry, microtechnology and biotechnology, with practical applications to the design of systems that involves the scaling of single or multiple lab processes into small volumes of fluids required to achieve similar results on a macro scale. The advent of this technological breakthrough has led the development of Micro-Total-Analysis-Systems (μ-TAS)[5] which is dedicated to the integration of the entire sequence of lab processes to perform chemical analysis and can also be used in diverse application other analysis [6]. The advent of this technological breakthrough has led the development of Micro-Total-Analysis-Systems (μ-TAS)[5] which is similar to LOAC platforms because it involves the integration of the entire sequence of lab processes to perform chemical analysis that can be used for diverse application other analysis [6]. This conventional science behind this technology depends on the behaviour of continuous liquid flow through microfabricated channels. Moreover, actuation of flow is mostly implemented with the external assistance of micro-pump, which are complicated and cumbersome. Also, the physical properties of fluids at the microscale can differ from the generic behaviour of macro-scale quantity in factors such as surface tension and energy dissipation, and fluidic resistance. Microfluidics analyses how these properties can change, and how they can be worked around, or exploited for specific design requirements. The revolutionary idea of fitting an entire laboratory on a chip (Figure1.1) was motivated by the electronic industry providing an entire computer on a microelectronic circuit chip. In a typical scenario, the samples need to be collected from the site and sent to specialised laboratories for analysis, which is a cost-intensive and time-consuming process. On the other hand, miniaturised laboratory analysis techniques offer small volume requirement which means only small

quantities of reagents are needed, reducing costs and waste. Moreover, the Analysis times are also efficiently shortened since efficiencies are usually higher when working on a smaller scale with operational simplicity compared to existing expensive, large size and time-consuming laboratory-based analysis techniques. All these benefits that include fast scan time, portability, cost reduction, disposability, reduced consumption of reagents and efficiency are revolutionising clinical diagnostics and many biochemical laboratory procedures by these means making the lab-on-a-chip technology ideal for near-patient and point-of-care testing.

Rapid Development of miniaturised laboratory diagnostic devices which have brought about an enormous impact on modern society's health and life owes its progress to the achievements in the field of microfabrication and microfluidics technology in recent years. Since then, there has been tremendous interest in harnessing the full potential of this approach and, consequently, the development of many microfluidic devices and fabrication methods. Materials such as (poly-dimethyl siloxane) (PDMS) and (Polymethyl methacrylate) (PMMA) have emerged recently as excellent alternatives to the silicon and glass used in early devices fabricated by MEMS (micro-electromechanical systems) processes [7]. The increase in popularity of their utilization in the manufacturing of microfluidic devices stems from low cost, excellent optical transparency, suitable mechanical/chemical properties and simple fabrication procedures.

This Simplified device fabrication and the possibility of incorporating densely integrated microvalves into designs [8][9]have helped microfluidics to explode into a ubiquitous technology that has found applications in many diverse fields. While the area of microfluidics is rapidly advancing and complex operations have become possible, limitations still appear in the form detection methods that may not always scale down positively, leading to low signal-to-noise ratios. Moreover, due to the chemical and physical properties of the fluid at microscale conditions, choice of reagent properties in design requirement becomes imperative.

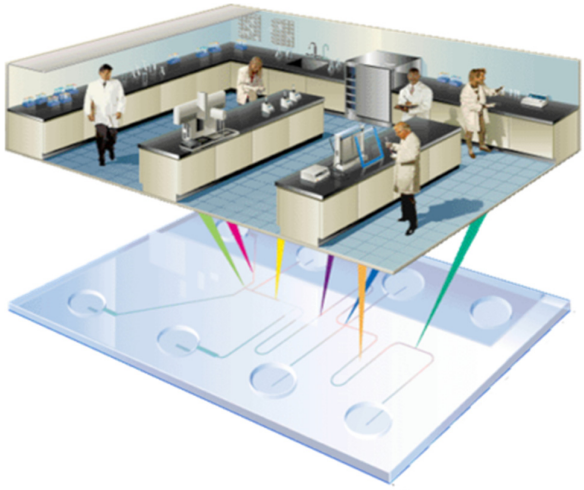

Figure 1.1. Illustration miniaturization of conventional laboratory to a chip

1.2 POINT OF CARE DIAGNOSTIC

Also known as point-of-care-testing (POCT) [10]is peripheral laboratory testing or Near Patient Testing (NPT) that involves any analytical test performed for or by a patient outside the conventional medical laboratory

setting. The principal concept behind POCT is to provide quick identification of diseases at the time the test is carried out. This innovation improves the likelihood that the patient, physician, and care team will receive the results faster thus making room for immediate clinical management decisions to be made. Examples of POCT includes sexually transmitted diseases (STD) testing, blood glucose testing, blood gas and electrolytes analysis, infectious disease testing, urine strips testing, pregnancy testing and much more.

Commercialising of this medical diagnostic innovation involves the combination of the POCT concept with microfluidic technology [9]. This combination has led to the production of Handheld and portable diagnostic kits that come either in multiple parts or compact integrated piece (all in one kit). Fig.1.2 and Fig.1.3 illustrates the various parts diagnostic kit that includes the sample collection platform (LOAC) and electronic identification component. On the other hand, the integrated diagnostic kit has both the sample and detection platforms in a compact piece, leading to possible trade-offs in reusability over compatibility.

The use of one device to test multiple predisposed disease symptoms has led the POCT leading industries leaning towards reusability. This approach encourages sound economic advantages in cost reduction and material wastage. Top amongst various design initiatives are the Disposable lab-on-chip platforms that can provide these POCT production companies with a convenient means to achieve this economic and versatility advantages. Furthermore, user-friendliness approach of diagnostic testing kits operation adds another dimension to the overall system, such that a semi-skilled operator or patient self-test can be carried out conveniently to achieve reliable results. With this quality, public acceptance and absorption become easier which improves marketability.

Figure 1.2. Picture of a disposable chip and automation control device.

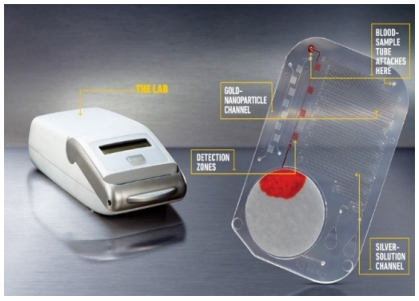

Figure 1.3. Picture of lab-on-a-chip with external automation [11].

1.2.1 ON-CHIP SAMPLE PREPARATION

Sample preparation is the initiation phase in the chip where the raw sample will be introduced to mix with the appropriate reagents. This process is the most important step in the full process of bio-analysis because it's the foundation for POCT chip efficacy (i.e. garbage in garbage out). For the nucleic acid test in conventional clinical practice, sample preparation involves extraction of DNA/RNA from a raw source of bio-fluid such as blood, saliva, urine or tissue section, etc.). The overall protocol can be divided into three significant steps: (1) Cell lysis; (2) DNA extraction; (3) DNA purification. Cell lysis is the prerequisite extraction process which involves the dissolution of the cell membrane release DNA/RNA. The fluid containing the lysed cells is referred to as lysate. Detergent lysis is the most extensively utilised method because its protocols are easily miniaturised on-chip [12]–[14]. Good examples of Detergents like SDS or Triton-X can effortlessly disrupt the cell membranes by solubilizing their phospholipids [15]. Furthermore, the use high temperature known as thermal lysis to break cell membrane is another adaptable on-chip protocol. For instance, thermal treatment on a microfluidic chip can seamless be integrated with a Polymerase Chain Reaction (PCR) thermal cycle [16], [17]. The use of ultrasound treatment, unlike the other techniques is it difficult to miniaturise this protocols on the chip as a result of the relatively large external device needed to function. Nonetheless, efforts and progress on its miniaturisation and efficiency to be realised on-chip [18], [19]. On the bright side, this method is a non-selective cell type and have a shorter lysis time in comparison to the others. Ultrasound creates minuscule gaseous cavitation from dissolved gases as a result of extreme pressure difference in the liquid. The implosion of the induced cavitation then creates shock waves comparable to several thousand atmospheres of pressure [20], [21] that is sufficient to break the cell membrane to release DNA fragment in length of hundreds bp's [20]. Lastly, another possible lysis mechanism is electrochemical lysis [31] that utilises hydroxide ions generated by electrolysis of buffer to disrupt cell membrane. Extraction of DNA from the lysate in most situations typically involves solid phase extraction (SPE) procedures. The nucleic acids subsequently released after lysis are purified in a reagent mixture suspension, followed by series of wash steps and elution for downstream amplification [22][15]. Nucleic acid purification is significant because some compounds found in clinical samples (especially those found in blood) [23] can inhibit subsequent PCR amplification technique. However, recently developed PCR assays that are less prone to inhibition with less cumbersome sample preparation have been adopted [24], [25]. It is also mentioning that so many isothermal technologies seem to be less affected by inhibitory compounds of bio-samples although DNA separation/purification is not always necessary if the lysate buffer is specially selected to circumvent the interference to PCR reaction. The most common method for on-chip DNA extraction is utilising magnetic beads coated with silica or functionalized groups (carboxyl [26], amine [26], biotin [38], nucleotide probes [27]) to separated DNA from lysate medium. This technique is easily adaptable on the chip due to the easy manipulation of microbeads within a compact system. Of recent, SPE using chitosan-coated magnetic beads [28][18] has been demonstrated without wash steps requirement by moving DNA bound to magnetic beads through a layer of liquid wax. A similar innovative approach that drastically eases sample preparation procedure is the coating of magnetic microparticles with chitosan [29]. Chitosan is a derivative of chitin extracted from crustacean shells that are commercially accessible, low-cost and biocompatible. It is a polysaccharide β-(1→4)-linked D-glucosamine (deacetylated unit) and N-acetyl-D-glucosamine (acetylated unit) that is predominantly suitable for charge switching owing to its wealth of amine groups that can be charge-regulated via pH. The amino group on chitosan has a pH of about 6.4 which makes chitosan cationic at pH lower 6.4 [30]. Under this circumstances, the chitosan can be

easily bound to a negatively charged DNA and then require a moderately high pH (for example, around 8.5) to efficiently elutes the DNA [29]. Chitosan has been applied in recent research to various grades of Whatman chromatography paper to serve as chitosan coated membranes [28]; that can be used for DNA extraction on a highly reproducible microfluidic platform.

1.2.2 DNA AMPLIFICATION

Amplification of DNA is the next phase where the small quantity of DNA purified from the preceding stages will be proliferated to achieve the anticipated concentration, which will be suitable for the detection strategy being employed. The two methods through which amplification process can be performed are traditional thermal cycling PCR or isothermal amplification technique. PCR can be described as a temperature-controlled and Enzyme-catalysed biochemical reaction that principally involves repeated thermal cycles carried out to ascertain enough copies of DNA to be detected and analysed. The aim of the process is to amplify short pieces of a longer DNA molecule [31]. A typical PCR amplification protocol involves a target DNA, a thermostable DNA polymerase, two oligonucleotide primers, deoxynucleotide triphosphates (dNTPs), reaction buffer and magnesium [32]. The external device used to facilitate this reaction is called a thermal cycler. This instrument is used to subject the chemical processes to a sequence of varying temperatures for specific amounts of time. For each protocol, inclusive of temperature variation and time makes a complete amplification cycle. The three steps of thermal cycling are (1) DNA melting; (2) Primers annealing; (3) Primers extension. In theory, each PCR cycle can double the amount of targeted sequence (amplicon) in the reaction. For instance, 20 cycles hypothetically multiply the amplicon by a factor of about one million in a matter of hours [33]. DNA melting is expected to occur around 95 °C for a short amount of time (15seconds to 2minutes) [15]. At this temperature (denaturing temperature, Td), the double-stranded DNA (dsDNA) uncoil from one another, producing the necessary single strand DNA (ssDNA) template for replication by the thermostable DNA polymerase. Subsequently, the primer annealing process is initiated by a reduction in temperature (annealing temperatures, Ta) approximately (40°C to 60°C) for about 15 to 60 seconds [33]. The cooling down of the temperature causes the oligonucleotide primers to form stable associations with the denatured target DNA and also serve as primers for the DNA polymerase. Finally, the extension process involves the synthesis of a new DNA by raising the temperature to about 70°C -74°C within 1 to 2 minutes [33], [34]. On the other hand, isothermal nucleic acid amplification technologies use a constant reaction temperature, which translates into less complicated and less expensive equipment such as water baths, resistive heaters (hot plates), or via exothermic chemical heating [35]. There are many different isothermal protocols, but the distinct advantages they share are suitability for low-cost applications and extreme analysis speed in comparison with PCR.

Loop-mediated isothermal amplification (LAMP) is one of the varied isothermal amplification that uses 4 to 6 primers with the capability of identifying 6 to 8 different sections of target DNA. LAMP well-suited for field diagnostics because it's very sensitive and fast [36]. Moreover, the analysis and amplification are so extreme that the magnesium pyrophosphate formed during the reaction can easily be observed [36].

A very popular isothermal technique that is still being employed in several diagnostic devices is helicase-dependent amplification (HDA). Similar to PCR, this system needs only two primers, and its protocol utilises the double-stranded DNA unwinding activity of a helicase to disconnect strands, enabling primer annealing and extension by a strand-displacing DNA polymerase [37].

Another commonly used technique in clinical diagnostics is Nicking enzyme amplification reaction (NEAR). NEAR is extremely fast and sensitive, capable of detecting small DNA target amounts in minutes. This process speedily produces many short nucleic acids from the target sequence by utilising a strand-displacing DNA polymerase initiated at a nick generated by a nicking enzyme [38]. A nicking enzyme (or nicking endonuclease) is an enzyme that breaks a double-stranded DNA into one strand to produce DNA molecules that are "nicked". This enzymatic hydrolysis occurs at specific recognition nucleotide sequences known as a restriction site [39], [40].

Strand displacement amplification (SDA) is also a commonly used clinical diagnostics procedure that utilises nicking enzyme. In this case, SDA relies on a strand-displacing DNA polymerase, to initiate at nicks created by nicking enzyme at a site contained in a primer. The nicking site is regenerated with each polymerase displacement step, resulting in exponential amplification. In summary, the major drawback of PCR is the time-consuming denaturation process that results in longer amplification period, typically thirty minutes or more in comparison to few seconds to minutes for isothermal amplification. However, isothermal amplification is not without their drawbacks as nonspecific amplification products are a common issue with their reactions [38].

Similar to SDA, a new technique termed recombinase polymerase amplification (RPA) was introduced in 2006 and is rapidly the diagnostic means of choice for the swift, explicit, and cost-effective identification of pathogens. This RPA advantage is as a result of their sample-preparation simplicity, minimal temperature requirements (25–42 °C), and readily available reagents in dried formats especially frozen. The main difference between PCR and RPA is substitution heat with protein enzymes for the necessary thermal denaturation process. The essential proteins required for strand-displacement activities that are necessary for exponential DNA amplification in the absence of thermal cycling comprise of the recombinase, single-strand DNA binding protein (SSB), and strand-displacing polymerase. Likewise, their combination has a high specificity and efficiency (10^4 fold amplification within 10 minutes) [41]. Even though RPA clinical results are similar to other techniques mentioned; there are also some obvious shortcomings. In comparison to LAMP, which enables flexible alterations to primers and probes by software manipulation; RPA is non-complaint as of yet. As a result, the optimal combination of several RPA primer and probe are required. More critical is the verification by gel electrophoresis that is usually inhibited by the presence of high molecular weight proteins. Thus, needing additional post-amplification purification. In all, RPA is certainly an auspicious isothermal molecular technique for point of care diagnostics.

1.2.3 DNA DETECTION

The final phase of the diagnostic process typically embroils differentiating the target-specific amplicons from non-specific amplification products, and it revolves around two standpoints; "real-time" or "endpoint detection". Endpoint detection uses Agarose gels for detection, thereby requiring simpler instrumentation and providing less complex outputs for clarification. A good example of a commonly used endpoint method to characterise DNA components is staining agarose gels with fluorescent dye (ethidium bromide) [42]. After staining the nucleic acids are subjected to electrophoresis before visualised through illumination with 300-nm UV light [43]. The dye ethidium bromide is very useful to detect both single and double stranded nucleic acids (DNA and RNA inclusive). However, there are limitations such as poor precision, low sensitivity, short dynamic range less than two logs, low resolution, not–automated process, size-based discrimination only, results are an analog representation, and ethidium bromide dyes are not very quantitative.

Real-time, on the other hand, integrate ongoing amplification reaction with detection. Real-time methods are far superior for quantitative analyte detection with a large dynamic range. Furthermore, real-time chemistries allow for the detection of PCR amplification during the early phases of the reaction. One of the most common DNA non-specific detection technique in PCR microfluidic chip is the combination of optical technology in conjunction with capillary electrophoresis [44], [45]. In this synthesis, the optical approach utilises the fluorescence signals from the binding interaction between the dye and the amplified amount of double-stranded DNA molecules [44], [46], [47], while capillary electrophoresis is used to separate the DNA molecules according to their sizes. Afterwards a DNA template concentration could be acquired before and after PCR or calculated from threshold value in real-time by fluorescent intensity difference. Although this method is very sensitive and extensively used in PCR, fluorescence-based methods are not acquiescent for miniaturisation and integration onto an all in one single-chip, as a result of the requirement of power-intensive laser light sources and an optical detection system of a reasonable size [48]. The use of sequence-specific electrochemical DNA sensors can be well suited for hand-held instruments. In this system, the sensing protocol involves the immobilisation of an oligonucleotide onto a transducer surface, and upon the hybridization of the complementary target sequence, the binding event is detected by electrochemical methods [49]. Furthermore, the signal detection from hybridization action that involves two primary methods termed labelled and label-free. In the first approach, target molecules will be labeled with specific identifiers and the signal can be generated from the interaction between the label and sensor. An example of such of label-based detection techniques is the Electrochemical and magnetic biosensors [50]. The electrochemical surface biosensor measures the active redox activity of active labelled target molecules in the form of electric signals. While the magnetic biosensor utilises the field of the magnetic bead tagged to the hybridised DNA molecule. This area is anticipated to change the underlying resistance of the GMR (giant magnetoresistance) sensor, and consequently, the signal can also be measured as a variation in the sensor electric current [50]. In the case of the label-free detection techniques, the signal is generated from the intrinsic properties of DNA molecules such as electric charge and mass variations. The total DNA mass on the surface of the sensor can be subjected to alterations from hybridization occurrence. These alterations can then be detected using a quartz crystal microbalance sensor. Charge variation at the surface of the sensor can also be detected by the use an underlying field effect sensor.

1.3 OBJECTIVES OF RESEARCH

The vision of Brunel Doclab research group is to develop a fully integrated Blister microfluidic device for point-of-care diagnostics with the capability of detecting single or multiple pathogens of infectious diseases. The device under development utilises Isothermal nucleic acid technology for amplification while real-time miniaturised fluorometric detection strategies are employed [9].

This thesis aligns with the group vision but is primarily focused on designing a fast, simple and disposable PDMS bio-cartridges capable of performing microfluidic functions necessary for its intend POCT use; DNA extraction, purification, amplification, and detection. These features involve of fluids transportation and storage. The storage purpose requires the use of on-chip reservoir mostly in the form of blisters that are capable of dispelling the fluids its hold when needed. On the other transportation, can be categorised into movement of pre-processed and post-processed fluids within the system. Pre-processed fluids are inflow or inbound fluids

into the reaction chambers they include reagents and bio-sample while the case of post-processed fluid involves fluid flowing outbound d from the reaction chambers into designated chambers for further processing. For both microfluidics functions to necessitate the preferred mundane POCT characteristics such as fast processing time, low cost per unit production, good precision, and disposability; well-designed networked microchannels, chambers, and fluid reservoir are of highly vital importance in the bio-chip modelling. Conventional existing bench-tops POCT devices take up to an hour to process extraction and purification. Exclusive of this process time is the amplification and detection time that also adds up to the overall process time. These developments have made fast and relatively low-cost diagnostic systems imperative in lab-on-chip modelling.

In design an optimised POCT biochip three designs were taken into considerations in other to achieve the design models that will ascertain a well coordinate lab sequence of operation, the specific objectives of this research are summarised as follows:

.

- Develop and fabricate a 3D design concept for a microfluidic cartridge capable of multiplexing fluid flow to six individual microchambers and also carry out precise flow regulation by the use of a passive valve

- Perform preliminary fluid flow experiment to test the efficacy of the newly fabricated microfluidic cartridge using coloured liquid dye as a substitute for laboratory reagents.

- Perform DNA sample preparation in the microfluidic cartridge by the use of chitosan paper, liquid waste treatment and also isothermal DNA amplification reaction in six microchambers.

- Develop and fabricate a 3D design concept for silicone rubber blister that can be integrated with the microfluidic cartridge. Then afterwards ascertain is efficacy by a fluid flow experimentation with coloured dye.

1.4 SUMMARY OF METHODOLOGY

To tackle the creative design process leading to fabrication and experimentation, two fundamental design processes can be used to illustrate the steps taken to developed a valid prototype model. As shown in Figure 1.5, process A involves three subsidiary steps that are used to conceptualise intricate parts that make up the internal fluid flow network of the microfluidic chip. These components include microchannels, interface ports (inlet and outlet), passive valve, multiplexer and reaction chambers.

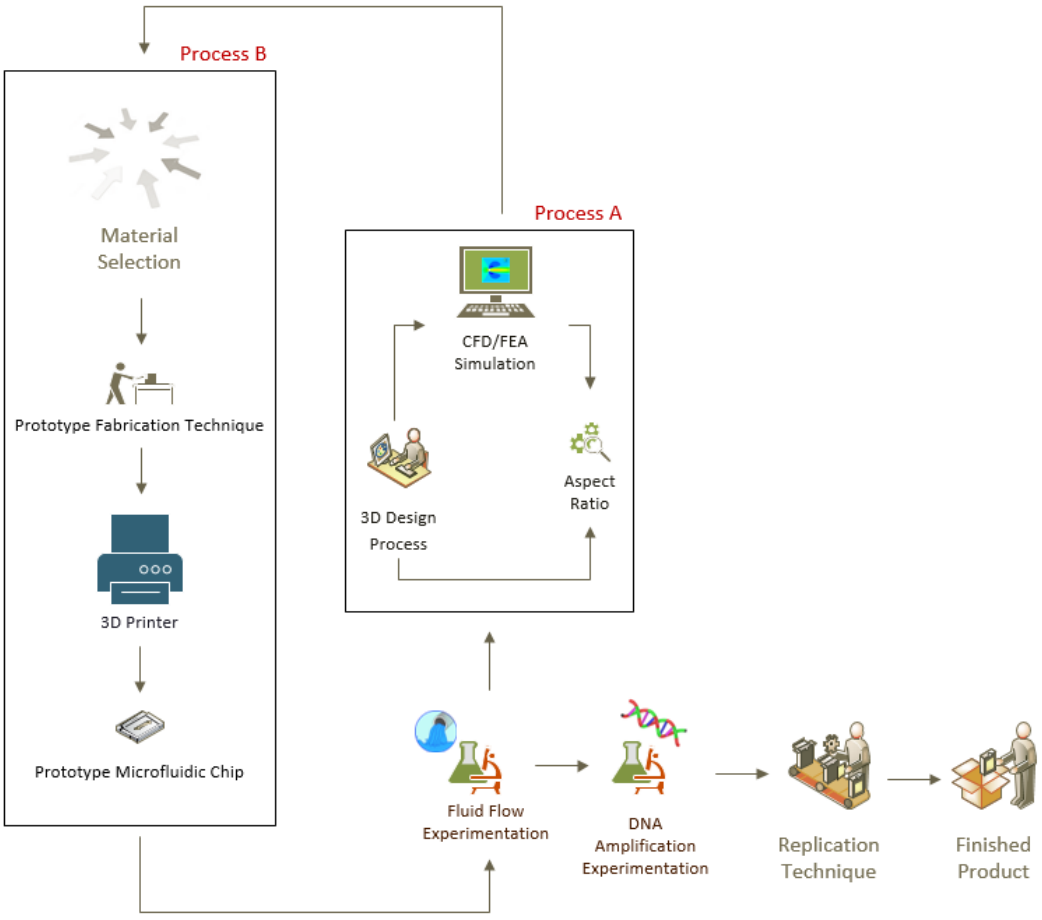

Figure 1.4. Design flow process for PDMS-glass chip fabrication

First and foremost, of these steps in the 3D design process involves creating 3D models that rely on aspect ratio specificity. The aspect ratio, on the other hand, was heavily dependent on the quality of the 3D printer to be used, which in this case was Viper si2 SLA system. As a result, the range of dimensions used in conceptualising the fluidic elements geometries was determined by the aspect ratio of the fabrication technique output. In other words, without a definite or clear idea of the prevalent and readily accessible means of manufacturing technology, most microfluidic designs will be hard to develop. For example, dimensions, well below 200 µm will require relative high cost and slow turnaround for production. Besides, research projects

need cost within reasonable margins while simultaneously allowing transition flexibility of design alterations from 3D prototype models to fabricated parts. The last step is process A is the CFD simulation that offers a far cheaper means of test the efficacy of the 3D design models without the need for fabrication. Two types of simulation were performed using water as the primary fluid since the anticipated reagents and sample template have densities similar to it. The first simulation was a multiphase flow simulation that was used to observe the behaviour of the primary fluid as it displaces the resident air within the volume domain. Since the chip, internally confined space is not a vacuum. Lastly, single phase simulation was also employed to understand the velocity trajectory and pressure drop within a particular aspect of the chip, especially the multiplexer and passive valve. During the simulation process, the passive valve design that is expected to regulate flow between to fluidic regions on the operational principle of pressure drop was successful. Likewise, the multiplexer which performs the most important function in the flow network by equally distributing the fluid to six designated amplification reaction chambers was also successful.

Process B involves the transformation of the digitised version of the 3d model to a physical entity. This process begins with the material selection process, of which PDMS was found to be the preferred choice. Subsequently, soft lithography a commonly used technique in PDMS microfluidics research was needed to cast the PDMS into the desired shape. As a result a 3D printer which was required to create the mould required for casting. Afterwards, sealing of the PDMS mould became imperative so as to avoid external interference except through the designated port interfaces. The sealing process involved installing the chitosan paper into the central reaction chamber and Sodium Polyacrylate powder into the waste reaction chamber before using the corona plasma corona treater to functionalize both the PDMS mould and glass surfaces to create a strong bond when they pressed against each other.

In-between the process A and process B was the fluidic experimentation process which served as a final validation test of the fully conceived cartridge before the anticipated DNA experiment. Furthermore, any time the design was found wanting the process A to B was restarted and remained in loop still all microfluidic functionalities were confirmed before the approved cartridge was then certified for DNA amplification experiment.

1.5 CONTRIBUTION TO KNOWLEDGE

The following contributions to knowledge are claimed:

- The design of silicone rubber blister with the capability to serve as both a reservoir and fluid pump for a particular volume of liquid. This specific fluid capacity is the anticipated amplification amount required to perform successful isothermal DNA reaction on six micro reaction chambers. Furthermore, the blister possesses the considerable mechanical strength to prevent unnecessary breakage while at the same time flexible enough to deflect appropriately during vigorous compression necessary for fluid pumping.

- The design of microfluidic cartridge capable of performing DNA sample preparation (DNA extraction, purification and elution) on chitosan paper. The configuration of this model entails the use of an embedded chitosan membrane. This membrane was preinstalled in the designated reaction chamber for sample preparation during the fabrication process.

- The design of a multiplexer to connect multiple micro-chambers in a parallel configuration for simultaneous fluid flow distribution. This innovative design provides the means for the cartridge bearing six standalone amplification chambers to receive fluid simultaneously for isothermal DNA amplification reactions.

- Conversion of the RPA DNA amplification experiment performed in a laboratory using microcentrifuge or PCR tubes to microfluidic cartridge based platforms. This conversion procedure is the most important step in point of care diagnostics because it involves the altering the specified liquid solution constituents into different components to achieve similar laboratory results. In this thesis, similar improvisation was made to alter the particular liquid mixture of reagent, proteins, sample DNA and other necessary chemicals so to comply with the designed microfluidic cartridge.

- Provision of a waste treatment within a microfluidic cartridge to prevent hazardous waste contaminating the immediate environment. During DNA purification process, excess or unwanted fluid containing biological substances that may constitute health and safety concerns are required to be contained within the chip before appropriate disposal. As a result, innovative protocols were developed in this thesis to convert the liquid waste to gel by the use of a proprietary substance.

1.6 THESIS STRUCTURE

- Chapter Two: Literature Review

  This section discusses the science, technology and materials needed for designing the POCT microfluidic cartridge and their relationship with one another.

- Chapter Three: Design and Fabrication of Microfluidic Cartridge

  In this section, the 3D prototype design model of the PDMS microfluidic chip was performed. Also, the use of multiphase and single-phase flow simulation analysis is utilised to affirm the design concept before fabrication. The overall fabrication process involves manufacturing a PDMS based microfluidics chip from a 3D printed mould design by the use of soft lithography and plasma bonding technique to seal the cartridge.

- Chapter Four: Fluid Flow Experimentation

  In this chapter, a preliminary test using liquid dyes as a substitute for reagents was carried in anticipation of the DNA amplification experiment to verify the efficacy of the chip design and functionalities in comparison to CFD results.

- Chapter Five: DNA Amplification Experimentation

  In this chapter, a DNA sample Preparation and amplification experiment was performed on the chitosan bearing microfluidic cartridge. The process involved the use of a proprietary product called TwistAmp basic kit from TwistDx company based in England. This basic kit comprises of all enzymes and reagents required to perform a positive and negative DNA amplification experiments on the PDMS-glass cartridge. Afterwards, DNA Agarose Gel Electrophoresis was employed as the endpoint method to assess the amplification success.

- Chapter Six: On-chip Blister Design and Fabrication

  The highlights of this section include the 3D design process, material evaluation process and fabrication technique utilised to produce a blister which would serve as a passive pump and liquid storage device on the microfluidic chip. Also, discussed here were the specific protocols used, in other to integrate blister into the PDMS cartridge mould. Also, fluid flow experimentation involving a blister filled with liquid dye was expected to dispense liquid into the microchannels of the PDMS cartridge was also performed in this section as a preliminary DNA experiment.

- Chapter Seven: Conclusion and Recommendations

  An overview of the characteristics of a DNA hybrid cartridge consisting of glass and PDMS was discussed and analysed. Furthermore, the chapter also gave an overview of the successful design process used to achieve a functional PDMS-glass cartridge for DNA amplification while also affirming the design concepts and empirical results.

1.7 PAPERS PUBLISHED

- **2016-** Ereku L, Mackay R, Balachandran W, Ajayi K. Review of Commercially Available Microfluidic Materials and Fabricating Techniques for Point of Care Testing. Sensors and Transducers. 2016: 202(7):1-24
  (Appendix A)

- **2014**- L.T. Ereku, R.E. Mackay, W. Balachandran, K. Ajayi. Continuous Flow Pressure Driven Microfluidic Techniques for Point of Care Testing, Sensors and Transducers, 170 (5); 1-18
  (Appendix B)

- Mackay R.E., Craw P., Manoharanehru B., Chaychian S., Ereku T., Sivanesan T., Ahern J. Hudson C., Baker M., Kremer J., Naveenathayalan A., Powell Z., Evans R., Manivannan N., Balachandran W. A Molecular Diagnostic Point of Care Platform for Rapid Detection of Sexually Transmitted Infections. Sensors in Medicine, London, Mar 2014

- Recombinase Polymerase Amplification Using a Multiplexing Cartridge for Low Cost Point of Care Diagnostics. Luck T. Ereku, Angel Naveenathayalan, Ruth Mackay, Branavan Nehru, Wamadeva Balachandran,

- Design and Fabrication of a PDMS microfluidic Multiplexing Cartridge

  Luck T. Ereku, Angel Naveenathayalan, Ruth Mackay, Wamadeva Balachandran,

- Design of Silicone Elastomeric Blister for Microfluidic Multiplexer Cartridge

  Luck T. Ereku, Angel Naveenathayalan, Ruth Mackay, Wamadeva Balachandran

2. LITERATURE REVIEW

2.1 INTRODUCTION

This section gives an introduction and detailed description of the science, technology and material properties needed for the development of the POCT Microfluidics cartridges. As anticipated, the sample fluids or reagent utilised in this device is expected to be in a continuous phase. Thus, the science discussed here is constrained to laminar flow mechanics, since it's a better micro hydrodynamic representation of a pressure driven flow within the cartridge when observed experimentally or simulated in 3D. Likewise, the effect of viscosity, surface tension and capillarity on microchannels are brought into considerations for both single-phase and multiphase continuous flows. On the other hand, the material properties analysis which is a prerequisite requirement for chip fabrication was carried out over a wide range of available materials and their unique physical and chemical properties suitability in microfluidic applications. Also, the advantages and drawbacks of various commercially available microfabrication techniques were also discussed.

2.2 MICROHYDRODYNAMICS

Since most microfluidic systems operate at low Reynolds numbers, the physical properties of fluids at the microscale can differ from the generic behaviour of macro-scale quantities in factors such as surface tension, energy dissipation, and fluidic resistance. The field of micro-hydrodynamics analyses how these properties can change, and how they can be worked around, or exploited for specific design requirements. In microfluidic systems, fluid movement can be categorised under two means of fluid transportation; which are a continuous flow and discrete flow.

Continuous flow is d¦efined by the incessant and seamless flow of fluid/fluids (miscible or immiscible) which are composed of molecules that collide with one another within a confined boundary (microfabricated channels). Moreover, these molecules are assumed to obey the continuum assumption [51], which considers fluid being made up of particles in a continuous phase rather than in a discrete phase. As a result, physical properties such as pressure, density, temperature, and velocity of infinitesimally small fluid particles are assumed to vary continuously concerning one another [52]. Most pressure-driven POCT devices to operate under these means of liquid transportation. Some examples of pressure driven flow which makes use of

micropumps, plungers or mechanical blisters utilise this means of fluid transportation. Furthermore, non-mechanical techniques such as sound waves or a combination of capillary forces with electrokinetic mechanisms (e.g. electro-osmotic flow) [53], [54]also utilise this means.

On the other hand, discrete microfluidics commonly known as droplet microfluidics utilises minute or discrete volume of fluid in the form of droplets contained within an immiscible continuous phase as means of transportation [55], [56]. The small volumes of fluid are isolated from each other in continuous motion offer the opportunity of novel solutions to today's biomedical engineering challenges for innovative POCT protocols and therapeutics. For instance, droplets allow a significant reduction in sample volumes to be analysed, leading to the corresponding reduction in cost. Furthermore, compartmentalization in droplets improves assay sensitivity by increasing the effective concentration of rare species and reducing the time needed to reach the detection threshold [57], [58]. In addition, the platform dimensional scaling advantage encourages controlled and rapid mixing of fluids in the droplet reactors, resulting in significantly reduced reaction time, accurate generation and repeatability of droplet operations. Droplet microfluidics incorporates two distinct methods which are digital microfluidics and segmented flow microfluidics [59], [60].

One of the important properties shared by both types of fluid flow is viscosity (μ); which can be described as the ratio of shear stress to velocity gradient. Viscosity describes the resistance of a liquid to any deformation caused by either external body immersed in fluid or between different layers [61]. In addition, the higher surface to volume ratio, higher mass heat transfer ratio, and low Reynolds number are other characteristic properties of fluids in microsystems.

Another major feature endemic at the micro-scale is the flow disposition which is practically defined as laminar flow. Laminar flow or steady flow occurs when fluids move in parallel layers, exhibiting no disorder between their repetitive layers [62], [63]. In fluid dynamics, the velocity of flow varies from zero at the walls to a maximum along the centre line with the flow regime characterised by high momentum diffusion and low momentum convection since there are no cross currents perpendicular to the direction of flow, nor eddies [64], [65]. At low velocities, the particles of these fluids are very organised, enabling them to move in straight lines parallel to the pipe walls which in turn inhibit lateral mixing as a result of the adjacent layers sliding past each other effortlessly. When taking into consideration scientific and empirical observations of fluid flows in microchannels of a microfluidic device, Reynolds number of much less than one is observed [64]–[66]. This type of flow is also known as creeping motion or Stokes flow, and it is an extreme case of laminar flow where viscous (friction) effects are much greater than inertial forces [67]–[69],. This relationship is defined as Reynolds number as a dimensionless parameter and is given by the ratio of inertial force (ρV^2L^2) to viscous force (μVL) as follows.

$$Re = \frac{inertial\ force}{viscous\ force} = \frac{\rho V^2 L^2}{\mu VL} = \frac{VL}{v} \qquad (2.1)$$

$$v = \frac{\mu}{p}\left(\frac{m^2}{s}\right)$$

Where, V is the characteristic velocity of the fluid, L is the characteristic length of the geometry, ρ is the fluid density, μ is the fluid dynamic viscosity, and v is the kinematic viscosity of the fluid.

In microfluidics, it is usually assumed no gravity, incompressibility, and dominant viscous forces. The flow of fluid through a microfluidic channel can be characterized by the Reynolds number, similar to equation 2.1:

$$Re = \frac{LV_{avg}\rho}{\mu} \qquad (2.2)$$

Where, V_{avg} is the average velocity of the flow, L is the most relevant length scale, ρ is the fluid density and μ is the fluid dynamic viscosity.

The Velocity of fluid flow through a control volume can be described by the complete Navier-Stokes (N-S) equations. These equations can be derived from the principles of conservation of mass, momentum and energy. Navier-stokes equations are a non-linear set of differential equations which explain the motion of fluid in general. This equation is defined by applying Newton's second law to a fluid motion by the assumption of continuum fluid and small fluid velocity compared to the speed of light. The general form of these equations has no solution and is used in computational fluid dynamics. Also, the equations do not dictate position but rather a velocity. A solution of the Navier–Stokes (N-S) equations is called a velocity field or flow field, which is a description of the velocity of the fluid at a given point in space and time. Once the velocity field is solved for, other quantities of interest (such as flow rate or drag force) may be found. The complete equation is shown below [70]:

$$\rho\left[\frac{\partial v}{\partial t} + v \cdot \nabla v\right] = -\nabla p + \nabla \mathbb{T} + \mathrm{f} \qquad (2.3)$$

Where v is the flow velocity, ρ is the fluid density, p is the pressure, is the (deviatoric) stress tensor, and f represents body forces (per unit volume) acting on the fluid and ∇ is the Del operator.

The general form of N-S equations can be simplified by the assumption of incompressible flow which is common in microfluidics [71]. This assumption simplifies the form of N-S equations and can be written as the following:

$$\rho\left[\frac{\partial v}{\partial t} + v \cdot \nabla v\right] = f_{pressure} + f_{friction} + f_{volume} \qquad (2.4)$$

Where, $\partial v/\partial t$ is the unsteady acceleration, $v \cdot \nabla v$ is the convective acceleration, ρ is the density, $_{\text{pressure}}$ $(-\nabla p)$ is the pressure gradient, $_{\text{friction}}$ $(\mu \nabla^2 v)$ is the viscosity of the fluid, $_{\text{volume}}$ $(-\rho g)$ is the body force of fluid.

In microfluidics, the fluid flow is mostly described by Poisson equation. This equation can be derived from N-S equations by applying boundary conditions in micro-channels. When solid walls bound a fluid, the fluid velocity is assumed zero at the liquid-solid interface. This process is as a result of molecular interactions between two phases which force the fluid molecules to seek the momentum and energy equilibrium of solid surface. This phenomenon is called no-slip condition and will be used as a boundary condition at the interface between the fluid and solid surfaces. Therefore the simplification of N-S applies the following conditions for two-dimensional flows [71], [72]:

- No slip at the wall
- Infinitesimal gravity, $\rho g = 0$
- Convection effect is negligible, $v \cdot \nabla = 0$
- Laminar flow (steady flow), $\partial v/\partial t = 0$

Therefore, Poisson equation for a pressure driven flow is given as:

$-f_{pressure}$ ($-\nabla p$) is the pressure gradient = $_{friction}$ ($\mu \nabla^2 v$) is the viscosity of fluid

$$\nabla p = \mu \nabla^2 v \tag{2.5}$$

The two-dimensional Cartesian co-ordinates of equation 2.42 are expressed as [71];

$$\frac{dp}{dx} = \mu \frac{\partial^2 u}{\partial y^2} \tag{2.6}$$

2.2.1 VISCOSITY EFFECT

In general, the viscosity is the quantity that describes a fluid's resistance to flow. Fluids resist the relative motion of immersed objects through or besides them as well as the motion of layers with differing velocities within them in any flow [73]–[75]. These layers move at different velocities, and the fluid's viscosity arises from the shear stress between the layers that ultimately oppose any applied force. Viscosity is important because it acts as an opposing force in the mixing of two liquids [74]. The viscosity of fluid might change by changing the temperature or pressure but if the viscosity of a fluid is constant at all shear rates at constant temperature and pressure; the fluid is known as Newtonian. The relationship between the shear stress and viscosity and velocity in the Newtonian fluid can be described as follows [76]:

$$\tau = \mu \frac{\partial u}{\partial y} \tag{2.7}$$

In which, $\boldsymbol{\tau}$ is the shear stress; μ is the fluid dynamic viscosity coefficient (du/dy) is velocity gradient.

The viscosities of most liquids (Newtonian) decrease with increasing temperature, and vice versa [76]. As the temperature increases, the average velocity of the molecules in liquid increases and the amount of time they expend "in contact" with their nearest neighbors decreases. Thus, as temperature increases, the average intermolecular forces decrease [74], [77]. Another factor is pressure, the viscosity is normally independent of pressure, but liquids under extreme pressure often experience an increase in viscosity. Since liquids are normally incompressible, an increase in pressure doesn't result in bringing the molecules significantly closer together i.e. increase in pressure doesn't register a significant change in viscosity of an incompressible fluid [61], [71].

In the case of non-Newtonian fluids, the viscosity is a function of mechanical variables such as shear stress or time. These fluids are also directly affected by temperature and are classified as shear-thinning and shear-thickening [76]. Materials that thicken when worked on or agitated are called shear-thickening fluids because they experience a decrease in viscosity under shear stress are described as shear-thinning fluids. Blood falls into this category and is also known as a Bingham plastic [76] because it requires a threshold shear stress for it to make a transition from a high viscosity to a low viscosity fluid. The blood fluid must reach a shear rate of about 100 (1/sec) to be assumed Newtonian and after this shear rate is reached the viscosity is about five times as great as the viscosity of water [78]. Urine at room temperature can be categorized as a Newtonian fluid because it contains about 95% of water [78].

2.2.2 SURFACE TENSION EFFECT AND CAPILLARITY PHENOMENON

The cohesive forces between the liquid molecules are responsible for this phenomenon of surface tension that allows the surface of a liquid to resist an external force as a result of imbalance molecular attractive forces at

the interface [70], [79]. In a bulk solution, each molecule is pulled equally in every direction by neighbouring liquid molecules, resulting in a net force of zero. The molecules at the surface do not have other molecules on all sides of them and, therefore, are pulled inwards. Therefore creating some internal pressure and forces on the liquid surfaces that contact to the minimal area available [80].

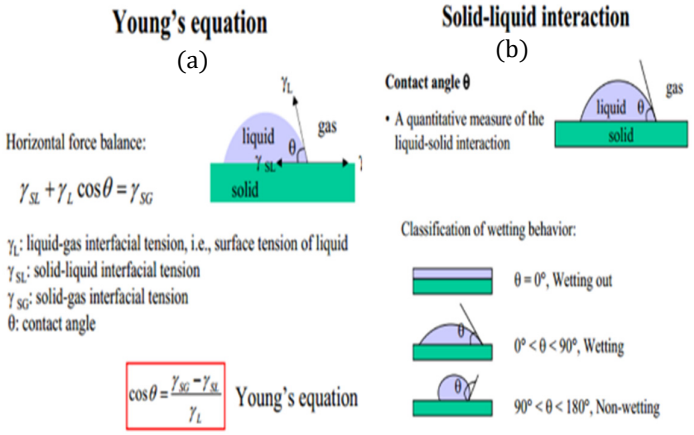

Figure 2.1. Young equation depiction of solid-liquid interaction in ambience air, this schematic shows the surface tension forces at the contact line. (a) Liquid drops placed on a flat surface try to adopt spherical cap shape in other to minimize the surface energy. (b) The surface wettability in relationship to liquid-surface angle [79].

The surface tension depicted in Figure 2.1 is the excess energy per unit area of the fluid surface when it is in contact with another material) or phase (solid or fluid) [81], which in turn largely determines the spherical shape of the fluid droplet placed on a solid surface. Young's equation shows a liquid droplet in contact with a solid surface and ambient air (Figure 2.1a). The equilibrium forces due to the surface tensions at the liquid-gas (γ), solid-liquid (γ_{SL}) and solid-gas (γ_{SG}) interface dictate the contact angle, $\theta_Y = (\gamma_{SG} - \gamma_{SL})/\gamma$ of the liquid on the solid [79]. On the other hand, Figure2.1b describes the wettability of the internal surface that is a major criterion in micro-hydrodynamics for controlling the flow. This phenomenon is solely based on the contact angle of water on the solid surface; the surface can either be classified as hydrophilic (water-loving, $\theta_Y < 90^o$) or hydrophobic (water hating, $\theta_Y > 90^o$) [82]. One of the major side effects of high surface tension in fluid flowing through a conduit is that is friction resistance between the solid-fluid interfaces. Due to this surface tension, a stream of fluid splits to form several small droplets to minimize the total surface energy [79] as a result the surface tension tend to zero, this is known as "Rayleigh-Plateau instability". In general, increasing the temperature of liquid will decrease its surface tension. Likewise, Surfactants can also be used to lower the surface tension of a liquid [75], [83]. Besides, this procedure can also be applied to interfacial tension between two liquids or that between a liquid and gas.

In micro-scaling, surface tension at the interface between the liquid surface and the microchannel surface is significant to the design, with dimensions on the order of microns, the lengths liquids will travel easily using the capillary force [82]. At a microscopic scale, with gravitational effects minimal, the surface-to-volume ratio increases due to the exceedingly small volumes employed. This characteristic improves the surface tension effect that shares a direct relationship with capillarity [81], [82].

The phenomenon known as capillary action/capillarity is the ability of a liquid to flow against gravity, inertia or flow spontaneously without the aid of an external force through a narrow space. This enclosure can be thin tubes, microchannels and porous materials such as paper or non-porous materials such as liquefied carbon fibre [76], [82]. In addition, it can occur due to inter-molecular attractive forces between the liquid and solid surrounding surfaces. Subsequently, at the micro-scale the gravity effect is infinitesimal, so the diameter of the tube or cross section of a channel has to suffice for the capillary process to be sustainable. So since the energy stored in surface tension is equivalent to the multiplication of the surface tension and surface area; therefore reduction in conduit surface area of any microfluidic system will naturally minimize surface energy that significantly eases fluid flow [81].

Putting this phenomenon in perspective with regards to microfluidics that deal with very narrow channels with liquids under infinitesimal gravitation and high viscous forces with amplified fluid-solid surface tension; capillarity consequently behaves as a medium through which fluid flow can be alleviated. Similarly, fluid flow velocity can also be controlled by altering the capillary surface energy. Capillarity, therefore, plays a major role in aiding fluid flow within the LOAC platform by requiring less external pressure or energy input needed to actuate the flow [71], [75].

2.2.3 PRESSURE DRIVEN FLOW

This phenomenon is also known as Poiseuille flow, and it exhibits a parabolic flow profile which is characterized by the liquid movement as a result of the pressure gradient between two or multiple points within the system. The liquid control is mostly constrained to a one-dimensional liquid flow in a straight, curved or circular microchannel (Figure 2.2) [71], [76], [77]. The nature of process entails the flow of fluid from a region of high pressure to a region of low pressure.

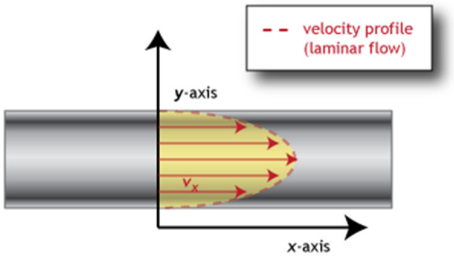

Figure 2.2. Schematic representation of the parabolic path way of liquid in a cylindrical conduit [84]

Fluid operations carried out on this platform are either capillary driven or linearly actuated. Capillary driven flow involves the high dependence on capillary forces which in turn rely on the channel geometry design (i.e. width, length, and height) and surface properties (hydrophobic or hydrophilic) [82]. On the other hand, linear actuated devices propel flow by mechanical displacement of liquid through the application of force. For instance, fluid stored in a reagent reservoir can be propelled by the aid of a plunger into a micro-conduit of negative pressure (Figure 2.3). The common denominator that makes all these methods of fluid actuation significant is the presence of the generated pressure gradient. Furthermore, novel methods such as electro-osmotic force can also be used to induce pressure driven flow through the insertion of in-channel electrodes of relatively small electric potentials [85], [86].

Simplified Navier-Stokes equations for pressure driven micro-flows characterized by the significantly reduced Reynolds number ($Re << 1$)

$$0 = -\nabla p + \eta \nabla^2 \vec{u} \qquad 2.8$$

Where, p is the pressure, u is the fluid velocity, and η is the dynamic viscosity of the liquid.

The Hagen-Poiseuille equation describes the relation between pressure and flow rate, In the case of cylindrical microchannel experiencing a parabolic flow is given below [87]:

$$\Delta P = \frac{8\eta LQ}{\pi r^4} \qquad 2.9$$

Where ΔP is, the pressure drop between the two ends of the cylindrical conduit, L is the total length of the channel, r is the radius, Q is the volumetric flow rate of the channel and v is the average flow velocity across the section.

In the case of planar channels with height, h, which is much less than the width w ($h << w$,) the solution of the Poiseuille flow gives [88], [89]:

$$\Delta P = \frac{12\eta LQ}{wh^3\left(1-\frac{h}{w}\left(\frac{192}{\pi^5}\sum_{n=1,3,5}^{\infty}\frac{1}{n^5}tanh\left(\frac{n\pi w}{2h}\right)\right)\right)} \qquad 2.10$$

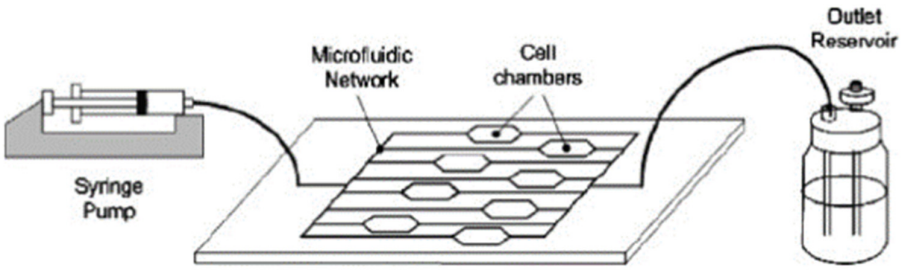

Figure 2.3. Schematic representation of external syringe pump used to supply typical pressure-driven microfluidic platform for living cell analysis [90].

2.2.4 ELECTRIC CIRCUIT ANALOGY CONCEPT OF FLUIDIC RESISTANCE

The concept of Hagen-Poiseuille equation rewritten as Ohm's law clearly depicts the average flow rate of a liquid within a microfluidic channel as proportional to the pressure gradient imposed on both ends of the channel (Figure 2.4) [91], [92].

$$\Delta P = R_H Q \qquad 2.11$$

The fluidic resistance R_H will depend on the geometry of the cross section (e.g. cylindrical and planar). For instance, equation 2.9 and equation 2.10 are the cylindrical and planar Hagen-Poiseuille circuit analogy representation of equation 2.12 and 2.13

$$R_H = \frac{8\eta L}{\pi r^4} = \frac{\Delta P}{Q} \qquad 2.12$$

$$R_H = \frac{12\eta L}{wh^3\left(1-\frac{h}{w}\left(\frac{192}{\pi^5}\sum_{n=1,3,5}^{\infty}\frac{1}{n^5}tanh\left(\frac{n\pi w}{2h}\right)\right)\right)} \quad 2.13$$

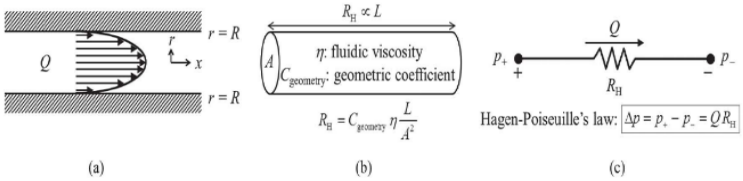

Figure 2.4. The graphical illustration of physical similarities between the flow of fluid and flow of electricity. (a) Poiseuille flows in a circular channel. (b) The hydraulic resistance of the circular channel $C_{geometry} = 8\pi$ for the circular channel). (c) Equivalent circuit symbol of a fluidic resistor for the hydraulic resistance and Hagen–Poiseuille's law analogous to a resistor for the electric resistance and Ohm's law [92].

This fluidic resistance is also known as hydraulic resistance and can be used to analyze the flow or pressure relationship within complex microfluidic networks. The validity of this concept relies on some basic assumptions. First of all, the flow is considered viscous, incompressible and homogeneous with no presence of convective mixing. Secondly, the steady-state and laminar flow nature of the flow exhibits a parabolic shape profile. Finally, the flow is considered to have a uniform pressure gradient across the microchannel length. By this means estimation of the laminar flow within circular or non-circular channels that are either infinite or finite in length can be with simple mathematical calculation. For instance, channels connected in series will be resolved by using "$R_H=R_{H1}+R_{H2}+R_{H3}+...R_{Hn}$" which will provide the estimated total fluidic resistance of the network. Whereas parallel channels network will have a total resistance of "$1/R_H=1/R_{H1}+1/R_{H2}+1/R_{H3}+...1/R_{Hn}$" [92].

There is an extensive range of diverse applications of this pressure driven systems in the microfluidic platforms. These include the use of plungers, syringes, micropumps (peristaltic and piezo-electric), gas expansion principles, pneumatic displacement of membranes, blisters, etc. The advantage they share is the simplicity in design and fabrication processes. They are also economical and affordable but suffer the disadvantages of reproducibility and limited ability to support very complicated microfluidic processes [93].

2.2.5 MULTIPHASE FLOW

This type of flow is mostly attributed to microscale dimensions involving multiple fluids existing in their individual flow fields or a shared flow field. Each fluid in this flow is separated by a discernible interface, unlike multicomponent flow that has the fluids mixed

at a molecular level and shares the same mean velocity, pressure, and temperature fields [94], [95]. Multiphase flow is a more complicated condition because each fluid component may have different physical and chemical properties in the same or different phases (gas, liquid or solid). Good examples are cases involving liquid-gas flow that usually have the liquid as the primary phase which may be continuous, while the gas as the secondary phase which may be dispersed (air bubbles) or continuous.

The distinct models used in computational fluid dynamics simulation are [96]:

- Lagrangian dispersed phase model (DPM)
- Eulerian-Eulerian continuous phase model (CPM)
- Eulerian Granular model
- Volume of fluid (VOF) model
- Algebraic Slip Mixture Model (ASMM)
- Cavitation Model

Similarly, flow regimes are also very significant in determining flow characteristics of each fluid component in relation to their initial volume fraction. Since each fluid is expected to be Immiscible fluids divided by a clearly-defined interface they, therefore, have to occupy a finite space about one another in the fluid domain. Although this is only expected at before the computation solver starts analysing their projected movement in space and time.
Figure 2.5, is a good example of initial volume fraction state.

Below is the formula for determining volume fraction in a fluid domain:

$$Volume\ Fraction\ of\ a\ Phase\ = \frac{volume\ of\ the\ Phase\ in\ a\ cell/domain}{volume\ of\ cell/domain} \qquad 2.13$$

The various types of flow regime present available are:

- Multiphase flow can be classified by the following regimes:
- Bubbly flow: Discrete gaseous or fluid bubbles in a continuous fluid
- Droplet flow: Discrete fluid droplets in a continuous gas
- Particle-laden flow: Discrete solid particles in a continuous fluid
- Slug flow: Large bubbles (nearly filling cross-section) in a continuous fluid
- Annular flow: Continuous fluid along walls, gas in center
- Stratified/free-surface flow: Immiscible fluids separated by a clearly-defined interface

In this thesis, Volume of fluid (VOF) model multiphase modelling and Stratified/free-surface flow regimes are given preference because they both fit suitably into the simulation and experimental analysis of the POCT chip.

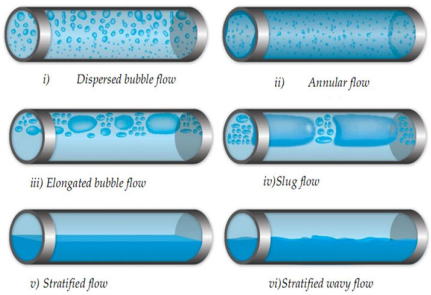

Figure 2.5. Illustration of Gas-liquid flow regimes in horizontal pipes [94].

2.1.5.1 VOLUME OF FLUID MODEL

This computational method is most suitable for flow where multiple Immiscible fluids have a distinctly defined interface and phase regardless of shared or individual velocity. For example, stratified flows such as; liquid-liquid (oil-water), (Liquid-Gas (oil/water-air) or Liquid-Liquid-Gas (oil-water-air) is clearly illustrated by Figure 2.6. The relative motion of the interface is tracked in the computational domain by the solver as the fluids against each in the domain. Given that most liquids are infinitesimally compressible in comparison to gases Steady or transient tracking of any liquid-gas interface is achieved by the specific numerical interfacial surface tension. For instance, air-water interfacial tension is 0.07275n/m.

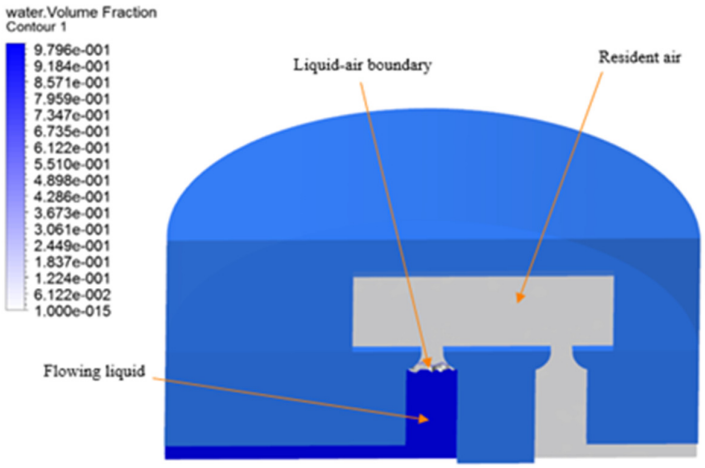

Figure 2.6. Illustration of volume fraction of air-water.

Below is the mathematical assumption used by Ansys fluent [94],[95] for fluid volume occupation in a computational domain at an initial state and specific phase. The formal also defines the interface boundary between the fluids in the same or different phase.

- For volume fraction of k^{th} fluid, three conditions are possible:

  i. $\varepsilon_k = 0$ if the cell is empty (of the kth fluid)
  ii. $\varepsilon_k = 1$ if the cell is full (of the kth fluid)
  iii. $0 < \varepsilon_k < 1$ if cell contains the interface between the fluids

Simulation and tracking of the relative motion of the interface(s) between phases are determined by solution of a volume fraction continuity equation for each phase [96]:

$$\frac{\partial \varepsilon_k}{\partial t} + u_j \frac{\partial \varepsilon_k}{\partial x_i} = S_{\varepsilon_k} \qquad 2.14$$

The equation below is used to solve one set of momentum equations for all fluids 32:

$$\frac{\partial (\rho u_j)}{\partial t} + \frac{\partial (\rho u_i \rho u_j)}{\partial x_i} = -\frac{\partial \rho}{\partial x_j} + \frac{\partial}{\partial x_i} \mu \left(\frac{\partial u_i}{\partial x_j} + \frac{\partial u_j}{\partial x_i} \right) + \rho g_j + F_j \qquad 2.15$$

2.3 MICROFLUIDIC LARGE SCALE INTEGRATION

Microfluidic large scale integration shares semblance to an electronic circuit that has diverse patterns of wiring circuitry responsible for taking current from one point to another [98]–[100]. However, this is a microfluidic tool that entails microfluidic channel networks integrated with thousands of micromechanical valves and hundreds of individually accessible reservoirs [101] organised systematically to carry out complex POCT, medical or biochemical applications. These plumbing networks have microvalves that open or close on the pneumatic pressure applied due to elastic membranes that are situated between a liquid-guiding layer and pneumatic control-channels [102]. The overall configuration involves combining several microvalves more multifaceted units like micropumps, mixers, multiplexers, etc. having hundreds of units on one single chip.

2.3.1 MICROFLUIDIC MULTIPLEXER

The fluidic multiplexer is a key component of large microfluidic scale integration networks because it contains a blended arrangement of binary valves in patterns that significantly allow specific addressing of a large number of independent chambers. It also increases the processing power of fluidic network exponentially via bifurcated network of microchannels to specific outlets and enabling complex fluid manipulations with a minimal number of controlled inputs [103].

They are usually designed to be connected to independent microchamber where similar or different biochemical reactions can be initiated. Generally, they can be categorised into two modes of operations. These are either non-sequential or programmable sequential flow functionalities. A sequential fluidic network (is mostly an active device that contains a blended arrangement of active valves in patterns that significantly allow specific addressing of a large number of independent chambers or outlet. Thus, for their highly precise and programmable operations, they offer more cumbersome and complex means of fluidic operation. Likewise, dependency on expensive electro-mechanical devices such as syringe pump, active valves and other external devices are mostly certain. On the other hand, non-sequential mechanism offers pre-planned or random pattern of flow within the bifurcated channels. For what non-sequential multiplexer lack in precision or flexible mode of operation, it makes up in less dependency in external or active microfluidic devices. As a result, they offer a more simplified and low-cost solution for liquid distribution.

2.3.2 MICROMIXER

Micromixing in microfluidic devices is achieved with the assistance of laminar flow, confined space constraint and significant small aspect ratio of microchannel which are endemic factors in miniaturization. In addition the significant small length advantage drastically increases the effect of diffusion and advection necessary for mixing to occur [104]. Correspondingly the channel geometries of micromixers are also designed to decrease the mixing path and increase the contact surface area [104], [107]. Induced mixing at the microscale is classified as being passive or active. Passive mixers depend solely on pumping energy, while active mixers make use of an external energy source to achieve mixing.

Active mixing uses external excitation to initiate time-dependent perturbations that stir and agitate the streamlines within the fluid for the sole purpose of accelerating the mixing process [108]. They are categorized with respect to the type of external perturbation energy such as acoustic (ultrasonic)-driven [109], thermal-induced [110], pressure field-driven [111], magneto-hydrodynamic [112], electrokinetic [113],

dielectrophoretic [114], [115] or electro-wetting [116]. The prominent advantage age of Active micromixers is better mixer efficiency in comparison to passive mixers [117]. However, they suffer from the inconvenience cumbersome integration encumbrance from their peripheral devices e.g. actuators, which in the end lead to complex and expensive fabrication process [104]. Furthermore, the use of ultrasonic waves, high-temperature gradients lead to extensive damage biological fluids or matrices. Some groups have used silica particles impregnated with Fe_3O_4 to actively mix fluids in a microchamber using a magnetic field from either a permanent rotating magnet or an electromagnet [118]. The Figure below shows the use of 5 mm neodymium-iron-boron magnetic particles (MQP-15-7, Magnequench International, Inc, Singapore) for optimum active mixing performance at an optional upper-frequency limit of 100 Hz [119]. This time-dependent microfluidic operation utilises flow mixing patterns of two dye streams (black and white) in the presence of ciliated structures as depicted Figure 2.8. In general, active mixers are not a popular choice when applying microfluidics to chemical and biological applications [120]. Overall, implementation of such devices in practical applications is limited.

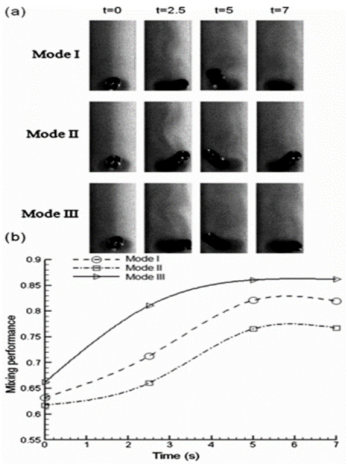

Figure 2.7. Time-dependent flow mixing behaviour in three different beating modes (a) and the 2D graphical corresponding mixing performance (b) [119].

Passive mixing devices depend exclusively on the energy from fluid pumping and judicious use unique channel designs to constrain the flow configuration and therefore increase mixing velocity by reducing the diffusion length and optimising the contact surface area between the different fluids [66], [104]. A good example is the use of a serpentine microchannel structure to coerce the fluid in mixing; as depicted in Figure2.9. Molecular diffusion and chaotic advection are the main reason this mass transport phenomenon are possible. Moreover, the design modifications carried out to aid the influence of the internal laminar flow and mixing time reduction is achieved by splitting the fluid stream using serial or parallel lamination [121], [122]. For instance, hydrodynamically focusing mixing streams [123], injecting bubbles of gas (slug) or liquid (droplet) into the flow [124], [125] or improving chaotic advection using ribs and grooves fabricated on the channel walls [126], [127]. Unlike active mixers, passive mixers are less costly and involve simpler fabrication methods; they are far better to integrate into more complex LOC platforms [104].

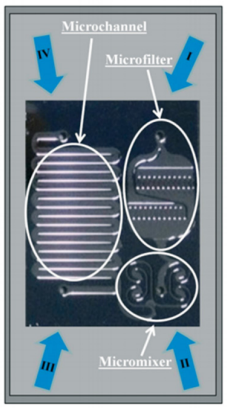

Figure 2.8. A picture of a microfluidic chip consisting of microfilter, micromixer and microchannel. (I–III) Inlets for additional samples, lysis buffer, washing and elution buffer. (IV) Outlet for gathering of the extracted DNA [116].

2.3.3 MICROPUMPS

Since the Reynolds number is typically low in Microsystems, several different means of achieving fluid flow control in microfluidics have been developed. The selection of a pump is mostly biased to mostly moderate performance and low-cost applications, provided that other requirements, like reproducibility and operational stability, can be satisfied.

The majority of these miniaturised pumps come under the classification of electric/electronic(Figure2.10), magnetic, external pressure generators, manual and passive pump systems [128]. Examples of electric/electronic pumps are the piezo actuator, electro-osmotic and peristaltic pumps, while the case of magnetic systems is represented in the form of magnetohydrodynamic pumps and ferrofluidic pump. Piezo-electric, electro-osmotic and peristaltic pumps can be used for complex microfluidic operations and can be fabricated cheaply. The case of piezo-electric pumps which are the most compact pumps can be used for intermediate flow rates (µl) while electro-osmotic pumps due to their simplicity can be easily integrated into a microsystem. These integrated pumps are mostly the preferred choice for contemporary applications which requires multiple and complex fluidic operations, although the pressure produced by fluid motion cannot be necessarily considered independent of scale (miniaturisation).

Commonly used manual pumps are syringes and blisters, the former entails a plunger pushing fluid through a cylindrical cavity while the latter is a fluid enclosed diaphragm that is compressible and deformable as shown in Figure 2.10 Whereas passive pumps makes use of surface tension or capillary effect to drive fluid flow. The Figure 2.11 shows a passive system that utilises a flexible diaphragm and vent hole that is simultaneous blocked when priming the pump, then released to substantially drive fluid at a constant rate through a designated microchannel.

On the other hand, the main benefit of these low-cost syringe pumps and blisters is their ability to initiate flow rate across microchannels irrespective of the fluidic resistance. This is because the fluid traffic is largely dependent on the forced displacement of the plunger or finger blister (Figure 2.2.6) which in this case is sufficient (mechanical advantage). On the other hand, the main drawback of manual pumps is the development of pulsatile flows at low flow rates and lack of adequate flow control required for complicated fluid flow sequence.

Finally, the external pressure generators are mostly mechanical computer-controlled mechanical devices that can excite pressure when connected to the microfluidic chip. They can also exist as hydrostatic generators which depend on gravity to cause pressure difference for fluid flow. Most of these devices are expensive and are not easy to integrate into standalone microfluidic platforms. However, these simple and low-cost pumps generate the required pressure difference needed for fluid flow by varying the altitude of the liquid to air (atmosphere) interface within different reservoirs. This technique makes it impossible for applications in closed fluid flow systems. In all cases, whether the pump is external or integrated, pressure differences within the system are inferior to those produced by external sources.

.

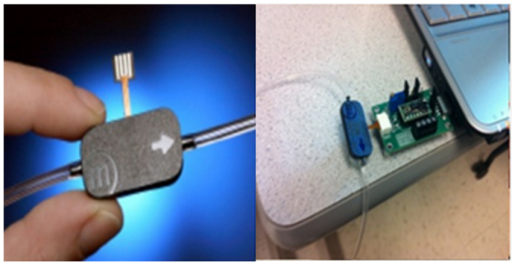

Figure 2.9. Disposable microfluidic pump (Bartels Mikrotechnik mp6 Micropump) capable of pumping both air maximum flow: 18 ml/min (300 Hz) and water maximum flow: 7 ml/min (100 Hz). It is made up of a heat and chemical resistant plastic covering (30 x 15 x 3.8 mm³), weigh 2grams, 2 piezo actuators, 0 - 70 °C operating temperature and an estimated 5000 hours live time [129].

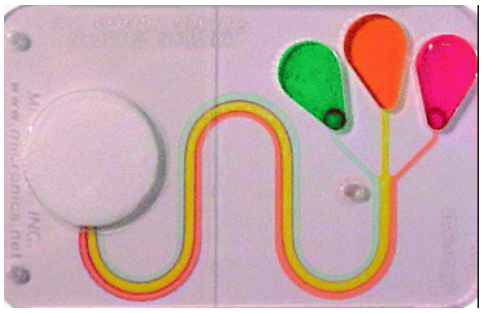

Figure 2.10. Passive pumping mechanism operated by a wicking pad that requires prerequisite priming action by finger bellows [9]

(a) (b)

Figure 2.11. Example of blister packaging in microfluidics. (a) Deposable blister design packs by Accel Biotech, taken from www.accelbiotech.com (b) Minifab 3D prototype blister integrate microfluidic cartridge, Taken from www.minifab.com.au.

2.3.4 MICROWELLS

Also known as multi-well is a flat plate with multiple arrays patterned holes which serve as miniature test tubes [130], [131]. These miniaturised systems when integrating to microfluidic platforms offer precise delivery and manipulation of fluid through microchannels as well as offering a significant reduction in sample and reagent usage (fig.2.13). Micro-well are mostly used in cell sorting [132], culture [133], [134] and trapping [135], [136].

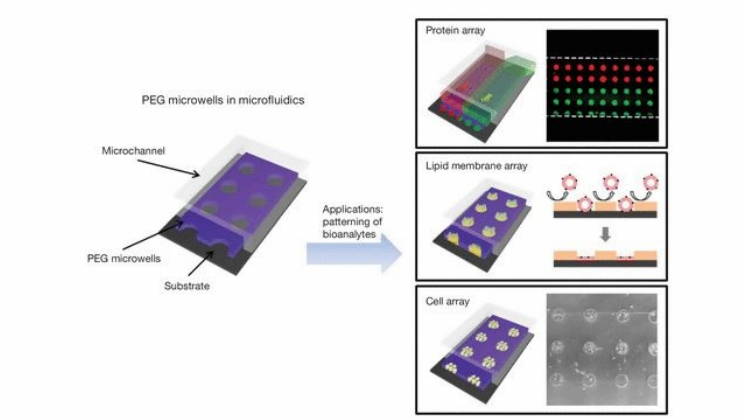

Figure 2.12. A graphical depiction of Poly (ethylene glycol) (PEG) Microwells integrated with PDMS fabricated microchannels for protein, lipid membrane and cell patterning [132].

2.3.5 MICROVALVES

The capacity to manipulate fluid flow using valves is indispensable in many microfluidic applications [137]. There are two types of valves: passive valves that require no energy and active valves that require energy for operation. The type of valve used in a device depends on the amount and type of control needed for the application [128], [138].

Active valves often depend on external physical stimulation or macroscale devices to control the actuation. They are also possessing complicated fabrication process involving three or multiple layers within the multifaceted chip. The principle of operations usually involves a flexible membrane or diaphragm that can have its geometrical shape altered by stimuli to resist or allow fluid flow through a fluidic channel. A good example of the commonly used membranes is PDMS; which relies on pneumatic pressure stimulation mostly driven by air to deflect the valves accordingly [139]–[142]. Likewise, hydrogel-based microvalves [143], [144] are good examples of thermos-responsive valves that can open or close a fluidic line. Some recent designs include an electromagnetically actuated microvalve [145] that require specific range of magnetic field strength for valve control. On the other hand, Passive valves are micro-check valves [146], [147] that far simpler and require fewer fabrication procedures. Although, fig 2.29 show certain similarities both active and passive share; such as the use of a PDMS membrane to restrict flow in one direction. Passive valve principle of operations involves the use of geometrical features to temporarily limiting fluid flow in only one direction as a result of a pressure differential. Although surface tension, fluid viscosity and hydrophobicity all come into play to aid the microvalve effectiveness [148]. The Figure 2.14 shows a fundamental principle of operation of a passive valve

when taking into consideration the geometrical anomalies of an abrupt change in width between two microchannels on a hydrophobic substrate. It's expected that a considerable pressure would be needed to push the fluid across the restriction. This threshold pressure required to break through the passive valve is expressed by the Hagen-Poiseuille expression for a rectangular channel and can be calculated from (2.23) [149]

$$\Delta P_1 = \frac{12L\mu.Q}{wh^3} \qquad 2.23$$

where **L** is the length of the microchannel, **μ** is the viscosity of the fluid, **Q** is the flow rate, **w** is the width, and **h** is the height of the microchannel.

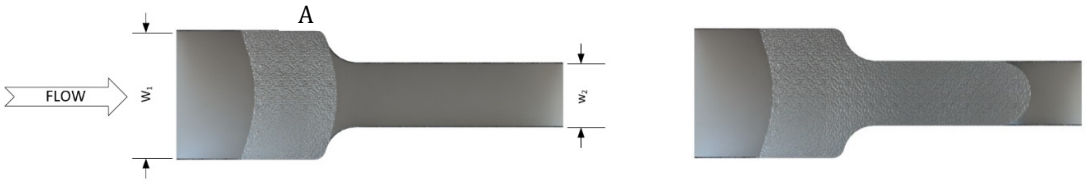

Figure 2.13. A schematic of fluid flow through an abrupt junction passive microvalve.

At point A which indicates the abrupt change in width from a larger section to a smaller section, the fluid flowing across will encounter significant increasing in pressure required to push the further through the narrow path. Besides, if the flow is at a low-velocity, the surface tension will be dominant, thereby increasing the flow resistance. This flow resistance is ephemeral and can be regulated by the pressure differential shown in equation 2.23. In the case of the threshold pressure needed to push the liquid into the narrow channel, when the flow is expected in that direction the method for this geometry can be derived from the principle of virtual work [150]. As expected the inflowing fluid into the narrow channel would experience a higher surface-area-to-volume ratio, resulting in significant increase in the surface energy of the system. Below is the expression for the threshold pressure needed to overcome the passive valve:

$$\Delta P_2 = 2\sigma\, cos(\theta_C)\left[\left(\frac{1}{w_1}+\frac{1}{h_1}\right)-\left(\frac{1}{w_2}+\frac{1}{h_2}\right)\right] \qquad 2.24$$

Where $\mathbf{w_1}$ is the width of inlet channel, $\mathbf{h_1}$ is the channel depth, $\mathbf{h_1}$ is the channel depth, **σ** is the surface tension, $\boldsymbol{\theta_c}$ is the fluid contact angle with the hydrophobic substrate. The most common channel geometry, have equal depth along the microchannel. Hence, setting $\mathbf{h_1}=\mathbf{h_2}$ simplifies equation 2.24 to:

$$\Delta P = 2\sigma\, cos(\theta_C)\left[\left(\frac{1}{w_1}-\frac{1}{w_2}\right)\right] \qquad 2.25$$

When the threshold pressure has been breached, that is representative of the pressure sufficient to overcome the passive valve; the fluid experience a short-lived rapid increase in velocity. From then onwards minimal pressure differential is required to maintain flow through the narrow channel.

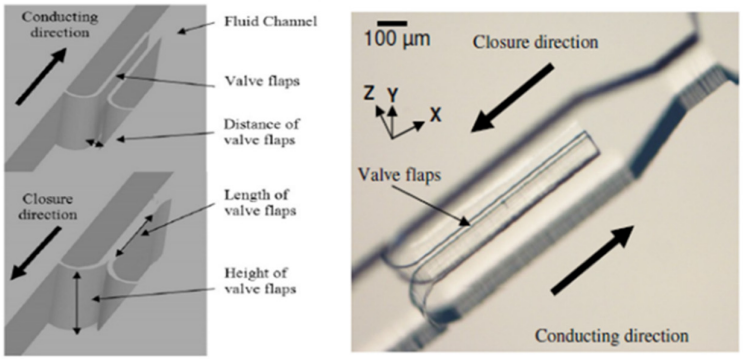

Figure 2.14. The passive design is based on two extruded symmetric flexible PDMS-based cantilever bars which act as valve flaps). The distance of the valve flaps is 20µm, the height of the valve flaps is 70µm and the length of the valve flaps is 300, 550, 700, and 1000µm, respectively [151].

2.3.6 MAGNETO-HYDRODYNAMICS

Magnetohydrodynamics (MHD) involves the interaction between the flow of an electrically conducting fluid and magnetic fields. This interaction between the electric currents and magnetic fields results in an indigenous pressure known as Lorentz body forces on conductive fluids (Figure 2.16) (ferrofluid, a buffer solution or cell media) [152]–[154]. This generated force can then be used to propel, stir and manipulate the fluids; since most applications use buffers and solutions that are often electrically conductive i.e. capable of transmitting electric currents through the solutions [152].

$$F = JxB \qquad 2.25$$

The MHD force is represented by F, while J and B are depicted as the electric current density and magnetic field.

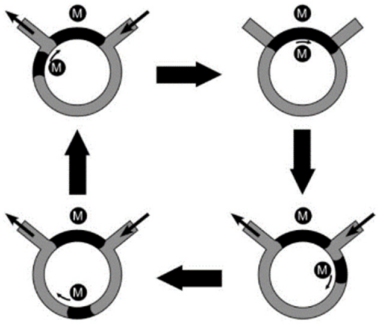

Figure 2.15. The principle operation of a circular ferrofluid pump used to manipulate fluids with ferrofluid plugs in circular microchannels [98].

In the domain of microfluidics, miniature devices are needed to carry out a large number of operations, MHD offers a sophisticated means to manipulate fluid flow in microdevices without a need for mechanical components. For example, many MHD pumps can be integrated on a lab-on-chip device to enable complex fluidic operations that can be done automatically on a single platform as shown in Figure 2.16 [153], [155]. MHD micropumps [156]can be used to pump several conducting liquids especially high conductivity fluids. These fluids are sometimes present in the aqueous solutions used in medical/biological applications; hence MHD pumps are suitable for POCT. Lab-on-chip applications typically require the use of pumps and valves which are usually cumbersome to implement. In an MHD setting, most of the network's channels are equipped with individual electrodes which can be intelligently controlled in the presence of a magnetic field to direct fluid flow along any desired path without a need for mechanical valves [157]. This operation can be used to generate higher flow rates at relatively small electrode potentials, typically below $1V$ [157]. This difference in potential gives MHD an advantage over electroosmosis as liquid flow does not depend on the chemical nature of the capillary surface [158]. One of the major main disadvantages of this technique is that of the generated Lorentz body forces which scale unfavourably as the conduit's dimensions are reduced. Thus, constraining MHD most applications to channel sizes with characteristic dimensions on the order of 100μm or larger [157]. Besides, ionisation effect causes the bubbles generation which greatly inhibits the flow rate. The effect of Bubble generation is minimized by reversing the direction of the applied voltage which can be done by using an alternating current driving mechanism to improve their performance [156].

2.3.7 DIELECTROPHORESIS

Dielectrophoresis (DEP) technique can be used to manipulate, transport, separate and sort diverse categories of bioparticles in microfluidics although DEP is mostly used as a particle separation technique[159]–[161]. DEP is a tool that can be effectively used for nucleic acid hybridization, purification and characterisation in POCT devices [162]. While other areas such as manipulation and transportation still require extensive research. As a good separation technique, it makes use of a polarisation effect that occurs when a non-conductive/dielectric liquid is placed in the presence of a non-uniform electric field [53], [87], [163]–[165]. If the polarisation effect of the particle supersedes that of the suspending medium, the particle movement will tend towards the region of higher field strength (positive DEP), while the reverse case will cause the particle to move towards the low potential area (negative DEP). The particles in question maintain an overall net charge of zero regardless of their original randomly oriented state or polarised state. A time-average DEP force applied on a spherical particle can be represented as the equation below [166], [167]:

$$(f) = [2\pi r^3 \varepsilon_0 \varepsilon_m Re|f_{CM}|\nabla E_{rms}^2] + \left[4\pi r^3\ \varepsilon_0\ \varepsilon_m\ Im|f_{CM}|\ \sum_{x,y,z} E_{rms}^2\ \nabla\varphi\right] \quad 2.26$$

$$f_{DEP} = 2\pi r^3 \varepsilon_0 \varepsilon_m Re|f_{CM}|\nabla E_{rms}^2 \quad 2.26a$$

$$f_{TW-DEP} = 4\pi r^3\ \varepsilon_0\ \varepsilon_m\ Im|f_{CM}|\ \textstyle\sum_{x,y,z} E_{rms}^2\ \nabla\varphi \quad 2.26b$$

Where **r** is the radius of the particle, ε_o= 8.854×10−12 F/m is the permittivity of the vacuum, ε_m is the dielectric constant of the medium, f_{CM} is a complex variable known as Clausius–Mossotti factor, E_{rms} is the root-mean-square value of the applied electric field, and ϕ is the phase component of the electric field. The first part (a) of equation (2.26) can be referred to as 'classical DEP force'. This is the force responsible for pushing the particles towards or away from the regions of strong electric field, i.e. microelectrode tips, on the polarity of Re[f_{CM}]. For example, If Re[$_{fCM}$] > 0 the particle is pushed towards the regions of strong electric field and such a motion is termed positive DEP response. On the other hand, if Re[fCM]<0 the particle is driven away from the regions of strong electric field and exhibits a negative DEP response (Figure 2.17a) [168].

Subsequently, the second part (b) is called 'travelling wave (TW) DEP force'. In this case, the force causes particles to move towards or away from the direction of the wave propagation, according to the polarity of Im (imaginary) [fCM]. For instance, if Im[fCM] > 0 the particle travels towards the smaller phase regions and such a motion is designated a co-field TW response. Alternatively, if Im[fCM] < 0 the particle tends to move towards the larger phase regions and such a motion is called an anti-field TW response (Figure 2.17b).

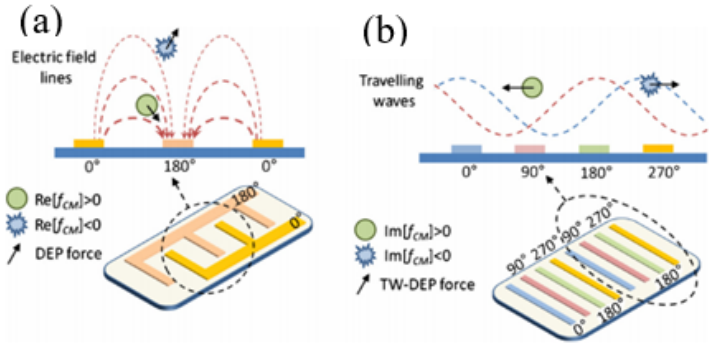

Figure 2.17. Non-uniform electric field can be created by metallic microelectrodes patterned on a substrate: (a) the spatial non-uniformity of electric field magnitude induces classical DEP force, while (a) the spatial non-uniformity of the phase component induces TW-DEP force [121]. Hydraulic resistance and Hagen–Poiseuille's law analogous to a resistor for the electric resistance and Ohm's law [92].

$$f_{CM}(\varepsilon_P^*, \varepsilon_m^*, \omega) = \frac{\varepsilon_P^*(\omega) - \varepsilon_m^*(\omega)}{\varepsilon_P^*(\omega) + 2\varepsilon_m^*(\omega)} \qquad 2.27$$

f_{CM} is the dipolar Clausius-Mosotti factor which is the characterising parameter of a Dielectrophoretic particle [54].

ε_p, ε_m are the complex permittivities of the particle and the medium respectively.

In turn, the complex permittivity is given by:

$$\varepsilon = \varepsilon_r - i\frac{\sigma}{\omega} \qquad 2.28$$

Where ε_r is the dielectric constant; **σ** is the conductivity; **ω** is the frequency of the applied Electric Field, and *i* is $\sqrt{-1}$

Furthermore, since they all exhibit a substantial amount of dielectrophoretic activity in the presence of non-uniform electric fields, the requirement for pre-charged particles in the system is not a prerequisite condition [168]. The strength of the force exerted by this electric field is directly proportional to the electrical properties of the particles' shape, size and operational frequency of the field. As a result, particles with great sensitivity can be manipulated by a designated electric field. Electric field generation requires fabrication of precise electrodes for the particles attraction; likewise, these particles may also require formation of intricate channels for effective separation. It may have certain disadvantages for use with some particles if their response to the field is not strong enough to be detected. In general, dielectrophoresis is a good technique for use in Novel methods like binary separation [169], travelling wave DEP [170] and light-induced DEP [171] have been performed. In the case of light-induced DEP, light-induced dielectrophoretic forces are used to manipulate aqueous droplets immersed in an electrically nonconductive liquid such as oil with a light intensity as low as 400 $\mu W/cm^2$ [171].

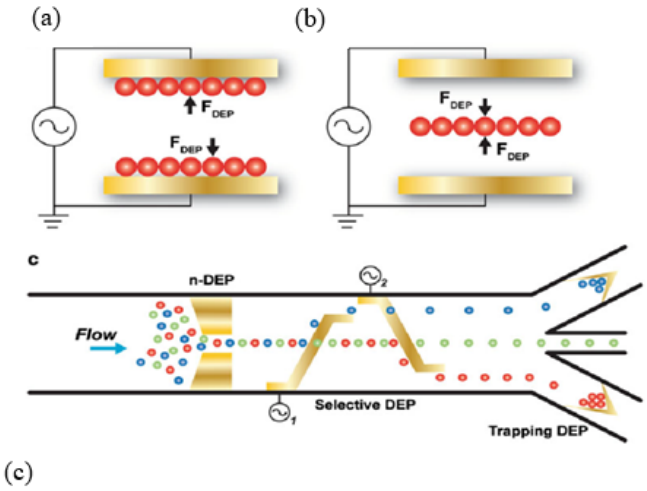

Figure 2.16. Dielectrophoretic (DEP) separations can be positive (pDEP) as shown in (a) or (b) negative (nDEP) which affects where cells are positioned within a field. (c): gives a basic depiction of DEP been utilized in different microfluidic systems [160].

Microfluidic devices as the principle of operation is simple and requires less hardware and can also be applied to non-conductive liquids (Figure 2.17). Conversely, it covers a wide-span of the potential application when compared to standard electrophoresis which requires the spatially uniform electric field to pull a charged particle towards the electrode with opposite charge. Of recent researchers, have found ways to use dielectrophoresis-based continuous-flow technique for gene vaccination production. This innovative technique [161] demonstrates the quick and efficient separation of parental plasmid, miniplasmid, and minicircle DNA as shown in Figure 2.18.

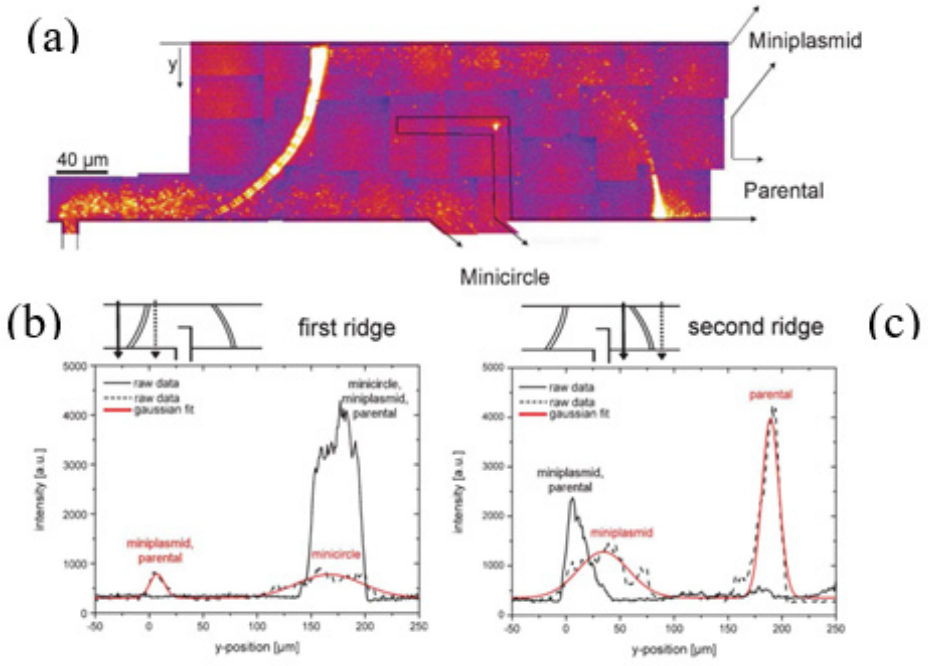

Figure 2.17. Separation of the parental plasmid, miniplasmid and minicircle DNA. (a) Combination of the fluorescence microscopy images. A mixture of the parental plasmid, miniplasmid and minicircle DNA is inserted towards the ridges from a side channel (each yellow spot represents one distinct DNA molecule). At the first ridge, the minicircle DNA is separated out of the mixture and directed into a separate channel. The parental plasmid and miniplasmid DNA are deflected and drift towards the second ridge, where only the parental plasmid DNA is deflected. Thus, all three species are retrieved in separate channels. (b) and (c) Fluorescence intensities up- and downstream of the two ridges. The scan paths are portrayed over the graphs. The black lines signify the scans upstream of the ridge; the dashed lines symbolize the scans downstream of the ridge. The red lines are Gaussian fits. (b) At the first ridge the resolution was Res = 1.10. (c) At the second ridge the resolution was Res = 1.25. Consequently, a complete separation of the three species was achieved with very high separation efficiency [104].

2.4 MICROFLUIDIC MATERIALS

In microfluidics, the properties of Material are very crucial because it affects both functionality and manufacturability. Consequently, the selection process is the foremost consideration for any successful design and fabrication methods of POCT devices. For instance, device performance is critically tied to balancing functional requirements that are related to the physical and chemical properties of the intended material.

2.4.1 REQUIRED PROPERTIES

The anticipated physical properties required mostly revolves around mechanical resilience (modulus of elasticity), visual characteristics (optical) and high-temperature tolerance. Mechanical properties describe the rigidity (hardness) or elastic nature of the device. Hardness features are mostly utilized for the framework where rugged handling is required. Furthermore, since most POCT chips are subjected to relatively high pressures flow when external pumps are utilised. Thus, the designated material are expected to resist rupture. As for the utility of elastic materials, their characteristics are mostly employed in the internal membranes of micropumps and microvalves. The temperature, on the other hand, is needed for chemical reaction or processing done on the chip. For instance, polymerase chain reaction (PCR) relies on repetitive heating and cooling cycles for rapid DNA melting and enzymatic replication, during which the temperature fluctuates between 52°C and 96°C [31], [172]. Thus, a material of considerable temperature resistance is a requirement. Another important feature is the surface properties which dictates the solid-fluid interface relationship. A good example is the surface interaction between microchannel surfaces and active fluids (reagent). These interactions can be described physically as surface hardness and roughness which are the main factors that determine hydrophobic or hydrophilic characteristics. When the surface is hydrophilic, capillary flow is enhanced, while the opposite applies to hydrophobic surfaces. Although, in recent times innovative methods such as surface modification techniques are being employed to treat specific surface to adhere specific surface requirements. Regarding requirements, hydrophilic patches are required to accelerate flow, while hydrophobic patches for stopping fluid flow [173]. [173]. A common surface modification technique is plasma treatment [174]. Applications involving optical properties is usually associated with fluorescence which is the emission of electromagnetic radiate

In in this case Ultra Violet (UV) light to aid chemical reaction or DNA detection. This real-time fluorescence detection system [174]. Applications involving optical properties is usually associated with fluorescence which is the emission of electromagnetic radiation in this case Ultra Violet (UV) light to aid chemical reaction or DNA detection. This real-time fluorescence detection system [175]–[177] are usually employed lab-on-a-chip applications. Thus the degree of material transparency becomes highly significant.

Chemical resistance (inertness), antifouling and disposability are also vital requirements in material selection. Chemical resistance involves a material surface reaction to chemicals (organic solvent, water, along with others). An overview of physical properties for common microfluidic polymers and material are clearly depicted in [178]. The main interest in this reaction is the whether the contact surface and overall nature of the material is altered or not. This alteration relates to absorption and adsorption of the small molecules of solvents in contact with the material surface. Whereas, when the concerned chemicals or reaction are of biological connotations the term biocompatibility is used in reference to the material. For instance, absorption of organic solvents in PDMS fabricated chip causes swelling of the chip, which results to distortion of the microchannels

[179], [180]. Therefore, the fluid flow within the channels are impaired and might lead to building up of excessive back pressure in the pumping mechanism. Similarly, antifouling otherwise known as Protein fouling is the accumulation of proteins on a surface, especially in microchannels. Fouling of surfaces in microfluidics devices, predominantly, when the protein or enzymatic solutions are often used creates both restrictions of flow channels of very small dimensions and also alter the surface chemistry of the channels [181], [182]. The above-listed surface modification techniques are usually applied to improve microfluidic functionalities. Material Disposability comes in two folds which can be identified as cost and eco-friendliness. Material cost plays a major role in chip prototyping and commercialization because at low-cost microfluidic POCT device prototyping research is made easier while affordability aids commercialization (Table 2.3) of new design products. The factors that determine cost are the material availability and cost of synthesis or production. Inexpensive materials tend to be ubiquitously available in the market while at the same time easy and cheaper to synthesise. Since polymers commonly used in microfluidics device fabrication are non-biodegradable, recycling becomes the best effort that helps reduce the high rates of plastic pollution. Then again there have been the recent use of biodegradable polymers [183] in microfluidics device in tissue engineering [184], [185].

2.4.2 SILICON

Considering the wide variety of microfabrication processes for microfluidic and MEMS devices which are largely inherited from microelectronics fabrication; therefore, making silicon by far the most prevalent substrate material in use. Before the rapid growth of interest in polymer materials for MEMS, silicon was the most important material for microelectronics because of its semiconductor properties. Although brittle when stressed to the point of fracture, silicon is remarkably effective as a mechanical material [186]. The crystalline structure of silicon inhibits gas permeability; which is one of the necessary characteristic vital for cell culturing in microfluidic systems [134]. It also exhibits linearly elastic behaviour below its yield strength with no hysteresis and suffers no plastic deformation or creep except under very extreme temperatures well beyond relevance to microfluidic applications. As a result, their high material stiffness makes it very difficult for the fabrication of mechanically movable microfluidic structures (diaphragms) required for microvalves and pumps; which fair better under soft and flexible materials. Though, silicon is still a utilised material for moulds replication in microfluidics.

Silicon is also prevalent in microfluidics in the form of polysilicon (i.e., polycrystalline silicon) and amorphous silicon. In both cases, the silicon is typically deposited as thin films by vapour deposition and can be doped for electronic device functionality. Polysilicon is used in many diverse ways for surface micromachined sensors and actuators. For example, in the case of actuation, polysilicon has been used for electrostatic diaphragms [187] and as heating elements for micropumps. Properly doped polysilicon is also effective for sensing elements based on capacitive displacement [188] and piezoresistive strain measurement. Another unique aspect of silicon is that it can be made highly porous with good uniformity by an anodic electrochemical etch process. Porous silicon has an extremely high surface-to-volume ratio, which is particularly advantageous for applications with surface reactions involving catalysis, adsorption and desorption [189].

2.4.3 GLASS

The term glass usually refers to materials that are predominately amorphous silicon dioxide (SiO2), also known as silica. Varieties of glass are made by including other compounds such as sodium carbonate, calcium oxide,

and boron oxide to produce different thermal, mechanical, and optical characteristics. Like silicon, glass is rigid, dimensionally stable (thickness of 30μm can be handled) and relatively brittle. Many common categories of glass are optically transparent, making glass favourable for applications that require imaging or optical methods of detection for fluids particles. Glass is a very convenient substrate for microfluidic devices because it is readily available and typically cut into rectangular slides or circular wafers. For applications, such as capillary electrophoresis, glass microchannel chips are routinely produced as either commercial off-the-shelf products or even semi-custom layouts. Unless specifically engineered for electrical conductivity, conventional glass exhibits sufficient electrical insulation such that it can serve as a substrate for direct patterning of conductive metal lines and functional electrodes [190], [191].

A common way of creating channels in glass substrates is by wet etching, typically with a concentrated hydrofluoric acid. Wet etching of glass occurs isotropically and typically produces rounded profiles with low aspect ratio. Holes and channels in glass substrates can be fabricated by ultrasonic drilling and laser ablation. There are also formulations of photosensitive glass that exhibit spatial etch selectivity when exposed to UV radiation through a mask [192]. Although the majority of glass microfluidic devices use slides or wafers, glass in other forms can also be used to fabricate channel-like structures using spin-on-glass [193] or sputtered films. A good example of a commonly used derivative is borosilicate glass. It has an excellent ability to resist strong acids, saline solutions, strong oxidising and corrosive chemicals. In the same way, their chemical inertness exceeds that of most metals and other materials because at temperatures above 100 ˚C they still retain their inertness for a long period. Economically, they are easily mass produced and readily available in differs thickness.

2.4.4 FUSED SILICA QUARTZ

Fused silica quartz is dissimilar to quartz which is a crystalline material whereas fused silica quartz is amorphous, just like other glass forms they are that are mostly made up of silica in its non-crystalline form. They can be manufactured using several different processes. Prominent amongst this is a vitreous method (splat-quenching or melt-quenching) used to form the quartz by heating the material to its melting point and rapidly cooling it, while the fused used Silica is formed by fusing high purity silica in a specially designed furnace. The overall procedure is carried out at extremely high temperatures, over 500^0C. The microfluidic device fabrication processes with this material are similar in precision to the ones used in the electronics industry. For instance, the channels for fluid flow are etched into materials by photolithography processes. While in the case of multi-patterned layers can be very accurately aligned, and fused together. Recently Engineers at Dolomite can now etch optically smooth features with depths of up to 150microns which is far deeper than most available solutions in the marketplace which can only offer depths in the area of 20microns [194].

In comparison to glass, quartz is much harder with great thermal shock resistance. It also has an excellent chemically inertness; fused silica quartz can handle the high concentration of acids except for hydrofluoric acid even at low concentrations. They do have superior optical properties (UV transparency) in comparison to glass and can be used for applications such as flow cytometry (cell sorting and cell counting). For example, Institute of Photonic Technology in Germany, in collaboration with the Department of Internal Medicine have developed a Quartz microfluidic chip that can be used for tumour cell identification using Raman spectroscopy

in combination with optical traps [195]. Some other benefits include non-auto-fluorescent and non-porous characteristics making it a preferred material for applications in the POCT.

2.4.5 METALS

Metals are obviously distinguished by having significantly higher electrical conductivity than other categories of materials used in microfluidics. Accordingly, metals are frequently used for electrical functional components such as electrodes, conducting lines, or signal interface contacts. As conductors of electricity, metals may also be used to modify electromagnetic fields, which may subsequently be used in novel ways for applications such as biological cell manipulation[196]. Another functional merit for metals is high thermal conductivity. For example, a heat spreader based on micro heat pipe design has been constructed from layers of copper and brass for microprocessor cooling [197], [198]. The relatively high mechanical strength of metals favours their use for high-pressure applications, compared to polymer materials. Some metal alloys that have favourable magnetic properties have been incorporated into functional components such as nickel- iron rotors for active mixing [199], [200]. Magnetic components have also been combined with deformable polymer structures for functionality as micropumps [201] and microvalves. Some microfluidic devices also take advantage of shape memory alloys. Nickel-titanium (NiTi), which changes from its austenite phase to its martensite phase upon cooling and the corresponding shape change, can be used for device actuation.

Gold, nickel, and copper are among the most commonly used metals in microfluidic devices. Gold is often the material of choice for electrical purposes because of superior resistance to corrosion and oxidation, even though other materials such as copper have lower electrical resistivity (1.7×10^{-6} Ωcm for copper versus 2.2×10^{-6} Ωcm for gold). Nickel, copper, and alloys based on nickel or copper are favourable for structures made by electroplating and electroforming. Single nickel electroforming step is a good example of commercially viable means of making a metal microfluidic structure such as ink-3Djet print heads [202]. In contrast to gold and copper, the much higher resistivity of platinum (10.6×10^{-6} Ωcm) makes it favourable for resistive heating. Other metals such as aluminium and tungsten are prevalent in microelectronics but less common in microfluidic devices.

Recent publications have shown that gold, silver and gold-silver alloy nanoparticles [203] now offer an alternate solution to optical detection through resonant light scattering spectroscopy (RLS) [204]. This unconventional route approaches the perspective of gold and silver particles as substitutes for fluorescent probes in certain microfluidic applications. Still, the possibility of dark field RLS detection [204] and quantitation of metal nanoparticles in POCT devices are opening thought-provoking potentials for the advance development of microfluidic detection systems [205], [206].

Another important role of metals in microfluidic device fabrication is tooling. Even if the final device made of a different material, it is sometimes beneficial to have finely patterned tooling to transfer the relevant geometry by hot embossing or other moulding technique. This system facilitates more rapid high-volume manufacturing with good repeatability. One approach, for example, is to begin with laser micromachining of patterned tooling in a thin metallic sheet, then to transfer the pattern by hot embossing onto a thermoplastic (PMMA) master, and to complete the process with the casting of PDMS atop the PMMA master [207].

2.4.6 PAPER

Paper-based microfluidics" or "lab on paper," provides an innovative system for manipulation and analysis of fluid for a variety of applications. They are typically made up of cellulose or cellulose polymer that possess excellent compatibility trait with several medical diagnostics applications and can be chemically modified to integrate an extensive range of functional groups that can be covalently bound to DNA or proteins [208], [209]. Just like most papers they are easy to stack, store, transport, depose (burning) and most especially available in a wide range of thicknesses (0.07-1 mm) [210].

Besides, unlike conventional microfluidics, its preference to fluid flow by capillary driven forces makes it requires little or no ancillary pump which often requires external power assistance.

These systems integrate some of the capabilities of conventional microfluidic devices with the simplicity of strip diagnostic tests [211], [212]and can be referred to as micro-pads (μPADs). μPADs are very significant in comparison because they provide bio-analyses that are more rapid, less expensive, and more highly multiplexed than contemporary analyses. They require only minute volumes of fluid and very minimal external supporting equipment or power because fluid movement in μPADs is controlled principally by capillarity and evaporation. Their Features can be identified by a variety of 2D and even 3D microfluidic channels that have been created on paper to confine and manipulate fluid flow within the predesigned pathways on paper [213].Unlike orthodox microfluidic devices that have their microchannels fabricated by etching or moulding channels into PMMA, glass, PDMS, or other polymers; instead, μPADs make use of patterning sheets of paper into hydrophilic channels constrained by hydro hydrophilic cellulose fibres of paper allowing aqueous fluids to wick along the channels. The flow rate of the wicking is contingent on the characteristics of the paper, ambient conditions (temperature and relative humidity) and most especially dimensions of the channel. Furthermore, the cellulose matrix can be combined with conducting carbon or metal fibres [211]. This innovative configuration provides electrically conducting or magnetically responsive patterns on the μPADs. The microfluidic paper technology is already used extensively in as a point-of-care device in developing countries where healthcare and disease screening is expensive and not readily available due to low-infrastructure and limited trained medical and health professionals [211], [214].

2.4.7 POLYMER

As a result, the growing demands for cheap and disposable POCT devices during the early 1990s, the selection of suitable materials has gradually shifted from the conventional materials such as silicon and glass towards polymers. This gradual change, which was eased through by the advent material technological progress, can be considered a major innovation in the field of microfluidics POCT that is primarily needed in various biomedical and clinical applications. Compared to other types of materials, polymers represent a wide variety of material characteristics for microfluidic devices [215], [216]. They have relatively low mechanical strength, low melting point, and high electrical resistance. The main advantage that polymers offer is that they can be engineered or synthesised to exhibit certain chemical and physical properties required for targeted functionality such as optical transparency, chemical resistance, stiffness and most especially surface energy.

Polymers chemical classification is based on monotonous structural blocks called monomers that are capable of being bonded chemically to other molecules in long chains to form large-sized molecules. These macromolecules or polymers can be used to create diverse material properties from their monomers by

polyaddition [217] reaction or polycondensation [218]. The most frequently used monomer chemistries Acrylates and vinyl polymers, Epoxy resins, Thiol–enes, Polyurethanes, Siloxanes.

Epoxy polymers are typical derivatives of glycidyl or oxirane group and can be created from a synthesis of Bisphenol A epoxy resin, Bisphenol F epoxy resin, Bisphenol F Novolac epoxy resin, Aliphatic epoxy resin and Glycidylamine epoxy resin [219]. Further details of the chemistry engineering of epoxy can be found in this textbook [220]. A good example of an epoxy-based polymer is SU8, which is a commonly used substrate for making a master mould for photolithography technique. The "8" in SU-8 stands for the eight epoxy groups in a bisphenol- A Nova lac glycidyl ether a single molecule cul ar structure. SU8 photolithography produces a Good adhesion and high aspect ratio negative photoresist that allows for the creation of deep channel microfluidic structures and as well as variant depth through multiple UV light exposure [221] (this technique will be discussed in the microfabrication section). Also, they are also suitable polymers material choice for prototyping techniques such as stereolithography [222], [223].

The thiol-ene reaction is acknowledged as a click chemistry reaction given the reactions' maximum yield, fast rate, stereoselectivity and thermodynamic driving force [224]. They are compounds with sulphur hydrogen groups also known as alkene hydrothiolation; which is an organic reaction that forms alkyl sulphide [225]. They are commercially produced from mixing monomers such as trithiol with triene or tetrathiol with triene in varying ratios wich are calculated on the amount of free thiol and allyl(ene) groups in the monomer structure [226]. Subsequently, the mixed ratios can then be cured rapidly under UV light through free-radical polymerization at ambient temperature and pressure [227]. Thiol-ene chemistry are now seen as PDMS substitutes in soft lithography [228]–[230] for bioanalytical applications because they are not prone to protein fouling [231], [232] to swelling upon contact with organic solvents [233], absorption of small hydrophobic molecules [234] and Most importantly high elastic modulus (PDMS is frequently restricted to comparatively low working pressures of about 1 bar [235].They are mostly utilized in microfluidics for surface engineering and microchannel patterning [236].

Acrylate monomers are typically derivatives of acrylic acid [237] which consist of vinyl hydrogen and the carboxylic acid, while vinyl monomers are consist of the vinyl group [238] or ethylene. However, acrylates are industrially easier to synthesise than pure vinyl polymers which are toxic and difficult to handle. An example of a simple acrylic acid synthesise is the methyl methacrylate which has its vinyl hydrogen and carboxylic acid hydrogen substituted by methyl groups to form poly(methyl methacrylate) (PMMA) [239], typically known for their transparency. On the other hand, vinyl chloride can be polymerised [240] with the assistance of a radical a catalyst to form of polyvinyl chloride (PVC) which is widely used the material.

Polyurethanes (PU) polymers also known as polycarbonates are created by the reaction of two monomers di-isocyanate and a polyol that contains containing hydroxyl groups in the presence of a catalyst or by ultraviolet light stimulation [241]. There are of high relevance in microfluidic prototyping because of their suitability in the creation of moulds [242] and as structures [243] in microfluidic devices. This polymer also serves as another alternate to PDMS because they are not prone to protein fouling especially when biofluids are involved for example blood [244]. However, they are relatively expensive and not usually transparent.Polyurethanes robust reaction mechanism can be tailored to fit two typical forms in microfluidics which include elastomers and surface coatings. Elastomeric polyurethane (PU) which can be derived from bio-source such as castor oil (CO) [243]. This elastomer can be used to produce microvalves elastomer in microvalves that can be integrated with microfluidic devices [245]. Also, microchannel formation and sealing (both reversible and nonreversible) is

easily attainable in PU components using partial curing [243].One the other hand the coating specification applies to surface modification for good compatibility with a wide range of solvents and chemical resistance.

Siloxane polymers have mostly been used in microfluidics device prototyping for last two decades. They are chemically a class of polymers that exhibit an interchanging silicon–oxygen polymer with each pair of silicon centres separated by one oxygen atom to form backbone chains that are very elastic. Consequently, this renders most siloxanes; elastomers. A principal example is a polydimethylsiloxane (PDMS) that methyl groups as the main polymer backbone. PDMS are of significant importance due to their low critical surface tension, flexibility, chemical resistance and surface hydrophobicity in nature. This defining features of PDMS make it a very versatile material for the creation of microfluidic devices [246]. Commercial PDMS comprises of the polymer matrix (often aromatic siloxanes) and a curing agent which activates ring opening polymerization or similar crosslinking. This process usually involves the use of moulds or a solid master that gives the expected shape of the PDMS when cured. This process is known as casting [247]. A substitute method of curing similar to thiol-ene involves the use of a catalyst (typically a platinum catalyst) on a mixture of SiH and vinyl terminated polysiloxanes. A detailed analysis of the synthesis and characterization of siloxanes are found in this text [220].

On the other hand, physical and mechanical properties of polymers can be categorised into three rudimentary temperature dependent parameters in the form of glass transition temperature (Tg), heat distortion temperature (HDT) and decomposition temperature (TD). Glass transition temperature (Tg), which is of considerable technological importance has its derivation from the molecular comportment of the polymer material. It's an amorphous change unique to only polymers that involve reversible hardened or softening above or below a threshold temperature. As the polymer absorbs heat, up to a certain temperature, the intramolecular friction holding each fragment/monomer in the polymer chain is weakened by the relative motion as a result of absorbed energy. At this point, already hard polymers will have larger segments of their polymer chain moving freely, leading to a substantial softening of the material. On the other hand, when already soft polymers cooled below their Tg they become hard and brittle, like glass. The case of heat distortion temperature (HDT) describes the maximum temperature for which a polymer material susceptible to mechanical failure from stress as it would simply give way beyond this temperature. The last important parameter, decomposition temperature (TD), is the point at which the physical characteristics of the polymer is permanently altered as a result of the total breakdown of the polymer chains. The physical attributes of most polymers can be categories as thermoset, thermoplastics and elastomers.

Thermosets (duroplastic materials) often called resins are usually liquid at room temperature. They typically formed from a corresponding monomer that undergoes a crosslinking by a chemical reaction, photoinitiator or thermo-initiator for polymerization. Initiated chemical reaction is done by mixing the monomer with a curing agent. While crosslinking initiated physically by light (photoinitiator) are typically UV irradiation and curing induced at a temperature typically above 200^0C [248], [249] are a good example of thermo-initiator reaction. All these curing (cross-linking) processes involve an irreversible chemical reaction and once taken place the polymer becomes rigid with a significant increase in molecular weight and higher melting point. Furthermore, the crosslinking forms close-fitting and solid three-dimensional network that are usually stable at room temperature. When subjected to unrestrained heating, the cured material results in reaching the decomposition temperature earlier than the melting point which will eventually decompose the polymer. Consequently, a thermoset material cannot be melted and re-modelled after undergoing curing process because their Tg is

typically rather high and close to the decomposition temperature (TD) so, therefore, they burn instead of melting. As a result, thermosets, cannot be recycled therefore less eco-friendly. Well on the brighter side they do possess good dimensional stability, thermal stability, chemical resistance and electrical insulation properties, which makes them suitable for fabrication of microfluidics devices. Archetypal examples of thermoset polymers in microfabrication are the resist materials for microfluidic applications, especially the photoresist (negative & positive) SU-8 (see Photolithography).

Elastomers typically known as silicone rubber are polymers with glass transition temperatures characteristically lower than the normal operating room temperature. When they are cooled to their Glass Temperature, there is less mobility between the polymer chains that eventually results in the material becoming brittle and less elastic. Just as their name (elastomer/rubber) they are known to undergo elastic deformation as a result of very weak inter-molecular forces with generally low Young's modulus and high failure strain rate in comparison with other materials. They also share similar characteristics with thermoset with regards to TD even though thermoplastic elastomer does exist. Engineered thermoplastic elastomers (TPE's), are one of the most multipurpose polymers available [250] because of the combined performance properties of thermoset rubber with the processing ease of today plastics. As a result, there is versatility of design options and better cost-reduction opportunities. The most commonly used elastomer in microfluidics prototyping is PDMS, and recently, fluorinated elastomers (FKM/FFKM) [251]–[253] have gained significant traction in the community. These materials are exhibit number of properties that make them excellent materials for microfluidics that include very low critical surface tensions, high biocompatibility and outstanding chemical resistance. As well most of these fluorinated elastomers have their glass transition temperatures well below room temperature.

Since elastomers are usually soft, flexible and able to deform elastically without extensive pressure, they are therefore an ideal material for active microfluidic components such as membrane and mechanical valves needed for microvalves or micropumps. Furthermore, they are also suitable for the creation of deflectable channels in regards to TPE material [250], [254].

Thermoplastics Compared to thermosets is made up of linear molecular chains not cross-linked. This polymer chain configuration supports easy movement within the polymer chains bulk as intermolecular forces weaken rapidly at high temperatures. Most thermoplastics do have high molecular weight and with unrestricted heating at temperatures above their Tg, they melt into a viscous liquid and then solidifies upon cooling [255], unlike thermosets that decompose. Thermoplastics, therefore, can be moulded or reshaped by heating. There two classes of this polymer. First of all, is the amorphous thermoplastic, which has intermingled molecular chains with no crystalline structure present within the material. This polymer Chain disorder leads to intermolecular twisting and coiling since there is no crystalline structure present. Consequently, this means the materials are susceptible to failure above the glass their transition point due to low Heat distortion temperature, HDT. In additional, there are known for mostly their transparent or translucent, low tendency to creep, good dimensional stability, low tendency to warp, brittleness, low chemical resistance sensitive to stress cracking.

On the other hand, Semi-crystalline is denser than amorphous since the degree of crystallinity is proportional to density measurement [256], [257]. These thermoplastics have some macromolecules in the form of crystalline structures dispersed throughout the material. As a result of this crystalline regions, the materials have a tendency to be very hard (resilient intermolecular forces); and capable of withstanding mechanical stress above the glass transition temperature (high Heat distortion temperature). Their material properties are characterized by being translucent or opaque, good fatigue resistance, toughness, and good chemical resistance.

Polymers and other microfluidic materials with their relative commercial viability and general microfluidic use can be found in [178].

2.4.8 MATERIAL BONDING PROPERTIES

Bonding in microfluidics is a vital process that involves sealing two or more substrates arranged in a specific configuration that forms the internal environment of the Lab-on-a-chip (LOC) devices. This internal environment consists of microfluidic elements such as microchannels, mixer, valves, reaction chambers, fluidic connectors (inlet port and exit port). The Bond strength which is a significant factor in the sealing process can be reversible (relatively weak) but most commonly used applications are irreversible (permanent). Similarly, the bond interface is also another significant factor for consideration because it must provide appropriate chemical or solvent compatibility to avert degradation during usage, without compromising the dimensional integrity of the microchannels as a result of deformation during the bonding process.

The main concerns for the bond interface include surface chemistry, optical properties, material compatibility and uniformity of the channel sidewalls. Likewise, the already bonded substrates required to constraining the reagents, solvents and bio-samples in specific volumes while also preventing unrestrained dispersion of liquids along wettable areas. Furthermore, External contaminants (dust, etc.) are prevented from coming into the chip. Likewise, the anticipated fluid waste is restricted from going to outside world (biohazard). Finally, evaporation which is the main antagonist of fluid sample and reagents in the chip are brought to a minimal level especially during thermochemical reactions.

The Selection of bonding techniques depends mostly on the materials characteristics and type of constraints imposed by the application. Several bonding techniques are available, both past and recent are covered in this review journals [258]–[260]. However, this thesis discusses the commonly used techniques in microfluidics substrate bonding which include adhesive bonding, thermal fusion bonding, solvent-based bonding, localised welding and Surface treatment and modification.

In general, microfluidic bonding techniques, can be characterised as either indirect or direct. Indirect bonding involves the use of an extra layer apart from the substrates in concerned. This layer is an adhesive that seals the two substrates and their encapsulated internal microfluidic elements together by charge interactions [261], [262]. The charge interactions can be a result of chemical (covalent) bonding or van derWaals forces [262], [263]. In contrast, direct bonding methods mate the substrates by molecular entanglement, which is mechanical interlocking of two surfaces by relative diffusion between them. This process is done without any additional materials added to the interface. It is distinguished by its ability to produce microchannels with homogeneous sidewalls [178].

2.4.9 ADHESIVE BONDING

Most commonly used adhesive are UV curable [264], with the bonding process performed by applying a thin layer of a high viscosity liquid adhesive which is then cured by UV light irradiation. This process is illustrated by in Figure 2.20 which shows adhesive layer bonding for PMMA substrates [265]. Another common, inexpensive method for adhesive bonding is the use of lamination films as low as 40 μm [264], [266] since most Commercial laminators are inexpensive and simple to use. The drawback to this system is intermediate adhesive layer mostly produces composite layer chip with inconsistent microchannel sidewalls and clogging

of microchannels. Furthermore, the bonded surfaces tend to have different chemical, optical and mechanical properties than the bulk substrate. Although an extensive range of UV-curable adhesives is accessible, they are derived from polyester or acrylate resins.

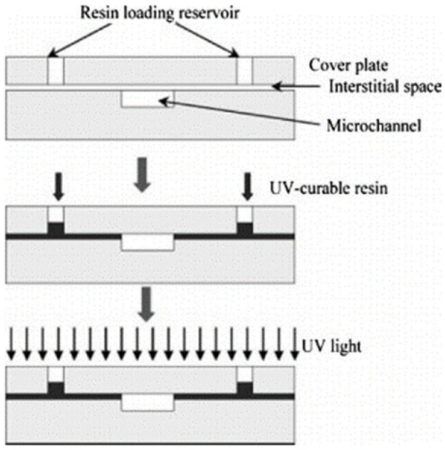

Figure 2.18. Capillarity-mediated resin introduction of UV-curable adhesive [304]. Copyright Wiley-VCH Verlag GmbH & Co. KGaA, copied with permission.

2.4.10 THERMAL FUSION BONDING

This direct technique involves the simultaneous application of pressure and heat on both substrates surfaces. This bonding process gives a moderately high bonding strength and is mostly applied to thermoplastic materials because the Substrates are heated to temperatures near or above the glass transition temperature (Tg). Although, unrestrained temperatures and pressures application or use of materials with different Tg may lead to microchannel distortion and collapse. Hence, the use of a programmable hot press [265], [267]–[269]such as high throughput roller laminator [270] that can properly regulate temperature, pressure, and time is vital to attaining high bond strength while preventing deformation of the embedded microchannels due to bulk polymer flow. The Use of this method will cause consistent stability of channel cross-sections to be attainable, as revealed in Figure 2.21; that shows the case of laser micromachined channels in PMMA [271].

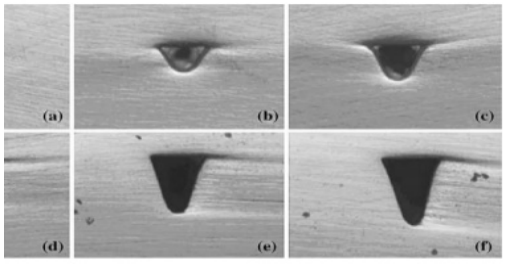

Figure 2.19. Cross-sectional views of enclosed laser micromachined PMMA channels, with increasing depth from a–f, thermally bonded at 18^0C, well above Tg, using a low bonding pressure below 20 kPa [271].

2.4.11 SOLVENT-BASED BONDING

This technique is similar to the adhesive indirect method because of it that it requires a solvent between the merged surfaces. However, in this case, the solvent used to bond the substrate together, temporarily soften and dissolves the material. Consequently, the surface molecules of the materials mix to form a permanent bond as the solvent evaporate [153]. Solvent bonding of thermoplastics makes use of polymer solubility in designated solvent systems to achieve entanglement of polymer chains across the interface. As a result, the polymer chains become mobile and can freely diffuse across the solvated layer, leading to the broad interweaving of chains between the surfaces to create exceptionally strong bonds [154]. PMMA substrates immersion in ethanol for at last ten minutes before joining them together under pressure is a simple illustration is a solvent bonding that has been performed by this group [274].

2.4.12 LOCALIZED WELDING

It's a direct bonding technique that is used on thermoplastic. It involves the use of ultrasonic energy to induce heating and to soften at the interface of the mating parts [275]. Another alternative method to is the use of microwave energy to heat embedded metal films located between the desired bond surfaces. An advantage of this technique is selective use of energy to locally target specific regions or uniformly all mating interfaces for bonding [276]. There are commercially viable systems operating at 35 kHz [277] that can be efficiently used on thermoplastic polymers such as PMMA (Poly(methyl methacrylate) and PEEK (polyetheretherketone).

2.4.13 SURFACE TREATMENT AND MODIFICATION

This form of direct bonding technique that functions by increasing the surface energy of the substrates required to bond. Increased surface energy helps to improve the hydrophilic properties of mating surfaces. As a result, mechanical interlocking and inter-diffusion of polymer chains between the surfaces are enhanced [278]. The substrates are held together by the generation of electrostatic interactions, and also surfaces possessing high specific energy in the form of polar functional groups can create hydrogen or covalent bonds across the interface that are capable of producing bond strengths beyond the cohesive strength of the bulk polymer [279]. Similar to localised welding, selective region use of a mask can be used to apply surface treatment and modification to specific regions. For example, PDMS layer to be bonded is covered with a masking material during corona discharge treatment to protect areas from exposure to the corona plasma so that only the unprotected surfaces are activated. Subsequently, the activated surfaces are hydrophilic, with chemically active functional groups that bind to other activated surfaces, while the masked areas remain unbounded [280], [281]. This example is an illustration of O2 plasma surface treatment done by the aid of corona discharge (Figure 2.22). Corona discharge used for bonding is a process by which an electrical discharge occurs between an electrically charged conductor (electrode) and the surface of a substrate. This occurrence is as a result of potential gradient (electric field) and ionisation of the neutral media fluid, typically air [282]. This fluid ionisation process creates a region of plasma around the electrode as free electrons randomly accelerate across the air gap in the presence of a high voltage discharge. Subsequently, when a substrate surface is positioned in the discharge path, high energy electrons create free radicals by colliding with the surface to break up their molecular bonds. These free radicals form various chemical functional groups [283], [284] required for effectively increasing surface energy and enhancing chemical bonding to another activated surface, in the

presence of oxygen (oxidational reaction). Examples of functional groups include carbonyl (-C=O-). Carboxyl (HOOC-), hydroperoxide (HOO-) and hydroxyl (HO-) groups [284], [285].

Ultraviolet light (UV), is a simpler alternative to plasmas for the enhancement of substrate surface energy. The Exposure of UV light to polymer substrates especially thermoplastics results in photodegradation, which is the primary mechanism creates photo-oxidation and breakup of polymer chains on the surface [286]. Typically, light exposure within the range of 300–400 nm is usually sufficient to break chemical bonds within most thermoplastics [287], [288].

.

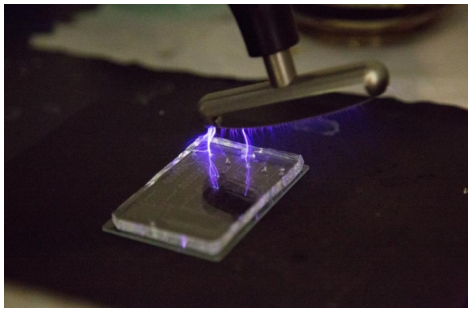

Figure 2.20. Corona discharge used to bond surfaces of PDMS to glass.

Table 2.1. Synopsis of general bonding techniques for microfluidic device [178].

Bonding Method	*Bonding Strength*	*Bonding Quality*	*Process Complexity*	*Bonding Time*	*Cost*	*Advantage*	*Limitation*	*Suitable Material*	*References*
Solvent bonding	High	Fair	Low	Low	Low	Simple, fast, low temperature, high bond strength, low cost	Soften polymer surface may collapse channel from un-optimized process	PMMA, PC, COC	[289]–[293]
Solvent Bonding with sacrificial Material	High	Good	High	Medium	Low	High bond strength, low cost, low channel collapse and clogging	Sacrificial material needed to be applied into channel before bonding and removed after bonding	PMMA	[294], [295]
Localized welding	Medium	Fair	Medium-high	Medium	Medium	Low temperature, localized bonding	Energy director (ultrasonic welding) or metal layer (microwave welding) are required	PMMA, PEEK	[296], [297]
Surface Treatment Bonding	Medium-high	Good	Medium	Medium	Medium-high	Low temperature bonding, low channel deformation	Surface chemistry changed after treatment	PMMA, PC, COC, PS, PET	[298]–[300]

Bonding Method	*Bonding Strength*	*Bonding Quality*	*Process Complexity*	*Bonding Time*	*Cost*	*Advantage*	*Limitation*	*Suitable Material*	*References*
Adhesive Printing Bonding	High	Fair	Medium-high	Short-medium	Low-medium	Low temperature, high bond strength, low channel clogging, controllable adhesive thickness	Scarification channel (contact printing) or printing mask (screen printing) required	PMMA. COC	[301], [302]
Adhesive interstitial Bonding	High	Fair	Low	Short	Low	Low temperature, high bond strength, low channel clogging, controllable adhesive thickness	Soften polymer surface may collapse channel from un-optimized process	PMMA	[303], [304]
Adhesive interstitial Bonding	High	Fair	Low	Short	Low	Low temperature, high bond strength, low channel clogging, controllable adhesive thickness	Soften polymer surface may collapse channel from un-optimized process	PMMA	[303], [304]
PDMS-interface bonding	Medium	Fair	Medium	Long	Medium	Simple, fast, low temperature, high bond strength, low channel clogging, low cost	Sacrificial material need applied into channel before bonding and removed after bonding	PMMA	[265]
Lamination film bonding	Medium	Fair	Low	Short	Low	Low temperature, compatible with PDMS microfluidics	Energy director (ultrasonic welding) or metal layer (microwave welding) are required	PMMA, PC, PS, PET	[289], [305], [306]
Thermal fusion bonding	Medium	Fair	Low	Long	Low-medium	Simple, fast, low cost, low temperature, no adhesive clogging	Surface chemistry changed after treatment	PMMA, PC, PS, Nylon, CO, PSU	[307]–[310]

2.5 PROTOTYPE FABRICATION TECHNOLOGY

The need to manufacture POCT devices at relatively cheap cost brought about rapid development microfabrication technology in the medical field. The earlier years of microfluidics devices were predominantly produced with techniques borrowed from the microelectronics field, and they predominantly involved materials like glass, quartz or silicon. However, the advent of new technological processes brought into focus the demand for devices which are disposable and inexpensive.

Contemporary techniques can be distinguished by their individual protocols employed to establish efficient channel network or fluid circuit in the chip. The chip functionalities, are largely defined by microchannel aspect ratio, with channel dimensions as low 0.5um to as large as 500um. As a result, choice of fabrication methods is tied to the anticipated channel dimensions on cost and production time. They can be divided into two areas: material depositing techniques and material removing technique.

2.5.1 MATERIAL DEPOSITING TECHNOLOGY

This technology represents the successive build of bulk material on a substrate or a Standalone structure which can be used directly or as a mould for replication of microfluidic components. Parts produced can be used Directly or bonded to achieve expected functionality, while the case of replication involves the indirect use of fabricated parts to create intended components for utilisation. In layer-to-layer manufacturing, a part is broken down into multi-slices that are then created and coupled using solvent or heat supported lamination or bonding processes. The materials used are usually wax, resin or powder. A good example of this techniques is 3D printing.

2.5.2 3D PRINTING

3D printing that utilises a layering accretion system to build solid structures from either liquid resin or powder from a digital file. This technology offers a broad range of methods to synthesise solid structures of various shapes or geometry that differ in physical characteristics on the method of production. These methods include stereolithography (vat Photopolymerisation), ink jetting, Binder Jetting, Material Extrusion and Powder Bed

2.5.3 STEREOLITHOGRAPHY

Stereolithography (STL) is a conventional additive layer-on-layer manufacturing technique. STL is one of the most significant rapid prototyping methods in the microfluidic research industry today. It can be used to create very fine structures and, more importantly, allows for fast turnaround of functional prototypes used directly or replication moulds. The basic process is called Vat Photopolymerization [311], it involves consecutive ‘printing’ thin layers of a curable material, e.g., a UV curable material, cumulatively on top of another by the use of UV Laser beam. The three-dimensional model (3D CAD design) is divided into thin micro multiple layers before light exposure. Upon exposure to UV light, the surface of the liquid resin solidifies. This hardening process is responsible for forming successive individual layers of the anticipated 3D object and is carried out repeatedly till the 3D object is formed [312].

The Parts produced, based on this technique do have the considerable mechanical toughness and are capable of high detail definition. However, they do have some disadvantages such as post production that involves

immersion in a chemical bath to eradicate unwanted resin before being cured in an ultraviolet oven. Likewise, the support structures which are interminably present can be challenging and time-consuming to remove. Their dependency on UV light has gradually being reduced as recent improvement of photoinitiators, have afforded several options in the choice of light not restricted to UV. As a result, extensive range of high-intensity light sources of differing visible wavelengths can be used as a choice for polymerization [313], [314].

2.5.4 3D INKJET PRINTING

Inkjet 3D printing process is similar to regular inkjet paper printer but in this case light curable resins and wax instead of inks. In this combination, the wax is expected to create spatially constrained volumes which are to be filled with the light curable resins. The sequence of layer building involves an array of nozzles that create droplets of heated low viscous wax that instantaneously form cavities which are subsequently spotted with resin before cured by light exposure.

Similar to STL this system can be used for an extensive range of microfluidic fabrications involving mould replications. Although their final product finish is not as detailed as STL; they are still relatively close in comparison. Furthermore, the print mixture of UV curable acrylic resins and waxes makes easy post cleaning process because the waxes serve as supporting materials that can be removed easily. The foremost downside of inkjet printing is that most parts produced from this technique cannot be used directly because due to low chemical or biological compatibility [315].

2.5.5 BINDER JETTING

The technology was originally developed at the Massachusetts Institute of Technology in 1993. The technological process of layering involves the use of glue applied through jet nozzles to bind together powder based particles spread in equal layers using a slider that guarantees a smooth and even surface. The building space is typically a platform onto which a thin layer of powder is spread cumulatively to form the shape of a programmed 3D object. After the consecutive accumulation of layers, the finished part is typically tempered to allow full curing of the glue. Subsequently, the non-bound powder particles are then cleaned off.

This system pales in comparison to STL or 3Dinkjet in product finish but what it lacks in finishing it makes up in cost and faster turnaround. Conversely, the major setback of this technique is the dominant chemical and physical properties of the part created is defined by the glue used. Also, parts created by this process can't be transparent because of the solid particles combination. Likewise, inconsistent binding of particles can result in porosity which makes it highly unsuitable for direct microfluidic use because of potential leakages. Again, this method is mostly suitable for mould creation for microfluidic chip models of bigger aspect ratio because the difficulty of removing powder from long and narrow channels.

2.5.6 MATERIAL EXTRUSION

The Fused deposition modelling (FDM) technology is a commonly used material extrusion technique. The process involves a precise control of heated material through a plastic filament or coiled metal wire. Two nozzle builds layers; one for the primary material and another for the support structure. The primary nozzle extrudes molten material forcefully out in both horizontal and vertical directions before hardening. The material mostly used are Acrylonitrile Butadiene Styrene (ABS) and Polylactic acid (PLA). Concurrently, secondary

nozzle also typically ejects water soluble material for internal structures while low mechanical strength structures for external support. FDM has a unique advantage from other techniques, due to its ability to create multi-materials components without the need of specific polymer modifiers [316]. Thus materials with different chemical or physical properties can be applied (including stiffness and colour) subsequently. Acrylonitrile butadiene styrene (ABS) is a commonly used material in FDM while conventional polymers such as PC, PCL, PP or PS can be used as well in this process. The main weakness of FDM is the inconsistent definitions of the part geometrical structure as a result of the layer deposition characteristics that tend to mirror vivid shapes of the cylindrical wire used for layer formation 269. As a result, the final microchannel surfaces are rough, and sidewall shapes are skewed. This disadvantage disqualifies direct microfluidic use because the skewed channels can cause flow obstruction, leakages and most especially surface binding issues. Still, FDM can be suitable for mould replication because of fast turnaround, low cost of fabrication and no post curing.

2.5.7 POWDER BED

This process is similar to binder jetting, but in this case, a high-powered laser is used to fuse Small particles plastic, metal, ceramic or glass powders into a concise bulk of the anticipated 3D object. Unlike binder jetting, the chemical and biological compatibility of the created parts is defined only by the bulk material properties. The most commonly used technique for this process is Selective laser sintering (SLS) which builds up layers by using a laser beam to scan selectively across the surface of the powder bed. After each cross-section is scanned, the fused powder mass bed is lowered by one layer thickness before a new layer is applied on top and the routine is repeated until the object is completed. In SLS there is no requirement for support structure since all untouched powder remains become support for the sintered ones.

As of yet, this technique suffers major limitations in either direct use or indirect (mould replication) use in microfluidic research because the created parts are porous thus leading to mechanical toughness and surface finishing impairment.

2.5.8 LITHOGRAPHY

It a hybrid of both material removing and deposition technology. It is essential to note that lithography can be defined regarding direct use only. In the broad spectrum of prototyping, techniques lithography leans towards material deposition, although it requires material removal techniques as a complementary process to achieve the anticipated functioning POCT chip. The rudimentary process behind is selective lithography imprinting, which involves creating patterns on specific areas while simultaneously protecting areas not preferred untouched. For instance, ink can be used to create patterns on a material while the areas that are expected to be untouched are covered with wax. Good examples of these techniques that can be utilized for microfluidics fabrication are optical and x-ray lithography.

2.5.9 OPTICAL LITHOGRAPHY

Optical lithography makes use of UV light to transfer geometric patterns onto sensitive materials are known as photoresist on the surface of a substrate. The commonly used substrate and photoresist are a silicon wafer and SU-8. The process starts with the deposition of silicon dioxide (SiO_2) which serves as a barrier layer on

the surface of the wafer. Subsequently, a technique is known as spin coating[317], [318] is used to build the required height in micrometres by uniform layer on layer deposition on the wafer surface. Irradiation is then applied through a glass photomask that can cause the exposed resist to either be more soluble (positive resist) or less soluble (negative resist). For positive resists, the dissolution by solubility that occurs due to light exposure is washed away by the developer solvent to leave precise openings surrounded by walls of resisting untouched. The exact opposite is the case for negative resists as exposure to light induces polymerization that causes the resist to be insoluble to the developer solution, whereas the unexposed area is then removed by the developer solution.

The main advantage of this technique above others is the closure of micro-channels which is inclusive in the fabrication method without any additional bonding process. Micro-channel development depends on several key factors which include resisting material, spin rotational speed, the power of exposure and tilting angle of the substrate. Likewise, this newly created channels can also be sealed by creating a second SU-8 layer on top by similar light exposure and developer treatment. Also, the use of SU-8 can also allow on-chip integration to other SU-8 created functional components, like micropumps, microvalves, and complex microfluidic networks The recent improvement in technology has afforded cheaper, and faster alternative using dry film resist (DFR) [319], [320]. DFR offers numerous advantages over liquid resist (SU8) such as good adaptability, exceptional adhesion to any substrate, decent flatness, no requirement of liquid handling, even resist distribution, low energy exposure, low cost and short processing time. However, the main challenge of this method is the setting up cost which is relatively very high in comparison to other techniques even though DFR have cheaper to setup than SU-8. Furthermore, SU-8 are predisposed to large internal stress and once developed; they are very difficult to be removed from structures. Likewise, both liquid and a DFR require a uniform flat substrate to create precise structures; they also are not effective in create non-flat surface structures and require an extremely clean room environment for its protocols.

2.5.10 X-RAY LITHOGRAPHY

Lately, X-ray lithography has been adapted [321]–[323] for fabricating polymer microchannels using PMMA as substrate. PMMA is a suitable material for this process because of its high sensitivity to X-ray absorption (mild X-rays of 0.7-0.8mm) and degradation. This technique is similar to the positive resist technique of optical lithography. But in this case, the photomask that bears the geometrical patterns is made of gold. Gold is a typical X-ray absorber because of its high atomic number, and the mask thickness depends on of the intensity of the exposure. For example, the gold mask must be approximately five to ten micrometres thick to absorb x-rays with energy in the range of 5 keV to provide corresponding depth into PMMA of several hundred micrometres [324]. As the thick gold layer absorbs X-rays, the sections that are transparent to the X-rays are degraded. On the other hand, the photoresist which is PMMA can be spun as one single layer, multiple layers or joined as a pre-cast commercial sheet. The sheet is joined to the substrate by the liquid monomer, MMA. After the exposure, the degradation of PMMA into soluble oligomer [325] before they are dissolved in a developing solvent comes as a result of X-ray induced scission reactions.

This technique yields better high aspect ratio structures than photolithography because X-ray operates at a much shorter wavelength than UV light, even Deep UV (DUV)[326] light and also provide increased lateral resolution. However, their setup cost goes into millions of dollars, and operating cost can run into hundreds of dollars per hour just to recuperate the actual operating expenses. Nevertheless, subsequent duplicates PMMA

moulds can be made from the master synchrotron made a mold reduce cost by injection moulding or hot embossing. This method is mostly suited from replication, not direct use.

2.5.11 MATERIAL REMOVING TECHNOLOGY

Unlike material depositing techniques, material removing techniques create structures by locally removing material from designated parts of bulk. In microfluidics techniques such as laser ablation, micromilling or etching are commonly used. These methods typically create negative spaces that form the microchannels and fluidic elements in substrates. However, they are not suitable when the cost of the substrate is a major concern.

2.5.12 ETCHING

This technology is one of the earliest fabrication method used in microelectronics or MEMS involving silicon and glass. Likewise, they have mostly being used as a complementary process in techniques as optical lithography and micromachining. Due to current trend glass, microfluidics components seem to be the preferred choice in the POCT field due to its physical characteristics of transparency. Etching techniques are categorised either as dry or wet etching. When the material is removed from it can do by either process it can either be isotropically (uniformly in all directions) or anisotropic etching (constant surface area and uniformity in depth). The major difference between the two processes is the material removal rate which is faster in wet-etching and can be subjected to varying temperature or the concentration of the wetting agent. However, both require mask similar to optical lithography so only unmasked areas will be touched. In dry etching, the removal process is done by physical, chemical or both means. Physical dry etching utilises plasma that generates bombarding ions, electrons or photons with high kinetic energy to knock out the atoms from the substrate surface, which in turns results in material disintegration by evaporation. While, the case of chemical dry etching don't require actual liquid etchants but instead gas etchant such as tetrafluoromethane (CH_4), sulphur hexafluoride (SF_6), nitrogen trifluoride (NF_3), chlorine gas (Cl_2), or fluorine (F_2) [327] to cause surface ablation. A commonly known combination (physical and chemical) is called reactive ion etching. This process is the most extensively used dry etching technic because it's faster and able to achieved better resolution than both the physical and chemical results. The method of operation involves dissociation of enchanting molecules to more reactive species by high energy collision from plasma ionisation reaction.

On the other hand, wet etching involves exposing the substrates to corrosive solvents in liquid form. As the liquid etchant diffuses across the exposed surfaces, a reduction-oxidation reaction occurs between the liquid-solid interfaces causing degradation. Furthermore, the rate degradation determines is determined by the concentration of the etchant. Isotropic wet etching uses a combination of hydrofluoric acid, nitric acid, and acetic acid (HNA) as etchant solvent for silicon. While, potassium hydroxide (KOH), ethylenediamine pyrocatechol (EDP), or tetramethylammonium hydroxide (TMAH) are some of the anisotropic wet etching agents for silicon [328]. The major advantages dry etching is anisotropic etch profile is easily attainable, enchant consumption is relatively small. Whereas, wet etching requires simple equipment and possess high substrate selectivity. For the disadvantages, dry etching requires complex equipment and protocols, while their substrate material selectivity is very low. On another hand wet etching chemical cost are relatively high, and small geometries precisions are not consistently accurate (prone

to undercutting) [329], [330]. In general, it is possible to use this technique for replication mold or direct use in microfluidic chips fabrication.

2.5.13 LASER ABLATION

This micromachining process involves using a powerful laser to shape or create geometric structures on a substrate. Just as lithography and etching techniques discussed ablation might be achieved by exposure through a mask. The defining difference between the substrate and mask is the significant absorption at the laser wavelength. For the mask, they are expected to have very low absorption, e.g. most metals. A good example of a commonly used substrate is PMMA due to its significant absorption of the emission wavelength of the laser (i.e. 427 °C for PMMA) [331]. Alternatively, direct-write maskless systems can still be used to create channels and other microfluidic structures. In this process, the laser is held at a constant position while the platform that bears the substrate is moveable. This technique has a better turnaround because the design of the microchannel network can be changed quickly during the prototyping process instead of time spent designing new masks. One the other hand, the drawback of this method is the inability to mass produce parts since they are made in a sequential manner.

In general, the shape develops by laser ablation are usually square or rectangular with straight edges. Moreover, laser-ablated channels have far worse surface roughness than most material removing techniques. The degree of roughness is highly reliant on the absorption of the polymer at the excimer wavelength. While, the depth of laser-ablated channels is dependent on many parameters including polymer absorption, laser power, pulse rate, and some passes made across the channel. There are varieties of commercially available plastics such as polycarbonate, polystyrene, cellulose acetate, and poly(ethylene terephthalate) [306], [332], [333] that can be used to fabricated microchannels using ArF excimer laser (193 nm)[334].

2.5.14 MICROMILLING

micromilling process involves micro-cutting that is characterized by the mechanical interaction of a fast spinning piercing tool that causes splintering within specifically defined paths on the substrate. The residue of this process is usually in the form of chips [335] that can be easily blown or washed off. This method is mostly suited to mould replication in microfluidics, and the type of material general used as substrate are metals (e.g. aluminium). Although polymers can also be subjected to this process, they are highly selective due to their comparable mechanical strength to metals. PMMA is a good example of commonly used polymers because of its good mechanical strength, thermal resistance, and dimensional stability. Furthermore, PMMA optical transparency also provides a major advantage. The capability of producing high-quality microchannels and other geometric structures are determined by the material, diameter and sharpness of the cutting tools. The main cutting tools in this miniaturisation process are cemented carbide and diamond. Both tools achievable minimum width of the microchannels is proportional to the diameter of the tool. There are commercially available carbide tools down to the size of 5µm while diamond is within the Range of 100µm. However, tools below 100µm are prone to unpredictable failures. In the case of tool sharpness, diamond mills are within the range of 50nm and are capable of surface roughness Ra 10nm with no burrs (channel edge roughness). Whereas, carbide mills have a sharpness around 1µm to 10µm [336]with considerable burrs.

The major shortcoming of micromilling is the difficulty in defining small geometric structures consistently due to excessive tool failure. Furthermore, they do have expensive setup cost but are relatively cheaper in

comparison to lithography. On the bright side, Micromilling is a capable and cost-effective technique to fabricate PMMA microfluidics for research purposes.

2.5.15 MICRO ELECTRICAL DISCHARGE MACHINING

Micro Electrical Discharge Machining (EDM) is quite similar with the principals of macro Electrical Discharge Machining the only difference is the plasma channel diameter. Micro-scale EDM is a thermal process that utilises electrical discharges to erode electrically conductive materials. Since the materials only applicable are metals, this easily categorises this method as means for mould making. This process involves two electrodes that are separated by a dielectric medium, then brought together to a specific threshold were the dielectric medium breaks down and becomes conductive. As a result, sparks will be generated between the electrodes that create a successive surge of thermal energy. When this thermal energy is released, it causes the material surface to melt and evaporate rapidly, creating voids. The precise control of the energy magnitude regarding voltage and current can help create micro features on any electrically conductive material. Since μEDM is a no-contact and no-force process in comparison to micromilling they can easily be used to cut micro features of complex shapes and thin walled microchannels without distortion. Moreover, the μEDM process leaves no burrs. The major drawbacks are the use of only conductive materials, i.e., (insulators) are out of the process. Moreover, setup cost is more expensive than conventional micromilling.

2.6 PROTOTYPE REPLICATION TECHNOLOGY

This technological process is employed for the sole purpose of replicating parts and components that are integral to the entire POCT chip formation at a mass production level. Commercial viability is also key to this process, as a low cost at high quality improves marketability. Consequently, this is targeted towards end users, but some of its methods can also be utilized in research prototyping. A typical process involves selection of precision fabrication technique to create a master mould that bears the intended design to be replicated through a specific process to several parts.

2.6.1 INJECTION MOLDING

In this replication method, wet or dry etching techniques are employed to create structures with higher aspect ratios [337] and precise geometrical features on a silicon substrate. Subsequently, nickel electroformed [337] is the process used to produce the metal master mould by electroplating a layer of metal, with a thickness within the range of few micrometres to a few millimetres. Metal masters are a lot stronger and longer lasting than masters made of silicon, glass or polymers. They can be utilised to yield hundreds of thousands of injection moulded parts with features microfluidic elements. The replication process involves the nickel electroformed being mounted onto a mould insert and the polymer of choice is melted to a viscous liquid when pushed by a mechanical screw through a heated chamber. Afterwards, the liquid polymer is injected at high pressure into the mounted mould (with nickel electroformed), and as contact is made with the mould walls, the heated polymers start to cool down, resulting in well-defined solid features [338]. Injection moulding technique is very versatile and almost any plastic part, or component can be made efficiently. PMMA [339] and PC [340] are good examples of polymers used in this replication process. The major advantage of this technique is accuracy; it can be used to produce channel sizes ranging from10μm to few hundred micrometres. Their major

Limitation is that they are not cost effective for research prototyping since few copies are required with a frequent change of designs.

2.6.2 HOT EMBOSSING

This method shares a similar process to injection moulding in the case of metal master mould preparation. However, this technique involves the use of a hydraulic press to imprint the master mould forcefully on a polymer material after it has been softening to a temperature close to the T_g. The stamp with the mould design is applied at low pressure for a period less than 10 minutes on the plastic. As a result, plastic, microchannel features are the exact mirror of the metal stamp. Alternatively, this same process can still be done in plastic at room temperature, but high pressures. Though the turnaround time is a lot shorter, the product finishing is much more dependent on numerous constraints including imprinting pressure, imprinting time and properties of the plastic itself [340]. Moreover, the lifespan of room temperature imprinting is a lot shorter than at elevated temperature.

Hot embossing or room temperature imprinting can be successive done on several types of plastic with excellent device-to-device reproducibility. Good examples of plastics include polystyrene (PS)[341], polyethylene tetra phthalate glycol (PETG)[342], polymethylmethacrylate (PMMA)[343], polyvinylchloride (PVC), and polycarbonate[344]. Just like injection moulding their downside is the setup cost and lack of flexibility in design altering needed for prototyping research.

2.6.3 SOFT LITHOGRAPHY

Soft lithography is a widely used rapid and efficient way to create microfluidic prototypes. This method is a very cost effective and is used extensively for research for research purposes. As with all other techniques described thus far, a positive relief master may be needed, but not necessary in silicon. As for this technique, since its research inclined the turnaround time is highly dependent on the fabrication method of making the master mould. As of recent 3D printing techniques have been useful in fulfilling this requirement because of the flexibility involved in design changes endemic in rapid prototyping. In the case of material utilised, an elastomeric polymer that is liquid at room temperature is required to be cast onto the master mould and allowed to cure at a high temperature. Subsequently, the cured material with the micropatterns is bonded to another substrate more likely glass, before they are functional. A commonly used material for this process is PDMS because of its favourable mechanical and optical properties. PDMS is a mixture ratio of a prepolymer and curing agent. A standard mix ratio is 10:1 (i.e. 10g of prepolymer to 1g of curing agent) [246]. As a result, the mechanical properties of PDMS can be narrowly altered by either increasing the prepolymer to reduce elastic modulus or increasing curing agent to increase elastic modulus. The curing process of PDMS can occur slowly at room temperature or speedily at a slightly elevated temperature (generally 40–70 °C for PDMS) before they are peeled off the mould. Polyurethane elastomer is an excellent alternative to PDMS as it has better relative mechanical strength [345] with optical transparency. However, the protocols involved in casting are very stringent and do have potential health [346] concerns.

The major drawback in soft lithography is the design limitation since most moulds are created as either positive or negative the outcome of the cast is a 2.5-Dimensional (2.5-D) object that requires another layer substrate (glass or similar material) to complete it. Although, the fabrication of 3-D is not somewhat impossible but will

require several designs of moulds, that are individually representative of different layers in a multi-layer three-dimensional structure [347].

2.7 SUMMARY

Viscosity and surface tension and wetting stood out to be the most important factors in designing the microfluidic cartridge due to the larger surface to volume ratio in the microchannels. The common purpose they share is to provide fluid flow with minimal drag and ease of manipulation during transit. For viscosity, since most of the anticipated transport fluids and chemical reagent share similar characteristics with water-based solutions, and the viscosity of water is usually sufficient and appropriate in most microfluidic devices. Therefore, viscosity will only be critical in oil based or highly viscosity fluid systems which are beyond the scope of this thesis. The case of surface tension is mostly applicable in interfacial tension that exists in multiphase flow at liquid-gas interfaces. At this boundary, the cohesion of liquid molecules at the surface is greater than the adhesion of the gas molecules. Consequently, considerable surface tension at the interface can reduce adverse bubble formation in continuous the flow. Similar to surface tension is the wetting phenomenon that is primarily concerned with the solid-liquid interface. In microfluidics, the solid microchannels surfaces can either be described as hydrophobic or hydrophilic respect to the fluid interface. In hydrophilic channels, which are known to have minimal boundary slip, the fringe particles of the transport fluid tend to have a stronger adhesive relationship with its surface than cohesion with themselves. As a result, they are a significant influence in the phenomenon of capillarity, which is a self-perpetuating fluid motion that enables fluid spread easily on surrounding adhesive surfaces. This mostly advantageous in enhancing fluid motion in microchannels with minimal means of fluid actuation. Although they are helpful in fluid transport, fluid manipulation or handling may require a more complicated process and most of all; they are susceptible to drag which can interfere with the delicate interfacial tension at the liquid-gas interface in a pressure driven flow. Thus, they may be easily prone to bubbles formation. On the plus side, they are preferable more in biochemical reactions involve liquid separations. On the other hand, hydrophobic surfaces offer considerable boundary slip due to the negligible adhesive interactions with the fluid particles. Thus, there will be less fluid contact, resulting in minimal drag between the surfaces. In comparison to fluid motion of on hydrophilic surfaces that self-actuating, hydrophobic surfaces, requires an existential force such as pressure to propel the fluid through the microchannels. This attribute makes them more susceptible to manipulation in a pressure actuated flow system. Furthermore, advancement in technology has offered innovative surface modification techniques that can be used to create favourable wetting characteristic on a material to be utilised for specific microfluidic applications.

For instance, surface roughness can be a means to amplify hydrophobicity while the use of surfactant or plasma treatment to increase the surface energy that will enhance hydrophilicity. Thus, the understanding of the interactions between the biomolecules and surfaces play a major role in the material selection process.

Amongst the various material discussed polymers as the substrate has shown better significance due to their wide range of physical characteristics suitable for microfluidic applications. Practical cases are their mechanical resilience, transparency and high-temperature tolerance and biocompatibility that form the major features needed for core chip functions such as DNA amplification and detection. PDMS, PMMA, PC and COC tend to be most widely used polymers due to their low cost, ease of fabrication and market availability.

However, other materials that pale in comparison to polymers such as metals, silicon, etc. which don't account for the bulk parts of the POCT chip, do contribute to other microfluidic elements creation or enhancement. For instance, silicon can be used for electromechanical components such as electrostatic diaphragms for valves or pumps. Also, gold can be used as alternate means of optical high-sensitivity detection by in microfluidic channels by Resonant light scattering spectroscopy. On the other hand, fabrication techniques mainly revolve around setup cost, production cost, surface roughness, the simplicity of operation and aspect ratio definition. Of all the above attributes mentioned, none of the fabrication technique discussed offers a total solution. Moreover, it can be deduced that as the surface finish and aspect ratio improves there is a significant correspondence in the product and setup cost. Besides, prevalent technology makes some of these techniques not yet appropriate for POCT device creation because of the poor surface finishing or the limited choice of materials that can be processed with their respective protocols. Nonetheless, 3D print offers a reasonable solution in academic or research environment as a result of the recent improvement and commercial availability of printers in the marketplace. While for the commercial aspect, hot embossing and injection moulding are the still the best available option as of yet.

3. DESIGN AND FABRICATION OF CARTRIDGE

3.1 INTRODUCTION

In this section, a 3D concept model of a microfluidic cartridge was designed to achieve rudimentary functions of DNA extraction, purification, and amplification. The concept model of the microfluidic cartridge entails element such as inlet, outlet, chambers, valve, multiplexer and most importantly the microchannels that link all components up. Taking into cognizant the knowledge gain from the literature review, the choice of material was PDMS, while the means of cartridge fabrication was soft lithography. Likewise, the means of sealing the cartridge was done utilising the plasma bonding technique also described in chapter two. 3D printing which was key in determining the aspect ratio of design modelling process was chosen as a means fabricate moulds required for casting the PDMS structure. Furthermore, the principle of passive valve operation, discussed in the literature review was also considered when designing the passive valve and multiplexer which are both required for the chip to perform its primary functions. The means of validating the prototype cartridge model was done by the use of computational fluid dynamic simulation.

3.2 DESIGN OBJECTIVES:

The design process aimed to fabricate a microfluidic cartridge capable of performing complex fluid handling operations that are representative of laboratory chemical protocol in a continuous flow process. In order to achieve this cartridge functionality, the following objectives were met:

- Design a 3D model microfluidic chamber that will perform DNA extraction and elution.
- Design a 3D model microfluidic waste chamber that will handle waste treatment
- Design a 3D model microfluidic chambers that will perform DNA amplification
- Design a multiplexer to distribute fluid to the designated amplification chambers
- Design a passive valve to regulate flow within the cartridge
- Perform computational fluidic dynamics simulation to validate the cartridge functions
- Fabricate the concept cartridge model by soft lithography using PDMS and a 3D printed mould
- Performing a sealing process with glass slide using plasma the bonding technique

3.3 DESIGN GEOMETRY OF FLUIDIC ELEMENTS

This chapter is primarily concerned with the interconnectivity and interdependency between the inlet, outlet, microchannels and chambers on the chip. Each pair of fluidic elements plays unique roles within the distribution flow network. Likewise, their dimensions and geometrical configurations are prerequisite parameters for determining flow characteristics of the anticipated fluid movement. The predefined sectional boundary of the chip was derived from a "50mm x 75mm" glass microscope slide. This slide provides the area which all the fluidic elements will be positioned spatially to one another in the flow network. In the case of depth of the chip, 4mm provides material thickness sufficient to enhance strength as well as provide excess space regarding the height of fluidic elements. The Solid Works 3D design software is the means utilised to create 3D prototype design concepts.

Lab-on-a-chip protocols are the prerequisites before any design conceptualization, and in this section, a summarised version is utilised to form a fluid flow pattern on the positive mould (detailed experimental protocols are discussed in the amplification chapter). The pre-requisite aspect ratio of 0.5 mm was used to define most of the microchannels within the microfluidic chip model design as depicted in Figure 3.1. This aspect ratio was the preferable choice when the relative sizes of other fluidic element and most the available 3D printer quality were all taken into consideration. Detailed design configurations of the other modular features of the cartridge are discussed in the later sections of this chapter. The below are the required fluidic elements:

- One amplification inlet port
- One sample inlet port
- Six amplification outlet ports
- One waste outlet port
- One central reaction chamber (CRC)
- One waste reaction chamber (WRC)
- Six amplification reaction chambers (ARC)
- One passive valve
- One non-sequential multiplexer
- Microchannel network of 0.5mm aspect ratio (Figure 3.1)

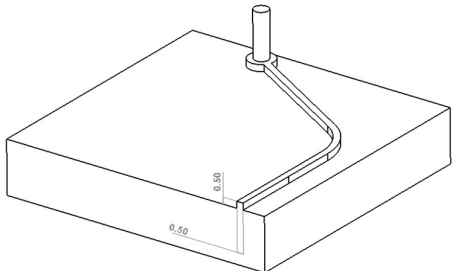

Figure 3.1. Pictorial illustration of microchannel aspect ratio of (unit mm).

3.3.1 3D GEOMETRY DESIGN OF INLET AND OUTLET PORTS

The design concept revolves around apertures that fit with individual microfluidic external fittings and connectors (e.g. syringe) for mostly the case of the inlet. Although, they may also apply to outlets if the

processed sample is to be extracted for post-processing in the case of DNA gel analysis. In all, outlets and inlets as supposed to be open enough to permit airflow and sufficiently reduce environmental or ambient interference. The Figure 3.2 depicts the design configuration used.

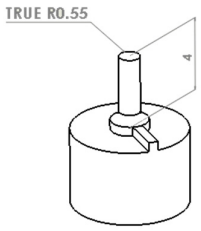

Figure 3.2. 3D geometrical design of inlet and outlet (unit mm).

3.3.2 3D GEOMETRY DESIGN OF CENTRAL REACTION CHAMBER

This design aims to create a chamber with functions such as; less flow resistance (that aids quick fill-up) and minimal air bubbles formation. It is also worth mentioning that it is imperative for this specific design functions should have experimental repeatability. Furthermore, the design also took into consideration space management and anticipated fluid volume capacity due to the insertion of a chitosan membrane within the chamber Figure 3.3b. The chosen shape is trapezoidal, and Figure 3.4a shows the dimensions of the reservoir geometric design. The volume capacity of the central reaction chamber (CRC) is 115 µL without the chitosan, but have a net volume 65 µL with the chitosan thickness of 650µm. The determinant factor for the liquid capacity was deducted from the experimental liquid sample requirement.

3.3.3 3D GEOMETRY DESIGN OF WASTE REACTION CHAMBER

The reasons for a circular waste chamber are space management and proximity to the reaction chamber. Smooth and quick waste deposition in the waste chamber was significant to the chip function as a result proximity of both reaction chambers was imperative in the design modelling. The proximity of the waste chamber to the reaction chamber was imperative. Likewise, as a result of proximity space management (Figure 3.3a) was considered because a high-volume capacity bigger than the CRC was required. Furthermore, circular chambers require less space in comparison to trapezoidal chambers for equal volume due to their cross-sectional area. The capacity of the design model (Figure 3.3c) is 220 µL which is twice the volume of the CRC. This volume disparity, provide sufficient room to accommodate the total volume expelled from the CRC as well as the chemical waste treatment that involves volume expansion.

Chemical waste treatment primary functions are to store and treat the liquid from expelled CRC. In other words, the main purpose is to prevent waste fluid in the WRC from going into the immediate environment to biological pollution. This chemical process involves the use of proprietary superabsorbent polymers (SAP) also referred to as Sodium Polyacrylate. These polymers are extremely hydrophilic and can absorb and retain extremely large quantities of a liquid relative to their mass (about 500 times its weight). Below are the physical properties of the gotten from the manufacturers [348]:

- Appearance: White Powder
- Absorption Capacity: De-ionized water 400 times
- Absorption Capacity: 0.9% NaCl solution 60 times

- Bulk Density: g/cm3 0.6
- pH: 6 to 8

SAP does have the capability to be concentrated up to 99.9% liquid and then solidify in gel-like substance within forty to fifty seconds depending on the chemical nature of the waste liquid. For instance, it is indicated by the manufacturer that 35g will solidify approximately 800ml of liquid. So, therefore, by mathematical deduction of cross multiplication: 10 grammes of SAP (Figure 3.3c) will solidify approximately 220ml of liquid. This liquid amount (220ml) is about four times the capacity of the central reaction chamber (Figure 3.3b) with chitosan and twice without. With this liquid volume design consideration, a proper contingency for excess fluid is made available.

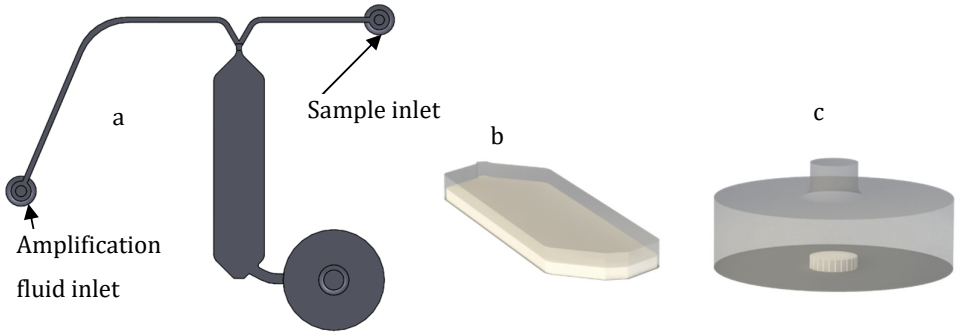

Figure 3.3. (a) 3D geometry design of central reaction and waste chambers. (b) Central reaction chamber with chitosan. (c) Waste reaction chamber with Sodium Polyacrylate (Superabsorbent powder).

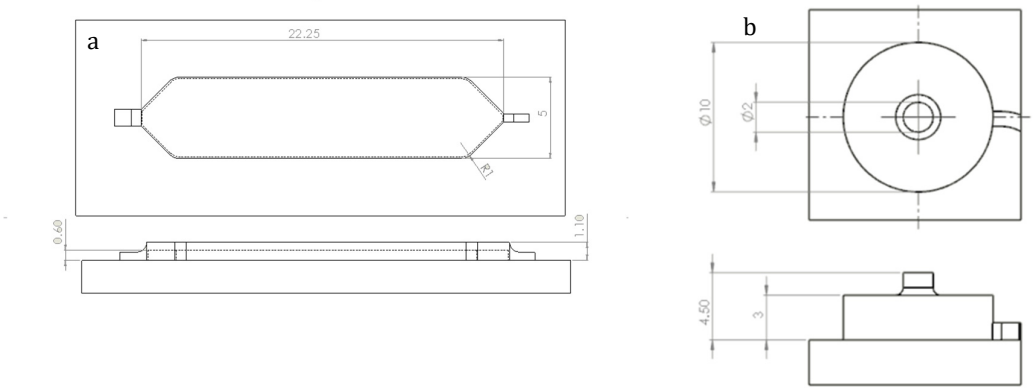

Figure 3.4. (a) 2D schematic diagram of central reaction chamber. (b) 2D schematic diagram of waste reaction chamber.

3.3.4 3D DESIGN OF A MICROFLUIDIC AMPLIFICATION CHAMBERS

The geometrical design of this chamber is prescribed from previous research was done by Doclab at Brunel University [349], that made use of similar chamber design and spatial configuration. This choice of reservoir design was chosen as a result of the real-time Fluorescence DNA detection device [350] manufacture specifically for the geometrical shape characteristics. Focus, in this thesis, was to use this design features, but in this case, six chambers were connected in a parallel configuration. This configuration enables fluid filling

up simultaneously within a very short period. So below is the 3d design concept of the parallel linked amplification chambers (Figure 3.5). Volume capacity of each chamber is 35µL which is aligned with the amplification reaction requirement.

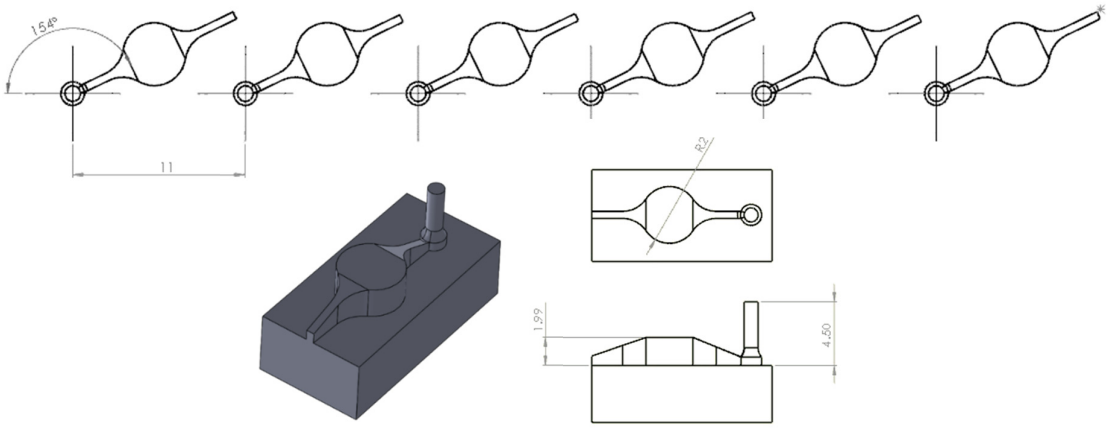

Figure 3.5. Prearranged design formation of amplification chambers (unit mm).

3.4 3D DESIGN OF PASSIVE MICROVALVE

The passive valve design in this thesis utilises a geometrical feature to control or regulate fluid flow between to key process termed first half and second half which are properly illustrated in more detail in later sections. Furthermore, this device also brings to together the main sections of the microfluidic cartridge (Figure 3.6) as shown in Figure 3.7. Fluid flows into the WRC for processing indicates the end of the protocols within the first half of the experimental process. As fluid volume builds up in the waste reservoir, the passive valve temporally restricts flow to microfluidic multiplexer till the start of the second half process. Figure 3.9 shows the fluid flow overreach into the multiplexer during the waste volume fill-up process. This action is critically needed to avoid complicated fluid handling mechanisms, while at the same time prevent contaminants from entering the amplification chambers which may have an adverse effect on the overall experimental results. Figure 3.8 gives a vivid process involving several test configurations used to develop an efficient passive valve. Although, the variables tested were restricted to a range of values from “200 to 500 microns” aspect ratio that was within the resolution capacity of the 3D printer (Viper SLA stereolithographic printer) used.

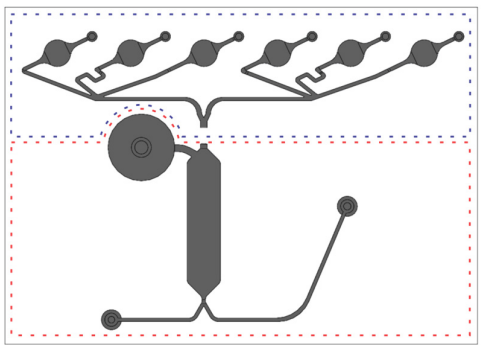

Figure 3.6. Separation of chip into two distinct sections by the use of red and blue dotted lines.

From the figure above the section bounded by red dotted lines are representative of the sequence involving fluidic processes within the CRC and WRC, while the processes that occur within the multiplexer and ARC are represented by the blue dotted lines. Each section is connected to another by a passive valve. The mechanics of the passive valve design involves the use of a narrower channel to bridge to similar channels of similar geometries. This geometric interruption is responsible for regulating flow between each section by hindering flow temporally as a result of pressure variation across the narrow channel. The (narrowness Figure 3.8) of the passive is proportional to the passive valve resistance which relies heavily on the aspect ratio finish of the 3Dprinter due to the microstructure required.

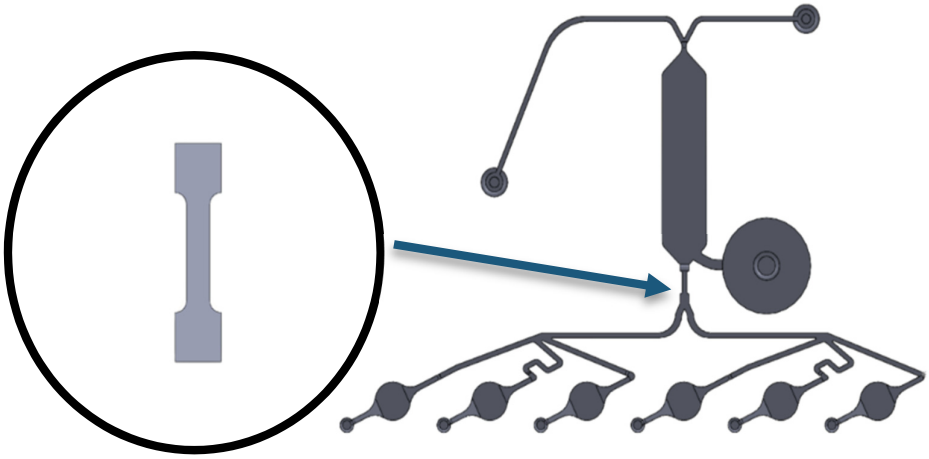

Figure 3.7. Illustration showing the use passive valve to bridge the two main sections of the microfluidic chip

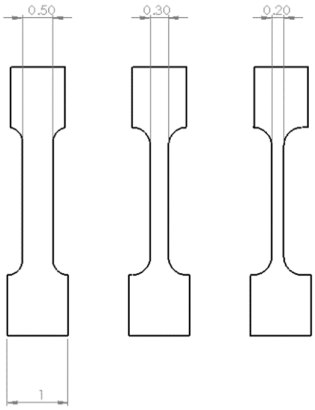

Figure 3.8. Schematic diagram of the different narrow width thickness of the passive valve tested by simulation.

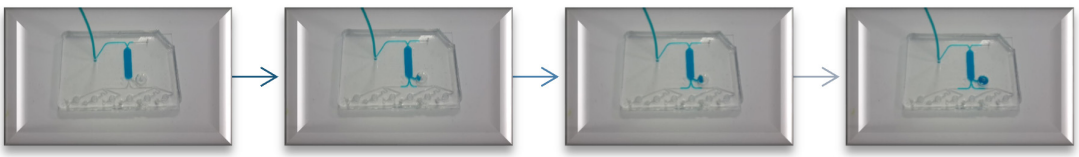

Figure 3.9. Fluid flow overreach in the multiplexer during the waste chamber filling process as a result of the absence of a passive valve.

3.4.1 MULTIPHASE FLOW SIMULATION OF PASSIVE VALVE

In this simulation, the computational domain of the test model is filled with air at the initial stage. Unlike single phase flow, that assumes the model to be a vacuum that will be filled gradually by an independent fluid. The initially filled region will be progressively displaced by another fluid inflow into the computational domain. Both the fluids in this simulation a separated by an Interfacial surface tension boundary that prevents unwanted mixture of the fluids. Although, constraints such as wall condition, pressure, the speed of flow and most especially geometrical shape may cause a temporary rupture in the interfacial boundary film; leading to air bubbles formation. The goals of this experiments are to ascertain proper filling of both chambers without air bubble formation, and time it takes before the passive valve seal is breached.

Below are the boundary conditions for the experiment carried out using Ansys Workbench CFX.

Initial Boundary conditions:

- Simulation time 20 seconds
- Chamber volume 50µL
- Air @ 25^0C (fills the chamber)
- Ambient pressure 1 atm
- Air density 1.185 kgm^{-3}
- Inlet-Water flowrate 8µL/s
- Water density 998 kgm^{-3}
- Water (liquid)-Air (gas) Interfacial surface tension 0.072Nm
- Wall (solid)-liquid (water) surface tension hydrophobic condition
- Free surface flow

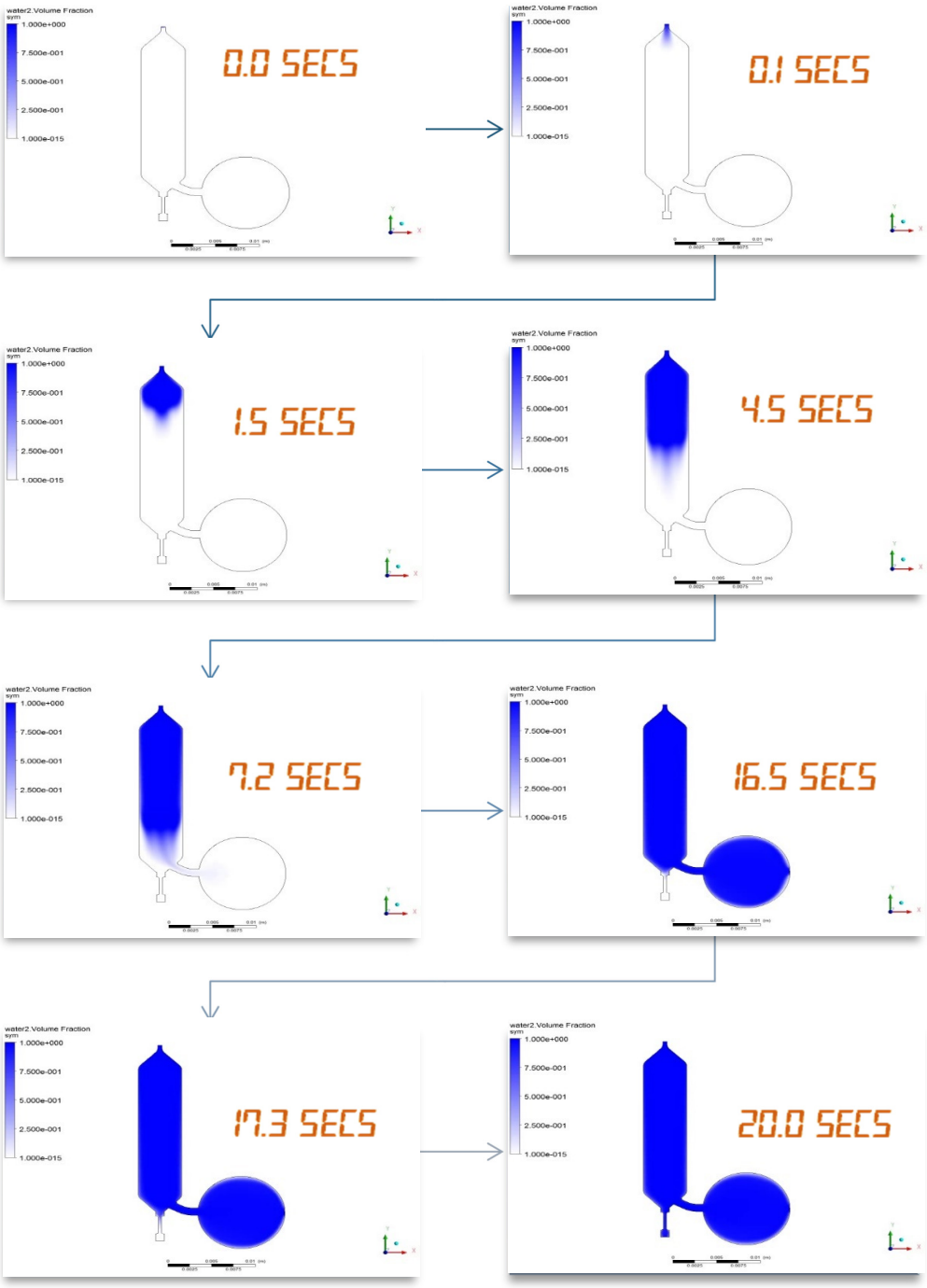

Figure 3.10. Multiphase simulation showing flow regulation of fluid by a pressure sensitive passive valve (300μm width)

3.4.2 SINGLE PHASE FLOW SIMULATION OF PASSIVE VALVE

Unlike multiphase simulation, single phase involves only one fluid moving through a vacuum while simultaneously interacting with the geometrical constraints within the defined volume domain. As a result, the variation of pressure and inflow velocity within the domain will be captured.

Below are the boundary conditions for the experiment carried out using COMSOL Multiphysics.

Initial Boundary conditions:

- Ambient pressure 1 atm
- Inlet-Water flowrate 8µL/s
- Water density 998kg/m^3
- No slip boundary condition

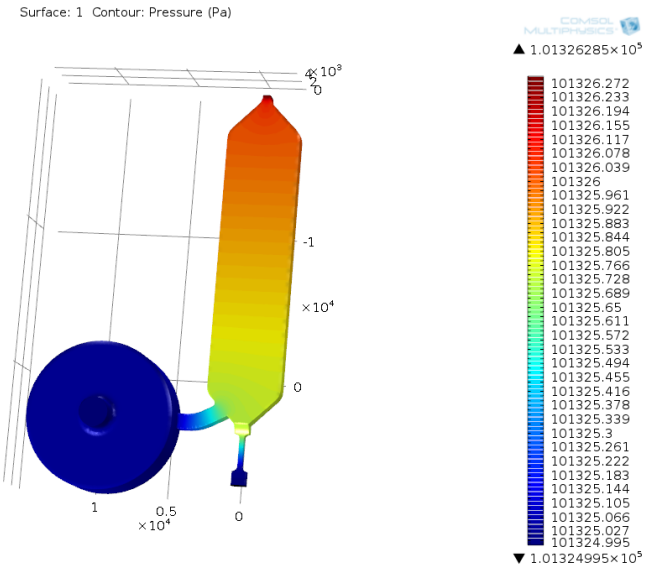

Figure 3.11. Depiction of pressure variation within the volume domain as fluid move from central chamber to the waste chamber and also the passive valve (300µm width).

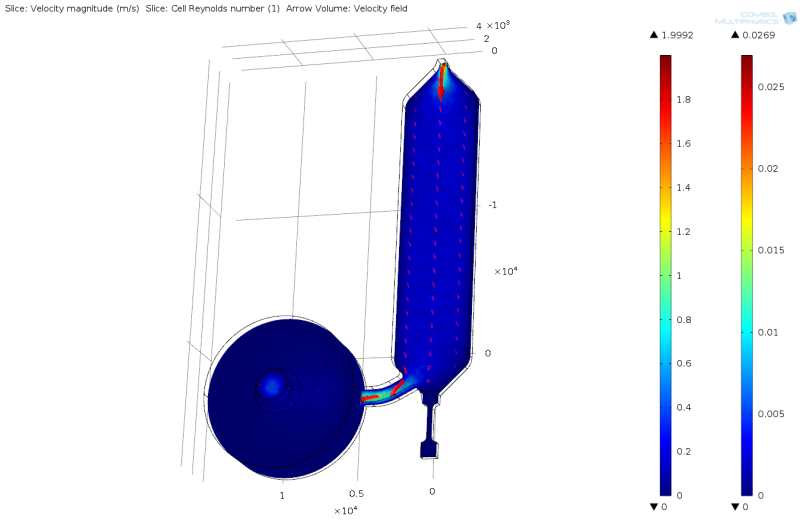

Figure 3.12. Illustration of flow velocity variation in the volume domain as flow moves waste channel and passive valve (300µm width). The first legend on the right-hand side indicates the Reynolds number, while the second legend highlights flow velocity in metres per seconds (m/s).

3.4.3 SIMULATION ANALYSIS OF PASSIVE VALVE

The simulation performed in Figure 3.10, 3.11 and 3.12 were done on three different passive valve thickness as shown in Figure 3.8. After this simulation exerscise, the width thickness of 300µm was selected. The empirical methods were used for this deduction.

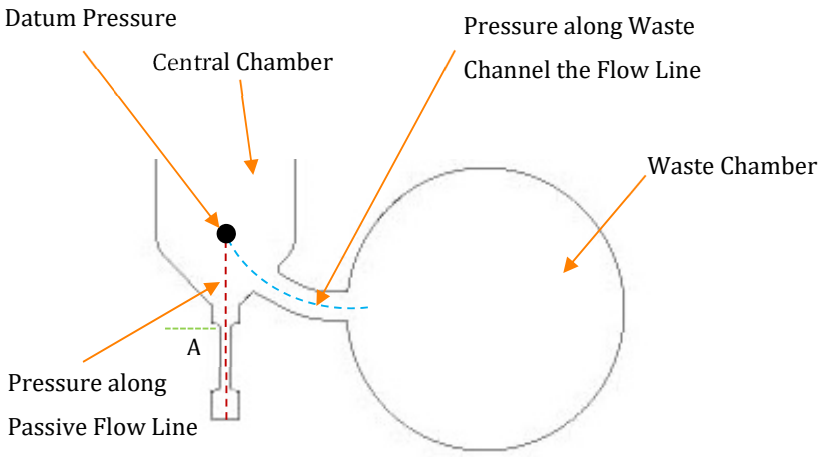

Figure 3.13. Schematic diagram showing the means of deriving the pressure drop along the passive valve of various narrow width thickness (300µm, 400µm and 500µm) and channel waste chamber of various by a single phase CFD simulation.

In Figure 3.13, two broken lines (red and blue) originate from a common nodal point where pressure was expected to be equal. The red line indicates pressure variation for all the different width, while the blue line represents the waste channel flow. Furthermore, the green line which is highlighted by the marker A specifies the region where the pressure seal likely breaks. At this threshold point the maximum buildup of pressure stalls. The simulation results at a flowrate of using water at 8µL/s are graphically illustrated in Figure 3.14, as it highlights the individual pressure differential of all the selected narrow passive valve widths along with the waste channel. The graph shows the why the flow preferably moves to the waste channel by the disproportionate pressure variation of the blue line in comparison with the others. This flow singularity can be illustrated in Figure 3.12, as it shows a transient acceleration of flowrate from (0.0092m/s to 0.0128m/s) into waste channel.

Likewise, the reference point **A** depicts the transitional point between the more extensive and narrow section where the valve seal has a high probability of failure. An interesting repetitive pattern which shows pressure steadily decline at a very listless pace as it approaches the reference marker A. Afterwards, there is a sharp decline in pressure as the flow progressively moves past the narrow section. This phenomenon explains the sudden and short-lived rapid increase in velocity as fluid enters the constricted channel due to a sudden drop in pressure. From then onwards minimal pressure differential is required to maintain flow through the narrow channel. When comparing all three dimensions, the 500 microns valve already indicates a rapid drop in pressure

before fluid gets to the reference point A (101325.8158 Pa). At this point the valve has a high probability failure rate in contrast to the 200 and 300 microns valves that exhibited steady decline. Although, 200 microns valve (101325.9567 Pa) show a better potential than the 300 microns (101325.9009 Pa); it was not preferred.

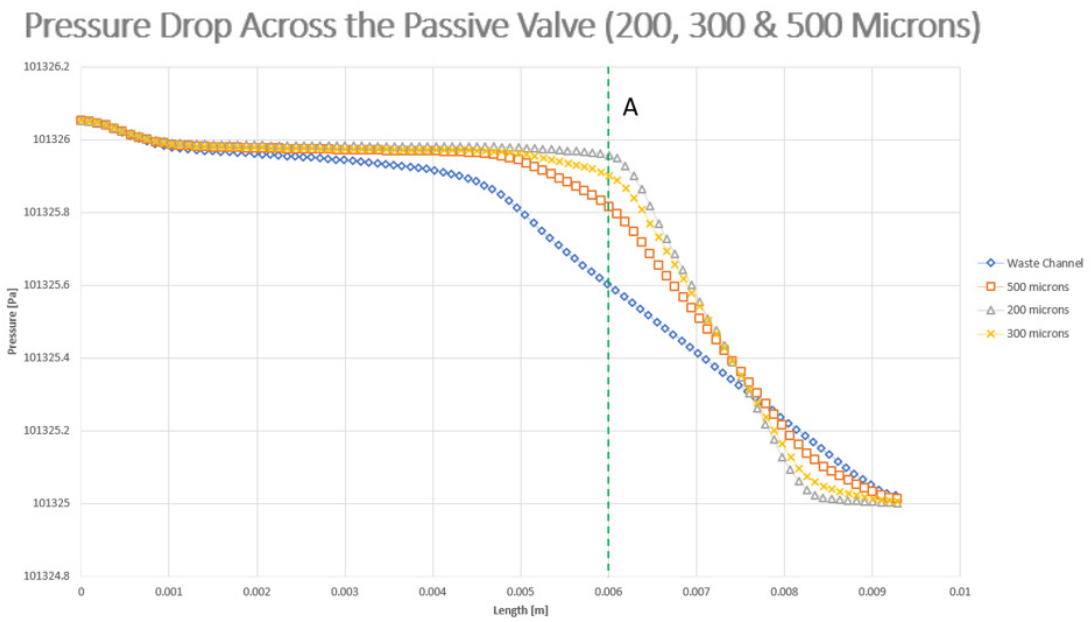

Figure 3.14. Line graph showing the pressure along passive valves width (300µm, 400µm and 500µm) in comparison with the pressure along the channel leading to the waste chamber.

There are three critical reasons for this choice. First, the 200 microns dimension is very close to the 3D printer most exceptional aspect ratio which may give room for inconsistent geometrical layer formation. Secondly, the pressurized high flow at a rate within the region of 10µl/s may result in liquid shearing along the narrow channel dominated by high surface tension due to its hydrophobic characteristics and a large surface to volume ratio. This drawback may result in air bubble formation mostly when multiple fluids are expected to be used on a single cartridge serially; resulting in the valve functionality impairment. However, the possibility of this occurrence can be mitigated by significantly reducing the length of the passive valve. The Third factor brings into focus time constraint as shown in Figure 3.10 that utilizes Ansys multiphase CFD simulation to depict water been regulated to the waste chamber before the 300 microns valve seal breaks above the period of 17 seconds. As a result, a slimmer version of the valve will require need more time which may not be suitable for the overall fluid processing time of the microfluidic cartridge. Also, the use of excessive pressure to compensate for very narrow conduit may be counterproductive since relatively flowrate systems are more manageable and sustainable.

3.5 3D DESIGN OF A MICROFLUIDIC MULTIPLEXER

The design of a parallel circuit that is utilised in distributing equal amplification reagents simultaneously to the six amplification reaction chambers (ARC). The spatial configuration of the multiplexer channels circuit is

contingent on the limited space as illustrated in (Figure 3.6) as the dotted blue lines. Furthermore, Figure 3.6, also shows critical node points (a, b and c) that were specifically chosen to be key distribution points for each six ARC. Node "a" is the main distribution point that creates two different microchannel paths to node "b" and "c" equidistant from each other. Furthermore, since each of chambers was prearranged as secondary nodes (b1, b2 and b3) are directly interlinked to primary node "b" at equal distance. Likewise, secondary node (c1, c2 and c3) are linked to primary node "c" at equal distance. For unique cases, such as serpentine microchannel link between b-b2 and c-c2 are a result of space management consideration when equal distance is to be applied to all secondary links (b-b1, b-b2, b-b3, c-c1, c-c2 and c-c3). Each of this secondary links of equal length from their primary nodes a form a non-sequential multiplexer that divides the dispensed amplification reagent into six equal volumes to be delivered to the amplification reservoirs.

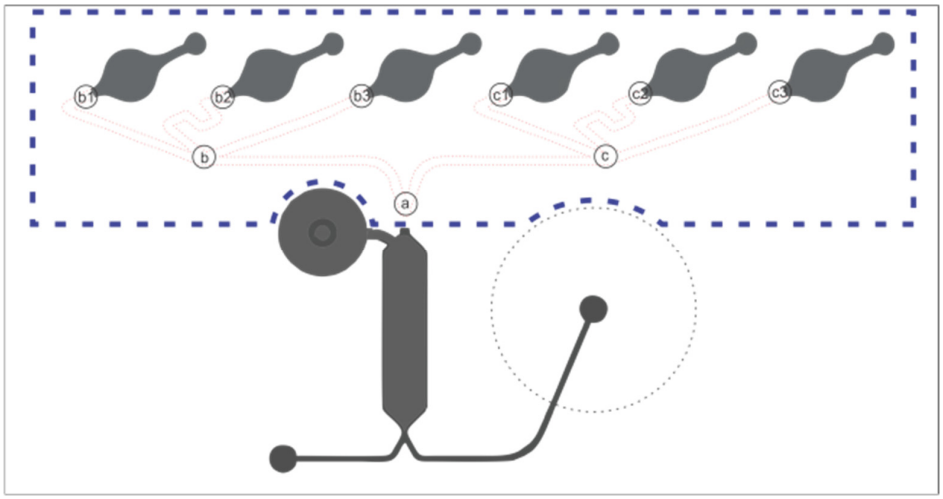

Figure 3.15. Spatial configuration of a 0.5mm aspect ratio multiplexer microchannels linked to the six amplification chambers

3.5.1 MULTIPHASE FLOW SIMULATION OF MULTIPLEXER

The simulation protocols and parameters employed here are similar to that of the passive valve. The goal of this simulation observes the capability and efficiency of the multiplexer to fill each of the six amplification chambers. Below are the Initial Boundary conditions for the experiment carried out using Ansys Workbench CFX.

- Simulation time 30 seconds
- Inlet-Water flowrate 8µL/s
- Water density 998 kgm^{-3}
- Ambient pressure 1 atm

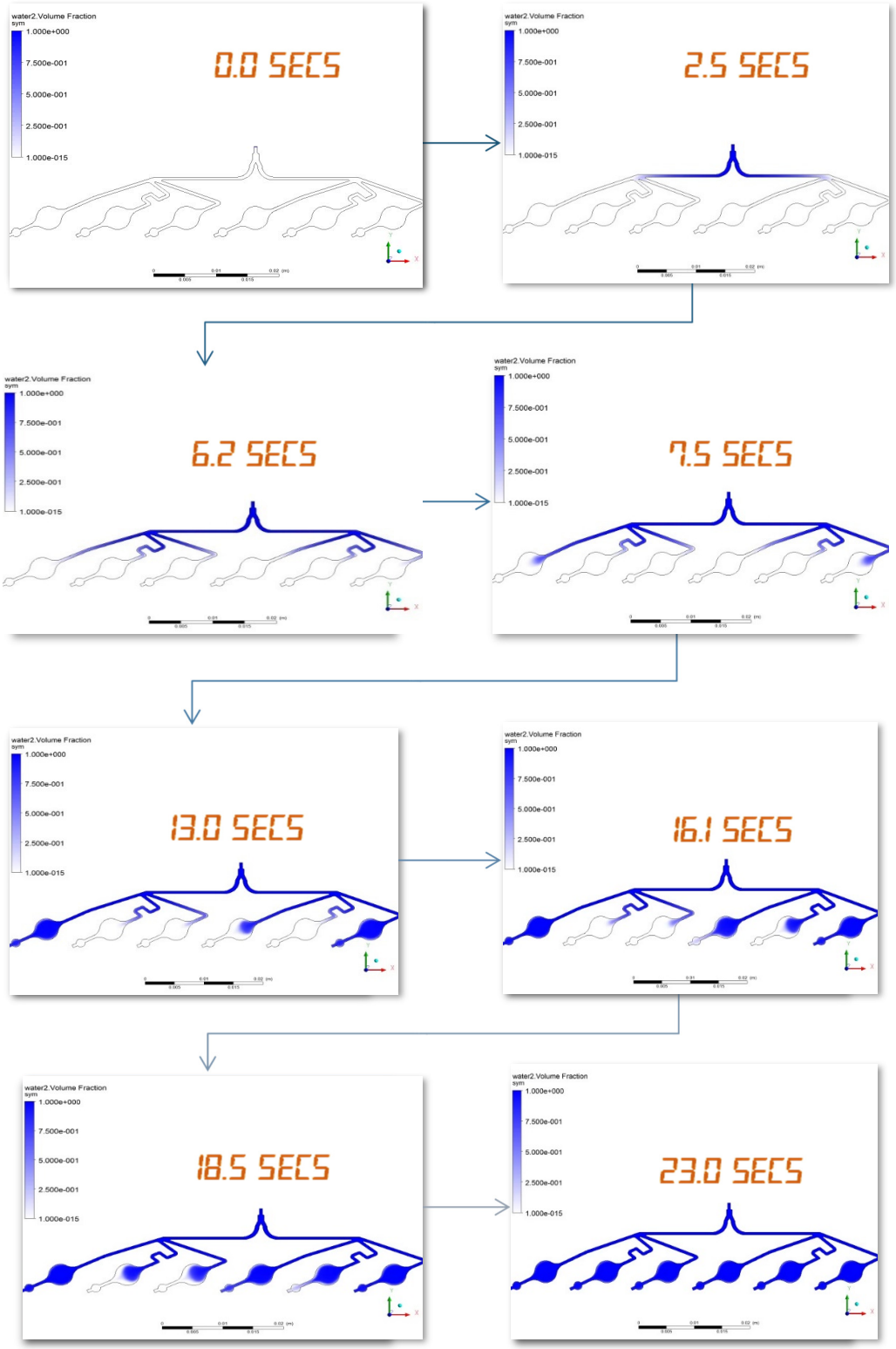

Figure 3.16. Ilustration of the filling of the ARC by gradual displacement of the prevalent air by the inflow of water.

3.5.2 SINGLE PHASE FLUID FLOW SIMULATION OF MULTIPLEXER

The goal of this experiment was to deduct the change in fluid flow velocity through multiplexer bifurcated microchannels as well as the pressure drop across each of them. Below are the boundary conditions for the experiment carried out using COMSOL Multiphysics.

Initial Boundary conditions:

- Inlet-Water flowrate 8µL/s

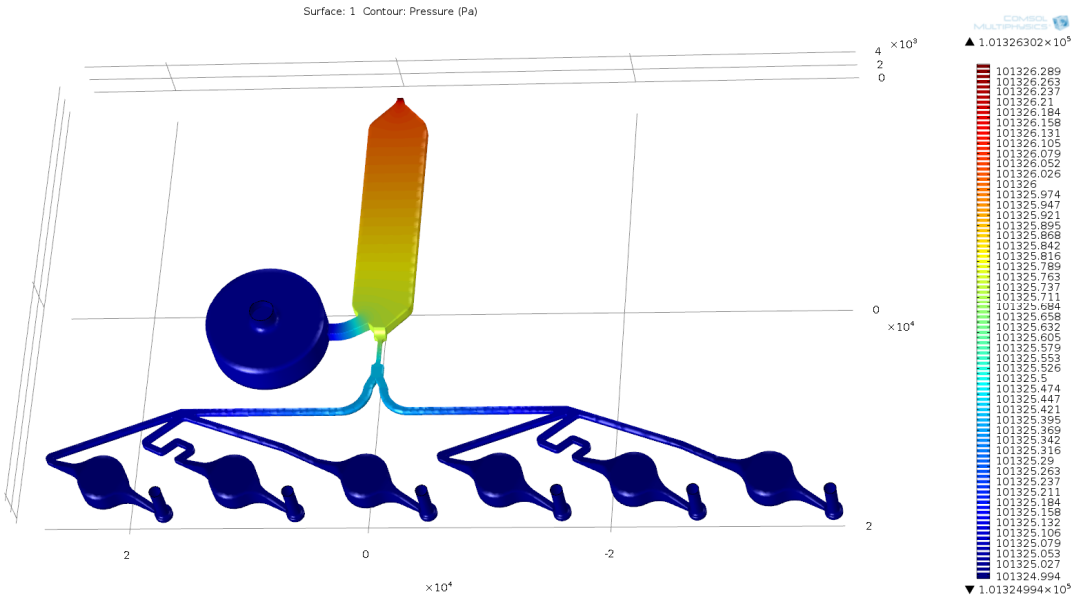

Figure 3.17. Illustration of pressure variation within the volume domain as fluid move from central chamber through the passive valve (300µm width) to the multiplexer for distribution the amplification reservoirs.

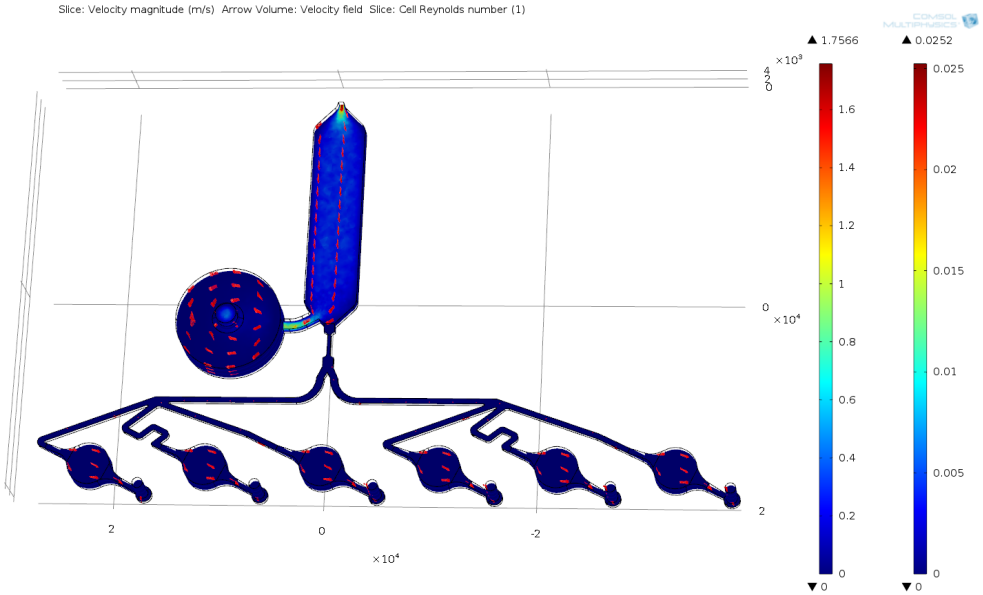

Figure 3.18. Depiction of flow velocity variation in the volume domain with passive valve of (300µm width) connected to a multiplexer. The first legend on the right-hand side indicates the Reynolds number, while the second legend highlights flow velocity in metres per seconds (m/s)

3.5.3 SIMULATION ANALYSIS OF MULTIPLEXER

The primary goal was meant to be achieved with the multiphase and single phase simulation. The multiphase simulation displayed in Figure 3.16 was used to observe the fluid filling pattern of the bifurcate microchannels as well as their ability to completely fill up all six connected chambers. At the 6.2 seconds mark of Figure 3.16, it shows similar fluid distribution along the six multiplexer veins with subtle differences which mainly as a result of the difference in geometrical features such as microchannel bends and elbows. Subsequently, as flow progressed the liquid filling amongst the six chambers could be seen as unconventional as it developed into a non- sequential pattern. In summary the multiphase showed the efficacy of the multiplexer to fill up the all six chambers in no particular order.

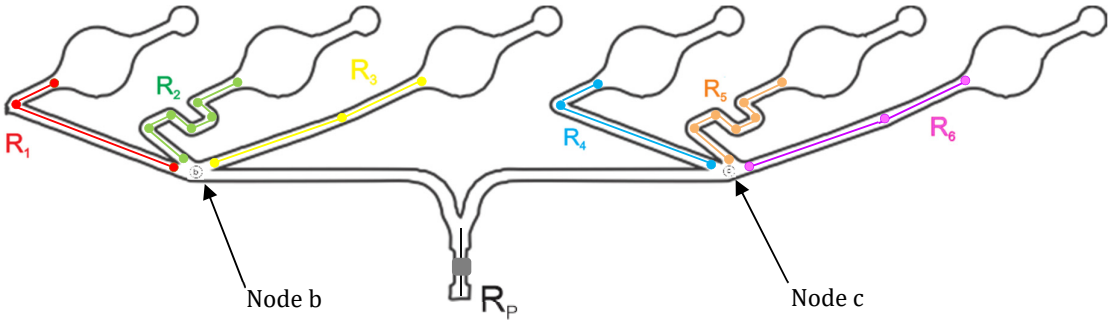

Figure 3.19. Vein outline in the multiplexer to indicate flow pathway from designated nodal points b and c

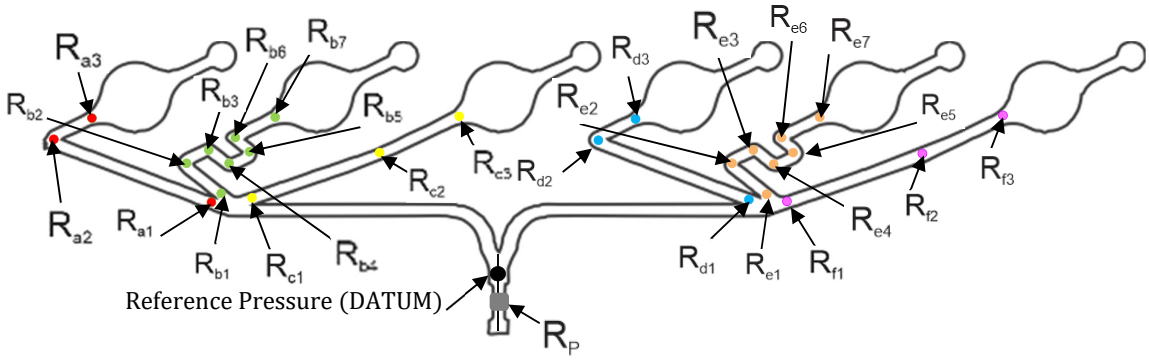

Figure 3.20. Selected pressure points where pressure drops are most critical

Single phase simulation was deployed to investigate the subtle flow resistance in the multiplexer channels and also the anomaly in the filling pattern in the ARC. During this flow process, subtle fluctuations in pressure and velocity were expected. This anticipated instability in flow velocity is depicted in Figure 3.18. In the Figure, the average speed in all reaction chambers is less than or equal to a Reynolds number of 1. As for the rest areas inclusive of the multiplexer and passive valve the change in flow is very subtle. Similarly, in the case of pressure in the volume domain; it can be observed in Figure 3.17 pressure variation from of flow from the passive valve to all outlet ports of the ARC are within the range of 101325.5 Pa to 101325.0 Pa. This pressure variation is vividly captured in the multiplexer by the use of flow distribution vein outlines illustrated in Figure 3.19 (**R_1**, **R_2**, **R_3**, **R_4**, **R_5** and **R_6**) which have their origins from node **(b** and **c)**. Pressure drop analysis performed on the outlines are represented graphically in the (Figure 3.20) on each vein hailing from their designated nodes.

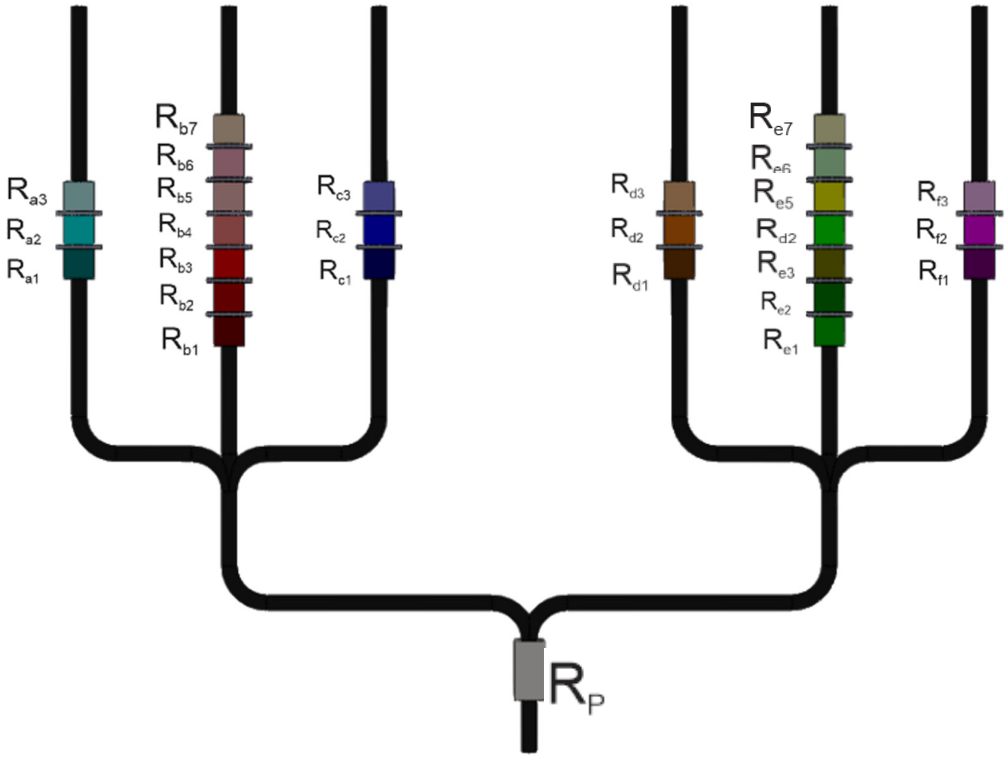

Figure 3.21. Representation of critical pressure points in Figure 3.18 as electronic resistors on a conducting wire.

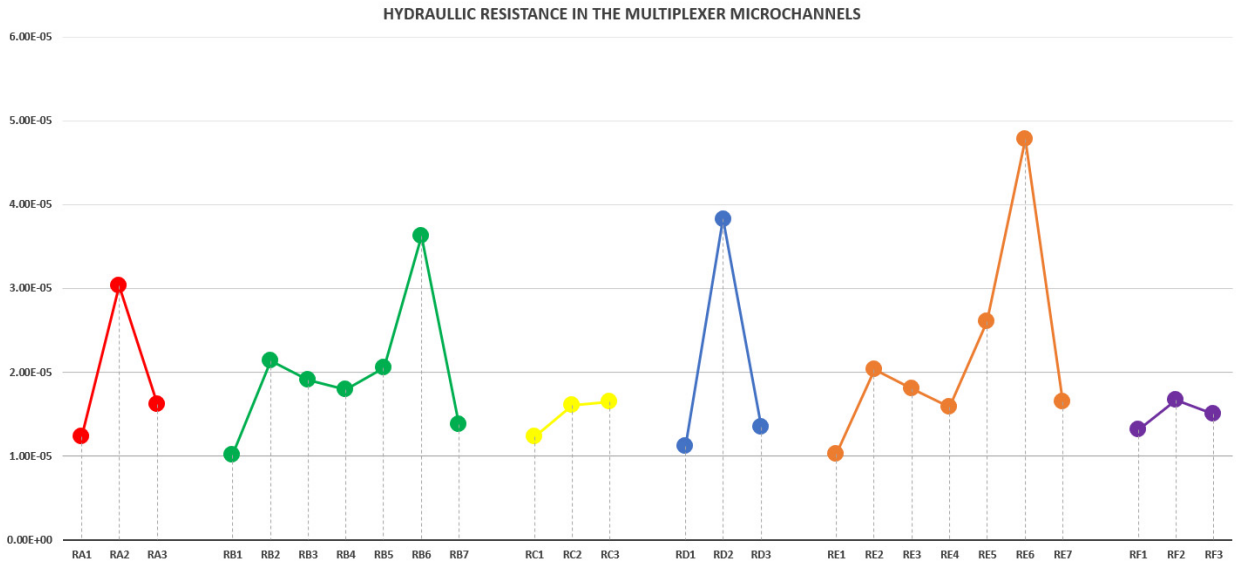

Figure 3.22. Graphical illustration of fluidic resistance at the critical pressure points shown in Figure 3.20

Table 3.1. The derivation of fluidic resistance from critical pressure points concerning datum pressure. Note due to the subtle change in pressure registered at nine decimal places, the equal depiction of decimal numbers on the table was very difficult to achieve.

CHANNEL DESIGNATION	PRESSURE (MPA)	PRESSURE DROP ΔP (DATUM-R)	FLOWRATE Q [MM^3/S]	HYDRAULIC RESISTANCE ΔP/Q (NS/MM^5)
DATUM PRESSURE	0.101331054			
RA1	0.101326406	4.64811E-06	3.78E-01	1.23E-05
RA2	0.101325531	5.52375E-06	1.82E-01	3.03E-05
RA3	0.101325359	5.69569E-06	3.51E-01	1.62E-05
RB1	0.101326418	4.63618E-06	4.57E-01	1.01E-05
RB2	0.101326179	0.000004875	2.28E-01	2.14E-05
RB3	0.101326008	5.04681E-06	2.64E-01	1.91E-05
RB4	0.101325853	0.000005201	2.91E-01	1.79E-05
RB5	0.101325706	5.34814E-06	2.61E-01	2.05E-05
RB6	0.101325595	5.45932E-06	1.51E-01	3.62E-05
RB7	0.101325394	5.66070E-06	4.11E-01	1.38E-05
RC1	0.101326447	4.60697E-06	3.75E-01	1.23E-05
RC2	0.101325780	0.000005274	3.28E-01	1.61E-05
RC3	0.101325394	5.66052E-06	3.43E-01	1.65E-05
RD1	0.101326432	4.62263E-06	4.13E-01	1.12E-05
RD2	0.101325587	5.46766E-06	1.43E-01	3.83E-05
RD3	0.101325404	5.65039E-06	4.19E-01	1.35E-05
RE1	0.101326406	4.64817E-06	4.55E-01	1.02E-05
RE2	0.101326166	0.000004888	2.41E-01	2.03E-05
RE3	0.101325991	5.06367E-06	2.82E-01	1.80E-05
RE4	0.101325841	5.21380E-06	3.31E-01	1.58E-05
RE5	0.101325700	5.35431E-06	2.06E-01	2.60E-05
RE6	0.101325588	0.000005467	1.14E-01	4.78E-05
RE7	0.101325428	5.62675E-06	3.41E-01	1.65E-05
RF1	0.101326372	4.68257E-06	3.57E-01	1.31E-05
RF2	0.101325707	5.34724E-06	3.21E-01	1.67E-05
RF3	0.101325388	5.66629E-06	3.77E-01	1.50E-05

Further analysis was carried out on the fluidic resistances at specific junctions (Figure 3.20 and 3.21) where pressure loss was expected to critical. Hagen pousilles equation was used to calculate the fluidic resistance as shown in Table 3.1. It also worth noting that the reference pressure to used determine the pressure drops in each critical point was chosen at node "a." at this point flow velocity is redeveloping again, pressure is stable, and most importantly flow distribution originates there. The anticipated fluctuation of the resistances in each location is captured accurately in Figure 3.22 graph which shows a mirror-like a behaviour between branches of similar geometrical structures. For instance, branch R_1 having a resistance of ($\mathbf{r_{A1}}$, $\mathbf{r_{A2}}$ and $\mathbf{r_{A3}}$) show similarities to branch $\mathbf{R_4}$ of resistance ($\mathbf{r_{D1}}$, r_{D2} and $\mathbf{r_{D3}}$). Correspondingly, branch R_2 having a resistance of ($\mathbf{r_{B1}}$, $\mathbf{r_{B2}}$ and $\mathbf{r_{B3}}$) show similarities to branch R_5 of resistance (r_{E1}, r_{E2} and r_{E3}) and R_3 with R_6. However, the stark dissimilarities between the $\mathbf{R_{Bn}}$ series and $\mathbf{R_{En}}$ series are came a result of the slight geometrical difference in dimensions (1.e they don't share the same dimensions).

In the case of the non-sequential filing of the amplification chamber, the geometrical features of each ARC outlet were taken into consideration. From the Figure 3.23b, a flow line method similar to the passive valve analysis was employed across the broad and narrow regions of the ports. These features are similar to a passive valve as flow moves from a wide section to a narrow section and as a result, there will be resistance to flow due to pressure. This pressure in pressure was captured in the Figure 3.24, that show the various drop in pressure across each port when liquid enters their chamber.

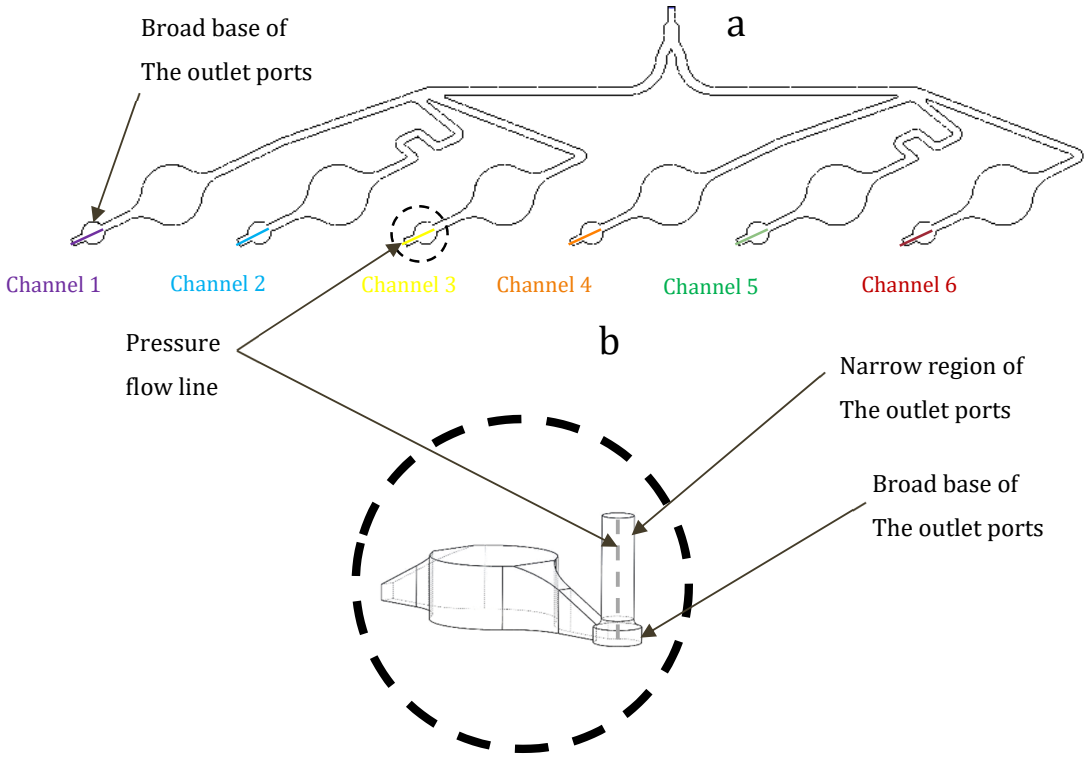

Figure 3.23. (a) 2D illustration of the Multiplexer connected to six amplification chambers with pressure lines along their exit ports. (b) Magnified 3D depiction of the pressure lines the outlet ports that offer characteristics similar to a passive valve due to its geometric features.

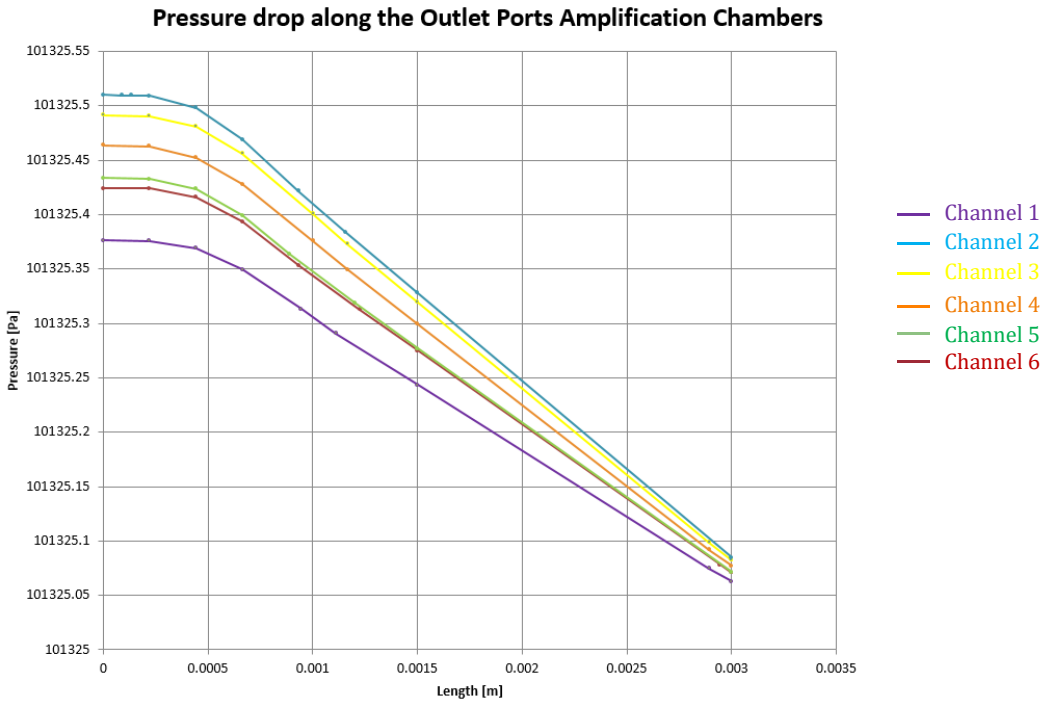

Figure 3.24. Line graph showing the pressure along all the outlet port lines of the amplification chambers.

Figure 323 shows a planar section of the provisional passive valve that was representative of the 3D outlet port utilized for flow simulation. The intended functionality of this innovation was to ensure all microchambers get filled appropriately after passing through the unconventional patterned multiplexer.

As expected there will be measurable pressure differential to instigate sufficient interferences as flow temporally ceases (Figure 3.23) if any chamber fills up until all are full in a non-sequential flow pattern. When taking into consideration this non-sequential filing of the designated microchambers, a flow line method similar to the passive valve analysis was employed across the broad and narrow regions of the ports. These features are similar to a passive valve as flow moves from a wide section to a narrow section and as a result, there will be resistance to flow due to the pressure differential. This pressure drop was captured in the Figure 3.24, that show the various drop in pressure across each port when liquid enters their chamber.

3.6 CARTRIDGE PROTOTYPE PRODUCTION

The composition of the cartridge was PDMS and a 75mm x 50mm glass slide. The PDMS was intended to hold or bear the internal geometric structures that form the unique modular elements in a complete microfluidic flow circuit. The glass, in turn, was meant to seal the chip to prevent unwarranted liquid leakage. Soft lithography was the selected means to fabricate the chip by the use of a positive 3D printed mould (Figure 3.25). Below was the list of the equipment required:

Key apparatus:

- Metal (stainless steel) Jig
- 3D mould
- Electric Oven
- Vacuum pump/ Centrifuge
- Corona Plasma Treater

3.6.1 3D PRINTING OF POSITIVE MOULD

As discussed in the previous chapter the microfluidic moulds were designed using Solidworks CAD software and saved as STL files. PDMS based chips can be divided into two major components which are the negative PDMS mould and glass slide. The use of 3D printers to is to create positive moulds which will be utilised for making negative PDMS mould. This thesis made use of two types of printers: (1) Objet30 Pro and (2) Viper si2 SLA system. Objet30 Pro is a 3D inkjet printer that utilises photopolymer for layer deposition and wax as support material (chapter 2), while 3d systems Viper SLA utilises stereolithographic technique for printing parts. For most of the supportive parts Objet30 Pro was preferred due to turnaround speed, but for the primary or established design models, Viper si2 SLA printer was preferred due better resolution and definition (Figure 3.28).

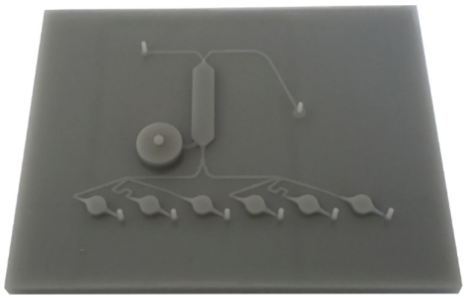

Figure 3.25. 3D printed positive mould used for creating negative PDMS mould. Created by viper si2 SLA printer.

3.6.2 SOFT LITHOGRAPHY PDMS PROTOCOL

Mixing and Degassing:

It is necessary to carry out this protocol in a clean environment to avoid surface contamination since PDMS chips rely on clean glass/plastic substrate to bond properly. Dow Corning's Sylgard 184 is the typical choice of PDMS for microfluidics. This two-part chemical system involves a mix ratio of cross-linking agent A with siloxane agent B. The mix ratio is usually 1:10 (agent A: agent B) shares a direct relationship with the mechanical properties of the PDMS produced. For example, increasing the curing agent ratio in the mixture results in increased rigidity of the PDMS. Upon mixing, the PDMS solution was hand stirred for 1-2 minutes and then placed in a degassing chamber where the air is sucked out by a vacuum pump at regular intervals for about fifteen minutes. Alternatively, a centrifuge can also be used as means of degassing PDMS mixture. Since

the mixture is a highly viscous Newtonian liquid solution air bubbles will rise naturally to the surface as it is spun in a circular motion. Using this technique the mixture was stirred for 8 minutes. These Mixing and de-airing process was carried out to avoid air bubble problems that can be localised or widespread, inhibiting the gel properties or cure characteristics of the PDMS mould.

Application of PDMS to the mould:

The moulds were cleaned by rinsing with isopropanol alcohol and then di-ionized water to remove any dust or contamination. Subsequently, the printed mould was placed into a custom-made stainless steel jig as shown in (Figure 3.26) before the thoroughly mixed degassed PDMS is poured in gently. The design specification of the jig frame is expected to hold the positive mould while simultaneously providing geometric definitions for the PDMS to cure.

PDMS Curing:

Below are various oven temperature to curing period given in the Sylgard 184 Silicone Elastomer data sheet [351].

- Cure Time at 25ºC 48 hours
- Heat Cure Time at 55ºC 4 hours

However, as a result of the low glass transition temperature of the 3D printed moulds, the oven was set at a temperature of 55° C to cure PDMS for 4 hours.

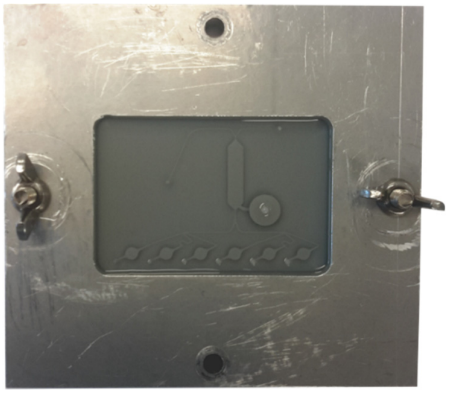

Figure 3.26. Encased 3D printed mould in a metal filled with liquid PDMS.

3.6.3 PRODUCTION OF CHITOSAN MEMBRANE

Chitosan membrane is one of key components that is required to achieve successful DNA Amplification. The location of this membrane was in the central trapezoidal chamber of the cartridge. The list below was the necessary materials required to produce a membrane thickness of 650 microns.

Materials required:

- acetic acid
- Chitosan
- DI H_2O
- 500µm Whatman paper
- GPTMS ((3-Glycidyloxypropyl)trimethoxysilane)

Fabrication Protocols:

i. For a 10mL solution dissolved chitosan in 2v/v% acetic acid in DI H2O
ii. Fully dissolve the chitosan in the acetic acid solution using a magnetic stirrer, this can take up to 24 hours for the high weight percentage solutions, do not add heat. (Vigorous stirring should not be used, chitosan is non-Newtonian)

iii. Add 10uL of GPTMS once chitosan is fully dissolved.
iv. Add solution immediately to membrane/surface substrate.
v. Leave the membranes for 8 hours
vi. Rinse the membranes in 10mM acetic acid solution to remove excess chitosan that is not cross-linked to the surface substrate.
vii. Dry in oven at 60^{o}C overnight or until dry.

3.6.4 BONDING AND SEALING TECHNIQUE

The cured PDMS was removed from the mould (Figure 3.27); a handheld corona treater, BD20-AC (Electro-Technic Products Inc., US), was used to bond the PDMS to a 75x50mm glass slide [352]. The corona device is used at a relatively low level to produce a steady but lax corona with marginal crackling and sparking before the wire electrode is passed back and forth approximately quarter inch above each bonding surface for twenty seconds. The treated surfaces are then pressed together and left untouched for at least one hour at 45° C for the glass-PDMS (Figure 3.28) surface interface to bond correctly. Optimal bond strength was observed when the glass-PDMS chip was left overnight.

Figure 3.27. Cured negative PDMS mould still attached to positive 3D printed mould

a b

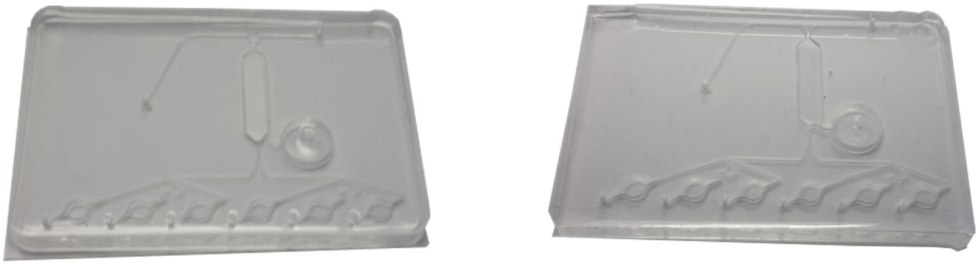

Figure 3.28. (a) Bonded PDMS-glass chip with chitosan membrane in the central reaction chamber. (b) bonded PDMS-glass chip with no chitosan membrane

3.7 PDMS-GLASS CARTRIDGE CHARACTERISTICS

As a result of the high surface-to-volume ratio in microfluidic cartridges, the interaction between liquid compounds present in the microchannels and the channel wall material are more amplified compared to lower surface-to-volume ratios of macro (conventional) systems. Moreover, since precise fluid control and flow stability are critical for successful DNA analysis in microfluidics-based systems; material surfaces with intrinsic hydrophobic or hydrophilic natures were brought into focus. In this research, PDMS and glass which are the most widely used materials microfluidics research were used to produce a hybrid cartridge for DNA amplification. The principal reasons for this choice were due to the simplicity of fabrication, low cost, biocompatibility, and optical transparency. As a result, two different types of surfaces with different energy level will interact directly with the fluid flowing along the channels. Figure 3.28 is representative of the microchannel pathways in the cartridge used in this thesis. It also gives a vivid picture of PDMS to glass surface ratio of 3:1 microchannel configuration, were hydrophobic PDMS (contact angle $\approx 110^0$) is bonded to hydrophilic glass (contact angle ≈24) by plasma treatment. Although, during the bonding process that involves plasma treatment, the glass and PDMS surface are made more hydrophilic even this effect is ephemeral [353]. Recent studies have shown that if the already bonded cartridge is further exposed to 70W of plasma power at an extended treatment of over five minutes, the PDMS surface will remain hydrophilic for more than six hours [353].

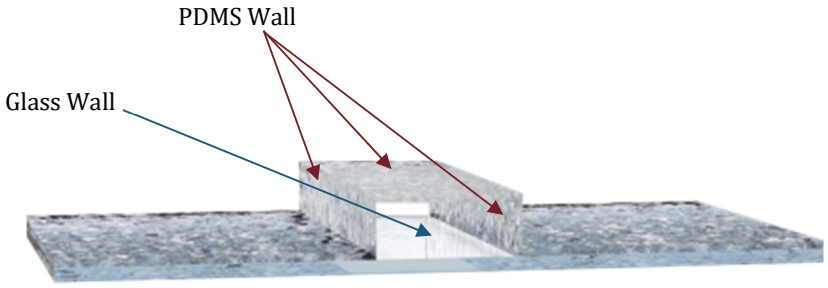

Figure 3.29. Illustration of a glass sealed rectangularly shaped polydimethylsiloxane microchannel structure that is exemplary of general PDMS-glass cartridge.

In other to understand this multi-surface phenomenon, a case scenario of homogeneity was inferred, such as PDMS-PDMS or glass-glass. First of all, channel walls that are entirely hydrophilic will have favourably high capillarity that requires less power consumption. Furthermore, biological molecules and chemical synthesis work preferably quick and efficient well on wettable surfaces [354], as seen in cases of biomolecules separation experiments. Good examples are electrophoretic separation [355] and blood plasma separation on a chip [356]. On the downsides, flow manipulation is usually complicated and challenging since these kinds of the surface may require activities such as fluid properties modification (e.g. viscosity), or sophisticated surface modification technique like hydrophobic coating [357] on specific surfaces. In contrast, hydrophobic flows can be easily manipulated by pressure and geometrical constraints. For instance, vector quantity such as flow velocity can easily be altered by varying pressure or geometric aspect ratios. Also, since there is less contact between the solid-liquid interface that results in minimal drag, the flow is more stable and easy to control. The disadvantage of this low energy surface is their relative adsorption [358] of an extensive variety of hydrophobic

molecules to their surfaces. For example, PDMS suffers from significant protein fouling due to its hydrophobic surface nature. Thus, these gathering of protein aggregates on a surface may limit the practical use of PDMS-based cartridges from microfluidic applications [359], [360].

When both surfaces are combined their individual positive effects provide significant advantages to the microfluidic cartridge, while the adverse consequences on both sides are considerably brought under control. Although, there are more hydrophobic surfaces to hydrophilic surfaces (3:1). As a result, the overall microchannel surface characteristic will sway more to the hydrophobicity. For instance, the hydrophilic glass surface aids flow through capillary action and appropriate spreading of fluid across the surfaces, while the hydrophobic PDMS surfaces provide sufficient fluid flow management options and less vulnerability to bubble formations [361]. Also, the PDMS drawbacks of adsorption will be minimised since the presence of glass provides expeditious biochemical reactions and even uncontrolled capillarity (high energy surface) will be considerably managed.

3.8 SUMMARY

This section was divided into three stages. The first stage is the 3D geometry design of the functional fluidic elements on the chip such as inlet, outlet, reaction chambers, multiplexer and six amplification chambers. These components were all design in anticipation of computational fluid dynamic (CFD) analysis. The major aspects of the design process include central reaction chamber (CRC) where the chitosan membrane will be located and the waste reaction chamber (WRC) where fluid leaving the CRC will be treated. Also, designing of a multiplexer with multiple microchannels capable of the equal delivery volume of fluid in six prearranged amplification reaction chambers (ARC) was achieved here. Moreover, multiplexer geometry was attached to the CRC and WRC though a passive flow with the sole function of flow regulation between the three components.

The second stage entails the use of CFD simulation to affirm or ascertain the efficacy of fluid flow within the three major entities: CRC, WRC, multiplexer, and ARC. The aim of the flow analysis was to observe noticeable flow resistance which will be observable in the velocity and pressure parameters in certain vital geometrical areas such as multiplexer burifications and passive valve. Afterwards, Data deduction made from this CFD analysis and use of graphs and pictorial illustrations were also employed to highlight the noticeable changes. These changes include flow velocity, relative pressure and fluidic resistance. Analysis assisted in the selection of the preferable width of 300 microns for the passive valve.

A good illustration was multiphase flow simulation which showed proper water-air interfacial surface tension necessary to prevent air bubble formation. Likewise, there was a uniform distribution of flow in the multiplexer to simultaneously fill-up the six amplification chambers. Also, there was also accurate regulation of flow by the passive, to first redirect fluid to fill up the waste chamber before going to the multiplexer. As a result, the two essential elements, multiplexer and a passive valve which have their functions imperative to the success of the category was enough approval for the last stage.

The last stage involved the chip fabrication process already expounded in the literature review. The soft lithography process was successfully carried out using a positive 3d printed mould to create a negative PDMS mould that bears the internal and interconnected microfluidic elements geometrical structures. Afterwards, the newly casted PDMS mould was then permanently sealed or bonded to a glass slide by plasma surface treatment using a corona treater. The result was a successful PDMS-glass chip.

4.EXPERIMENTAL VALIDATION OF CARTRIDGE

4.1 INTRODUCTION

In this section, an experiment was performed with the cartridge produced during the fabrication process. The first fluid flow experiment was conducted on the cartridge without the embedded chitosan membrane to draw an observable comparison between the previous CFD simulated model and real-time laboratory fluid flow experiment. Afterwards, different cartridge bearing chitosan was to ascertain if the presence chitosan would yield similar results before the main DNA amplification experiment was performed.

The preliminary fluid flow experiment conducted here was done with two sample dye solutions representative of sample DNA and amplification reagent. Yellow dye was used for DNA solution while blue dye for the amplification reaction. Furthermore, the efficacy of the passive valve to perform DNA purification protocol that is imperative in DNA sample preparation was tested. Likewise, the capability of the multiplexer to distribute flow to designated amplification chambers was also tested. The full experimental protocols were then divided into three categories: (1) DNA extraction by chitosan, (2) DNA purification and waste treatment, (3) DNA elution and amplification. Through these experimental protocols, additional validation of the microfluidic cartridge was ascertained before expensive laboratory reagents were to be used on it for DNA amplification.

In the DNA experiment, the chitosan bearing microfluidic cartridge required two categories of test. First was the control that had no presence of DNA; regarded as the negative DNA experiment. This negative test was used to confirm or validate the second experiment bearing DNA, which was represented as the positive DNA experiment. The means of achieving this goal was done with the assistance of a proprietary product called TwistAmp basic kit [362] from TwistDx company [363] based in England. By default, this kit was intended to perform recombinase polymerase amplification by using miniature pellet tubes, contrary to this thesis objectives. As a result, efforts were made in this thesis to adjust the volume and chemical enzymes or reagents required, so similar results derived with PCR tubes can be achieved utilising a chitosan bearing microfluidic PDMS-glass cartridge. Afterwards, an endpoint analysis was required to ensure successful DNA amplification and Agarose Gel Electrophoresis was the selected means of achieving these results.

4.2 OBJECTIVES OF EXPERIMENT:

The list of objectives below was developed ascertain the designed and the fabricated microfluidic cartridge was able to perform its primary functions that include DNA extraction, purification, elution and amplification in a continuous fluid flow process.

- To achieve comparable results with the CFD simulation by performing fluid flow test using coloured dye solutions on a cartridge without chitosan.
- To ascertain microfluidic cartridge can perform its expected functionalities when a chitosan membrane is embedded in its central reaction chamber.
- To establish the use of passive to regulate flow during DNA purification
- To establish the utilization of a multiplexer to disseminate flow to six amp0lifiaction reservoirs
- To establish the use of sodium polycarbonate powder for internal liquid waste treatment for biohazard prevention.
- To achieve successful DNA amplification by altering the chemical and volumetric composition of an RPA basic kit to suit the protocols required using chitosan membrane.
- To establish a defined continuous fluid flow protocols using syringe pumps for the DNA extraction, purification, elution and amplification process for with and without chitosan membrane.
- To attest successful DNA amplification took place in the chip by conducting an endpoint analysis using Agarose gel electrophoresis on the positive and negative extracted solutions from the cartridges.

4.3 VOLUMETRIC ANALYSIS

The fluid flow experimentation is categorised into three major processes; (1) DNA sample volume, (2) wash Volume and (3) amplification volume. Each picture shown in Figure 4.1 is representative of the different flow process. Furthermore, the total volume of each process takes into account the fluidic chambers and microchannels interconnections. Below is the formula used to define specific process volume:

$$\text{T}otal\ volume\ = residual\ volume\ + specific\ volume$$

$$V_T = V_r\ + V_s \qquad 4.1$$

$\text{V}_T = total\ volume$ (exclusive of the fluid in the syringe pump tubing connectors)
$V_r = residual\ volume$ (excess volume residing in the inlet microchannels leading to the CRC)
$V_s = specific\ volume$ (specific volume targeted for DNA analysis)

Sample volume:
Figure 5.1a. Shows the total volume necessary for DNA sample fluid. The value is given as 125µL for volume without chitosan and 75µL with chitosan.

$V_r = 10\mu L,\ V_s = 65\mu L$ (with chitosan), $V_s = 115\mu L$ (without chitosan)

$V_T = 75\mu L$ (with chitosan), $V_T = 125\mu L$ (without chitosan)

Wash volume:

Figure 5.1b. Shows the total volume necessary for flushing waste sample fluid. This volume in this domain entails the DNA sample and waste chamber volume. The total waste volume required is similar to the total volume of the sample fluid since air which is the flushing fluid is passed through the same inlet port.

The value is given as 125µL for volume without chitosan and 75µL with chitosan.

$V_T = 75\mu L$ (without chitosan), $V_T = 125\mu L$ (with chitosan)

Amplification volume:

Figure 5.1c. Shows the total volume required for performing successful amplification by filling the CRC and most especially the ARC via the multiplexer. The value is given as 370µL for volume without chitosan and 320µL with chitosan.

$V_r = 15\mu L$, $V_s = 305\mu L$ (with chitosan), $V_s = 355\mu L$ (without chitosan)

$V_T = 320\mu L$ (with chitosan), $V_T = 370\mu L$ (without chitosan)

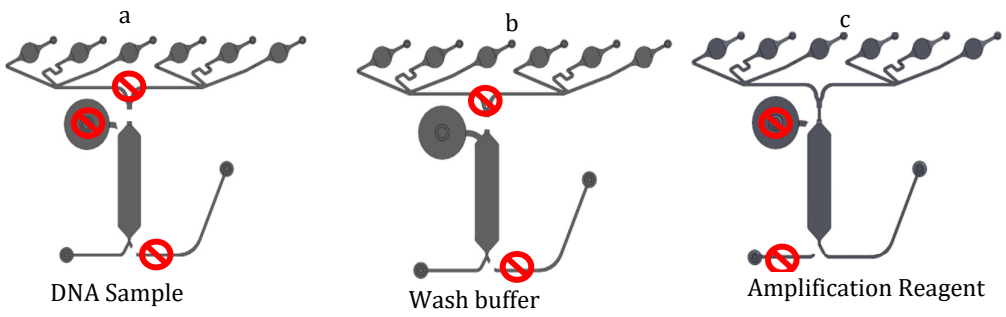

Figure 4.1. (a) flow processes involving only central reaction chamber. (b) flow processes involving the central and waste reaction chamber. (c) flow processes involving the central reaction chamber, multiplexer and amplification reaction chamber.

4.4 FLUIDIC EXPERIMENTAL MATERIALS

All the experiments performed in this section had their peculiarities, but they all shared similar materials equipment. Below is the list of materials used for both the fluid flow and DNA amplification experiment.

MATERIALS:

- Yellow liquid dye: DNA sample representation volume
- Blue liquid dye: Amplification reagent representation volume
- Sodium Polyacrylate (Superabsorbent Powder): waste solidifier as known as slush powder

- Chitosan membrane
- Synthetic DNA
- RPA basic kit primers and reagents
- Tris (hydroxymethyl) aminomethane MWT 121.4 g/mol
- MES (2-(N-morpholino) ethane sulfonic acid) buffer
- KCl
- Di-ionized water

APPARATUS

- Luer fittings, Luer adapters and accessories
- PTFE Teflon tubing coil 1/16-inch (outer diameter) x 1/32 inch (internal diameter)
- PDMS microfluidic chip
- Electrically powered syringe pump
- Electric hot plate

4.5 FLUIDIC EXPERIMENTAL PROTOCOL

The Three key samples required for these experiments were the DNA sample solution, amplification mixture and air volume as wash fluid. For each solution, a different volume is required as shown in the volumetric analysis. As a result, the experimental protocols for both solutions for cartridges with or without chitosan was different. To ensure simplicity of operation, the protocols were dived into first half and second half processes. In the first half DNA extraction by chamber fluid filling and purification by passive valve was expected to take place. While the second half entailed the DNA elution and amplification process.

The development of each protocol required several experimental tests before a suitable flowrate required for each testing was chosen. A peculiar case during this testing process was the appropriate selection of precise flowrate required to quickly flush the chamber with air without causing air bubble formation in chamber containing chitosan membrane that is hydrophobic. Furthermore, there is a consistent buildup of pressure in the waste chamber as the liquid entering reacts instantaneously with the sodium polycarbonate powder. As a result, the flushing or purification time had to be quick enough to prevent premature breaking to the passive valve seal due to the pressure difference. A time range of 15 to 20 seconds was sufficient to achieve optimal purification process. Shown below are the time and flowrate protocols developed for the experiments.

4.5.1 FLOW CONDITIONS WITHOUT CHITOSAN

The first half (DNA extraction and purification):

i. 100µl of yellow liquid dye is pumped in for 45 seconds @ 180µl/min (DNA extraction)
ii. Interlude of 30 seconds (reaction simulation period)
iii. 125µl of air (flush) is pumped in for 16 secs @ 480µl/min (DNA purification)
iv. Interlude of 30 seconds (waste treatment period)

Second half flow (DNA amplification):

v. 135µl of blue liquid dye is pumped in for 35 secs @ 240µl/min (DNA elution)
vi. Interlude of 30 seconds (reaction simulation period)
vii. 235µl of blue liquid dye is pumped in for 70 secs @ 240µl/min (DNA Amplification)

4.5.2 FLOW CONDITIONS WITH CHITOSAN

The first half (DNA extraction and purification):

i. 100µl of yellow liquid dye is pumped in for 23 seconds @ 180µl/min (DNA extraction)
ii. Interlude of 30 seconds (reaction simulation period)
iii. 75µl of air (flush) is pumped in for 10 seconds @ 480µl/min (DNA purification)
iv. Interlude of 30 seconds (waste treatment period)

The second half (DNA amplification):

v. 85µl of blue liquid dye is pumped in for 21 seconds @ 240µl/min (DNA elution)
vi. Interlude of 30 seconds (reaction simulation period)
vii. 235µl of blue liquid dye is pumped in for 70 seconds @ 240µl/min (DNA Amplification)

4.6 EXPERIMENTAL RESULTS AND ANALYSIS WITHOUT CHITOSAN

A control experiment was used to evaluate and compare the flow of fluid within the chip without the presence of a chitosan paper in the CRC. Considering this experiment to be a mock DNA amplification experiment, the flow analysis can be broken down into first half and second half processes. In this segment is a simpler summary of the overall process is discussed; a more detailed illustration of the DNA amplification process will be discussed in details in later in this chapter. One of the first half processes involves the extraction of DNA. This process is illustrated by the Figure 4.2 by the inflow of 100µl to partially fill the CRC to 85% capacity. Subsequently, the wash process is then initiated to flush excess fluid into the waste chamber. Figure 4.3 describes this process by the use of air to flush the yellow dye in the waste chamber to be solidified by the slush powder to prevent further fluid outflow from the chip through the waste outlet. Finally, the second half processes start with the introduction of the amplification fluid into the CRC to release DNA. Figure 4.4, captures this process vividly when 110µl of blue dye is pumped into the CRC. Afterwards, Figure 4.5 shows the remaining 235µl being pumped into the six amplification reservoirs. This last process is representative of the newly released DNA being pushed into all the ARC's for the amplification reaction.

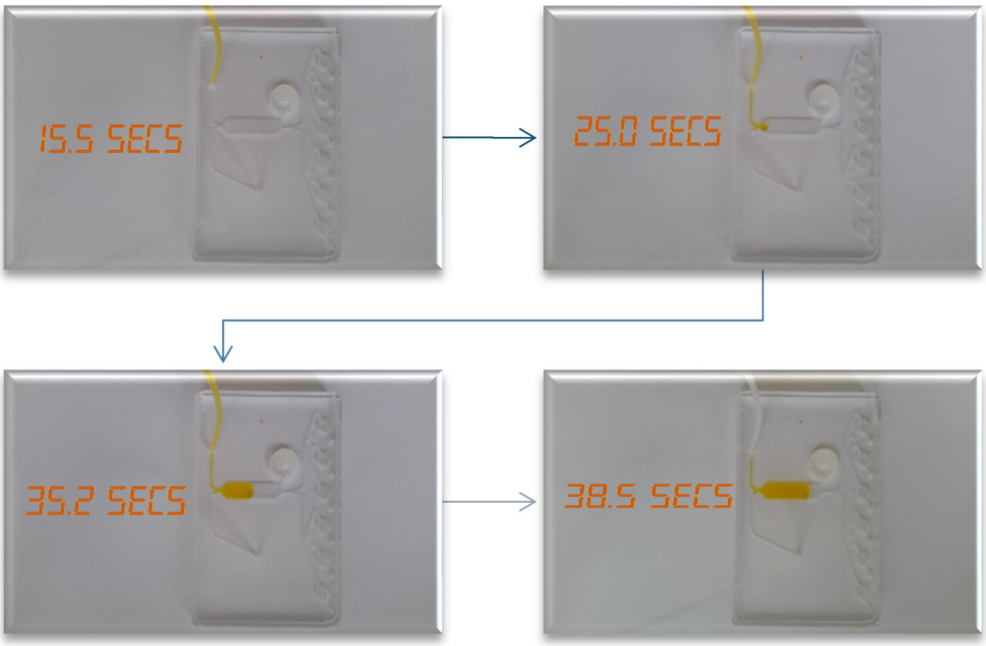

Figure 4.2. Partial filling of the central reaction chamber with yellow dye to indicate DNA extraction

Figure 4.3. Flushing of yellow dye with air into the waste reaction chamber to represent DNA purification

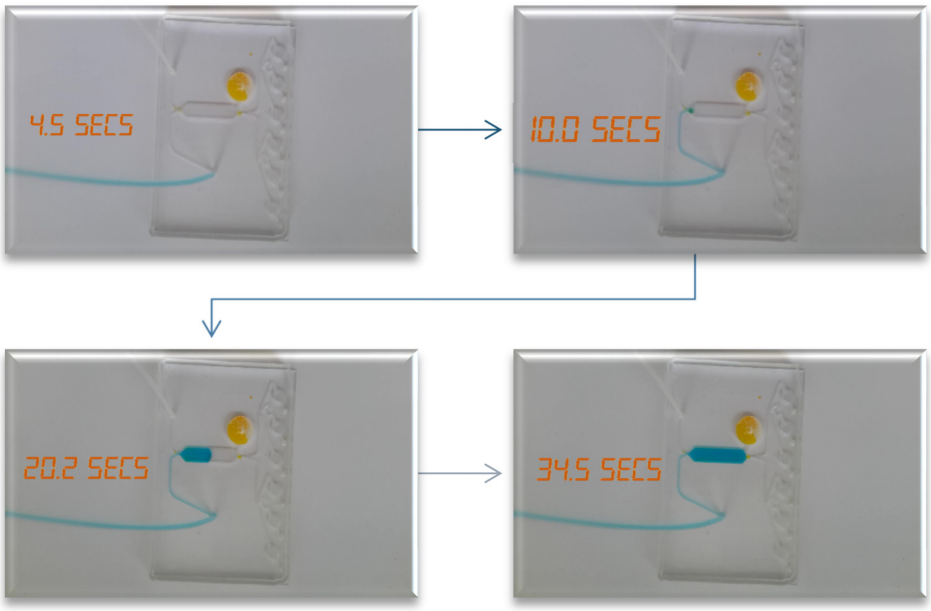

Figure 4.4. Filling of the central reaction chamber with blue dye to represent DNA elution protocol

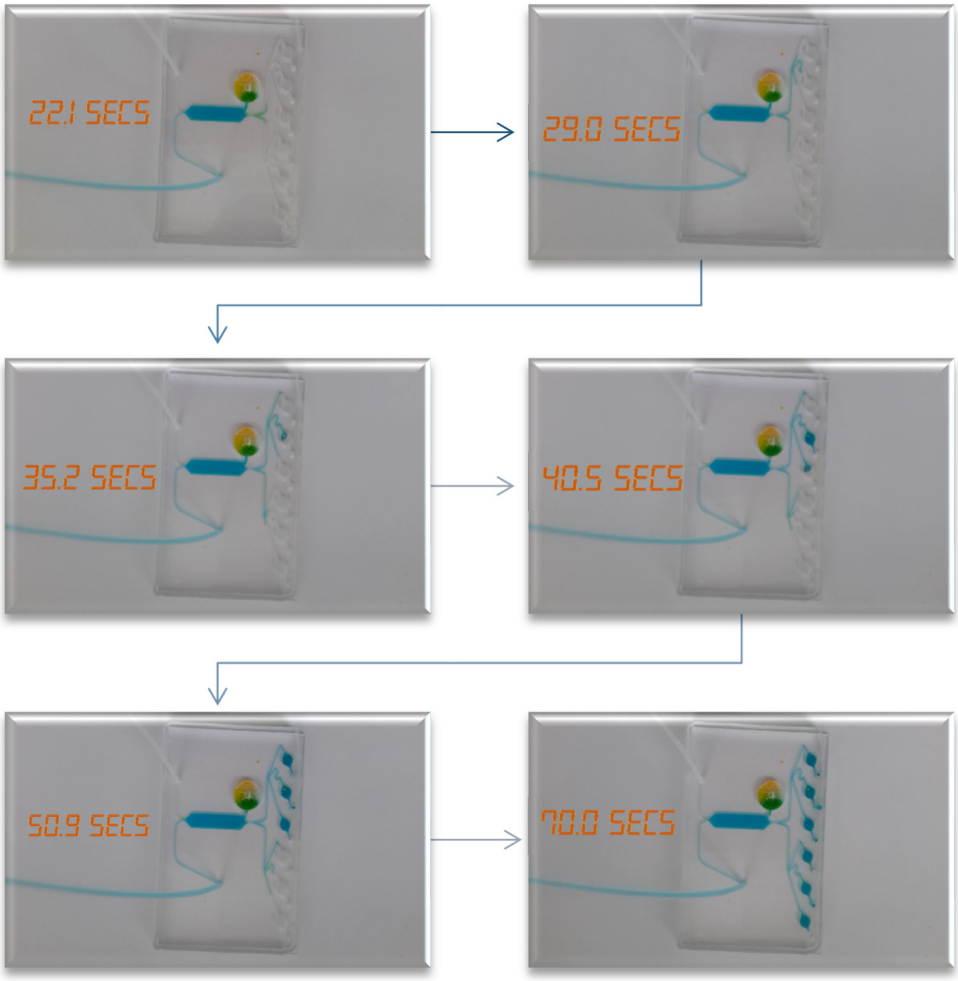

Figure 4.5. Filling of the amplification reaction chambers with blue dye via the multiplexer for DNA amplification reactions.

There were expected observable differences in the filling pattern of 3D simulated flow and real-time multiplexer because this a non-sequential device. In the CFD simulation, the fluid build-up in the multiplexer differs slightly since the simulation applied a non-slip boundary condition to its material surfaces. Therefore, the subtle changes in the simulated flow in each multiplexer vein were dependent on geometrical features in contrast to the flow experimentation that shows more resistance to fluid motion during as they spread through the multiplexer. This additional resistance effect can be attributed to surface properties of the hybrid cartridge that composes of PDMS and glass that form flow pathways of high surface to volume ratio where surface tension is very dominant. As a result, dissimilarities flow patterns were expected.

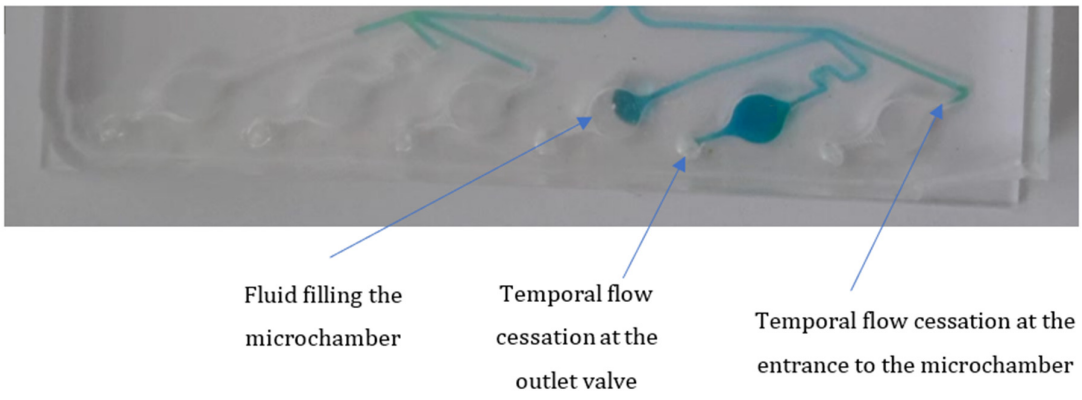

Figure 4.6. Illustration of the outlets port of the amplification behaving similarly too passive by temporally restricting flow.

Moreover, the CFD depiction of microchamber chamber fill-up process was similar to the fluid experiment since they both were haphazard and non-sequential. Although the particular order of their filling was different, two major effects differentiated both systems of operation as flow tend to cease before entering the chambers and then stop again at the outlet ports after the reservoir is filled (Figure 4.6). By observation, the first effect that causes the fluid entering the chamber to freeze temporally came as a result of the compressed resident air which wasn't displaced quickly enough due to the provisional passive valve in the shape of an outlet port. The consequence of this causes air pressure to push back at the liquid at the interfacial boundary layer (air-liquid surface tension) where their relative velocity to each other is infinitesimal due to laminar flow at low Reynolds number less than one. Since flow in the microfluidic circuit is dynamic, the effect of the air pressure will be broken by a transitional pressure differential at the lowest point. That means any of the connected microchambers with the relatively low air pressure will be the path of least resistance. Whereas, regions, where pressure is high, will remain frozen temporally. The second factor comes into play when the chamber has been filled, and flow ceases at the junction of the outlet valve. In this scenario, the effect of the hydrophobic nature of PDMS and geometrical structure of the outlet port creates a pressure seal that provides sufficient resistance to fluid flow. This seal remains intact till all chambers are filled, and pressure equalization occurs across all outlet ports. The overall of the phenomenon observed when filling the six microchambers via a multiplexer can be related to multiple passive valves simultaneously connected parallel to each other and also having their pressure seal dependent on the pressure drop across all valves.

4.7 EXPERIMENTAL RESULTS AND ANALYSIS WITH CHITOSAN

In this experiment, chitosan is present in the reaction chamber. As a result, there will be a significant reduction in volume capacity. Besides, the hydrophobic chitosan is expected to the absorbed minimal quantity of coloured dyes that passes through the CRC. In comparison with the control experiment, the specific sample volume required is 50µl (75% capacity of the CRC) of yellow dye instead of 100µL for DNA extraction (Figure 4.6), while the wash volume of air needed for purification is 75µL. After the wash, the chitosan apparently stained with yellow dye as shown in Figure 4.7. This stain may be representative of absorbed DNA. Likewise, when 50µl of blue dye is pumped to into the CRC as shown in Figure 4.8; the colour in the CRC changes to green. As a result of the blue dye mixing with the absorbed yellow dye on the chitosan. Also, the green colour outcome as a result of mixing may be representative of the chemical reaction to release DNA elution) from the chitosan. Finally, a total volume of 235µL is then subsequently pumped into the six amplification chambers. Figure 4.9 shows vivid colour green in each of the six chambers as a result of the continuous mix of the absorbed yellow dye and flowing blue dye. Just like the previous observations it may be inferred that the green colour mix flushed into the amplification reservoirs represent successful DNA transfer from the CRC to ARC for amplification.

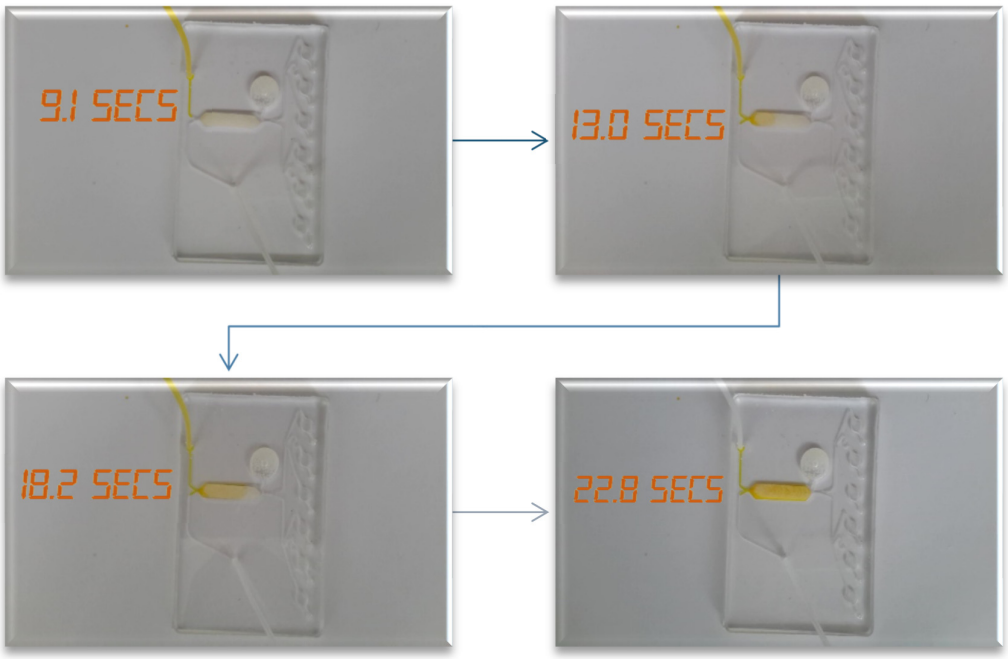

Figure 4.7. flow process involving filling of the central reaction with yellow dye and also wicking of the dye by the chitosan membrane (DNA extraction).

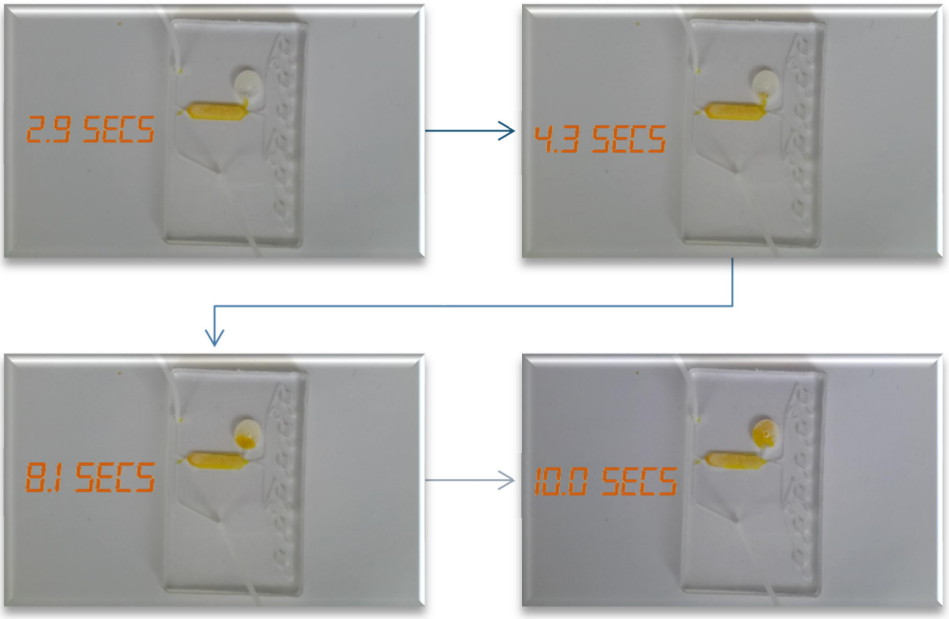

Figure 4.9. Flushing of unabsorbed the yellow dye by the chitosan with air into the waste reaction chamber (DNA purification).

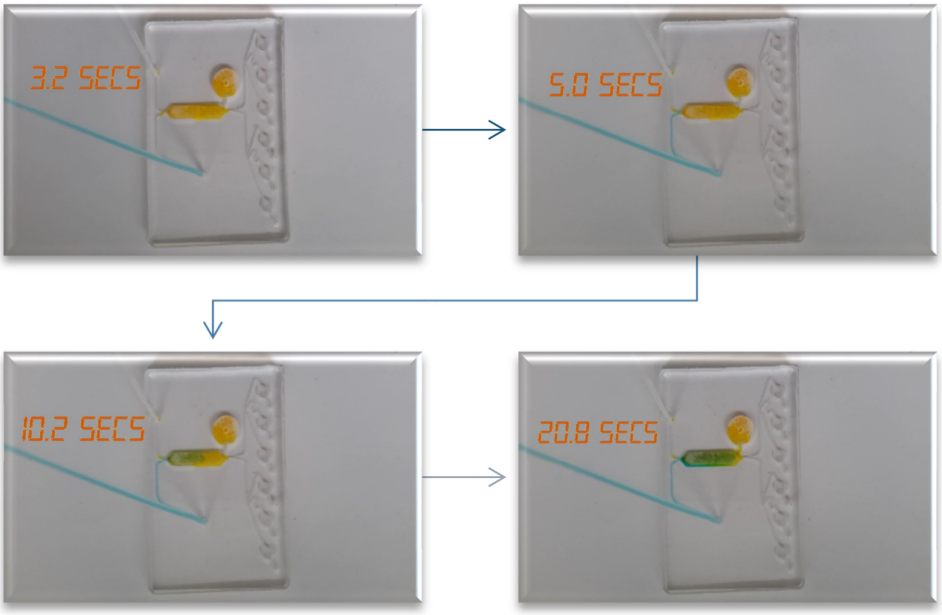

Figure 4.8. Filing of the central reaction chamber with blue dye that mixes with the absorbed yellow dye in the chitosan to form a green colour resolution (DNA elution).

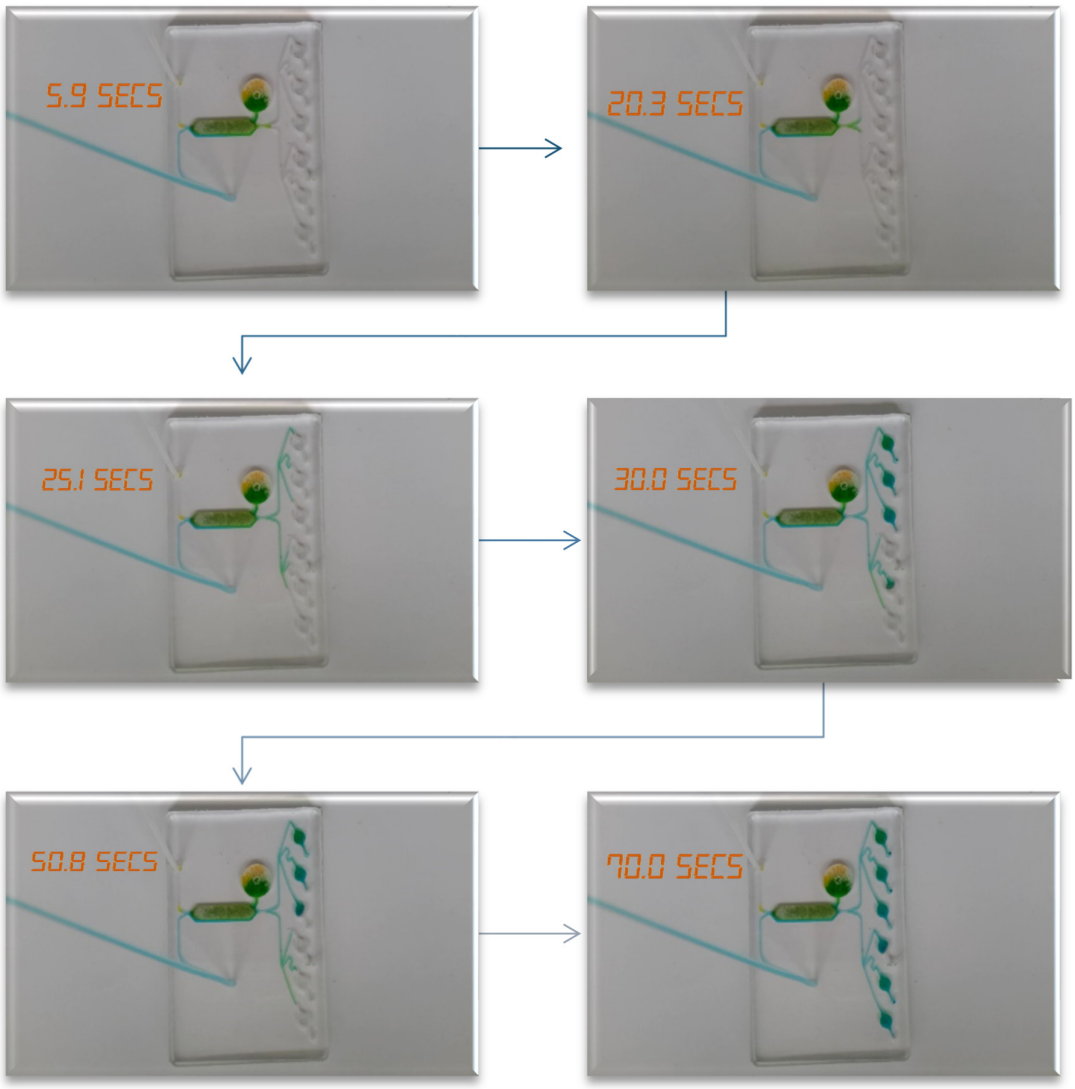

Figure 4.10. Filling of the amplification reaction chambers via multiplexer to give a greenish blue resolution (DNA amplification reactions).

4.8 RPA DNA AMPLIFICATION EXPERIMENT:

The experiments performed in this section required the use of synthetic DNA and RPA reagents instead of coloured dyes. Two microfluidic cartridges bearing chitosan (Figure4.11) were used, and the fluid flow protocols with chitosan were employed for these experiments to achieve the specific goals below.

- Perform negative and positive DNA extraction on-chip by the use of chitosan paper
- Perform negative and positive DNA purification on chip
- Perform negative and positive DNA elution on chip
- Perform negative and positive DNA amplification on chip
- Perform comparative end point analysis of positive and negative amplification results

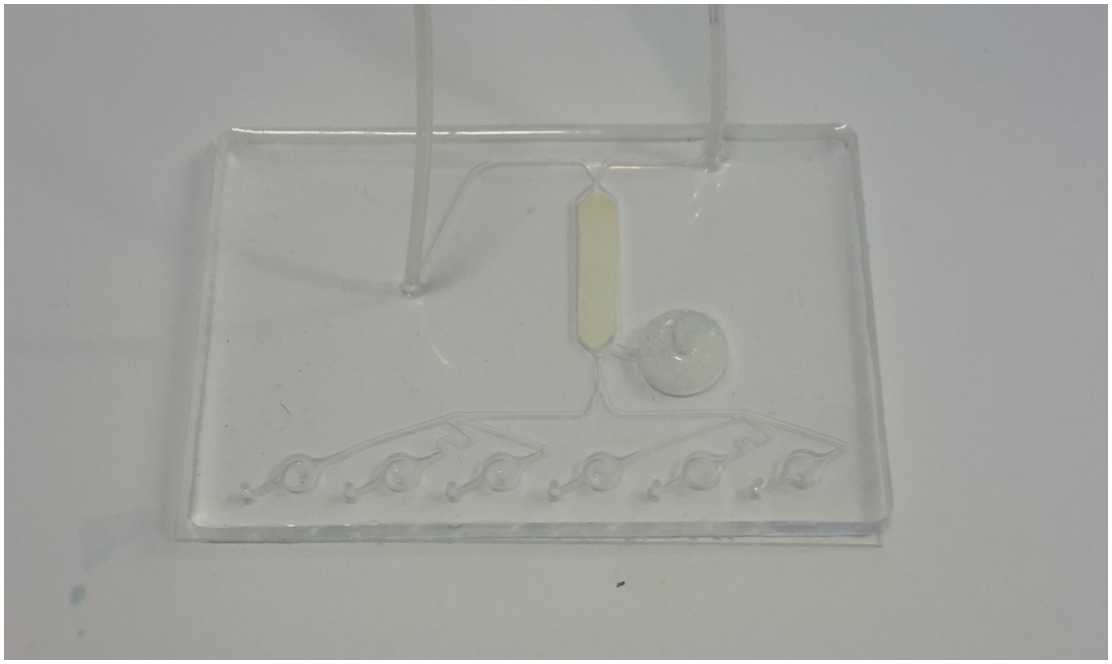

Figure 4.11. PDMS-glass microfluidic cartridge with embedded chitosan in reaction chamber, sodium poly acrylate powder in waste chamber and air-dried magnesium acetate in six amplification chambers.

The RPA protocol requires a single reaction volume of 50µl solution as shown in Table 4.1. In other to merge this experimental protocol with the microfluidic chip, two solutions had to be resolved. From Figure 1b, it can be seen that there are two inlets: (1) amplification reagent and (2) DNA sample. This improvisation was also meant to simulate a realistic scenario of field application of the cartridge where sample biofluid such as blood, urine or any format could be pumped through one inlet and another used for the chemical reagents stored or pumped through. In the same vein, this alteration also assisted in the DNA extraction process required.
The first solution, which was representative of the amplification solution involved the substitution of the DNA in the original version with Tris and KCl buffer that are mixed and pH adjusted to 9 in the modified version. This buffer was required to release DNA bound to the chitosan membrane. The second solution was formed from the previously removed DNA which was then added to an MES buffer. This buffer has a pH of 5.0 and is specifically needed for DNA extraction on Chitosan Paper. This selected extraction process utilized is pH dependent, and it involves the binding of DNA to the chitosan at pH 5.0 provided by the MES buffer. Subsequently, this bound DNA can then be released by the Tris-KCl solution of pH 9.0 already in the first solution. The third solution, which is similar to the second, was prepared to replace the DNA in the second mixture with de-ionized water. This mixture was meant to serve as the control, also referred to as negative DNA sample while the former as the positive sample.

The experiment starts with 100µl DNA of sample DNA solution allowed to fill the CRC to a capacity of 50µl partially, while the dry region of the chitosan was expected to get wet by wicking. On the other hand, the excess 50µl compensates for the extra volume needed in the microchannel, tubing and connectors that link the CRC and syringe pump. Subsequently, the extraction reaction begins after the filling process was achieved. After

two minutes, DNA purification is initiated which involves flushing the excess MES buffer by air to the waste chamber leaving only the wet and properly soaked chitosan membrane.

Table 4.1. Comparisons between the original TwistDx chemical and volume compositions [364] with the altered version used for the PDMS-glass chip for DNA amplification.

S/N	TWISTDX ORIGINAL VERSION (1 REACTION)	ORIGINAL SOLUTION MIXTURE	TWISTDX EXTEMPORIZED VERSION (1 REACTION)	MODIFIED SOLUTION MIXTURE	TOTAL SOLUTION MIXTURE (8 REACTIONS)
1	Tenth dilution of the positive control DNA (in dH2O)	10µl	Tris-Kcl reaction buffer	10µl	80µl
2	Primer A solution	4µl	Primer A solution	4µl	24µl
3	Primer B solution	4µl	Primer B solution	4µl	24µl
4	Rehydration buffer	29.5µl	Rehydration buffer	29.5µl	236µl
5	Magnesium acetate solution	2.5µl	Magnesium acetate solution	2.5µl	20µl
6	Total volume	50µl		50µl	384µl

After the liquid waste has solidified which takes about twenty to thirty seconds the amplification process was then initiated. The first step of the amplification process involves filling the CRC with amplification reagent solution to cause elution. The elution process takes about five minutes for a maximum yield of DNA at pH 9.0, which was then flushed through the multiplex to the ARC where pre-air dried 2.5µl of magnesium acetate was waiting to initiate the amplification reaction. The total volume used for initiating this reaction is 320µl. However, in Table 4.1. A reaction volume of 384µl (eight sample reaction) exclusive of the magnesium acetate was computed. The purpose of this selected volume was to compensate for the excess fluid in the microchannel network and syringe tubing connected to the amplification inlet.

The initiated recombinase polymerase amplification (RPA) reaction is a self-perpetuating process that requires the presence of two key proteins the Escherichia coli (RecA) [365]–[367] recombinase and single-strand DNA binding protein (SSB)[368], [369]. Although, other subsidiary proteins and cofactors aid the RPA process. A good example is T4 UvsY protein [370], [371] which is known to be a recombinase loading factor that supports RecA throughout the creation of the nucleoprotein filament [372], [373] with single-stranded oligonucleotide primers [374]. Other support factors such as Polyethene glycol [375], [376] act as a crowding agent to amplify the interactions of RPA core proteins with DNA, while creatine kinase uses from the pool phosphocreatine to generate adenosine triphosphate (ATP) and fuel the enzymes of the replication mechanism [41].

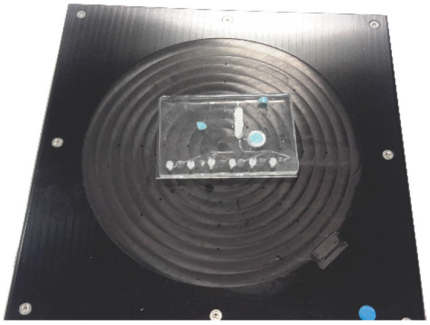

Figure 4.12. Illustration of amplification incubation using an electric hot plate

In RPA diagnostics [377], the mechanism of replication involves the strand-displacement of DNA polymerase that is necessary to extend the primer at a single of temperature (40–42 °C) [378]. Strand displacement activity involves nucleoprotein filament scanning double-stranded DNA (dsDNA) for homologous sequences that it needs to interact with to form a D-loop structure [377]. D-loop structure is the substratum of strand displacement that entails a local separation of DNA strands in which the matching strand is stabilised by SSBs and the target strand is hybridized with primer. While ATP hydrolysis by recA protein causes recombinase disassembly from the nucleoprotein filament allows primer extension by strand-displacing DNA polymerase to create a new template. Likewise, newly created DNA strands are repeatedly used for another round of DNA synthesis, thus repeating the RPA cycle. As a result, exponential duplication DNA molecules is triggered until exhaustion of the phosphocreatine pool [379].

4.9 EXPERIMENTAL COMPLICATIONS

There were slight complications during the experiment since both post-amplification analysis of the positive and negative reaction solution needed to be extracted of the cartridges. As result sealing of the cartridge was a difficult exercise that eventually leads to the loss of some fluid in some of the chambers by evaporation during the heating process on the hot plate (Figure 4.12). In the case of the fluid flow experimentation since both sample DNA and amplification reagents are colourless, it became reasonably difficult to observe or captures fluid progression easily.

4.10 END POINT DETECTION ANALYSIS

The anticipated outcome of the positive and negative experiment is to have the positive control reaction amplify DNA since the sample template has diluted DNA. Whereas, the negative control reaction is expected to be bland since no DNA was used in the experiment. So, in other to affirm this conjecture Gel electrophoresis analysis was carried out. The application of gel electrophoresis helps categorise sizes of long or short DNA fragments as a result of strand displacement activities according to a standard, or DNA ladder. This separation will be made possible by passing an electric current through the gel matrix to cause DNA fragments of the same length form a "band" on the gel. Since these fragments can't be seen by the eye, a DNA-binding dye is utilised to aid visualisation. In this analysis gel-red dye [380] was employed to visualise the RPA amplification products for both positive and negative chip experiments. This dye is a fluorescent chemical compound that can re-emit orange colour that exponentially intensifies after binding to DNA when excited by ultraviolet light at 300nm [43].

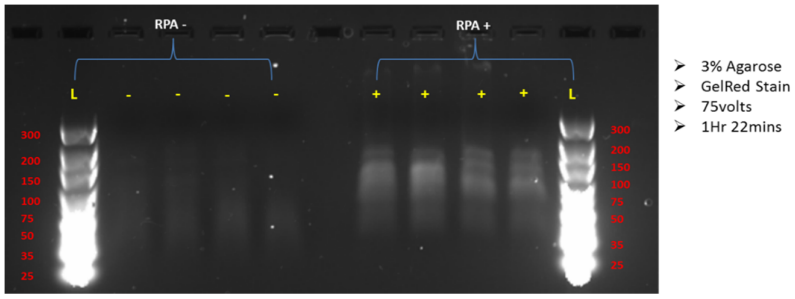

Figure 4.13. RPA amplicons detection by Agarose gel electrophoresis using a red DNA-binding dye. (a) Eight reaction gel results. (b) Twelve reaction gel results

The experimental procedure involves the use of 3% agarose gel that was stained with red dye and left for (1hour 20 minutes) at 75volts. Furthermore, the controlled DNA in the positive experiment has an amplicon product of 143bp's (±10%). So, therefore, ultralow gene ruler ladder was used at both end of the gel with a range of 300 – 10bps. These experiments were not without complications as clearly seen in Figure 5.3 that has only four results for each negative and positive gel analysis. This setback was due to evaporation loss (improper sealing) in the two chambers in each experiment. Nonetheless, the outcome of the positive gel showed significant evidence of DNA amplification within the range of 100-200bp's, and most importantly the negative control did not indicate that any DNA molecules were present or amplified.

4.11 SUMMARY

The purpose of this chapter was to test the ability of the newly developed hybrid microfluidic cartridge to perform the key fluid handling operations required for a successful DNA amplification experiment. The first experiment was carried out on a cartridge without chitosan in other to mirror the simulation analysis done in the previous chapter. Both the CFD and fluid flow analysis shared similar characteristics, but their major difference was in the effect of the surface tension in the surface to volume ratio microchannels and chambers. This was not properly captured in the simulation. As a result there were the slight noticeable difference in the fluid flow patterns in each case. The results of an experiment in the absence of chitosan were also achieved with the Cartridge with embedded chitosan membrane.

Afterwards, a DNA experiment was performed with a proprietary kit known as a TwistDx basic kit. The objective of the experiments carried out was to ascertain DNA amplification on the PDMS-Glass chip was possible. The TwistDx kit was used to perform to main experiments, which are the positive and negative control reaction. In the positive reaction, DNA template was included in the experimental setup, while di-ionized water was used instead of DNA for the negative reaction. After each experiment, the fluids in all six amplification chambers for both experiments were extracted for agarose gel electrophoresis. This endpoint analysis was expected to provide comparative analysis needed to confirm the experimental objectives and as anticipated the positive control reaction showed significant signs of amplification in all six chambers. Likewise, the negative without DNA showed no sign of amplification. Even though there were slight complications during the experiment, due to excessive evaporation when the cartridge was placed on a hot plate, the overall analysis was satisfactory. Therefore, it can be inferred that both positive and negative experiment was successful since there was no noticeable amplification on the negative gel result.

5. DESIGN AND FABRICATION OF AN ON-CHIP BLISTER

5.1 INTRODUCTION

In recent times, there have been several innovative steps taken to make chip-based microfluidics devices self-reliant without the need for complex external devices, which are usually bulky, expensive, and energy consuming. Amongst all, the innovative approach this thesis was concerned with was the area of fluid actuation. In this section, the design process for developing an inexpensive and disposable silicone elastic blister and its integration to the microfluidic cartridge was demonstrated. The primary functions of the blister were to serve as a fluidic pump as well as store reagents in the liquid form needed for the DNA amplification. The structure of this chapter is in five folds. First is the 3D concept design of the intended blister geometric structure and all accessories needed for it to be functional. The next step which was the most significant was the material selection process which involves selecting the appropriate silicone elastomer and subjecting it to a tensile stress test. The choice of silicone material used was a proprietary product termed Blu-stuff [381] while the tensile test performed on the material was an ASTM D412 standard test methods for rubber. Third on the list was the finite element analysis carried out on the blister to validate if the concept model and material properties will enable it to perform its primary functions efficiently. The fourth category was similar to the fabrication process of the cartridge that involves using a 3D mould to cast the desired shape from a liquid silicone material. Also, the casted blister mould was then integrated into the PDMS-glass chip by soft lithography. Finally, fluid experimentation was then performed on the blister PDMS-glass chip to determine its efficacy in microfluidic applications.

5.2 BLISTER DESIGN OBJECTIVES

Below are the procedures observed to ascertain the blister efficacy on the cartridge:

- To design a 3D model for a blister with specific liquid capacity needed to hold amplification reagent

- To design a blister capable of pumping fluid through a microfluidic cartridge network with minimal wastage.
- To successfully select a low-cost and mechanically reliable silicone elastomer as substitute to PDMS
- To successfully Install a blister on a PDMS-glass microfluidic cartridge
- To design a fluid control mechanism to regulate flow from blister to cartridge

5.3 BLISTER GEOMETRY DESIGN

The Figure 5.1, shows the final design of the internal and external shape of the blister to provide maximum compression that will result in minimal reagent wastage after series of trial with different model designs. During this designing process, three keys parameters were imperative:

i. Specific volume of reagent
ii. Fluid control mechanism
iii. Blister mechanical reliability (deformation)

The specific volume of reagent needed to perform a successful DNA amplification was derived from the previous experiment in chapter 4 (400µL). The design of the fluid compartment in Figure 5.1 shows unique features aimed at proper fluid expulsion with minimal wastage.
The microfluidic chip has two inlets (Figure 3.3a), one for biological sample and washes buffer while the other is for the amplification reagent. As a result, the blister inclusion into the POCT chip is appropriated to the amplification function because of its material cost and significance.

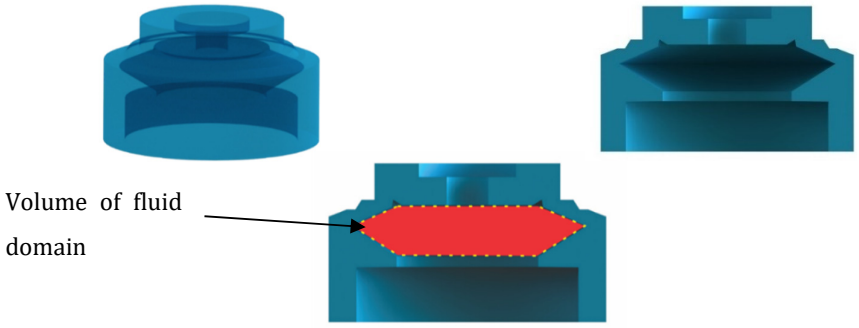

Figure 5.1. 3D sectional view of the blister model showing the region where fluid is

5.4 BLISTER FLOW CONTROL DESIGN

Similarly, the fluidic control mechanism is also a major determinant for defining the geometrical compartments within the blisters. There are two rudimentary functions expected of these flow control devices. First of all, they are expected to provide a leak-proof system for storing the fluid till the expected usage. Also, provide a means to expel the stored liquid into the microchannels in the chip. Two methods are described in this section.

5.4.1 FLOW CONTROL WITH MAGNETIC SEAL

The first method is a little complicated in the protocol of usage as it involves the use of magnets. Figure 5.2 shows the three key components required: (1) lock pin, (2) base washer and (3) 3mm magnet that was needed for this technique.

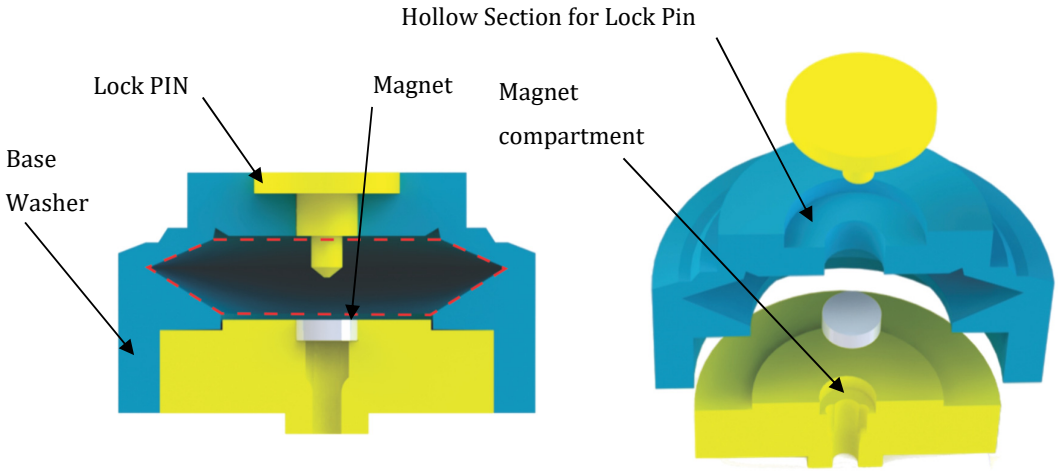

Figure 5.2. Fluid flow mechanism using a 3mm magnet lock

The hollow section above the blister in Figure 5.2 is required to hold the lock pin which is needed to hold the blister down by keying into the hole (interference tolerance) in the base washer to avoid negative suction pressure after the fluid store has been expunged. Likewise, the hole where the lock pin passes through also bears a wider indentation on the top surface that is meant to house the 3mm magnet. The purpose of this magnet was to prevent leakage from the fluid compartment. Upon the use of a 20kg-50 kg (not weight) pull strength magnet as shown in Figure 5.3a at proximity, the seal is broken and then flow permissible.

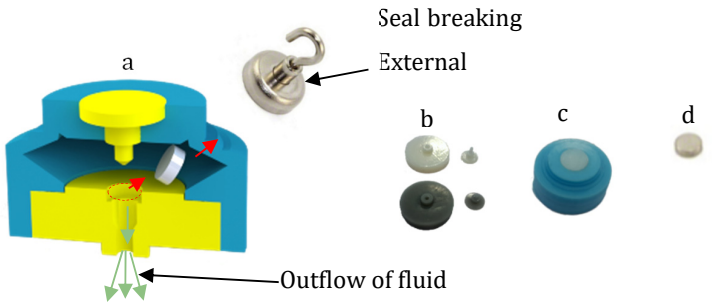

Figure 5.3. (a) Blister magnetic seal release demonstration. (b) base washer and pins 3D printed from Objet30 Pro (beige) and viper si2 SLA system (dark grey). (c) Complete blister assembly with flow

Finally, when reasonable force is applied by a solenoid or finger actuation, it's expected to allow fluid outflow in only one direction. The Figure 5.3b is the configuration for the blister with flow control mechanism.

5.4.2 FLOW CONTROL WITH RUBBER SEAL

The second method takes a much simpler approach shown in Figure 5.4. In this case, the internal magnet was replaced with a delicate elastic seal that easily breaks when the longer revised version of lock pin forcefully interacts with it. Subsequently, after the seal was broken and the blister is progressively depressed, the fluid within the blister floods the microchannels with liquid.

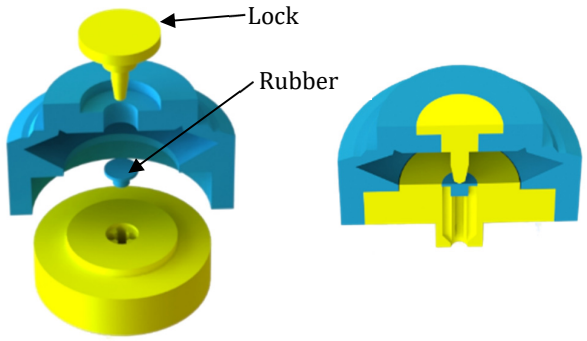

Figure 5.4. Alternate Flow control mechanism with fragile rubber seal

5.5 MATERIAL SELECTION OF BLISTER

The core material values required are the young modulus and ultimate tensile strength. Young modulus, the degree of stiffness or tendency for an object to deform under load. If its value is low, the material is more elastic while stiffer otherwise. This property defines the deformability and flexibility of the blister to undergo a geometrical transformation with the less applied load. Ultimate tensile strength is the threshold magnitude of stress that will cause failure. This stress evaluation was very significant, especially during the fabrication process when the casted material was to be peeled off the mould. A material with very low tensile strength will fracture easily. Likewise, when its deformed under considerable load, it's imperative that material breakage does not occur which may lead to loss of reagents.

PDMS was organically the first choice since it's an elastomeric material. PDMS Sylgard 184 (Dow Corning Corporation) as a material is a combination of two liquids; prepolymer (part A) and a cross-linker (part B). The mixing ratios of both liquids provide different values of young modulus and ultimate tensile strength. This means that the higher ratio (i.e. more part A) is inverse proportional to the young modulus. As a result, PDMS with low modulus tends to be softer and flexible. For example, Table 6.1 shows the fluctuation of young modulus and tensile strength of PDMS when a standardised test of ratio 10:1 (part A: part B) cured at various temperature. Although recent studies have shown 33: 1 ratio yields an approximate minimum value 0.577 Mpa, young modulus [382].

When the fabrication technique discussed later in this chapter was used on PDMS, it continuously suffered breakage during the disassembly process involving separation from the mould. This material failure came as a result of reasonable low tensile strength. Though, Table 6.1 shows a maximum tensile strength of 7.65 at 125 ^{0}C which is unreasonable to subject the 3d printed blister die (Figure 5.10) to because of its heat deflection temperature about (63^{0}C to 67^{0}C). Therefore, a material with flexible and strength similar to natural rubber was preferred. A proprietary silicone rubber termed "Blu-Stuff" with a standard mix ratio of 1:1 was selected

due to its physical similarities to PDMS but with a better tensile strength. Likewise, from an economical standpoint, Blu-Stuff is relatively available and cheap. The drawback to this material is transparency; since they are opaque, it is impossible to observe fluid movement within it.

5.6 MECHANICAL CHARACTERIZATION OF BLISTER

In this section, the elastic modulus and ultimate tensile strength were investigated by ASTM D412 - 15a Standard test. D 412 covers the tensile properties of vulcanised rubber, thermoset rubbers and thermoplastic elastomers and can be used to determine the Young modulus of the material.

Equipment used:

- Blu-Stuff silicone dumb bell (dog-bone) shaped mould
- Tensile testing machine with 30kN load capacity
- A PC based Software system with the capability to provide and calculate the raw data from the tensile test machine.
- Digital Vernier calliper

The aim of analysis:

i. To determine the Young modulus
ii. To determine ultimate tensile strength.

Experimental preparation and procedure:

i. Three "dumbbell" shaped specimens of Blu-Stuff are Produced (ASTM D412 Sample Shape) as shown in Figure 5.5b.
ii. Each specimen was loaded into tensile grips for individual testing as shown in Figures 5.5a.
iii. The tests begin by gradual separation of the tensile grips at a speed of 0.5 millimetres per second.
iv. The test ends by after specimen breaks (rupture).
v. Computational analysis is then carried out to determine the Young modulus

Table 6.5.1. Provides a standardised test of ratio 10:1 (part A: part B) cured at various temperature

Property	*Min Value*	*Max Value*	*Temperature (^0C)*	*Reference*
Young's modulus (MPa)	1.32 ± 0.07	2.46 ± 0.16	25	[382]
Ultimate tensile strength (MPa)	3.51 ± 1.11	7.65 ± 0.27	125	[382]

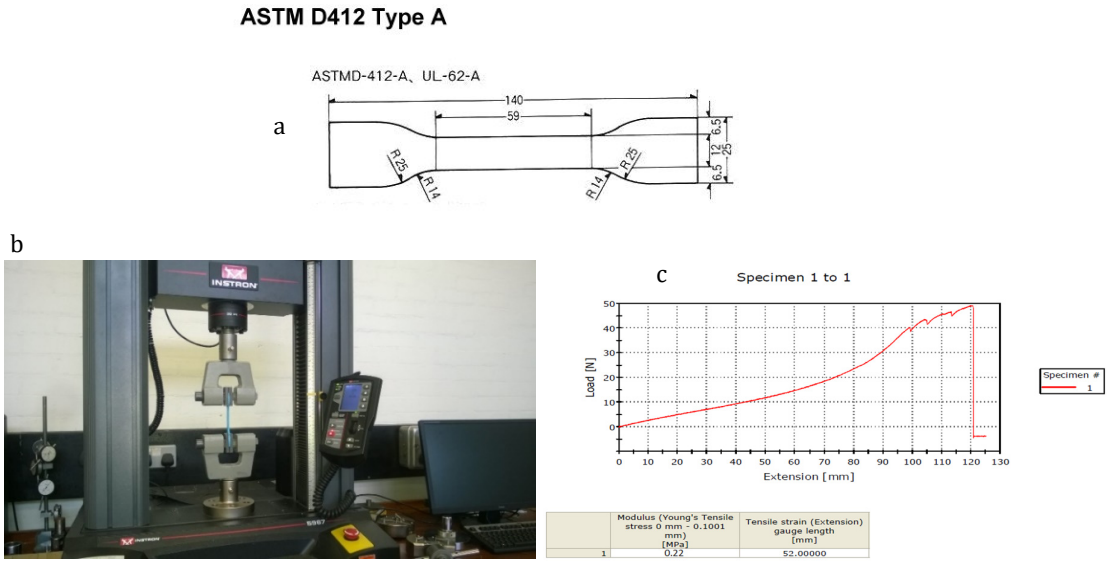

Figure 5.5. (a) Schematic diagram of ASTM D412 dumb bell (b) Silicone elastomer loaded on a tensile grip. Sample Shape. (c) Graphical illustration showing load versus extension

5.6.1 RESULTS AND DISCUSSIONS

The main difficulty faced during this tensile test for rubber or silicone elastomer was that 1kN load capacity machines are usually required, but due to availability and time constraint, a 30kN machine was used. As a result, a very slow rate of 0.5mm/s speed was used to offset the excessive force. Similarly, an extensometer which is recommended to improve the accuracy of the elongation measurement wasn't available for this experiment.

Ultimate tensile strength is derived from the division of the load at breaking point by the initial cross-sectional area as shown in Figure 5.6. Below is the formula used in the calculation.

$$ultimate\ tensile\ strength = \frac{(load\ at\ failure)}{original\ width \times original\ thickness)} \quad 6.1$$

From Figure 5.6, the initial width is 3mm; thickness is 1mm and load at failure is given as 49N

Therefore, $ultimate\ tensile\ strength = \frac{49}{3\times1}$

Ultimate tensile strength of Blu-stuff is approximately 16.33 MPa (table 6.2)

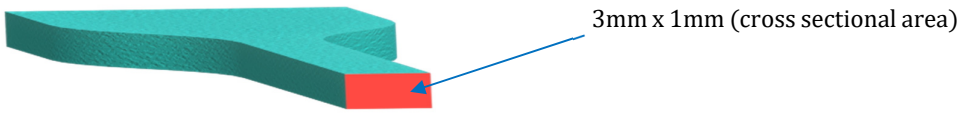

Figure 5.6. Cross section al of Blu-stuff silicone elastomer dumb bell mould.

Table 5.2. Mechanical properties of Blu-stuff silicone elastomer

PROPERTY	MIN VALUE	MAX VALUE
YOUNG'S MODULUS (MPA)	0.22	6.84
ULTIMATE TENSILE STRENGTH (MPA)	10.88	10.88

5.7 FINITE ELEMENT STRUCTURAL ANALYSIS

The results gotten from the tensile test were further used to analyse the blister deformation using Ansys static analysis software.

The aim of analysis:

- Useful volume Deformation
- Strain analysis

Material assignment:

- Blister: Blu-stuff
- Pin: rigid thermoplastic
- Washer: rigid thermoplastic

Boundary condition:

- Support: fixed
- Load: 10N (ramped)

5.7.1 USEFUL VOLUME DEFORMATION

In this analysis, the initial state of the blister was compared with the fully compressed state to anticipate the amount of fluid deposit in pocket spaces create by the deformation. These fluids deposits do not contribute to the total volume being pushed through the fluidic network. Therefore, they are regarded as nonfunctional or unusable volume. Likewise, good insight can be derived from this analysis to help determine appropriate volume consideration in blister shape and capacity design.From the Figure 5.7, it can be observed that a steady force was being applied to deform the blister from a uncompressed to a compressed state. Likewise, Figure 5.8 depicts the achievement of the design model in the compressed state with less air pocket spaces. Therefore, there will be minimum reagent wastage during fluid expulsion to the flow network.

5.7.2 FINITE ELEMENT ANALYSIS OF BLISTER COMPRESSION

Ansys static analysis software was used to determine the stress the blister undergoes when subjected to an external push force from human fingers or mechanical contrivance such as a solenoid. In this analysis, the force is expected to be consistently progressive as the blister gradually deforms with or without the back pressure from the internal fluid. The back pressure comes as a result of fluid being forced instantaneously from a high volume region to a micro capacity media such as a microchannel.

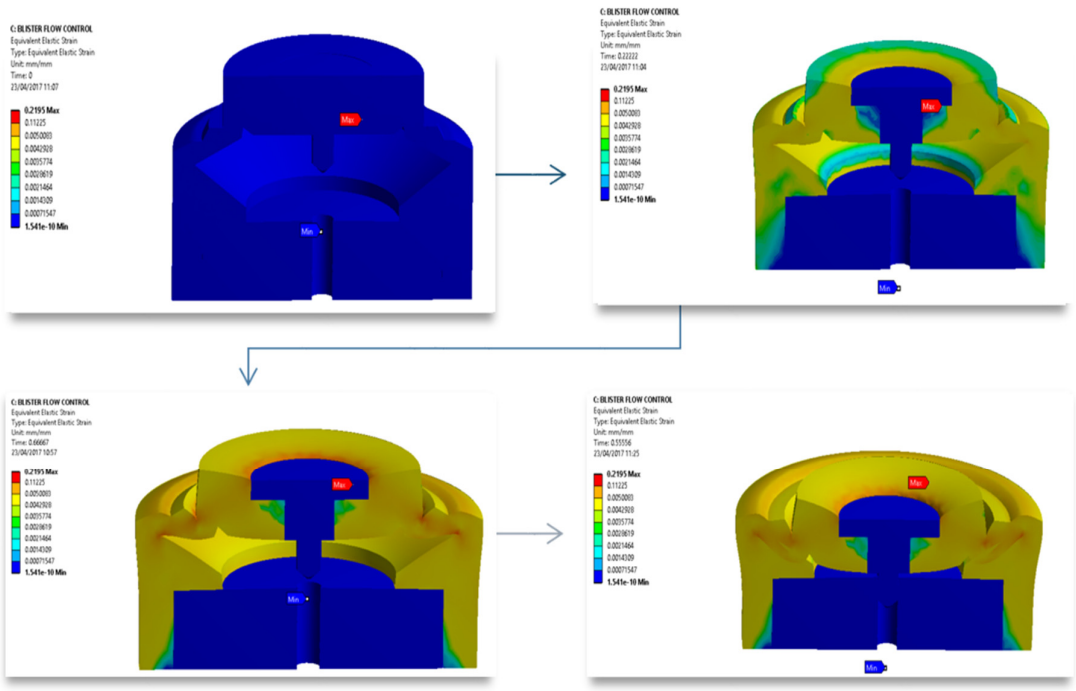

Figure 5.7. Static analysis on complete blister assembly showing gradual decompression of blister under a ramped forced of 10N.

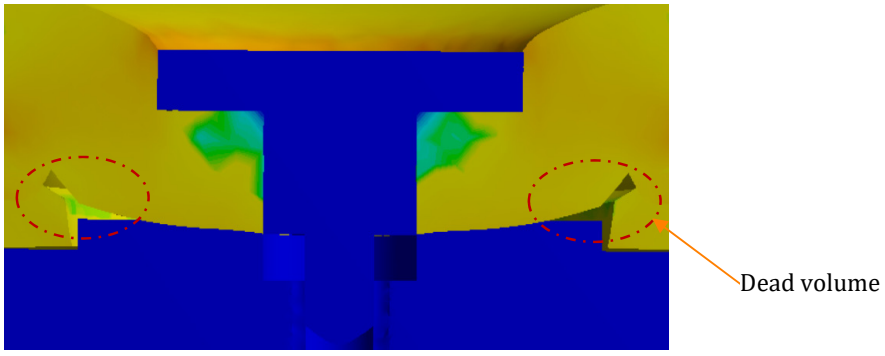

Figure 5.8. Illustration of a fully decompressed blister with minimal dead space volume.

5.8 BLISTER FABRICATION

Processing and Curing of Blister Material were similar to PDMS, Blu-Stuff requires two-part liquid mixing agents to initiate the polymerization reaction. Although the ratios are equal (1:1) the curing takes less than twenty minutes at room temperature. The preparation starts with the same volume of each liquid agent thoroughly mix for ten seconds before being poured into a mould to set. The replication technique applied in this process is similar to the injection moulding, although heat is not required since the material is already in liquid form. Figure 5.9 shows an assembly of the blister die which consists of a detachable plunger and a base mould. When both are put together their hollow cavities form the groove and path ways for the liquid elastomer to fill before setting.

Fabrication protocols:

i. Thorough mixing of the proprietary blu-stuff elastomer
ii. Pouring the liquid elastomer into the base mould cavity (Figure 5.10)
iii. Gradual Insertion of the die plunger, while poking for air bubbles
iv. Clearing excess liquid from the top of the die assembly
v. Blu-stuff left to set for twenty minutes
vi. Mould taking apart gently to remove newly from blister (Figure 5.11)

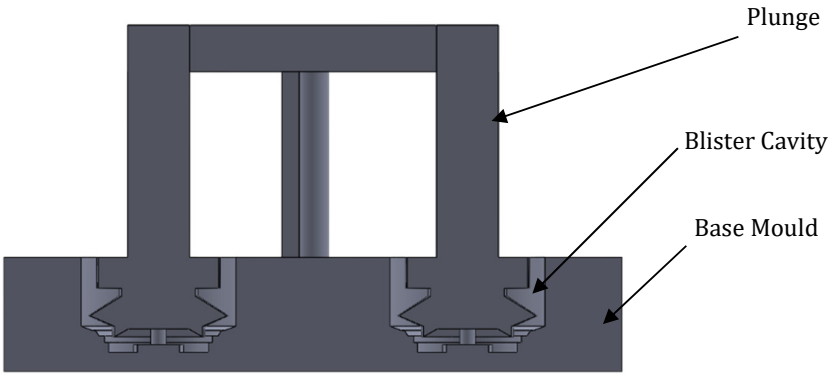

Figure 5.9. Illustration of the plunger and a base mould design configuration used for making blisters

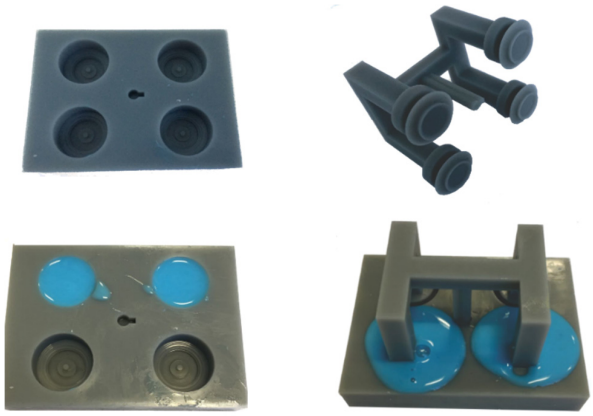

Figure 5.10. Fabrication of Blu-stuff elastomeric blister using 3D printed plunger and base mould

Figure 5.11. fabricated blu-stuff silicone elastic blister for microfluidic cartridge

5.9 ASSEMBLY OF FLUIDIC ELEMENTS ON CHIP

This section as depicted in Figure 8.1 shows the installation of the blister mechanism to the PDMS POCT prototype chip.

Fabrication protocols:

i. The 400µL capacity blister was prefilled with 320µl blue dye is installed on chip (Figure 5.12)
ii. Chip was then enclosed in the metal jig secured with bolts and nuts.
iii. PDMS is then poured to fill up the jig to a height of 5mm (Figure 5.13a)
iv. Jig was then placed in the oven for 4hrs at 65^0C
v. Set PDMS was then peeled off the mould (Figure 5.13.b) and bonded to a glass slide.
vi. Bonded PDMS-glass chip (Figure 5.13c) was then left in the oven 3hrs at 65^0C

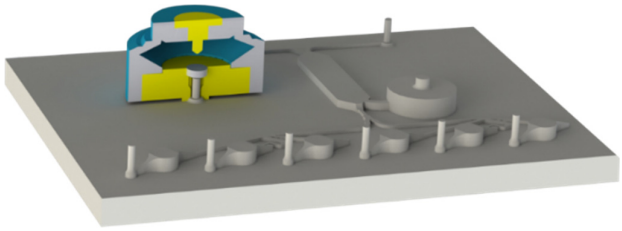

Figure 5.12. 3D design assembly configuration of positive mould microfluidic cartridge with a blister and its internal components

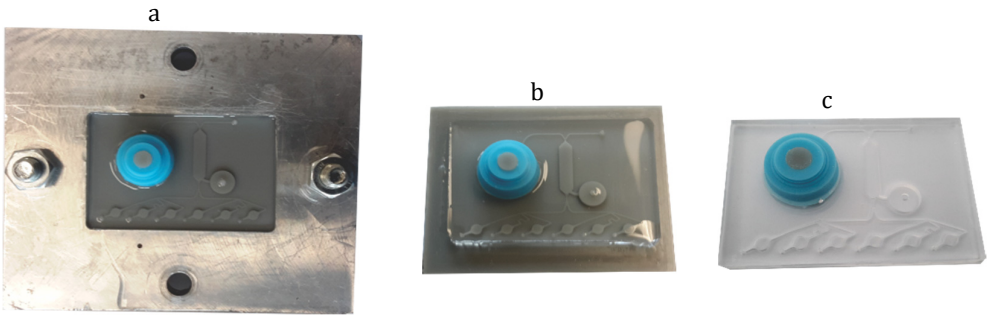

Figure 5.13. (a) Fluid filled Blister with positive mould chip is installed in a metal jig and filled with liquid PDMS. (b) Cured PDMS negative mould and blister still attached to positive chip. (c) Bonded glass slide with PDMS mould bearing a blister.

5.10 FLUID FLOW EXPERIMENTATION ON INTEGRATED CHIP

This experimentation is exclusive for amplification purpose. Similar to the previous experimentation on chapter 5, a coloured dye is used instead, regent. The targeted region for fluid dispensing is the shown in (Figure 4.1c) as the expected volume to be filled. This fluid filling process can only be achieved when the waste outlet is securely blocked. This blockage is done to prevent unwanted flow into the WRC that will result in unwanted wastage of liquid dye since the blister has a capacity of 400 µL and contains a specific liquid volume (370µL) that is needed for the amplification reaction.

Experimental protocols (magnet seal) design model:

i. The waste outlet was securely blocked
ii. Magnet with 30kg pull strength is held briefly for about two seconds at a distance of 1mm-2mm from the top of the blister (Figure 5.14).
iii. Next, the blister is gradually depressed at a slow pace
iv. Depression stops after the pin at the top of the blister keys into the washer below

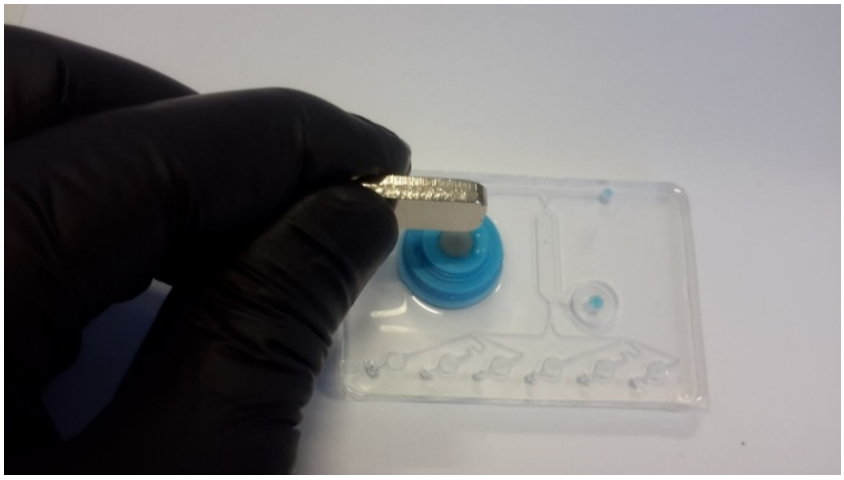

Figure 5.14. The use of magnet to release the miniature magnetic valve for fluid flow activation

5.10.1 EXPERIMENTAL RESULTS AND DISCUSSION

This experiment is similar to the previous fluid flow experiment performed without the use of chitosan. Although, in this case, only the DNA elution and amplification processes are considered. The Figure 5.15 illustrates the DNA elution process of filling the CRC with blue liquid dye representing amplification reagent. The elution process involved dispensing 135µL of liquid from the blister. Afterwards, the follow-up process shown in Figure 5.16 is the final liquid distribution by the multiplexer to fill-up the ARC for DNA multiplication. The whole experiment took place under a minute, with a varying flow rate which is dependent on the amount of pressure applied on the blister. The time jump observed in Figure 5.16 at the 11 seconds mark to 40 secs was as a result of a significant drop in pressure applied on the blister.

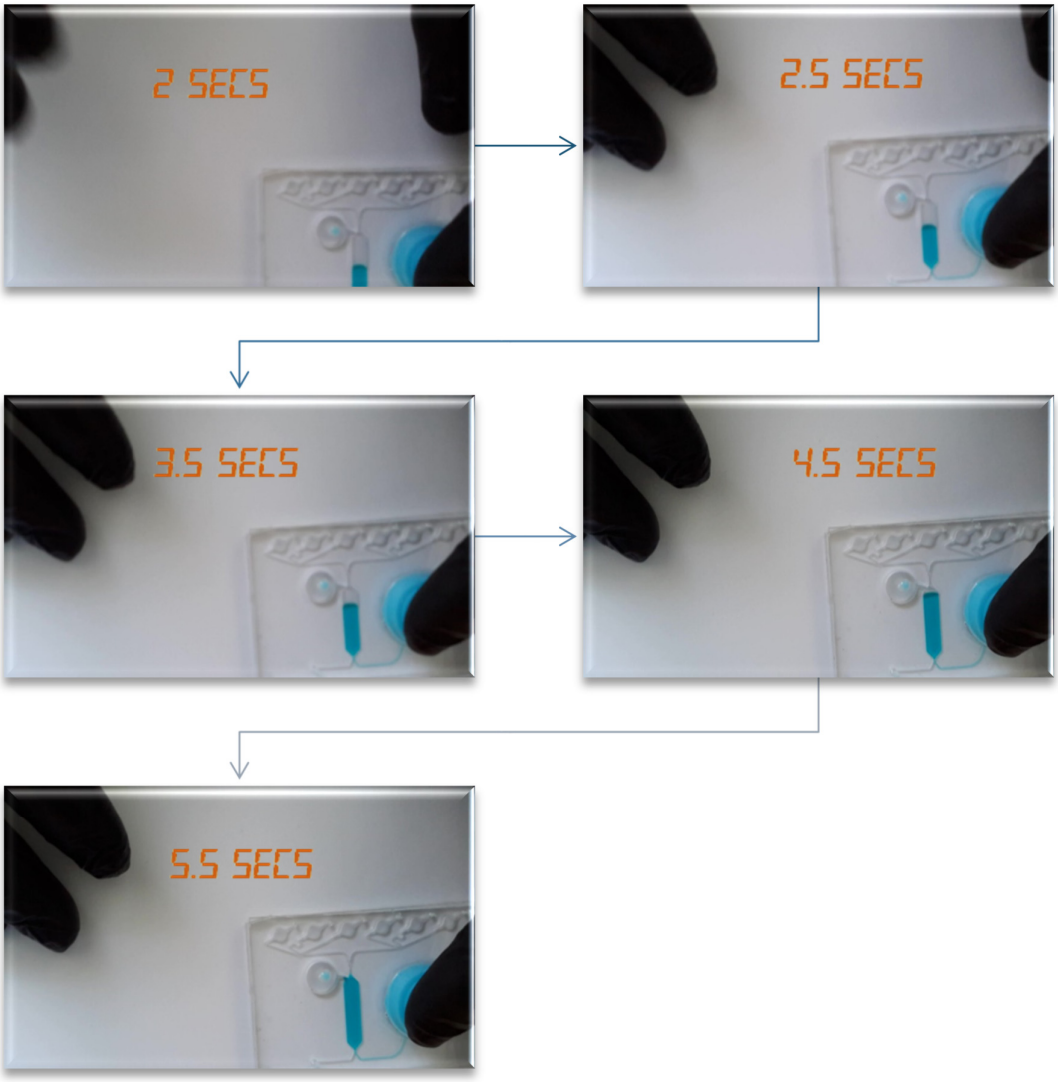

Figure 5.15. Pseudo DNA elution process that involved filling of the central reaction chamber with blue dye dispensed from the blister by finger compression.

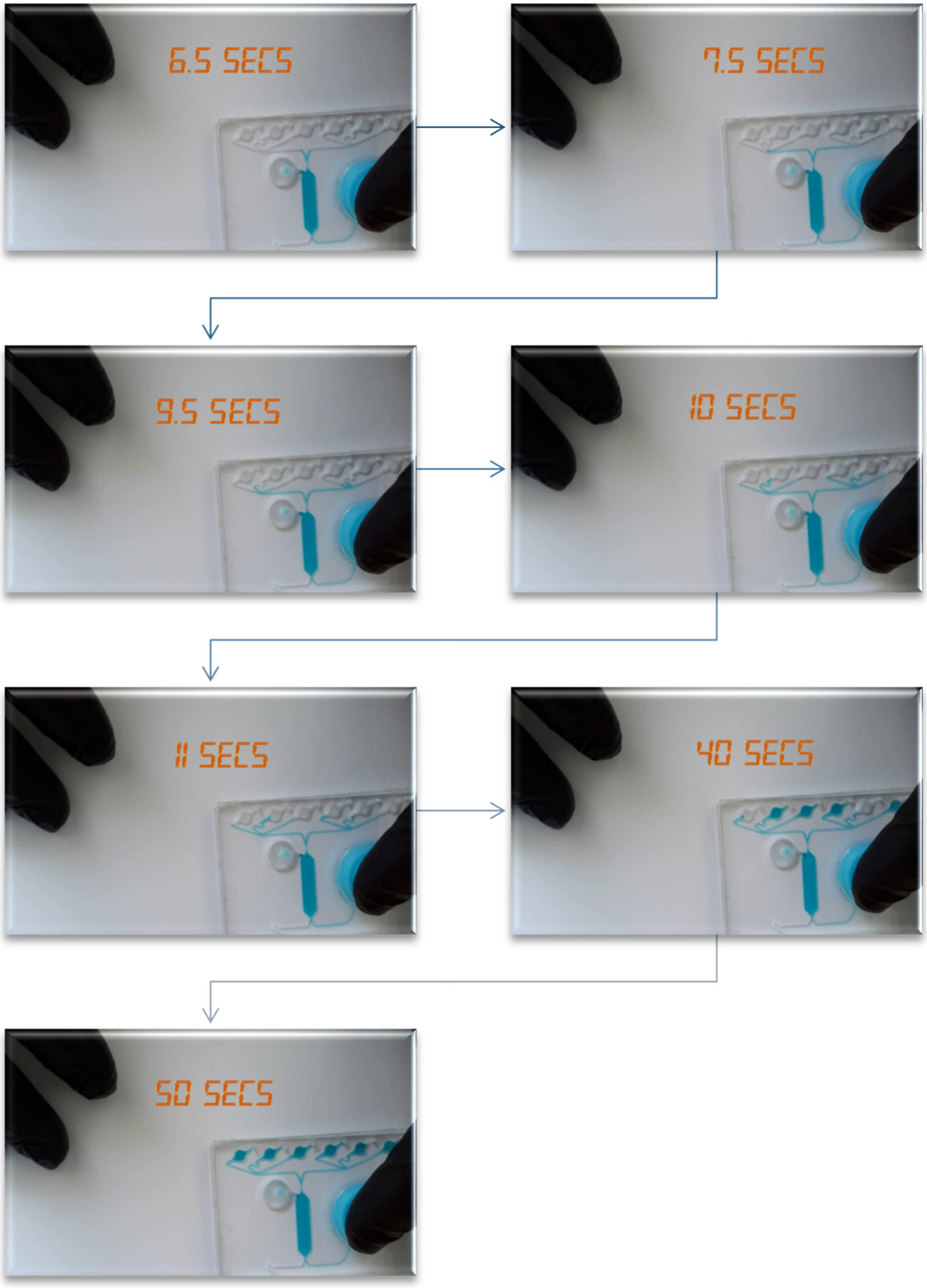

Figure 5.16. Extended finger compression exercise to Filling of the multiplexer and amplification reaction chambers by further finger compression.

5.11 SUMMARY

In designing this silicone elastomeric blisters, the material selection was critical amongst the process because it highlights the durability and particularly the ease of fabrication. The chosen material was a proprietary silicone elastomer called Blu-stuff due to its superior young modulus and tensile strength in comparison to PDMS. The geometry design for the blister was specifically chosen to provide adequate liquid volume and most especially allow appropriate deformation with less dead space volume to avoid wastage. The design merits were put to the test when an FEA simulation was performed on the 3D concept model prior to fabrication. The test successfully showed a fully compressed blister with minimal air pockets capable of housing liquid reagent that will reduce constituent wastage. As a result, the functioning blister showed promise of reagent savings. Another challenged resolved the interface mechanism between the blister and the cartridge. These mechanisms formed parts assembled to hold liquid in the blister before use. Two types of mechanism were described in this section. The only main difference between both setups was one of them uses a miniature magnet as a liquid flow stopper while the other a burstable rubber seal. After the successful fabrication of the blister with 3D printed moulds and subsequent use of soft lithography technique to integrate the blister with the cartridge. The mechanism that utilises a novelty use of a magnet for fluid control was employed in the fluidic experiment. At the start of the experiment, a small magnet with a pull strength 20kg was hovered about 1mm-2mm around the top of the blister to release the internal miniature magnet preventing flow from the blister. Afterwards, the 400µL capacity blister prefilled with 380µL of blue reagent was depressed to fill the 370µL microfluidic network similarly with Chapter 5 DNA elution and amplification experiment without chitosan. The slight 10µL difference in the experimental quantity required and prefilled blister was done in other to check wastage. In the end, after the blister was fully depressed all the required chambers were successfully filled as expected. So, therefore, it can be mathematical deducted that approximately three percent of the reagent was lost during this experiment. In conclusion, these auspicious results provide sufficient proof of concept that would warrant future DNA amplification experiment with prefilled reagent blister.

6.CONCLUSIONS

The core essence of microfluidics is scaling down conventional laboratory protocols to fit miniature devices that are highly required in a biomedical environment. So, in this thesis, a catalogue of the various steps, technology and science necessary to create a microfluidic cartridge capable of performing multiplex DNA amplification reactions was presented. The laboratory protocols that needed to be adapted involved DNA extraction, purification, elution and amplification. For these various steps specific, modular microfluidic elements were designed to fulfil the intended functionalities. Amongst the key features was the reaction chambers that were of three different categories. In no particular order, DNA sample preparation reservoir was centrally located trapezoidal and expected to house a chitosan membrane. This unique design was selected due to its streamline features that can handle multiple fluid filling processes without air bubble formations that be very challenging due to their adverse effects on bio-chemical reactions. The fluid process in this micro-compartment involves the use of chitosan to extract DNA by binding to it by the aid of a solution at pH 5.0 and then releasing it when a different mixture at pH 9.0 was pumped in. DNA purification which occurred between this extraction and elution processes required designing a waste reservoir capable of storing fluid waste internally, to assist the disposability of the cartridge. For this chamber design, the priority was volume. So, therefore, a circular shape which is concise and spatial suitable for the 75mm X 50mm cross-sectional area of the cartridge was selected. The high capacity volume that was twice the size of the extraction capacity was chosen to accommodate the use of sodium polyacrylate powder with antibacterial chemicals that rapidly expands in contact with the liquid. This liquid absorbing process was the preferred waste treatment process to prevent environmental contamination by converting extra fluid to gel-like substance. The last category is the region where amplification reactions were expected to occur, and for this cartridge, six microchambers were developed. Their intended design functions were similar to the extraction micro-reservoir requirements that favoured streamline flow to prevent air bubble formation. Although, they had much smaller volume since all six of them shared the extraction reservoir.

Apart from the interconnecting microchannels, there are also two main parts of the cartridge, which were designed specifically for fluid handling operations. They consist of a passive valve and multiplexer. This passive valve served as a useful microfluidic tool that is self-regulatory; requiring no external power input to control flow from the sample preparation to the waste chamber. The means to achieving this mechanism was

selecting a preferable geometrical configuration that created temporally pressure seal to prevent flow in a specific direction. This configuration consists of fluid moving from a large to narrow volume domain that generates relative high pressure that is required to be surpassed before fluid flow is permitted. On the other hand, the multiplexer was needed to distribute liquid simultaneously to the six amplification microchambers through a vein network of microchannels. All these designed modular elements combined through a series of interface ports and microchannels to form a closed loop microfluidic circuit that was subjected to a multiphase and single-phase simulations. The goal of the multiphase simulation was to observe the behavioural patterns of the fluid within the specified geometrical designed features to ascertain a semblance of reality. Whereas, single phase flow was used to accurately to deduct empirical values that can be analysed to improve or understand the relationship between the fluid and geometrical constraints of the microfluidic circuit. The is analyses proved useful in determining the best narrow width of the passive valve to be used.

The preferred means of fabrication was soft lithography that provided low-cost and less complicated means for producing a hybrid cartridge of PDMS and glass composition. These commonly used substrates are known to have different surface nature. PDMS is hydrophobic, while glass is hydrophilic. As a result, their combination produces a slightly different fluid flow pattern in comparison to the CFD simulations that made use of a no-slip boundary condition of wall surfaces. The internal microchannel walls of the cartridge were a ratio of 3:1 in favour of PDMS. That indicated that the overall wall wetting properties was more hydrophobic than hydrophilic. Empirically, these dominant wall characteristics provide more flow stability and control, while the recessive properties that are hydrophilic helped reduced resistance to flow by maximizing the contact area between the liquid-solid interface. In addition to the complimentary synergy of both surfaces; since hydrophobic surfaces are mostly not favourable to bio-chemical reaction the presence of hydrophilic glass helps mitigate the problem.

The nature of the DNA experiment performed on the cartridge entailed the use of synthetic DNA and an RPA basic kit that had to be altered volumetrically and chemically so as suit DNA sample preparation by chitosan. The volumetric process involved creating two key solutions namely; DNA sample mixture and amplification reagent. However, the chemical alterations involved introducing MES buffer pH 5.0 for DNA extraction and TRIS-KCl pH 9.0 solution for elution. Afterwards, a successful post-amplification technique using agarose gel electrophoresis was used to validate that multiplex amplification reactions took place in the cartridge. In other to improve the microfluidic cartridge to be compliant with present day demands for close circuit devices that are less dependent on power consuming syringe pumps especially in low resource settings. Efforts were made to design and fabricate a silicon elastomeric blister that could be easily installed on the chip. Two essential functions were required of this device which was fluid pumping and storage. After this innovation was put through a liquid flow experiment using coloured dye as substi8te for amplification reagent stored on the chip, it successfully demonstrated effectiveness and efficiency to be applicable.

In conclusion, this thesis can be said to have completed all its stated research objectives by using a relatively economical, flexible and hands-on approach for performing multiplex DNA amplification reactions on a single microfluidic cartridge. As of present STI's panel tests that involve that require several assays to run simultaneously resulting in high cost due to significant demand in equipment and reagent. Therefore, having a single microfluidic cartridge capable of handling multiple biological assays is promising and likewise a welcome addition to the prevalent state of the art technologies for the multiplex detection of pathogens related to the significant STI diseases. Moreover, implementation of this innovative cartridge design in low resource

settings, where near patient testing is usually needed can be conceivable with minimal dependency on clinical laboratories.

7.RECOMMENDATIONS AND FUTURE WORKS

7.1 RECOMMENDATIONS

These recommendations are the few insights and knowledge obtained during the DNA amplification experiments that can provide better results for future biological assays in line with this project.

7.1.1 PASSIVE VALVE:

In the thesis, only one geometrical design of passive valve was investigated within a limited 3D printer resolution. As a result, more work is needed to be done with various geometrical shapes that can act as efficient passive valves with the improved time sequence of fluid handling operations without generating any dead volume.

7.1.2 MULTIPLEXER:

The multiplexer utilised for this microfluidic cartridge was capable but unpredictable or non-sequential when filling the designate amplification chambers with liquid. As a result, efforts should be made to design a multiplexer that is effective and exceptionally predictable in its fluid filling pattern. So similar shapes of chambers to be filled can be arranged in a specific spatial configuration enabling fluid buildup in pre-planned orders.

7.1.3 SIMULATION ANALYSIS

In the simulation analysis used the microfluidic design the effect of surface tension was not accounted for. Since this hybrid cartridge composes of two different surfaces (hydrophobic and hydrophilic), effort should be made to run a similar simulation with the wall surfaces at specific adhesive contact angle. This contact angle is responsible for the characteristic of the wall when they interact with fluid. As a result, the no-slip boundary condition will not apply since a defined wetting characteristic of a microchannel wall will give a better semblance to a real-time fluid flow experiment.

7.1.4 DNA AMPLIFICATION EXPERIMENT:

There are areas of the DNA amplification fluid flow protocols that require improvement. Prominent amongst these was DNA elution amplification process that is concerned with harvesting the already extracted DNA from the chitosan membrane for amplification. The experimental protocols undertaken in this thesis involves filling the central reaction chamber completely with amplification reagent and then leaving it for a very short period. This pause or interlude is expected to help the elution process yield a maximum DNA harvest before the released DNA are then pumped into the amplification chamber. Therefore, to increase the DNA yield during the elution process, there should be repeated interlude after each complete chamber fill-up. For instance, if the time to fill up the reaction chamber is twenty seconds at a certain speed and the elution interval period is ten seconds, then after every twenty seconds the should be ten seconds pause till all the six amplification reaction chambers are filled. This new adjustment in protocol will help ensure maximum yield from the chitosan membrane.

7.2 FUTURE WORKS

In this section, the expedient use of this hybrid microfluidic cartridge for both academic research and commercial utilisation is discussed.

7.2.1 MATERIAL SELECTION:

PDMS substrate, a commonly utilised material with many attractive properties for device fabrication in the biomedical field, suffers significant fouling complications from protein adsorption due to its hydrophobic nature, which limits its practical use real biofluid samples. A good example of such biofluid is blood. This property makes PDMS use for long-term sustainable applications compromised. As result efforts will have to be made to use materials with similar characteristics, and better biocompatibility than PDMS. Such materials to be investigated will be PMMA and COC.

7.2.2 DNA DETECTION ON CARTRIDGE:

This prospective project is a lot more sophisticated because it entails the use of real-time detection technology to either serve as a complement or a replacement for more conventional detection means of identifying specific pathogens. This state-of-the-art technology provides the PDMS-glass cartridge with the capability to have DNA detection on the chip without relying solely on endpoint analysis involving fluid extraction from the chip. As result disposability of this cartridge can be truly realised, as all intended microfluidic and medical diagnostic. For successful implementation, other detection real-time systems such as electrochemical, magnetic beads base and optical Fluorescent Dye DNA Detection techniques would have to be tested.

7.2.3 AUTOMATION OF FLUID PROTOCOLS ON CARTRIDGE

A direct application to the already prescribed RPA protocols in Chapter 4 can be programmed on a device or platform capable of carrying out the DNA extraction, purification, elution and amplification protocol given that there are already prescribe time sequence for the fluid handling operations. This process will be capital intensive, that is why the implementation of the on-chip blister to hold some or most of the reagent will be a welcome prospect for simplicity of protocols and low cost of fabrication.

REFERENCES

[1] L. J. Kricka, “Microchips, microarrays, biochips and nanochips: personal laboratories for the 21st century.,” *Clin. Chim. Acta.*, vol. 307, no. 1–2, pp. 219–23, May 2001.

[2] D. Figeys and D. Pinto, “Lab-on-a-Chip : A Revolution in Biological and Medical Sciences A look at some of the basic concepts and,” 2004.

[3] A. K. Au, H. Lai, B. R. Utela, and A. Folch, *Microvalves and micropumps for BioMEMS*, vol. 2, no. 2. 2011.

[4] R. C. Anderson, X. Su, G. J. Bogdan, and J. Fenton, “A miniature integrated device for automated multistep genetic assays.,” *Nucleic Acids Res.*, vol. 28, no. 12, p. E60, Jun. 2000.

[5] J. West, M. Becker, S. Tombrink, and A. Manz, “Micro total analysis systems: Latest achievements,” *Anal. Chem.*, vol. 80, no. 12, pp. 4403–4419, 2008.

[6] D. R. Reyes, D. Iossifidis, P.-A. Auroux, and A. Manz, “Micro total analysis systems. 1. Introduction, theory, and technology.,” *Anal. Chem.*, vol. 74, no. 12, pp. 2623–2636, 2002.

[7] O. Geschke, H. Klank, and P. Tellemann, *Microsystem Engineering of Lab-on-a-Chip Devices*, vol. 258. Wiley-VCH, 2004.

[8] N. L. Jeon, D. T. Chiu, C. J. Wargo, H. K. Wu, I. S. Choi, J. R. Anderson, and G. M. Whitesides, “Design and fabrication of integrated passive valves and pumps for flexible polymer 3-dimensional microfluidic systems,” *Biomed. Microdevices*, vol. 4, no. 2, pp. 117–121, 2002.

[9] C. D. Chin, V. Linder, and S. K. Sia, “Commercialization of microfluidic point-of-care diagnostic devices,” *Lab Chip*, vol. 12, no. 12, pp. 2118–2134, 2012.

[10] V. Pribul and T. Woolley, “Point of care testing,” *PubMed*, vol. 31, no. 2, pp. 84–86, 2013.

[11] Prof Samuel, “International business times,” 2011. [Online]. Available: http://www.ibtimes.com/services/mostpopular.htm?date=2011-08-01&type=d&section=Health. [Accessed: 23-Aug-2011].

[12] J. Wang, Z. Chen, P. L. a M. Corstjens, M. G. Mauk, and H. H. Bau, “A disposable microfluidic cassette for DNA amplification and detection.,” *Lab Chip*, vol. 6, no. 1, pp. 46–53, 2006.

[13] J. Sambrook, E. F. Fritsch, and T. Maniatis, *Molecular cloning: A laboratory manual. Cold spring harbor laboratory press*. 1989.

[14] X. Chen, D. Cui, C. Liu, H. Li, and J. Chen, “Continuous flow microfluidic device for cell separation, cell lysis and DNA purification,” *Anal. Chim. Acta*, vol. 584, no. 2, pp. 237–243, 2007.

[15] J. Wu, R. Kodzius, W. Cao, and W. Wen, “Extraction, amplification and detection of DNA in microfluidic chip-based assays,” *Microchim. Acta*, vol. 181, no. 13–14, pp. 1611–1631, 2014.

[16] R. H. Liu, J. Yang, R. Lenigk, J. Bonanno, and P. Grodzinski, “Self-Contained, Fully Integrated Biochip for Sample Preparation, Polymerase Chain Reaction Amplification, and DNA Microarray Detection,” *Anal. Chem.*, vol. 76, no. 7, pp. 1824–1831, 2004.

[17] L. C. Waters, S. C. Jacobson, N. Kroutchinina, J. Khandurina, R. S. Foote, and J. M. Ramsey, “Microchip device for cell lysis, multiplex PCR amplification, and electrophoretic sizing.,” *Anal. Chem.*, vol. 70, no. 1, pp. 158–162, 1998.

[18] P. Belgrader, D. Hansford, G. T. A. Kovacs, K. Venkateswaran, R. Mariella, F. Milanovich, S. Nasarabadi, M. Okuzumi, F. Pourahmadi, and M. A. Northrup, “A minisonicator to rapidly disrupt bacterial spores for DNA analysis,” *Anal. Chem.*, vol. 71, no. 19, pp. 4232–4236, 1999.

[19] T. C. Marentis, B. Kusler, G. G. Yaralioglu, S. Liu, E. O. Haeggstrom, and B. T. Khuri-Yakub, “Microfluidic sonicator for real-time disruption of eukaryotic cells and bacterial spores for DNA analysis.,” *Ultrasound Med. Biol.*, vol. 31, no. 9, pp. 1265–1277, Sep. 2005.

[20] G. Erden and A. Filibeli, “Ozone oxidation of biological sludge: Effects on disintegration, anaerobic biodegradability, and filterability,” *Environ. Prog. Sustain. Energy*, vol. 30, no. 3, pp. 377–383, 2011.

[21] P. Marmottant and S. Hilgenfeldt, “Controlled vesicle deformation and lysis by single oscillating bubbles.,” *Nature*, vol. 423, no. 6936, pp. 153–156, 2003.

[22] C. W. Price, D. C. Leslie, and J. P. Landers, “Nucleic acid extraction techniques and application to the microchip.,” *Lab Chip*, vol. 9, no. 17, pp. 2484–94, 2009.

[23] K. A. Curtis, D. L. Rudolph, and S. M. Owen, “Rapid detection of HIV-1 by reverse-transcription, loop-mediated isothermal amplification (RT-LAMP),” *J. Virol. Methods*, vol. 151, no. 2, pp. 264–270, 2008.

[24] Z. Zhang, M. B. Kermekchiev, and W. M. Barnes, “Direct DNA amplification from crude clinical samples using a PCR enhancer cocktail and novel mutants of Taq,” *J Mol Diagn*, vol. 12, no. 2, pp. 152–161, 2010.

[25] M. B. Kermekchiev, L. I. Kirilova, E. E. Vail, and W. M. Barnes, “Mutants of Taq DNA polymerase resistant to PCR inhibitors allow DNA amplification from whole blood and crude soil samples,” *Nucleic Acids Res.*, vol. 37, no. 5, 2009.

[26] T. Nakagawa, R. Hashimoto, K. Maruyama, T. Tanaka, H. Takeyama, and T. Matsunaga, “Capture and release of DNA using aminosilane-modified bacterial magnetic particles for automated detection system of single nucleotide polymorphisms.,” *Biotechnol. Bioeng.*, vol. 94, no. 5, pp. 862–868, Aug. 2006.

[27] C.-H. Wang, K. Lien, J. Wu, and G. Lee, “Assay for the rapid detection of methicillin-resistant Staphylococcus aureus by using a microfluidic system with integrated loop-mediated isothermal amplification,” *Lab Chip*, vol. 11, no. 8, pp. 1521–1531, 2011.

[28] W. Cao, C. J. Easley, J. P. Ferrance, and J. P. Landers, “Chitosan as a polymer for pH-induced DNA capture in a totally aqueous system,” *Anal. Chem.*, vol. 78, no. 20, pp. 7222–7228, 2006.

[29] M. D. U. R. S. (COLUMBIA M. D. U. P. K. R. (LAUREL M. D. U. N. I. (COLLEGE P. M. D. U. C.

W. (NORTH P. M. D. U. White Ian M. (ELLICOTT CITY, “SINGLE-STEP DNA PREPARATION FOR POLYMERASE CHAIN REACTION USING MAGNETIC CHITOSAN MICROPARTICLES,” no. 20160340668. Nov-2016.

[30] K. R. Pandit, I. A. Nanayakkara, W. Cao, S. R. Raghavan, and I. M. White, “Capture and Direct Amplification of DNA on Chitosan Microparticles in a Single PCR-Optimal Solution.,” *Anal. Chem.*, vol. 87, no. 21, pp. 11022–11029, Nov. 2015.

[31] C.-M. Chang, W.-H. Chang, C.-H. Wang, J.-H. Wang, J. D. Mai, and G.-B. Lee, “Nucleic acid amplification using microfluidic systems.,” *Lab Chip*, vol. 13, no. 7, pp. 1225–42, Apr. 2013.

[32] C. A. Heid, J. Stevens, K. J. Livak, and P. M. Williams, “Real time quantitative PCR.,” *Genome Res.*, vol. 6, no. 10, pp. 986–94, 1996.

[33] promega, “Nucleic Acid Amplification PROTOCOLS & APPLICATIONS GUIDE PROTOCOLS & APPLICATIONS GUIDE,” 2015. [Online]. Available: https://worldwide.promega.com/~/media/files/resources/paguide/a4/chap1a4.pdf?la=en.

[34] C. Zhang, J. Xu, W. Ma, and W. Zheng, “PCR microfluidic devices for DNA amplification,” *Biotechnology Advances*, vol. 24, no. 3. pp. 243–284, 2006.

[35] P. Labarre, J. Gerlach, J. Wilmoth, A. Beddoe, J. Singleton, and B. Weigl, “Non-instrumented nucleic acid amplification (NINA): instrument-free molecular malaria diagnostics for low-resource settings.,” *Conf. Proc. ... Annu. Int. Conf. IEEE Eng. Med. Biol. Soc. IEEE Eng. Med. Biol. Soc. Annu. Conf.*, vol. 2010, pp. 1097–1099, 2010.

[36] Y. Mori, H. Kanda, and T. Notomi, “Loop-mediated isothermal amplification (LAMP): Recent progress in research and development,” *Journal of Infection and Chemotherapy*, vol. 19, no. 3. pp. 404–411, 2013.

[37] M. Vincent, Y. Xu, and H. Kong, “Helicase-dependent isothermal DNA amplification.,” *EMBO Rep.*, vol. 5, no. 8, pp. 795–800, 2004.

[38] Biolabs, “Isothermal Amplification,” 2014. [Online]. Available: https://www.neb.com/applications/dna-amplification-and-pcr/isothermal-amplification.

[39] F. J. J. Kane and A. Pokorny, “Mental and emotional disturbance with pentazocine (Talwin) use.,” *South. Med. J.*, vol. 68, no. 7, pp. 808–811, Jul. 1975.

[40] T. Ando, J. Takagi, T. Kosawa, and Y. Ikeda, “Isolation and characterization of enzymes with nicking action from phage T4-infected Escherichia coli.,” *J. Biochem.*, vol. 66, no. 1, pp. 1–10, Jul. 1969.

[41] O. Piepenburg, C. H. Williams, D. L. Stemple, and N. A. Armes, “DNA Detection Using Recombination Proteins,” *PLoS Biol.*, vol. 4, no. 7, p. e204, Jul. 2006.

[42] D. L. Smisek and D. A. Hoagland, “Agarose gel electrophoresis of high molecular weight, synthetic polyelectrolytes,” vol. 22, no. 5, p. 2270, 1989.

[43] J. Sambrook and D. W. Russell, “Detection of DNA in Agarose Gels,” *Cold Spring Harb. Protoc.*, vol. 2006, no. 2, p. 1, 2006.

[44] J.-G. Lee, K. H. Cheong, N. Huh, S. Kim, J.-W. Choi, and C. Ko, “Microchip-based one step DNA extraction and real-time PCR in one chamber for rapid pathogen identification.,” *Lab Chip*, vol. 6, no. 7, pp. 886–895, Jul. 2006.

[45] A. Manz, N. Graber, and H. M. Widmer, “Miniaturized total chemical analysis systems: A novel concept for chemical sensing,” *Sensors and Actuators B: Chemical*, vol. 1, no. 1–6. pp. 244–248, 1990.

[46] J. Liu, C. Hansen, and S. R. Quake, “Solving the ‘world-to-chip’ interface problem with a microfluidic matrix.,” *Anal. Chem.*, vol. 75, no. 18, pp. 4718–4723, Sep. 2003.

[47] Y.-K. Cho, J. Kim, Y. Lee, Y.-A. Kim, K. Namkoong, H. Lim, K. W. Oh, S. Kim, J. Han, C. Park, Y. E. Pak, C.-S. Ki, J. R. Choi, H.-K. Myeong, and C. Ko, “Clinical evaluation of micro-scale chip-based PCR system for rapid detection of hepatitis B virus.,” *Biosens. Bioelectron.*, vol. 21, no. 11, pp. 2161–2169, May 2006.

[48] T. H. Fang, N. Ramalingam, D. Xian-Dui, T. S. Ngin, Z. Xianting, A. T. Lai Kuan, E. Y. Peng Huat, and G. Hai-Qing, “Real-time PCR microfluidic devices with concurrent electrochemical detection,” *Biosens. Bioelectron.*, vol. 24, no. 7, pp. 2131–2136, 2009.

[49] T. M. H. Lee and I. M. Hsing, “DNA-based bioanalytical microsystems for handheld device applications,” *Analytica Chimica Acta*, vol. 556, no. 1. pp. 26–37, 2006.

[50] Y. Xu and E. Wang, “Electrochemical biosensors based on magnetic micro/nano particles,” *Electrochimica Acta*, vol. 84. pp. 62–73, 2012.

[51] G. Falkovich, *Fluid Mechanics (A short course for physicists)*. Cambridge University Press, 2011.

[52] Yue-kin Tsang, “basic fluid dynamics,” 2011. [Online]. Available: www-vortex.mcs.st-and.ac.uk/~yktsang/4520/basic_fluid.pdf.

[53] C. Hsueh and L. Y. Yeo, *Electrokinetically-Driven Microfluidics and Nanofluidics*. Cambridge University Press, 2009.

[54] Sukhatme, Sarvesh, Agarwal, and Ajay, “Bioengineering & Biomedical Science Digital Microfluidics : Techniques , Their Applications and Advantages,” *Creating, Transporting, Cutting, and Merging Liquid Droplets by Electro-wetting Based Actuation for Digital Microfluidic Circuits*, no. 12. 2012.

[55] R. Zengerle, “3 . Physics of Microfluidic Systems.”

[56] B. Liu, Y. Deng, B. B. Qin, and Z. Y. Li, “Application of Microfluidics Technology in Bioanalysis,” *Adv. Sci. Lett.*, vol. 4, no. 1, pp. 150–155, 2011.

[57] Y.-J. Shin and J.-B. Lee, “Machine vision for digital microfluidics.,” *Rev. Sci. Instrum.*, vol. 81, no. 1, p. 14302, 2010.

[58] Z. Xiao, M. Niu, and B. Zhang, “Droplet microfluidics based microseparation systems.,” *J. Sep. Sci.*, vol. 35, no. 10–11, pp. 1284–93, 2012.

[59] M. Abdelgawad and A. R. Wheeler, “The Digital Revolution: A New Paradigm for Microfluidics,” *Adv. Mater.*, vol. 21, no. 8, pp. 920–925, 2009.

[60] R. Zengerle and J. Ducrée, “Microfluidics roadmap: The trend to use low-cost technologies and microfluidic platforms,” in *Actuator 2004 9th International Conference on New Actuators 116th June 2004 Bremen Germany*, 2004, no. June, pp. 194–199.

[61] N.-T. Nguyen and S. T. Wereley, *Fundamentals and Applications of Microfluidics*, vol. 7. Artech House, 2002.

[62] R. F. Ismagilov, T. D. Rosmarin, J. A. Kenis, D. T. Chiu, W. Zhang, H. A. Stone, and G. M. Whitesides, “Pressure-driven laminar flow in tangential microchannels: an elastomeric microfluidic switch.,” *Anal. Chem.*, vol. 73, no. 19, pp. 4682–4687, 2001.

[63] T. Squires and S. Quake, “Microfluidics: Fluid physics at the nanoliter scale,” *Rev. Mod. Phys.*, vol. 77, no. 3, pp. 977–1026, 2005.

[64] R. Narasimha, “The Challenge of Fluid Flow,” no. August, pp. 67–79, 2005.

[65] D. Cheng, J. Greenwood, X. Zeng, and C. Lo, “Laminar Flow in Microfluidic Channels Laminar and Turbulent Flow • What is Laminar Flow ? – Layers of liquid that flow in a uniform fashion,” 2007.

[66] S. Hardt, K. S. Drese, V. Hessel, and F. Schönfeld, “Passive micromixers for applications in the microreactor and μTAS fields,” *Microfluid. Nanofluidics*, vol. 1, no. 2, pp. 108–118, 2005.

[67] H. Hasimoto and O. Sano, “Stokeslets and Eddies in Creeping Flow,” *Annu. Rev. Fluid Mech.*, vol. 12, no. 1, pp. 335–363, 1980.

[68] A. Groisman and S. R. Quake, “A microfluidic rectifier: anisotropic flow resistance at low Reynolds numbers.,” *Phys. Rev. Lett.*, vol. 92, no. 9, p. 94501, 2004.

[69] D. J. Jeffrey and J. D. Sherwood, “Streamline Patterns and Eddies in Low-Reynolds-Number Flow,” *J. Fluid Mech. Digit. Arch.*, vol. 96, no. 2, pp. 315–334, 1980.

[70] G. K. Batchelor, *An Introduction to Fluid Dynamics*, vol. 76, no. 8. Cambridge University Press, 1967.

[71] F. White, *Viscous Fluid Flow*. McGraw-Hill Education, 2005.

[72] W. J. Layton, *Introduction to the Numerical Analysis of Incompressible Viscous Flows*, vol. 6, no. 2/3. Society for Industrial and Applied Mathematics (SIAM), 2008.

[73] L. D. Landau and E. M. Lifshitz, *Fluid Mechanics*, vol. 6, no. 1. Pergamon Press, 1987.

[74] M. Dolz, J. Delegido, A. Casanovas, and M.-J. Hernández, “A Low-Cost Experiment on Newtonian and Non-Newtonian Fluids,” *J. Chem. Educ.*, vol. 82, no. 3, p. 445, 2005.

[75] U. Miyamoto, “One-Dimensional Approximation of Viscous Flows,” *J. High Energy Phys.*, vol. 2010, no. 10, p. 17, 2010.

[76] Glen Elert, “viscosity,” 2013. [Online]. Available: http://physics.info/viscosity/.

[77] R. Nave, “Laminar Flow,” *HyperPhysics*, 2005. [Online]. Available: http://hyperphysics.phy-astr.gsu.edu/hbase/pfric.html.

[78] C. Lenz, A. Rebel, K. F. Waschke, R. C. Koehler, and T. Frietsch, “Blood viscosity modulates tissue perfusion – sometimes and somewhere,” *Transfus. Altern. Transfus. Med.*, vol. 9, no. 4, pp. 265–272, 2007.

[79] D. Mampallil and S. D. George, “Microfluidics – A Lab in Your Palm,” *resonance*, no. July, pp. 682–690, 2012.

[80] J. E. Winandy and T. F. Shupe, “FROM HYDROPHILICITY TO HYDROPHOBICITY : A CRITICAL REVIEW : PART I . WETTABILITY AND SURFACE BEHAVIOR Cheng Piao,” *Wood Fiber*, vol. 42, no. 4, pp. 490–510, 2010.

[81] A. D. Buckingham, P. W. Fowler, and J. M. Hutson, “Theoretical Studies of van der Waals Molecules and Intermolecular Forces,” *Chem. Rev.*, vol. 88, no. 6, pp. 963–988, 1988.

[82] P.-G. De Gennes, F. Brochard-Wyart, D. Quéré, and B. Widom, *Capillarity and Wetting Phenomena: Drops, Bubbles, Pearls, Waves*, vol. 57, no. 12. Springer, 2004.

[83] J. Eggers, “Nonlinear dynamics and breakup of free-surface flows,” *Rev. Mod. Phys.*, vol. 69, no. 3, pp. 865–930, 1997.

[84] penn state, “Velocity profile of laminar flow in a pipe,” 2012. [Online]. Available: http://accessibility.psu.edu/longdescription. [Accessed: 04-Aug-2013].

[85] T. E. McKnight, C. T. Culbertson, S. C. Jacobson, and J. M. Ramsey, “Electroosmotically Induced Hydraulic Pumping with Integrated Electrodes on Microfluidic Devices,” *Anal. Chem.*, vol. 73, no. 16, pp. 4045–4049, Jul. 2001.

[86] D. Dutta and J. M. Ramsey, “A microfluidic device for performing pressure-driven separations.,” *Lab Chip*, vol. 11, no. 18, pp. 3081–8, Sep. 2011.

[87] Brian J. Kirby, *Micro- and Nanoscale Fluid Mechanics: Transport in Microfluidic Devices*. Cambridge University Press, 2009.

[88] M. J. Fuerstman, P. Deschatelets, R. Kane, A. Schwartz, P. J. A. Kenis, J. M. Deutch, and G. M. Whitesides, “Solving Mazes Using Microfluidic Networks,” *Langmuir*, vol. 19, no. 11, pp. 4714–4722, Apr. 2003.

[89] R. J. Cornish, “Flow in a Pipe of Rectangular Cross-Section,” *Proc. R. Soc. A Math. Phys. Eng. Sci.*, vol. 120, no. 786, pp. 691–700, Oct. 1928.

[90] T. Glawdel and C. L. Ren, “Electro-osmotic flow control for living cell analysis in microfluidic PDMS chips,” *Mech. Res. Commun.*, vol. 36, no. 1, pp. 75–81, Jan. 2009.

[91] S. D. Hudson, “Poiseuille flow and drop circulation in microchannels,” *Rheol. Acta*, vol. 49, no. 3, pp. 237–243, 2009.

[92] K. W. Oh, K. Lee, B. Ahn, and E. P. Furlani, “Design of pressure-driven microfluidic networks using electric circuit analogy.,” *Lab Chip*, vol. 12, no. 3, pp. 515–45, Feb. 2012.

[93] Elveflow, “flow control in microfluidics devices,” 2011. [Online]. Available: http://www.elveflow.com/microfluidic-reviews-and-tutorials/nanofluidics-microfluidics-and-millifluidics.

[94] Ove Bratland, “Pipe Flow Assurance,” 2016. [Online]. Available: http://www.drbratland.com/PipeFlow2/chapter1.html. [Accessed: 22-Sep-2016].

[95] A. CFD, “Multiphase Flow Modeling,” 2016. [Online]. Available: https://www.sharcnet.ca/Software/Ansys/17.0/en-us/help/cfx_mod/i1384390.html.

[96] Ansys Fluent, “Modeling Multiphase Flows,” 2016. [Online]. Available: http://read.pudn.com/downloads119/ebook/505117/Fluent Modeling Multiphase Flows.pdf. [Accessed: 22-Sep-2016].

[97] Andre Baker, “Multiphase Flows,” 2012. [Online]. Available: http://www.bakker.org/dartmouth06/engs150/14-multi.pdf. [Accessed: 22-Sep-2016].

[98] S. Kaneda and T. Fujii, “Integrated microfluidic systems.,” *Adv. Biochem. Eng.*, vol. 119, no. June, pp. 179–194, 2010.

[99] R. H. W. Lam, K. F. L. K. F. Lei, J. H. M. Lam, and W. J. Li, “Digitally Controllable Large-Scale Integrated Microfluidic Systems,” *2004 IEEE International Conference on Robotics and Biomimetics*. Ieee, pp. 301–306, 2004.

[100] B. Gray, “Novel interconnection technologies for integrated microfluidic systems,” *Sensors Actuators A Phys.*, vol. 77, no. 1, pp. 57–65, 1999.

[101] T. Thorsen, S. J. Maerkl, and S. R. Quake, “Microfluidic large-scale integration.,” *Science*, vol. 298, no. 5593, pp. 580–4, Oct. 2002.

[102] J. Melin and S. R. Quake, “Microfluidic large-scale integration: the evolution of design rules for biological automation.,” *Annu. Rev. Biophys. Biomol. Struct.*, vol. 36, pp. 213–31, Jan. 2007.

[103] J. Melin and S. R. Quake, “Microfluidic Large-Scale Integration: The Evolution of Design Rules for Biological Automation Microfluidics: the study and manipulation of fluidic behavior on the nanoliter scale and below,” *Annu. Rev. Biophys. Biomol. Struct*, 2007.

[104] L. Capretto, W. Cheng, M. Hill, and X. Zhang, “Micromixing within microfluidic devices.,” *Top. Curr. Chem.*, vol. 304, no. April, pp. 27–68, 2011.

[105] D. W. L. D. W. Lee and Y.-H. C. Y.-H. Cho, “A quaternary microfluidic multiplexer using dynamic control of pressure valves having different thresholds,” *TRANSDUCERS 2009 2009 International SolidState Sensors Actuators and Microsystems Conference*. 2009.

[106] N. S. Korivi and L. J. L. Jiang, “A polymer microfluidic multiplexer,” *Proceedings 2007 IEEE SoutheastCon*. 2007.

[107] C.-Y. Lee, C.-L. Chang, Y.-N. Wang, and L.-M. Fu, “Microfluidic Mixing: A Review,” *Int. J. Mol. Sci.*, vol. 12, no. 5, pp. 3263–3287, 2011.

[108] G. G. Yaralioglu, I. O. Wygant, T. C. Marentis, and B. T. Khuri-Yakub, “Ultrasonic mixing in microfluidic channels using integrated transducers.,” *Anal. Chem.*, vol. 76, no. 13, pp. 3694–3698, 2004.

[109] Z. Yang, H. Goto, M. Matsumoto, and R. Maeda, “Ultrasonic micromixer for microfluidic systems,” *Proceedings IEEE Thirteenth Annual International Conference on Micro Electro Mechanical Systems Cat No00CH36308*, vol. 93, no. 3. Ieee, pp. 266–272, 2000.

[110] J. Tsai, “Active microfluidic mixer and gas bubble filter driven by thermal bubble micropump,” *Sensors Actuators A Phys.*, vol. 97–98, no. 1–2, pp. 665–671, 2002.

[111] I. Glasgow and N. Aubry, “Enhancement of microfluidic mixing using time pulsing.,” *Lab Chip*, vol. 3, no. 2, pp. 114–120, 2003.

[112] H. H. Bau, J. Zhong, and M. Yi, “A minute magneto hydro dynamic (MHD) mixer,” *Sensors Actuators B Chem.*, vol. 79, no. 2–3, pp. 207–215, 2001.

[113] H.-Y. W. H.-Y. Wu and C.-H. L. C.-H. Liu, “A novel electrokinetic micromixer,” *TRANSDUCERS 03 12th International Conference on SolidState Sensors Actuators and Microsystems Digest of Technical Papers Cat No03TH8664*, vol. 1, no. 1. Ieee, pp. 107–115, 2003.

[114] H.-Y. Lee and J. Voldman, “Optimizing micromixer design for enhancing dielectrophoretic microconcentrator performance.,” *Anal. Chem.*, vol. 79, no. 5, pp. 1833–1839, 2007.

[115] J. Deval, P. Tabeling, and C.-M. H. C.-M. Ho, “A dielectrophoretic chaotic mixer,” *Technical Digest MEMS 2002 IEEE International Conference Fifteenth IEEE International Conference on Micro Electro Mechanical Systems Cat No02CH37266*, vol. 1, no. 3. Ieee, pp. 36–39, 2002.

[116] P. Paik, V. K. Pamula, M. G. Pollack, and R. B. Fair, “Electrowetting-based droplet mixers for microfluidic systems.,” *Lab Chip*, vol. 3, no. 1, pp. 28–33, 2003.

[117] Z. Wu and N.-T. Nguyen, “Convective–diffusive transport in parallel lamination micromixers,” *Microfluid. Nanofluidics*, vol. 1, no. 3, pp. 208–217, 2004.

[118] S. Mohamad and A. Gavin, “RESEARCH PAPER A magnetic bead-based DNA extraction and purification microfluidic device,” pp. 157–165, 2011.

[119] C.-Y. Chen, C.-Y. Lin, and Y.-T. Hu, “Magnetically actuated artificial cilia for optimum mixing performance in microfluidics.,” *Lab Chip*, vol. 13, no. 14, pp. 2834–9, Jul. 2013.

[120] Nguyen and Wu, “Micromixers - a review,” *J. Micromechanics Microengineering*, vol. 15, no. 2, pp. R1–R16, 2005.

[121] A. E. Kamholz and P. Yager, “Molecular diffusive scaling laws in pressure-driven microfluidic channels: deviation from one-dimensional Einstein approximations,” *Sensors Actuators B Chem.*, vol.

82, no. 1, pp. 117–121, 2002.

[122] N. Schwesinger, T. Frank, and H. Wurmus, “A modular microfluid system with an integrated micromixer,” *J. Micromechanics Microengineering*, vol. 6, no. 1, pp. 99–102, 1996.

[123] J. Knight, A. Vishwanath, J. Brody, and R. Austin, “Hydrodynamic Focusing on a Silicon Chip: Mixing Nanoliters in Microseconds,” *Phys. Rev. Lett.*, vol. 80, no. 17, pp. 3863–3866, 1998.

[124] A. Günther, M. Jhunjhunwala, M. Thalmann, M. A. Schmidt, and K. F. Jensen, “Micromixing of miscible liquids in segmented gas-liquid flow.,” *Langmuir Acs J. Surfaces Colloids*, vol. 21, no. 4, pp. 1547–1555, 2005.

[125] H. Song, J. D. Tice, and R. F. Ismagilov, “A microfluidic system for controlling reaction networks in time,” *Angew. Chemie*, vol. 42, no. 7, pp. 767–772, 2003.

[126] T. J. Johnson, D. Ross, and L. E. Locascio, “Rapid Microfluidic Mixing,” *Anal. Chem.*, vol. 74, no. 1, pp. 45–51, Dec. 2001.

[127] A. D. Stroock, S. K. W. Dertinger, A. Ajdari, I. Mezic, H. A. Stone, and G. M. Whitesides, “Chaotic mixer for microchannels.,” *Science (80-.).*, vol. 295, no. 5555, pp. 647–651, 2002.

[128] C. Zhang, D. Xing, and Y. Li, “Micropumps, microvalves, and micromixers within PCR microfluidic chips: Advances and trends.,” *Biotechnol. Adv.*, vol. 25, no. 5, pp. 483–514, 2007.

[129] Bartels, “mp6 Micropump,” 2012. [Online]. Available: http://www.bartels-mikrotechnik.de/index.php/mp6.html.

[130] J. L. Abell, J. D. Driskell, R. a. Dluhy, R. a. Tripp, and Y. P. Zhao, “Fabrication and characterization of a multiwell array SERS chip with biological applications,” *Biosens. Bioelectron.*, vol. 24, pp. 3663–3670, 2009.

[131] D. Mark, S. Haeberle, G. Roth, F. von Stetten, and R. Zengerle, “Microfluidic lab-on-a-chip platforms: requirements, characteristics and applications.,” *Chem. Soc. Rev.*, vol. 39, no. 3, pp. 1153–82, Mar. 2010.

[132] D. H. Kang, H. N. Kim, P. Kim, and K.-Y. Suh, “Poly(ethylene glycol) (PEG) microwells in microfluidics: Fabrication methods and applications,” *BioChip J.*, vol. 8, no. 4, pp. 241–253, 2014.

[133] J. Sambrook, E. F. Fritsch, and T. Maniatis, *Molecular Cloning: A Laboratory Manual*, vol. 3, no. 3. Cold Spring Harbor Laboratory Press, 2001.

[134] E. W. K. Young and D. J. Beebe, “Fundamentals of microfluidic cell culture in controlled microenvironments.,” *Chem. Soc. Rev.*, vol. 39, no. 3, pp. 1036–1048, 2010.

[135] S. Kühn, P. Measor, E. J. Lunt, B. S. Phillips, D. W. Deamer, A. R. Hawkins, and H. Schmidt, “Loss-based optical trap for on-chip particle analysis.,” *Lab Chip*, vol. 9, no. 15, pp. 2212–2216, 2009.

[136] P. Shah, X. Zhu, C. Chen, Y. Hu, and C. Z. Li, “Lab-on-chip device for single cell trapping and analysis,” *Biomed. Microdevices*, vol. 16, no. 1, pp. 35–41, 2014.

[137] K. W. Oh and C. H. Ahn, “A review of microvalves,” *J. Micromechanics Microengineering*, vol. 16, no. 5, pp. R13–R39, 2006.

[138] S. Shoji and K. Kawai, “Flow control methods and devices in micrometer scale channels.,” *Top. Curr. Chem.*, vol. 304, no. April, pp. 1–25, 2011.

[139] G. Fuhrt, T. Schnellet, and B. Wagnert, “Travelling wave-driven microfabricated electrohydrodynamic pumps for liquids,” *J Micromech Microeng*, vol. 4, pp. 217–226, Dec. 1994.

[140] H. P. Chou, M. A. Unger, and S. R. Quake, “A microfabricated rotary pump,” *Biomed. Microdevices*,

vol. 3, no. 4, pp. 323–330, 2001.

[141] S. Zeng, C. H. Chen, J. C. Mikkelsen, and J. G. Santiago, “Fabrication and characterization of electroosmotic micropumps,” *Sensors Actuators, B Chem.*, vol. 79, no. 2–3, pp. 107–114, Oct. 2001.

[142] H. Takao, M. Ishida, and K. Sawada, “A pneumatically actuated full in-channel microvalve with MOSFET-like function in fluid channel networks,” *Journal Of Microelectromechanical Systems*, vol. 11, no. 5. pp. 421–426, 2002.

[143] A. Terray, J. Oakey, and D. W. M. Marr, “Fabrication of linear colloidal structures for microfluidic applications,” *Appl. Phys. Lett.*, vol. 81, no. 9, 2002.

[144] Q. Yu, J. M. Bauer, J. S. Moore, and D. J. Beebe, “Responsive biomimetic hydrogel valve for microfluidics,” *Appl. Phys. Lett.*, vol. 78, no. 2001, pp. 2589–2591, 2001.

[145] J. S. Bintoro and P. J. Hesketh, “An electromagnetic actuated on/off microvalve fabricated on top of a single wafer,” *J. Micromechanics Microengineering*, vol. 15, no. 6, pp. 1157–1173, 2005.

[146] A. V. Lemoff and A. P. Lee, “AC magnetohydrodynamic micropump,” *Sensors Actuators, B Chem.*, vol. 63, no. 3, pp. 178–185, May 2000.

[147] H. Search, C. Journals, A. Contact, M. Iopscience, and I. P. Address, “3 . 5pm thin valves in titanium membranes,” *J. Micromechanics Microengineering*, vol. 2, no. 3, pp. 184–186, 1992.

[148] A. Gunderson and A. T. Filak, “Microfluidic dispensers based on structurally programmable microfluidic systems (sPROMs) and their applications for µTAS,” *Philosophy*, vol. 85, no. 9 Suppl, pp. S460-3, 2003.

[149] K. W. Oh, K. Lee, B. Ahn, and E. P. Furlani, “Design of pressure-driven microfluidic networks using electric circuit analogy,” *Lab Chip*, vol. 12, no. 3, pp. 515–545, 2012.

[150] K. Hosokawa, T. Fujii, and I. Endo, “Droplet-based nano/picoliter mixer using hydrophobic microcapillary vent,” *Technical Digest IEEE International MEMS 99 Conference Twelfth IEEE International Conference on Micro Electro Mechanical Systems Cat No99CH36291*. Ieee, pp. 388–393, 1999.

[151] I. Klammer, A. Buchenauer, G. Dura, W. Mokwa, and U. Schnakenberg, “A novel valve for microfluidic PDMS-based systems,” *2008 IEEE 21st Int. Conf. Micro Electro Mech. Syst.*, 2008.

[152] M. Ghassemi, H. Rezaeinezhad, and A. Shahidian, “Analytical Analysis of Flow in a Magnetohydrodynamic Pump (MHD),” *2008 14th Symposium on Electromagnetic Launch Technology*. Ieee, pp. 1–4, 2008.

[153] L. Wang, L. Flanagan, E. Monukf, N. L. Jeon, and A. P. Lee, “A MAGNETOHYDRODYNAMIC (MHD) MICROLFUIDIC PLATFORM FOR CELL SWITCHING,” no. May, pp. 276–279, 2005.

[154] M. Qin, “MICROFLUIDIC PUMPING WITH SURFACE TENSION FORCE AND,” 2011.

[155] N. Pamme, “Continuous flow separations in microfluidic devices.,” *Lab Chip*, vol. 7, no. 12, pp. 1644–59, Dec. 2007.

[156] F. Abhari, H. Jaafar, and N. A. Yunus, “A Comprehensive Study of Micropumps Technologies,” vol. 7, pp. 9765–9780, 2012.

[157] H. H. Bau, J. Zhu, S. Qian, and Y. Xiang, “A magneto-hydrodynamically controlled fluidic network,” *Sensors Actuators B Chem.*, vol. 88, no. 2, pp. 205–216, 2003.

[158] A. Homsy, “Characterization of MHD Pumps and their Applications in NMR Environments by,” 2006.

[159] S. K. Cho, Y. Zhao, and C.-J. C. Kim, “Concentration and binary separation of micro particles for

droplet-based digital microfluidics.," *Lab Chip*, vol. 7, no. 4, pp. 490–498, 2007.

[160] D. R. Gossett, W. M. Weaver, A. J. Mach, S. C. Hur, H. T. K. Tse, W. Lee, H. Amini, and D. Di Carlo, "Label-free cell separation and sorting in microfluidic systems," *Anal. Bioanal. Chem.*, vol. 397, no. 8, pp. 3249–3267, 2010.

[161] M. Viefhues, S. Wegener, A. Rischmüller, M. Schleef, and D. Anselmetti, "Dielectrophoresis based continuous-flow nano sorter: fast quality control of gene vaccines.," *Lab Chip*, vol. 13, no. 15, pp. 3111–8, Aug. 2013.

[162] K. Khoshmanesh, S. Nahavandi, S. Baratchi, A. Mitchell, and K. Kalantar-zadeh, "Dielectrophoretic platforms for bio-microfluidic systems.," *Biosens. Bioelectron.*, vol. 26, no. 5, pp. 1800–14, Jan. 2011.

[163] H. Morgan and N. G. Green, *AC Electrokinetics: Colloids and Nanoparticles*. Research Studies Press, Ltd., 2003.

[164] M. P. Hughes, *Nanoelectromechanics in Engineering and Biology*. 2002.

[165] P. Yager, G. J. Domingo, and J. Gerdes, "Point-of-Care Diagnostics for Global Health," *Annu. Rev. Biomed. Eng.*, vol. 10, no. 1, pp. 107–144, Jul. 2008.

[166] S. Bunthawin, P. Wanichapichart, A. Tuantranont, and H. G. L. Coster, "critical frequency for a spheroid in traveling electric field," pp. 1–13, 2010.

[167] R. Pethig, T. M. S., and R. S. Lee, "Enhancing Traveling-Wave Dielectrophoresis with Signal Superposition," *PubMed*, no. December, pp. 43–50, 2003.

[168] P. R. C. Gascoyne and J. Vykoukal, "Particle separation by dielectrophoresis," *Electrophoresis*, vol. 23, no. 13, pp. 1973–1983, 2002.

[169] T. S. Sammarco and M. A. Burns, "Thermocapillary pumping of discrete drops in microfabricated analysis devices," *AIChE J.*, vol. 45, no. 2, pp. 350–366, 1999.

[170] Y. Z. Y. Zhao, U.-C. Y. U.-C. Yi, and S. K. C. S. K. Cho, "Microparticle Concentration and Separation by Traveling-Wave Dielectrophoresis (twDEP) for Digital Microfluidics," *Journal Of Microelectromechanical Systems*, vol. 16, no. 6. IEEE, pp. 1472–1481, 2007.

[171] S.-Y. Park, S. Kalim, C. Callahan, M. A. Teitell, and E. P. Y. Chiou, "A light-induced dielectrophoretic droplet manipulation platform.," *Lab Chip*, vol. 9, no. 22, pp. 3228–3235, 2009.

[172] P. C. Winter and B. C. Hospital, "Polymerase Chain Reaction (PCR)," *Curr. Sci.*, vol. 199, no. December, pp. 1–5, 2005.

[173] K. Ellinas, a Tserepi, and E. Gogolides, "Superhydrophobic , Passive Microvalves With Controllable Opening Pressure , and Applications in Flow Control," no. October, pp. 344–346, 2013.

[174] D. Hegemann, H. Brunner, and C. Oehr, "Plasma treatment of polymers for surface and adhesion improvement," *Nucl. Instruments Methods Phys. Res. Sect. B Beam Interact. with Mater. Atoms*, vol. 208, no. 1–4, pp. 281–286, 2003.

[175] J. R. Epstein, I. Biran, and D. R. Walt, *Fluorescence-based nucleic acid detection and microarrays*, vol. 469, no. 1. 2002.

[176] F. Sinturel, O. Pellegrini, S. Xiang, L. Tong, C. Condon, and L. Bénard, "Real-time fluorescence detection of exoribonucleases.," *RNA*, vol. 15, no. 11, pp. 2057–62, 2009.

[177] M. Lee, C. Tan, L. Aw, C. Tang, M. Singh, S. Lee, H. Chia, and E. Yap, "Real-time fluorescence-based PCR for detection of malaria parasites," *J. Clin. Microbiol.*, vol. 40, no. 11, pp. 4343–4345, 2002.

[178] C. W. Tsao and D. L. DeVoe, “Bonding of thermoplastic polymer microfluidics,” *Microfluid. Nanofluidics*, vol. 6, no. 1, pp. 1–16, 2009.

[179] R. Dangla, F. Gallaire, and C. N. Baroud, “Microchannel deformations due to solvent-induced PDMS swelling.,” *Lab Chip*, vol. 10, no. 21, pp. 2972–2978, 2010.

[180] M. W. Toepke and D. J. Beebe, “PDMS absorption of small molecules and consequences in microfluidic applications.,” *Lab Chip*, vol. 6, no. 12, pp. 1484–1486, 2006.

[181] T. M. Sikanen, J. P. Lafleur, M.-E. Moilanen, G. Zhuang, T. G. Jensen, and J. P. Kutter, “Fabrication and bonding of thiol-ene-based microfluidic devices,” *J. Micromechanics Microengineering*, vol. 23, no. 3, p. 37002, 2013.

[182] S. Sommer, A. Ekin, D. C. Webster, S. J. Stafslien, J. Daniels, L. J. VanderWal, S. E. M. Thompson, M. E. Callow, and J. a Callow, “A preliminary study on the properties and fouling-release performance of siloxane-polyurethane coatings prepared from poly(dimethylsiloxane) (PDMS) macromers.,” *Biofouling*, vol. 26, no. 8, pp. 961–972, 2010.

[183] I. Vroman and L. Tighzert, “Biodegradable polymers,” *Materials (Basel).*, vol. 2, no. 2, pp. 307–344, 2009.

[184] K. R. King, C. C. J. Wang, M. R. Kaazempur-Mofrad, J. P. Vacanti, and J. T. Borenstein, “Biodegradable Microfluidics,” *Adv. Mater.*, vol. 16, pp. 2007–2012, 2004.

[185] A. Hsiao, J. Luecha, J. Kokini, and L. Liu, “Green microfluidics made of corn proteins,” *Proc. Annu. Int. Conf. IEEE Eng. Med. Biol. Soc. EMBS*, pp. 8400–8403, 2011.

[186] K. E. Petersen, “Silicon As a Mechanical Material.,” *Proc. IEEE*, vol. 70, no. 5, pp. 420–457, 1982.

[187] W. Callister and D. Rethwisch, *Materials science and engineering: an introduction*, vol. 94. 2007.

[188] C. Iliescu, H. Taylor, M. Avram, J. Miao, and S. Franssila, “A practical guide for the fabrication of microfluidic devices using glass and silicon,” *Biomicrofluidics*, vol. 6, no. 1, pp. 16505–1650516, 2012.

[189] E. H. M. Camara, C. Pijolat, J. Courbat, P. Breuil, D. Briand, and N. F. de Rooij, “Microfluidic Channels in Porous Silicon Filled with a Carbon Absorbent for GAS Preconcentration,” *TRANSDUCERS 2007 - 2007 Int. Solid-State Sensors, Actuators Microsystems Conf.*, 2007.

[190] M. G. Pollack, a D. Shenderov, and R. B. Fair, “Electrowetting-based actuation of droplets for integrated microfluidics,” *Lab Chip*, vol. 2, no. 2, pp. 96–101, 2002.

[191] P. Vulto, T. Huesgen, B. Albrecht, and G. a Urban, “A full-wafer fabrication process for glass microfluidic chips with integrated electroplated electrodes by direct bonding of dry film resist,” *J. Micromechanics Microengineering*, vol. 19, p. 77001, 2009.

[192] T. R. Dietrich, W. Ehrfeld, M. Lacher, M. Krämer, and B. Speit, “Fabrication technologies for microsystems utilizing photoetchable glass,” *Microelectronic Engineering*, vol. 30, no. 1–4. pp. 497–504, 1996.

[193] P. J. Moyer, R. Benrashid, P. Dupriez, and F. Farahi, “Applications of spin-on-glass for waveguide and micro-optical systems,” in *Micromachining Technology for Micro-optics and Nano-optics, January 28, 2003 - January 29*, 2003, vol. 4984, pp. 38–45.

[194] Dolomite, “Glass chip design guide,” 2012. [Online]. Available: http://www.microfluidicsinfo.com/glassmanufacturedolomite.pdf. [Accessed: 21-Dec-2015].

[195] S. Dochow, C. Beleites, T. Henkel, G. Mayer, J. Albert, J. Clement, C. Krafft, and J. Popp, “Quartz

microfluidic chip for tumour cell identification by Raman spectroscopy in combination with optical traps.," *Anal. Bioanal. Chem.*, vol. 405, no. 8, pp. 2743–6, 2013.

[196] H. Lee, a. M. Purdon, and R. M. Westervelt, "Manipulation of biological cells using a microelectromagnet matrix," *Appl. Phys. Lett.*, vol. 85, no. 6, pp. 1063–1065, 2004.

[197] C. Oshman, Q. Li, L.-A. Liew, R. Yang, Y. C. Lee, V. M. Bright, D. J. Sharar, N. R. Jankowski, and B. C. Morgan, "Thermal performance of a flat polymer heat pipe heat spreader under high acceleration," *J. Micromechanics Microengineering*, vol. 22, no. 4, p. 45018, 2012.

[198] S. W. Kang, S. H. Tsai, and M. H. Ko, "Metallic micro heat pipe heat spreader fabrication," *Appl. Therm. Eng.*, vol. 24, no. 2–3, pp. 299–309, 2004.

[199] S. H. Lee, D. van Noort, J. Y. Lee, B.-T. Zhang, and T. H. Park, "Effective mixing in a microfluidic chip using magnetic particles.," *Lab Chip*, vol. 9, pp. 479–482, 2009.

[200] L. H. Lu, K. S. Ryu, and C. Liu, "A magnetic microstirrer and array for microfluidic mixing," *J. Microelectromechanical Syst.*, vol. 11, no. 5, pp. 462–469, 2002.

[201] T. Pan, S. J. McDonald, E. M. Kai, and B. Ziaie, "A magnetically driven PDMS micropump with ball check-valves," *J. Micromechanics Microengineering*, vol. 15, no. 5, pp. 1021–1026, 2005.

[202] J. a. McGeough, M. C. Leu, K. P. Rajurkar, a. K. M. De Silva, and Q. Liu, "Electroforming Process and Application to Micro/Macro Manufacturing," *CIRP Ann. - Manuf. Technol.*, vol. 50, no. 2, pp. 499–514, 2001.

[203] C. A. Baker, C. T. Duong, A. Grimley, and M. G. Roper, "Recent advances in microfluidic detection systems.," *Bioanalysis*, vol. 1, no. 5, pp. 967–75, 2009.

[204] J. R. G. Navarro and M. H. V Werts, "Resonant light scattering spectroscopy of gold, silver and gold-silver alloy nanoparticles and optical detection in microfluidic channels.," *Analyst*, vol. 138, no. 2, pp. 583–92, 2013.

[205] Y. Lu, W. Shi, J. Qin, and B. Lin, "Low cost, portable detection of gold nanoparticle-labeled microfluidic immunoassay with camera cell phone," in *Electrophoresis*, 2009, vol. 30, no. 4, pp. 579–582.

[206] B. Kuswandi, Nuriman, J. Huskens, and W. Verboom, "Optical sensing systems for microfluidic devices: A review," *Analytica Chimica Acta*, vol. 601, no. 2. pp. 141–155, 2007.

[207] P. P. Shiu, G. K. Knopf, M. Ostojic, and S. Nikumb, "Rapid fabrication of tooling for microfluidic devices via laser micromachining and hot embossing," *J. Micromechanics Microengineering*, vol. 18, no. 2, p. 25012, 2008.

[208] W. Zhao, van den Berg, and Albert, "Lab on paper," *Lab Chip*, vol. 8, no. 12, pp. 1479–197, 2008.

[209] V. Orr, L. Zhong, M. Moo-Young, and C. P. Chou, "Recent advances in bioprocessing application of membrane chromatography," *Biotechnol. Adv.*, vol. 31, no. 4, pp. 450–465, 2013.

[210] D. S. Hage, "Affinity chromatography: a review of clinical applications.," *Clin. Chem.*, vol. 45, no. 5, pp. 593–615, 1999.

[211] A. W. Martinez, S. T. Phillips, G. M. Whitesides, and E. Carrilho, "Diagnostics for the developing world: microfluidic paper-based analytical devices.," *Anal. Chem.*, vol. 82, no. 1, pp. 3–10, Jan. 2010.

[212] A. W. Martinez, S. T. Phillips, Z. Nie, C.-M. Cheng, E. Carrilho, B. J. Wiley, and G. M. Whitesides, "Programmable diagnostic devices made from paper and tape.," *Lab Chip*, vol. 10, no. 19, pp. 2499–504, 2010.

[213] A. W. Martinez, S. T. Phillips, M. J. Butte, and G. M. Whitesides, “Patterned paper as a platform for inexpensive, low-volume, portable bioassays.,” *Angew. Chem. Int. Ed. Engl.*, vol. 46, no. 8, pp. 1318–20, Jan. 2007.

[214] X. Li, D. R. Ballerini, and W. Shen, “A perspective on paper-based microfluidics: Current status and future trends.,” *Biomicrofluidics*, vol. 6, no. 1, pp. 11301–1130113, Mar. 2012.

[215] H. Becker, “Microfabrication Technologies for Microfluidic Devices.”

[216] O. Rötting, W. Röpke, H. Becker, and C. Gärtner, “Polymer microfabrication technologies,” *Microsyst. Technol.*, vol. 8, no. 1, pp. 32–36, 2002.

[217] Y.-M. Han, H.-H. Chen, and C.-F. Huang, “Polymerization and degradation of aliphatic polyesters synthesized by atom transfer radical polyaddition,” *Polym. Chem.*, vol. 6, no. 25, pp. 4565–4574, 2015.

[218] T. Yokozawa and A. Yokoyama, “Chain-growth polycondensation for well-defined condensation polymers and polymer architecture,” *Chem. Rec.*, vol. 5, pp. 47–57, 2005.

[219] C. A. May, “Epoxy Resins: Chemistry and Technology,” 2nd ed., New York: Marcel Dekker Inc, 1987, p. 794.

[220] D. Braun, H. Cherdron, M. Rehahn, H. Ritter, and B. Voit, *Polymer synthesis: Theory and practice: Fundamentals, methods, experiments*. 2005.

[221] D. Sameoto and C. Menon, “Deep UV patterning of acrylic masters for molding biomimetic dry adhesives,” *J. Micromechanics Microengineering*, vol. 20, p. 115037, 2010.

[222] C. E. Corcione, A. Greco, and A. Maffezzoli, “Photopolymerization kinetics of an epoxy based resin for stereolithography - Calorimetric analysis,” *J. Therm. Anal. Calorim.*, vol. 72, no. 2, pp. 687–693, 2003.

[223] F. P. W. Melchels, J. Feijen, and D. W. Grijpma, “A review on stereolithography and its applications in biomedical engineering.,” *Biomaterials*, vol. 31, no. 24, pp. 6121–30, 2010.

[224] C. Nilsson, N. Simpson, M. Malkoch, M. Johansson, and E. Malmström, “Synthesis and thiol–ene photopolymerization of allyl-ether functionalized dendrimers,” *J. Polym. Sci. Part A Polym. Chem.*, vol. 46, no. 4, pp. 1339–1348, 2008.

[225] C. E. Hoyle and C. N. Bowman, “Thiol-ene click chemistry.,” *Angew. Chem. Int. Ed. Engl.*, vol. 49, no. 9, pp. 1540–73, 2010.

[226] N. B. Cramer, S. K. Reddy, A. K. O’Brien, and C. N. Bowman, “Thiol - Ene Photopolymerization Mechanism and Rate Limiting Step Changes for Various Vinyl Functional Group Chemistries,” *Macromolecules*, vol. 36, no. 21, pp. 7964–7969, 2003.

[227] J. M. Karlsson, F. Carlborg, F. Saharil, F. Forsberg, F. Niklaus, W. van der Wijngaart, and T. Haraldsson, “High-Resolution Micropatterning of Off-Stoichiometric Thiol-enes (OSTE) Via a Novel Lithography Mechanism,” *Proc. Micro Total Anal. Syst. 2012*, vol. 1600, pp. 225–227, 2012.

[228] C. F. Carlborg, T. Haraldsson, K. Oberg, M. Malkoch, and W. van der Wijngaart, “Beyond PDMS: off-stoichiometry thiol-ene (OSTE) based soft lithography for rapid prototyping of microfluidic devices.,” *Lab Chip*, vol. 11, no. 18, pp. 3136–3147, 2011.

[229] J. F. Ashley, N. B. Cramer, R. H. Davis, and C. N. Bowman, “Soft-lithography fabrication of microfluidic features using thiol-ene formulations,” *Lab Chip*, vol. 11, no. 16, pp. 2772–2778, 2011.

[230] P. Wägli, A. Homsy, and N. F. de Rooij, “Norland optical adhesive (NOA81) microchannels with adjustable wetting behavior and high chemical resistance against a range of mid-infrared-transparent

organic solvents," *Sensors Actuators B Chem.*, vol. 156, no. 2, pp. 994–1001, Aug. 2011.

[231] J. Zhou, D. a. Khodakov, A. V. Ellis, and N. H. Voelcker, "Surface modification for PDMS-based microfluidic devices," *Electrophoresis*, vol. 33, no. 1, pp. 89–104, 2012.

[232] D. Wang, M. Douma, B. Swift, R. D. Oleschuk, and J. H. Horton, "The adsorption of globular proteins onto a fluorinated PDMS surface," *J. Colloid Interface Sci.*, vol. 331, no. 1, pp. 90–97, 2009.

[233] J. N. Lee, C. Park, and G. M. Whitesides, "Solvent Compatibility of Poly(dimethylsiloxane)-Based Microfluidic Devices," *Anal. Chem.*, vol. 75, no. 23, pp. 6544–6554, Dec. 2003.

[234] R. Gomez-Sjoberg, A. A. Leyrat, B. T. Houseman, K. Shokat, and S. R. Quake, "Biocompatibility and Reduced Drug Absorption of Sol−Gel-Treated Poly(dimethyl siloxane) for Microfluidic Cell Culture Applications," *Anal. Chem.*, vol. 82, no. 21, pp. 8954–8960, Nov. 2010.

[235] T. Gervais, J. El-Ali, A. Gunther, and K. F. Jensen, "Flow-induced deformation of shallow microfluidic channels," *Lab Chip*, vol. 6, no. 4, pp. 500–507, 2006.

[236] M. Natali, S. Begolo, T. Carofiglio, G. Mistura, A. Uv, S. Sb-, U. V Sun-blocker, T. Pe, D. Corning, M. Glaeser, and B. Pdms, "Rapid prototyping of multilayer thiolene microfluidic chips by photopolymerization and transfer lamination.," *Lab Chip*, vol. 8, no. 3, pp. 492–4, 2008.

[237] V. Ervithayasuporn and S. Chimjarn, "Synthesis and Isolation of Methacrylate- and Acrylate-Functionalized Polyhedral Oligomeric Silsesquioxanes (T8, T10, and T12) and Characterization of the Relationship between Their Chemical Structures and Physical Properties," *Inorg. Chem.*, vol. 52, no. 22, pp. 13108–13112, Nov. 2013.

[238] M. W. Allsopp and G. Vianello, "Poly(Vinyl Chloride)," in *Ullmann's Encyclopedia of Industrial Chemistry*, Wiley-VCH Verlag GmbH & Co. KGaA, 2000.

[239] Y. Chen, L. Zhang, and G. Chen, "Fabrication, modification, and application of poly(methyl methacrylate) microfluidic chips.," *Electrophoresis*, vol. 29, no. 9, pp. 1801–14, 2008.

[240] A. Asadinezhad, M. Lehocký, P. Sáha, and M. Mozetič, "Recent Progress in Surface Modification of Polyvinyl Chloride," *Materials (Basel).*, vol. 5, no. 12, pp. 2937–2959, 2012.

[241] M. Soto, R. M. Sebastián, and J. Marquet, "Photochemical Activation of Extremely Weak Nucleophiles: Highly Fluorinated Urethanes and Polyurethanes from Polyfluoro Alcohols," *J. Org. Chem.*, vol. 79, no. 11, pp. 5019–5027, Jun. 2014.

[242] D. Qin, Y. N. Xia, and G. M. Whitesides, "Rapid prototyping of complex structures with feature sizes larger than 20 mu m," *Adv. Mater.*, vol. 8, no. 11, p. 917-, 1996.

[243] E. Piccin, W. K. T. Coltro, J. A. Fracassi da Silva, S. C. Neto, L. H. Mazo, and E. Carrilho, "Polyurethane from biosource as a new material for fabrication of microfluidic devices by rapid prototyping.," *J. Chromatogr. A*, vol. 1173, no. 1–2, pp. 151–8, 2007.

[244] W. Wu, K. N. Sask, P. R. Selvaganapathy, and J. L. Brash, "Fabrication of Polyurethane Microfluidic Channels and Their Surface Modification for Blood Contacting Application," pp. 1140–1142, 2011.

[245] W. Park, S. Han, and S. Kwon, "Fabrication of membrane-type microvalves in rectangular microfluidic channels via seal photopolymerization.," *Lab Chip*, vol. 10, no. 20, pp. 2814–7, 2010.

[246] T. Fujii, "PDMS-based microfluidic devices for biomedical applications," in *Microelectronic Engineering*, 2002, vol. 61–62, pp. 907–914.

[247] W. Schrott, M. Svoboda, Z. Slouka, M. Přibyl, and D. Šnita, "PDMS microfluidic chips prepared by a novel casting and pre-polymerization method," *Microelectron. Eng.*, vol. 87, no. 5–8, pp. 1600–1602,

2010.

[248] M. Georges, P. M. Kazmaier, and K. Gordon, “Narrow Molecular Weight Resins by Free-Radical Polymerization Process,” *Macromolecules*, vol. 26, pp. 2987–2988, 1993.

[249] D. Mardare and K. A. Matyjaszewski, “Free-radical polymerization process,” *U.S.* (Carnegie Mellon University, USA)., p. 5 pp., 1994.

[250] E. Roy, J.-C. Galas, and T. Veres, “Thermoplastic elastomers for microfluidics: Towards a high-throughput fabrication method of multilayered microfluidic devices.,” *Lab Chip*, vol. 11, pp. 3193–3196, 2011.

[251] N. S. G. K. Devaraju and M. A. Unger, “Multilayer soft lithography of perfluoropolyether based elastomer for microfluidic device fabrication.,” *Lab Chip*, vol. 11, no. 11, pp. 1962–1967, 2011.

[252] M. A. Kader and A. K. Bhowmick, “Novel thermoplastic elastomers from fluorocarbon elastomer, acrylate rubber and acrylate plastics,” *Rubber Chem. Technol.*, vol. 74, no. 4, pp. 662–676, 2001.

[253] Zrunek Gummiwaren, “Designing with Fluoroelastomers,” 2015. [Online]. Available: http://www.zrunek.at/viton-fkm-fpm-fluorelastomere/download/zruelast-fpm-designing-with-fluoroelastomers.pdf. [Accessed: 04-Jan-2016].

[254] Polyone, “THERMOPLASTIC ELASTOMER (TPE),” 2015. [Online]. Available: http://www.polyone.com/products/tpe/tpe-knowledge-center/tpe-faqs. [Accessed: 04-Jan-2015].

[255] M. Biron, *Thermoplastics and Thermoplastic Composites*. 2007.

[256] H. Quan, Z. M. Li, M. B. Yang, and R. Huang, “On transcrystallinity in semi-crystalline polymer composites,” *Composites Science and Technology*, vol. 65, no. 7–8. pp. 999–1021, 2005.

[257] D. A. Şerban, L. Maravina, and V. Silberschmidt, “Behaviour of semi-crystalline thermoplastic polymers: Experimental studies and simulations,” in *Computational Materials Science*, 2012, vol. 52, no. 1, pp. 139–146.

[258] P. N. Nge, C. I. Rogers, and A. T. Woolley, “Advances in microfluidic materials, functions, integration, and applications,” *Chem. Rev.*, vol. 113, no. 4, pp. 2550–2583, 2013.

[259] P. Abgrall and a-M. Gué, “Lab-on-chip technologies: making a microfluidic network and coupling it into a complete microsystem—a review,” *J. Micromechanics Microengineering*, vol. 17, pp. R15–R49, 2007.

[260] E. Verpoorte and N. F. De Rooij, “Microfluidics meets MEMS,” *Proc. IEEE*, vol. 91, no. 6, pp. 930–953, 2003.

[261] H. R. Brown, “Adhesion of polymers,” *MRS Bull.*, vol. 21, no. 1, pp. 24–27, 1996.

[262] J. Schultz and M. Nardin, “Theories and mechanisms of adhesion,” in *Handbook of adhesive technology*, New York: Marcel Dekker, 1994, pp. 19–33.

[263] A. V. Pocius, *Adhesion and Adhesives Technology*. München: Carl Hanser Verlag GmbH & Co. KG, 2012.

[264] Y. Temiz, R. D. Lovchik, G. V. Kaigala, and E. Delamarche, “Lab-on-a-chip devices: how to close and plug the lab?,” *Microelectron. Eng.*, vol. 132, pp. 156–175, 2014.

[265] W. Chow, W. Yin, K. F. Lei, G. Shi, W. J. Li, and Q. Huang, “Microfluidic channel fabrication by PDMS-interface bonding,” *Smart Mater. Struct.*, vol. 15, no. 1, pp. S112–S116, 2005.

[266] R. Wolf, “A technology decision – adhesive lamination or extrusion coating/lamination?,” *TAPPI Place Conf.*, 2010.

[267] K. F. Lei, S. Ahsan, N. Budraa, W. J. Li, and J. D. Mai, “Microwave bonding of polymer-based substrates for potential encapsulated micro/nanofluidic device fabrication,” *Sensors Actuators A Phys.*, vol. 114, no. 2–3, pp. 340–346, 2004.

[268] J. Li, D. Chen, and G. Chen, “Low-temperature thermal bonding of PMMA microfluidic chips,” *Anal. Lett.*, vol. 38, no. January, pp. 1127–1136, 2005.

[269] M. T. Arroyo, L. J. Fernández, M. Agirregabiria, N. Ibãez, J. Aurrekoetxea, and F. J. Blanco, “Novel all-polymer microfluidic devices monolithically integrated within metallic electrodes for SDS-CGE of proteins,” *J. Micromechanics Microengineering*, vol. 17, no. 7, pp. 1289–1298, 2007.

[270] C. K. Fredrickson, Z. Xia, C. Das, R. Ferguson, F. T. Tavares, and Z. H. Fan, “Effects of fabrication process parameters on the properties of cyclic olefin copolymer microfluidic devices,” *J. Microelectromechanical Syst.*, vol. 15, no. 5, pp. 1060–1068, 2006.

[271] Y. Sun, Y. C. Kwok, and N.-T. Nguyen, “Low-pressure, high-temperature thermal bonding of polymeric microfluidic devices and their applications for electrophoretic separation,” *J. Micromechanics Microengineering*, vol. 16, no. 8, pp. 1681–1688, 2006.

[272] I. R. G. Ogilvie, V. J. Sieben, C. F. a Floquet, R. Zmijan, M. C. Mowlem, and H. Morgan, “Solvent processing of PMMA and COC chips for bonding devices with optical quality surfaces,” *14th Int. Conf. Miniaturized Syst. Chem. Life Sci.*, no. October, pp. 1244–1246, 2010.

[273] F. Umbrecht, D. Müller, F. Gattiker, C. M. Boutry, J. Neuenschwander, U. Sennhauser, and C. Hierold, “Solvent assisted bonding of polymethylmethacrylate: Characterization using the response surface methodology,” *Sensors Actuators, A Phys.*, vol. 156, no. 1, pp. 121–128, 2009.

[274] H. H. Tran, W. Wu, and N. Y. Lee, “Ethanol and UV-assisted instantaneous bonding of PMMA assemblies and tuning in bonding reversibility,” *Sensors Actuators, B Chem.*, vol. 181, pp. 955–962, 2013.

[275] R. Truckenmüller, R. Ahrens, Y. Cheng, G. Fischer, and V. Saile, “An ultrasonic welding based process for building up a new class of inert fluidic microsensors and -actuators from polymers,” *Sensors Actuators, A Phys.*, vol. 132, no. 1 SPEC. ISS., pp. 385–392, 2006.

[276] Strong AB, *Plastics Materials and Processing*. New Jersey: Prentice Hall, 2000.

[277] R. Truckenmüller, P. Henzi, D. Herrmann, V. Saile, and W. K. Schomburg, “Bonding of polymer microstructures by UV irradiation and subsequent welding at low temperatures,” *Microsyst. Technol.*, vol. 10, no. 5, pp. 372–374, 2004.

[278] M. a Eddings, M. a Johnson, and B. K. Gale, “Determining the optimal PDMS–PDMS bonding technique for microfluidic devices,” *J. Micromechanics Microengineering*, vol. 18, no. 6, p. 67001, 2008.

[279] M. J. Shenton and G. C. Stevens, “Surface modification of polymer surfaces: atmospheric plasma versus vacuum plasma treatments,” *J. Phys. D. Appl. Phys.*, vol. 34, no. 18, pp. 2761–2768, 2001.

[280] Y. Jiang, Z. Hao, Q. He, and H. Chen, “A simple method for fabrication of microfluidic paper-based analytical devices and on-device fluid control with a portable corona generator,” *RSC Adv.*, vol. 6, no. 4, pp. 2888–2894, 2016.

[281] M. A. Johnson, E. Liddiard, and B. K. Gale, “A Masked Corona Discharge Method for Selective Bonding in PDMS for Microfluidic Applications.”

[282] U. Lommatzsch, D. Pasedag, A. Baalmann, G. Ellinghorst, and H. E. Wagner, “Atmospheric pressure

plasma jet treatment of polyethylene surfaces for adhesion improvement," *Plasma Process. Polym.*, vol. 4, no. SUPPL.1, pp. 1041–1045, 2007.

[283] M. R. Sanchis, V. Blanes, M. Blanes, D. Garcia, and R. Balart, "Surface modification of low density polyethylene (LDPE) film by low pressure O2 plasma treatment," *Eur. Polym. J.*, vol. 42, no. 7, pp. 1558–1568, 2006.

[284] TANTEC, "How Corona Treatment and Plasma Treatment works!," 2015. [Online]. Available: http://www.tantec.com/what-is-corona-treatment-and-plasma-treatment-and-how-it-works.html.

[285] Z. Wu, N. Xanthopoulos, F. Reymond, J. S. Rossier, and H. H. Girault, "Polymer microchips bonded by O2-plasma activation," *Electrophoresis*, vol. 23, no. 5, pp. 782–790, 2002.

[286] NM. Emanuel and A. Buchachenko, *Chemical Physics of Polymer Degradation And Stabilization*. Utrecht: VNU Science Press, 1987.

[287] N. S. Allen and M. Edge, *Fundamentals of Polymer Degradation and Stabilization*. New York: Elsevier, 1993.

[288] J. Malík and C. Kröhnke, "Polymer stabilization: present status and possible future trends," *Comptes Rendus Chim.*, vol. 9, no. 11–12, pp. 1330–1337, 2006.

[289] H. Klank, J. Kutter, and O. Geschke, "CO(2)-laser micromachining and back-end processing for rapid production of PMMA-based microfluidic systems.," *Lab Chip*, vol. 2, no. 4, pp. 242–246, 2002.

[290] K. W. Ro, J. Liu, and D. R. Knapp, "Plastic microchip liquid chromatography-matrix-assisted laser desorption/ionization mass spectrometry using monolithic columns," *J. Chromatogr. A*, vol. 1111, no. 1, pp. 40–47, 2006.

[291] X. Sun, B. A. Peeni, W. Yang, H. A. Becerril, and A. T. Woolley, "Rapid prototyping of poly(methyl methacrylate) microfluidic systems using solvent imprinting and bonding," *J. Chromatogr. A*, vol. 1162, no. 2 SPEC. ISS., pp. 162–166, 2007.

[292] Y. C. Hsu and T. Y. Chen, "Applying Taguchi methods for solvent-assisted PMMA bonding technique for static and dynamic ??-TAS devices," *Biomed. Microdevices*, vol. 9, no. 4, pp. 513–522, 2007.

[293] L. Brown, T. Koerner, J. H. Horton, and R. D. Oleschuk, "Fabrication and characterization of poly(methylmethacrylate) microfluidic devices bonded using surface modifications and solvents.," *Lab Chip*, vol. 6, no. 1, pp. 66–73, 2006.

[294] R. T. Kelly, T. Pan, and A. T. Woolley, "Phase-changing sacrificial materials for solvent bonding of high-performance polymeric capillary electrophoresis microchips," *Anal. Chem.*, vol. 77, no. 11, pp. 3536–3541, 2005.

[295] M. T. Koesdjojo, Y. H. Tennico, and V. T. Remcho, "Fabrication of a microfluidic system for capillary electrophoresis using a two-stage embossing technique and solvent welding on poly(methyl methacrylate) with water as a sacrificial layer," *Anal. Chem.*, vol. 80, no. 7, pp. 2311–2318, 2008.

[296] J. Kim and X. Xu, "Excimer laser fabrication of polymer microfluidic devices," *J. Laser Appl.*, vol. 15, no. 4, p. 255, 2003.

[297] A. A. Yussuf, I. Sbarski, M. Solomon, N. Tran, and J. P. Hayes, "Sealing of polymeric-microfluidic devices by using high frequency electromagnetic field and screen printing technique," *J. Mater. Process. Technol.*, vol. 189, no. 1–3, pp. 401–408, 2007.

[298] Y. Wang, H. Chen, Q. He, and S. A. Soper, "A high-performance polycarbonate electrophoresis microchip with integrated three-electrode system for end-channel amperometric detection,"

Electrophoresis, vol. 29, no. 9, pp. 1881–1888, 2008.

[299] P. Abgrall, L.-N. Low, and N.-T. Nguyen, "Fabrication of planar nanofluidic channels in a thermoplastic by hot-embossing and thermal bonding.," *Lab Chip*, vol. 7, no. 4, pp. 520–522, 2007.

[300] C. W. Tsao, L. Hromada, J. Liu, P. Kumar, and D. L. DeVoe, "Low temperature bonding of PMMA and COC microfluidic substrates using UV/ozone surface treatment," *Lab Chip*, vol. 7, no. 4, p. 499, 2007.

[301] J. Han, S. Lee, A. Puntambekar, S. Murugesan, J-W, C. Beaucage, and A. C. G, "UV adhesive bonding techniques at room temperature for plastic lab-on-a-chip," in *In:Proceedings of 7th International Conference Micro Total Analysis Systems*, 2003, pp. 1113–1116.

[302] F. Dang, S. Shinohara, O. Tabata, Y. Yamaoka, M. Kurokawa, Y. Shinohara, M. Ishikawa, and Y. Baba, "Replica multichannel polymer chips with a network of sacrificial channels sealed by adhesive printing method.," *Lab Chip*, vol. 5, no. 4, pp. 472–478, 2005.

[303] S. Lai, X. Cao, and L. J. Lee, "A Packaging Technique for Polymer Microfluidic Platforms," *Anal. Chem.*, vol. 76, no. 4, pp. 1175–1183, 2004.

[304] C. Lu, L. Lee, J. Juang, and Y. Je, "Packaging of microfluidic chips via interstitial bonding technique," *Electrophoresis*, vol. 29, no. 7, pp. 1407–1414, 2008.

[305] F.-C. Huang, Y.-F. Chen, and G.-B. Lee, "CE chips fabricated by injection molding and polyethylene/thermoplastic elastomer film packaging methods.," *Electrophoresis*, vol. 28, no. 7, pp. 1130–1137, Apr. 2007.

[306] M. A. Roberts, J. S. Rossier, P. Bercier, and H. Girault, "UV laser machined polymer substrates for the development of microdiagnostic systems," *Anal. Chem.*, vol. 69, no. 11, pp. 2035–2042, 1997.

[307] Y. Li, J. S. Buch, F. Rosenberger, D. L. DeVoe, and C. S. Lee, "Integration of Isoelectric Focusing with Parallel Sodium Dodecyl Sulfate Gel Electrophoresis for Multidimensional Protein Separations in a Plastic Microfludic Network," *Anal. Chem.*, vol. 76, no. 3, pp. 742–748, 2004.

[308] J. S. Buch, C. Kimball, F. Rosenberger, W. E. Highsmith, D. L. DeVoe, and C. S. Lee, "DNA Mutation Detection in a Polymer Microfluidic Network Using Temperature Gradient Gel Electrophoresis," *Anal. Chem.*, vol. 76, no. 4, pp. 874–881, 2004.

[309] Y. X. Wang, Y. Zhou, B. M. Balgley, J. W. Cooper, C. S. Lee, and D. L. DeVoe, "Electrospray interfacing of polymer microfluids to MALDI-MS," *Electrophoresis*, vol. 26, no. 19, pp. 3631–3640, 2005.

[310] D. S. W. Park, M. L. Hupert, M. A. Witek, B. H. You, P. Datta, J. Guy, J. B. Lee, S. A. Soper, D. E. Nikitopoulos, and M. C. Murphy, "A titer plate-based polymer microfluidic platform for high throughput nucleic acid purification," *Biomed. Microdevices*, vol. 10, no. 1, pp. 21–33, 2008.

[311] Loughborough University, "VAT Photopolymerisation," *[Online]*. 2016.

[312] C. W. Hull, "Apparatus for production of three-dimensional objects by stereolithography," 1986.

[313] R. Xie, D. Li, and S. Chao, "An inexpensive stereolithography technology with high power UV-LED light," *Rapid Prototyp. J.*, vol. 17, pp. 441–450, 2011.

[314] H. Lin, D. Zhang, P. G. Alexander, G. Yang, J. Tan, A. W. M. Cheng, and R. S. Tuan, "Application of visible light-based projection stereolithography for live cell-scaffold fabrication with designed architecture," *Biomaterials*, vol. 34, no. 2, pp. 331–339, 2013.

[315] A. Waldbaur, H. Rapp, K. Länge, and B. E. Rapp, "Let there be chip—towards rapid prototyping of

microfluidic devices: one-step manufacturing processes," *Anal. Methods*, vol. 3, no. 12, p. 2681, 2011.

[316] Stratasys Ltd, "FDM materials," *website*, 2014.

[317] Techische Fakultät Der Christian-Albrechts Universitat zu kiel, "Spin coating," *Basic Lab*, vol. 5, p. 62, 2002.

[318] D. B. Hall, P. Underhill, and J. M. Torkelson, "Spin Coating of Thin and Ultrathin Polymer Films," *Polym. Eng. Sci.*, vol. 38, no. 12, pp. 2039–2045, 1998.

[319] a. D. Radadia, L. C. L. Cao, H.-K. J. H.-K. Jeong, M. a. Shannon, and R. I. Masel, "A 3D micromixer fabricated with dry film resist," *2007 IEEE 20th Int. Conf. Micro Electro Mech. Syst.*, no. January, pp. 361–364, 2007.

[320] P. Vulto, N. Glade, L. Altomare, J. Bablet, L. Del Tin, G. Medoro, I. Chartier, N. Manaresi, M. Tartagni, and R. Guerrieri, "Microfluidic channel fabrication in dry film resist for production and prototyping of hybrid chips.," *Lab Chip*, vol. 5, no. 2, pp. 158–62, 2005.

[321] K. Ueno, F. Kitagawa, H.-B. Kim, T. Tokunaga, S. Matsuo, H. Misawa, and N. Kitamura, "Fabrication and characteristic responses of integrated microelectrodes in polymer channel chip," *Chem. Lett.*, vol. 29, no. 8, pp. 858–859, 2000.

[322] A. Kain, C. Mueller, and H. Reinecke, "High aspect ratio- and 3D- printing of freestanding sophisticated structures," *Procedia Chemistry*, vol. 1, no. 1. pp. 750–753, 2009.

[323] S. M. Ford, J. Davies, B. Kar, S. D. Qi, S. McWhorter, S. A. Soper, and C. K. Malek, "Micromachining in plastics using X-ray lithography for the fabrication of micro-electrophoresis devices," *J. Biomech. Eng. ASME*, vol. 121, no. 1, pp. 13–21, 1999.

[324] S. Gorelick, J. Vila-Comamala, V. Guzenko, R. Mokso, M. Stampanoni, and C. David, "Direct e-beam writing of high aspect ratio nanostructures in PMMA: A tool for diffractive X-ray optics fabrication," *Microelectron. Eng.*, vol. 87, no. 5–8, pp. 1052–1056, 2010.

[325] T. Beetz and C. Jacobsen, "Soft X-ray radiation-damage studies in PMMA using a cryo-STXM," *J. Synchrotron Radiat.*, vol. 10, no. 3, pp. 280–283, 2003.

[326] C. Jackson, P. Buck, S. Cohen, V. Garg, C. Howard, R. Kiefer, J. Manfredo, and J. Tsou, "DUV laser lithography for photomask fabrication," *Opt. Microlithogr. Xvii, Pts 1-3*, vol. 5377, pp. 1005–1016, 2004.

[327] J. Garra, T. Long, J. Currie, T. Schneider, R. White, and M. Paranjape, "Dry etching of polydimethylsiloxane for microfluidic systems," *J. Vac. Sci. Technol. A Vacuum, Surfaces, Film.*, vol. 20, no. 3, p. 975, 2002.

[328] D. Zhuang and J. H. Edgar, "Wet etching of GaN, AlN, and SiC: A review," *Materials Science and Engineering R: Reports*, vol. 48, no. 1. Elsevier Ltd, pp. 1–46, 2005.

[329] A. Misra, J. D. Hogan, and R. Chorush, "Wet and Dry Etching Materials," *Handb. Chem. Gases Semicond. Ind.*, no. 3, pp. 1–5, 2002.

[330] F. Laermer and A. Schilp, "Method of anisotropically etching silicon," 1996.

[331] H. Schmidt, J. Ihlemann, K. Luther, and J. Troe, "Modeling of velocity and surface temperature of the moving interface during laser ablation of polyimide and poly(methyl methacrylate)," *Appl. Surf. Sci.*, vol. 138–139, no. 1–4, pp. 102–106, 1999.

[332] J. S. Rossier, G. Gokulrangan, H. H. Girault, S. Svojanovsky, and G. S. Wilson, "Characterization of protein adsorption and immunosorption kinetics in photoablated polymer microchannels," *Langmuir*,

vol. 16, no. 22, pp. 8489–8494, 2000.

[333] J. S. Rossier, P. Bercier, A. Schwarz, S. Loridant, and H. H. Girault, “Topography, crystallinity and wettability of photoablated PET surfaces,” *Langmuir*, vol. 15, no. 15, pp. 5173–5178, 1999.

[334] D. V Ganin, S. I. Mikolutskiy, V. N. Tokarev, V. Y. Khomich, V. A. Shmakov, and V. A. Yamshchikov, “Formation of micron and submicron structures on a zirconium oxide surface exposed to nanosecond laser radiation,” *Quantum Electron.*, vol. 44, no. 4, pp. 317–321, 2014.

[335] L. Alting, F. Kimura, H. N. Hansen, and G. Bissacco, “Micro Engineering,” *CIRP Ann. - Manuf. Technol.*, vol. 52, no. 2, pp. 635–657, 2003.

[336] E. Shamoto and T. Moriwaki, “Ultaprecision Diamond Cutting of Hardened Steel by Applying Elliptical Vibration Cutting,” *CIRP Ann. - Manuf. Technol.*, vol. 48, no. 1, pp. 441–444, 1999.

[337] G. Ekstrand, C. Holmquist, A. E. Orlefors, B. Hellman, A. Larson, and P. Andersson, “Integrated cell based assays in microfabricated disposable CD devices,” in *Micro Total Analysis Systems 2000*, 2000, pp. 249–252.

[338] R. M. McCormick, R. J. Nelson, M. G. Alonso-Amigo, D. J. Benvegnu, and H. H. Hooper, “Microchannel electrophoretic separations of DNA in injection-molded plastic substrates.,” *Anal. Chem.*, vol. 69, no. 14, pp. 2626–30, 1997.

[339] Y. E. Yoo, T. H. Kim, T. J. Je, D. S. Choi, C. W. Kim, and S. K. Kim, “Injection molding of micro patterned PMMA plate,” *Trans. Nonferrous Met. Soc. China (English Ed.*, vol. 21, no. SUPPL. 1, 2011.

[340] Y. Xu, H. Lu, T. Gao, and W. Zhang, “Predicting the low-velocity impact behavior of polycarbonate: Influence of thermal history during injection molding,” *Int. J. Impact Eng.*, vol. 86, pp. 265–273, 2015.

[341] M. J. Choi, K. J. Cha, H. W. Kim, M. H. Na, B. K. Lee, W. Hwang, and D. S. Kim, “Microchamber/nanodimple polystyrene surfaces constructing cell aggregates fabricated by thermoset mold-based hot embossing,” *Microelectron. Eng.*, vol. 110, pp. 340–345, 2013.

[342] S. Qi, X. Liu, S. Ford, J. Barrows, G. Thomas, K. Kelly, A. McCandless, K. Lian, J. Goettert, and S. a Soper, “Microfluidic devices fabricated in poly(methyl methacrylate) using hot-embossing with integrated sampling capillary and fiber optics for fluorescence detection.,” *Lab Chip*, vol. 2, no. 2, pp. 88–95, 2002.

[343] L. J. Kricka, P. Fortina, N. J. Panaro, P. Wilding, G. Alonso-Amigo, and H. Becker, “Fabrication of plastic microchips by hot embossing.,” *Lab Chip*, vol. 2, no. 1, pp. 1–4, 2002.

[344] Y. J. Juang, L. Lee James, and K. W. Koelling, “Hot embossing in microfabrication. Part I: Experimental,” *Polym. Eng. Sci.*, vol. 42, no. 3, pp. 539–550, 2002.

[345] A. Mata, A. J. Fleischman, and S. Roy, “Characterization of polydimethylsiloxane (PDMS) properties for biomedical micro/nanosystems.,” *Biomed. Microdevices*, vol. 7, no. 4, pp. 281–293, 2005.

[346] HUNTSMAN, “A guide to thermoplastic polyurethanes (TPU),” *Huntsman*, p. 26, 2010.

[347] B. H. Jo, L. M. Van Lerberghe, K. M. Motsegood, and D. J. Beebe, “Three-dimensional micro-channel fabrication in polydimethylsiloxane (PDMS) elastomer,” *J. Microelectromechanical Syst.*, vol. 9, no. 1, pp. 76–81, 2000.

[348] recycphp, “Super absorbent Sodium.” [Online]. Available: http://recycphp.com/en/p/materials/sodium-polyacrylate/. [Accessed: 10-Nov-2016].

[349] P. Craw, R. E. Mackay, A. Naveenathayalan, C. Hudson, M. Branavan, S. T. Sadiq, and W. Balachandran, “A simple, low-cost platform for real-time isothermal nucleic acid amplification,”

Sensors (Switzerland), vol. 15, no. 9, pp. 23418–23430, 2015.

[350] M. Branavan, R. E. Mackay, P. Craw, A. Naveenathayalan, J. C. Ahern, T. Sivanesan, C. Hudson, T. Stead, J. Kremer, N. Garg, M. Baker, S. T. Sadiq, and W. Balachandran, "Modular development of a prototype point of care molecular diagnostic platform for sexually transmitted infections," *Med. Eng. Phys.*, vol. 38, no. 8, pp. 741–748, 2016.

[351] D. Corning, "Electronics Sylgard ® 184 Silicone Elastomer," *Prod. Datasheet*, pp. 1–3, 2013.

[352] S. O. Procedure, "ETP Corona Discharge Wand," vol. 73246, pp. 2–4, 2015.

[353] S. H. Tan, N.-T. Nguyen, Y. C. Chua, and T. G. Kang, "Oxygen plasma treatment for reducing hydrophobicity of a sealed polydimethylsiloxane microchannel," *Biomicrofluidics*, vol. 4, no. 3, p. 32204, Sep. 2010.

[354] J. C. McDonald and G. M. Whitesides, "Poly (dimethylsiloxane) as a Material for Fabricating Microfluidic Devices," *Acc. Chem. Res.*, vol. 35, no. 7, pp. 491–499, 2002.

[355] D. C. Duffy, J. C. McDonald, O. J. Schueller, and G. M. Whitesides, "Rapid Prototyping of Microfluidic Systems in Poly(dimethylsiloxane).," *Anal. Chem.*, vol. 70, no. 23, pp. 4974–4984, Dec. 1998.

[356] M. S. Maria, P. E. Rakesh, T. S. Chandra, and A. K. Sen, "Capillary flow of blood in a microchannel with differential wetting for blood plasma separation and on-chip glucose detection.," *Biomicrofluidics*, vol. 10, no. 5, p. 54108, Sep. 2016.

[357] J. Zhou, A. V. Ellis, and N. H. Voelcker, "Recent developments in PDMS surface modification for microfluidic devices.," *Electrophoresis*, vol. 31, no. 1, pp. 2–16, Jan. 2010.

[358] M. F. Mora, C. E. Giacomelli, and C. D. Garcia, "Electrophoretic effects of the adsorption of anionic surfactants to poly(dimethylsiloxane)-coated capillaries.," *Anal. Chem.*, vol. 79, no. 17, pp. 6675–6681, Sep. 2007.

[359] B. Huang, S. Kim, H. Wu, and R. N. Zare, "Use of a mixture of n-dodecyl-beta-D-maltoside and sodium dodecyl sulfate in poly(dimethylsiloxane) microchips to suppress adhesion and promote separation of proteins.," *Anal. Chem.*, vol. 79, no. 23, pp. 9145–9149, Dec. 2007.

[360] H. Makamba, J. H. Kim, K. Lim, N. Park, and J. H. Hahn, "Surface modification of poly(dimethylsiloxane) microchannels.," *Electrophoresis*, vol. 24, no. 21, pp. 3607–3619, Nov. 2003.

[361] P. Garstecki, a M. Gañán-Calvo, and G. M. Whitesides, "Formation of bubbles and droplets in microfluidic systems," *Bull. Polish Acad. Sci.*, vol. 53, no. 4, pp. 361–372, 2005.

[362] TwistDX, "TwistAmp Basic RT Quick Guide."

[363] Dr Niall Armes, "Recombinase Polymerase Amplification; a breakthrough alternative to PCR." [Online]. Available: http://www.twistdx.co.uk/our_technology/. [Accessed: 16-Nov-2016].

[364] TwistDX, "RPA reagent volume composition."

[365] T. Shibata, "recA protein," *Tanpakushitsu Kakusan Koso.*, vol. 32, no. 1, pp. 69–76, 1987.

[366] A. Dudas, E. Markova, D. Vlasakova, A. Kolman, Z. Bartosova, J. Brozmanova, and M. Chovanec, "The Escherichia coli RecA protein complements recombination defective phenotype of the Saccharomyces cerevisiae rad52 mutant cells.," *Yeast*, vol. 20, no. 5, pp. 389–396, Apr. 2003.

[367] S. C. Kowalczykowski, D. A. Dixon, A. K. Eggleston, S. D. Lauder, and W. M. Rehrauer, "Biochemistry of homologous recombination in Escherichia coli.," *Microbiol. Rev.*, vol. 58, no. 3, pp. 401–465, Sep. 1994.

[368] R. Gamsjaeger, R. Kariawasam, A. X. Gimenez, C. Touma, E. McIlwain, R. E. Bernardo, N. E. Shepherd, S. F. Ataide, Q. Dong, D. J. Richard, M. F. White, and L. Cubeddu, "The structural basis of DNA binding by the single-stranded DNA-binding protein from Sulfolobus solfataricus.," *Biochem. J.*, vol. 465, no. 2, pp. 337–346, Jan. 2015.

[369] M. J. Morten, J. R. Peregrina, M. Figueira-Gonzalez, K. Ackermann, B. E. Bode, M. F. White, and J. C. Penedo, "Binding dynamics of a monomeric SSB protein to DNA: a single-molecule multi-process approach," *Nucleic Acids Res.*, vol. 43, no. 22, pp. 10907–10924, Dec. 2015.

[370] S. Gajewski, M. B. Waddell, S. Vaithiyalingam, A. Nourse, Z. Li, N. Woetzel, N. Alexander, J. Meiler, and S. W. White, "Structure and mechanism of the phage T4 recombination mediator protein UvsY.," *Proc. Natl. Acad. Sci. U. S. A.*, vol. 113, no. 12, pp. 3275–3280, Mar. 2016.

[371] H. Xu, H. T. H. Beernink, and S. W. Morrical, "DNA-binding properties of T4 UvsY recombination mediator protein: polynucleotide wrapping promotes high-affinity binding to single-stranded DNA.," *Nucleic Acids Res.*, vol. 38, no. 14, pp. 4821–4833, Aug. 2010.

[372] W. C. Leite, C. W. Galvao, S. C. Saab, J. Iulek, R. M. Etto, M. B. R. Steffens, S. Chitteni-Pattu, T. Stanage, J. L. Keck, and M. M. Cox, "Structural and Functional Studies of H. seropedicae RecA Protein - Insights into the Polymerization of RecA Protein as Nucleoprotein Filament.," *PLoS One*, vol. 11, no. 7, p. e0159871, 2016.

[373] C. J. Ma, B. Gibb, Y. Kwon, P. Sung, and E. C. Greene, "Protein dynamics of human RPA and RAD51 on ssDNA during assembly and disassembly of the RAD51 filament.," *Nucleic Acids Res.*, Nov. 2016.

[374] J. D. Marks, M. Tristem, A. Karpas, and G. Winter, "Oligonucleotide primers for polymerase chain reaction amplification of human immunoglobulin variable genes and design of family-specific oligonucleotide probes.," *Eur. J. Immunol.*, vol. 21, no. 4, pp. 985–991, Apr. 1991.

[375] M. Jia, G.-Y. Sun, Y. X. Zhao, Z.-S. Liu, and H. A. Aisa, "Effect of polyethylene glycol as a molecular crowding agent on reducing template consumption for preparation of molecularly imprinted polymers," *Anal. Methods*, vol. 8, no. 23, pp. 4554–4562, 2016.

[376] Y. Phillip, E. Sherman, G. Haran, and G. Schreiber, "Common Crowding Agents Have Only a Small Effect on Protein-Protein Interactions," *Biophys. J.*, vol. 97, no. 3, pp. 875–885, Aug. 2009.

[377] R. K. Daher, G. Stewart, M. Boissinot, and M. G. Bergeron, "Recombinase polymerase amplification for diagnostic applications," *Clin. Chem.*, vol. 62, no. 7, pp. 947–958, 2016.

[378] K. Krolov, J. Frolova, O. Tudoran, J. Suhorutsenko, T. Lehto, H. Sibul, I. Mager, M. Laanpere, I. Tulp, and U. Langel, "Sensitive and rapid detection of Chlamydia trachomatis by recombinase polymerase amplification directly from urine samples.," *J. Mol. Diagn.*, vol. 16, no. 1, pp. 127–135, Jan. 2014.

[379] O. Piepenburg, C. H. Williams, and N. A. Armes, "Methods for multiplexing recombinase polymerase amplification." Google Patents, 2011.

[380] P. Gelred and P. Gelgreen, "GelRed™ & GelGreen™," pp. 1–2, 2001.

[381] "Blu-Stuff." [Online]. Available: http://blu-stuff.com/magento/. [Accessed: 04-Jun-2015].

[382] I. D. Johnston, D. K. McCluskey, C. K. L. Tan, and M. C. Tracey, "Mechanical characterization of bulk Sylgard 184 for microfluidics and microengineering," *J. Micromechanics Microengineering*, vol. 24, p. 35017, 2014.

[383] D. S. Kim, S. H. Lee, C. H. Ahn, J. Y. Lee, and T. H. Kwon, "Disposable integrated microfluidic biochip for blood typing by plastic microinjection moulding.," *Lab Chip*, vol. 6, no. 6, pp. 794–802,

2006.

[384] P. S. Nunes, P. D. Ohlsson, O. Ordeig, and J. P. Kutter, “Cyclic olefin polymers: Emerging materials for lab-on-a-chip applications,” *Microfluid. Nanofluidics*, vol. 9, no. 2–3, pp. 145–161, 2010.

[385] J. Wang, M. Pumera, M. Prakash Chatrathi, A. Rodriguez, S. Spillman, R. S. Martin, and S. M. Lunte, “Thick-Film Electrochemical Detectors for Poly(dimethylsiloxane)-based Microchip Capillary Electrophoresis,” *Electroanalysis*, vol. 14, no. 18, pp. 1251–1255, 2002.

[386] G. Bin Lee, S. H. Chen, G. R. Huang, W. C. Sung, and Y. H. Lin, “Microfabricated plastic chips by hot embossing methods and their applications for DNA separation and detection,” *Sensors Actuators, B Chem.*, vol. 75, no. 1–2, pp. 142–148, 2001.

[387] A. Piruska, I. Nikcevic, S. H. Lee, C. Ahn, W. R. Heineman, P. a Limbach, and C. J. Seliskar, “The autofluorescence of plastic materials and chips measured under laser irradiation.,” *Lab Chip*, vol. 5, no. 12, pp. 1348–1354, 2005.

[388] S. W. Rhee, A. M. Taylor, C. H. Tu, D. H. Cribbs, C. W. Cotman, and N. L. Jeon, “Patterned cell culture inside microfluidic devices.,” *Lab Chip*, vol. 5, no. 1, pp. 102–107, 2005.

[389] A. M. Taylor, S. W. Rhee, C. H. Tu, D. H. Cribbs, C. W. Cotman, and N. L. Jeon, “Microfluidic Multicompartment Device for Neuroscience Research.,” *Langmuir*, vol. 19, no. 5, pp. 1551–1556, 2003.

[390] C. Vannahme, S. Klinkhammer, U. Lemmer, and T. Mappes, “Plastic lab-on-a-chip for fluorescence excitation with integrated organic semiconductor lasers.,” *Opt. Express*, vol. 19, no. 9, pp. 8179–86, 2011.

[391] M. R. Monteiro, a. R. P. Ambrozin, L. M. Lião, and A. G. Ferreira, “Critical review on analytical methods for biodiesel characterization,” *Talanta*, vol. 77, no. 2, pp. 593–605, 2008.

[392] H. Wei, B. Chueh, H. Wu, E. W. Hall, C. Li, R. Schirhagl, J.-M. Lin, and R. N. Zare, “Particle sorting using a porous membrane in a microfluidic device,” *Lab Chip*, vol. 11, no. 2, pp. 238–245, 2011.

[393] M. Evander and M. Tenje, “Microfluidic PMMA interfaces for rectangular glass capillaries,” *J. Micromechanics Microengineering*, vol. 24, no. 2, p. 27003, 2014.

[394] C. K. Fredrickson and Z. H. Fan, “Macro-to-micro interfaces for microfluidic devices.,” *Lab Chip*, vol. 4, no. 6, pp. 526–533, 2004.

[395] H. Becker and C. Gärtner, “Polymer microfabrication technologies for microfluidic systems.,” *Anal. Bioanal. Chem.*, vol. 390, no. 1, pp. 89–111, Jan. 2008.

[396] J. Astorga-Wells, H. Jörnvall, and T. Bergman, “A microfluidic electrocapture device in sample preparation for protein analysis by MALDI mass spectrometry.,” *Anal. Chem.*, vol. 75, no. 19, pp. 5213–9, 2003.

[397] A. Egatz-Gómez, J. Schneider, P. Aella, D. Yang, P. Domínguez-García, S. Lindsay, S. T. Picraux, M. a. Rubio, S. Melle, M. Marquez, and A. a. García, “Silicon nanowire and polyethylene superhydrophobic surfaces for discrete magnetic microfluidics,” *Appl. Surf. Sci.*, vol. 254, pp. 330–334, 2007.

[398] J. Li, C. Liu, Z. Xu, K. Zhang, X. Ke, C. Li, and L. Wang, “A bio-inspired micropump based on stomatal transpiration in plants.,” *Lab Chip*, vol. 11, no. 16, pp. 2785–9, 2011.

[399] A. Végvári and S. Hjertén, “A hybrid microdevice for electrophoresis and electrochromatography using UV detection.,” *Electrophoresis*, vol. 23, no. 20, pp. 3479–86, 2002.

[400] W. W. Yang, Y. C. Lu, Z. Y. Xiang, and G. S. Luo, “Monodispersed microcapsules enclosing ionic liquid of 1-butyl-3-methylimidazolium hexafluorophosphate,” *React. Funct. Polym.*, vol. 67, no. 1, pp. 81–86, 2007.

[401] J. DENG, L. WANG, L. LIU, and W. YANG, “Developments and new applications of UV-induced surface graft polymerizations,” *Prog. Polym. Sci.*, vol. 34, no. 2, pp. 156–193, 2009.

[402] J. C. Mcdonald, D. C. Duffy, J. R. Anderson, and D. T. Chiu, “Review - Fabrication of microfluidic systems in poly (dimethylsiloxane),” *Electrophoresis*, vol. 21, pp. 27–40, 2000.

[403] J. C. McDonald, D. C. Duffy, J. R. Anderson, D. T. Chiu, H. Wu, O. J. Schueller, and G. M. Whitesides, “Fabrication of microfluidic systems in poly(dimethylsiloxane).,” *Electrophoresis*, vol. 21, no. 1, pp. 27–40, 2000.

[404] O. C. Jeong and S. Konishi, “Fabrication and drive test of pneumatic PDMS micro pump,” *Sensors Actuators, A Phys.*, vol. 135, no. 2, pp. 849–856, 2007.

[405] J. Goldowsky and H. F. Knapp, “Gas penetration through pneumatically driven PDMS micro valves,” *RSC Adv.*, vol. 3, no. 39, pp. 17968–17976, 2013.

[406] R. Mazurczyk, G. El Khoury, V. Dugas, B. Hannes, E. Laurenceau, M. Cabrera, S. Krawczyk, E. Souteyrand, J. P. Cloarec, and Y. Chevolot, “Low-cost, fast prototyping method of fabrication of the microreactor devices in soda-lime glass,” *Sensors Actuators, B Chem.*, vol. 128, no. 2, pp. 552–559, 2008.

[407] C.-H. Lin, G.-B. Lee, Y.-H. Lin, and G.-L. Chang, “A fast prototyping process for fabrication of microfluidic systems on soda-lime glass,” *J. Micromechanics Microengineering*, vol. 11, no. 6, pp. 726–732, 2001.

[408] A. Iles, A. Oki, and N. Pamme, “Bonding of soda-lime glass microchips at low temperature,” *Proc. 2006 Int. Conf. Microtechnologies Med. Biol.*, pp. 109–111, 2006.

[409] S. Jiguet, A. Bertsch, H. Hofmann, and P. Renaud, “Conductive SU8 photoresist for microfabrication,” *Adv. Funct. Mater.*, vol. 15, no. 9, pp. 1511–1516, 2005.

[410] G. Liu, Y. Tian, and Y. Kan, “Fabrication of high-aspect-ratio microstructures using SU8 photoresist,” *Microsystem Technologies*, vol. 11, no. 4–5. pp. 343–346, 2005.

[411] J. H. T. Ransley, M. Watari, D. Sukumaran, R. a. McKendry, and a. a. Seshia, “SU8 bio-chemical sensor microarrays,” *Microelectron. Eng.*, vol. 83, pp. 1621–1625, 2006.

[412] W. Park, S. Han, and S. Kwon, “Fabrication of membrane-type microvalves in rectangular microfluidic channels via seal photopolymerization.,” *Lab Chip*, vol. 10, no. 20, pp. 2814–2817, Oct. 2010.

[413] T. Schaller, L. Bohn, J. Mayer, and K. Schubert, “Microstructure grooves with a width of less than 50 μm cut with ground hard metal micro end mills,” *Precis. Eng.*, vol. 23, no. 4, pp. 229–235, 1999.

[414] B. Jang, S. Member, and A. Hassibi, “Biosensor Systems in Standard CMOS Processes : Fact or Fiction ?,” vol. 56, no. 4, pp. 979–985, 2009.

[415] P. Tabeling and Y. K. Lee, “Micro / Nanofluidic Processes Pressure - Driven Microfluidics Electrokinetics Of Particles And Fluids,” pp. 1–5, 2010.

[416] P. Tabeling, *Microsystem Engineering of Lab-on-a-Chip Devices.*, 2nd ed. Paris: Oxford University Press, 2005.

[417] P. Craw and W. Balachandran, “Isothermal nucleic acid amplification technologies for point-of-care diagnostics: a critical review.,” *Lab Chip*, vol. 12, no. 14, pp. 2469–86, Jul. 2012.

[418] J. H. Nichols, “Point of Care Testing,” *Clin. Lab. Med.*, vol. 27, no. 4, pp. 893–908, Dec. 2007.

[419] D. S. V. Omar, “Point of Care What is Point of Care (POC)?,” 2007.

[420] V. Hessel, H. Lowe, and F. Schonfeld, “Micromixers?a review on passive and active mixing principles,” *Chem. Eng. Sci.*, vol. 60, no. 8–9, pp. 2479–2501, 2005.

[421] G. S. Jeong, S. Chung, C.-B. Kim, and S.-H. Lee, “Applications of micromixing technology.,” *Analyst*, vol. 135, no. 3, pp. 460–473, 2010.

[422] Markus Deserno, “One-dimensional difusion on a finite region,” 2010. [Online]. Available: http://www.cmu.edu/biolphys/deserno/pdf/diffusion.pdf.

[423] K. Handique, B. P. Gogoi, D. T. Burke, C. H. Mastrangelo, and M. A. Burns, “Microfluidic flow control using selective hydrophobic patterning,” pp. 185–195, 1997.

[424] A. Puntambekar, J.-W. Choi, C. H. Ahn, S. Kim, and V. Makhijani, “Fixed-volume metering microdispenser module.,” *Lab Chip*, vol. 2, no. 4, pp. 213–218, 2002.

APPENDIX A

Sensors & Transducers

http://www.sensorsportal.com

[1] Luck EREKU, [1] Ruth MACKAY, [1] Wamadeva BALACHANDRAN, [2] Kolawole AJAYI

[1] School of Engineering and Design, Brunel University, Kingston Lane, Uxbridge, UK

[2] University of Lagos, Akoka, Lagos, Nigeria

[1] Tel.: +441895267378, fax: +441895258728

[1] E-mail: luck.ereku@brunel.ac.uk

During the last two decades silicon and MEMs technology had been the mainstay of early microfluidic devices. However, recent times have brought into focus the need for low cost and readily available materials capable of achieving the expected microfluidics physical and chemical requirements. Also what mentioning is the rapid improvement in microfabrication technology over the years, which has significantly aided new and cheaper ways to produce microfluidic Point-Of-Care-Testing devices commercially or for research purposes. This review article discusses the usefulness of a wide range of available materials and their unique properties suitability in microfluidic applications. Likewise, advantages and drawbacks of manufacturing procedures and outputs of different fabrication methods are also brought into focus. *Copyright © 2016 IFSA Publishing, S. L.*

Keywords: Fabrication Techniques, Material Selection, Microfluidics, Point of Care Testing, Lab-on- a-Chip.

---

1. Microfluidics Materials

In microfluidics, the properties of Material are very crucial because it affects both functionality and manufacturability. This therefore makes material selection the first consideration for successful design, fabrication and efficacy of microfluidic POCT devices. For instance device performance and proper material selection is critical for balancing functional requirements that is related to the physical and chemical properties of the intended material.

1.1 Generally Required Properties

The anticipated physical properties required, mostly revolves around mechanical resilience (modulus of elasticity), visual characteristics (optical) and high temperature tolerance. Mechanical properties describes the brittleness (hardness) or elastic nature of the device. Brittleness features are mostly utilized for the framework where rugged handling is required. Furthermore since most POCT chips are subjected to relatively high pressures flow when external pumps are utilized, thus the designated material are expected to resist rupture. As for the utility of elastic materials, their characteristics are mostly employed in the internal membranes of micropumps and microvalves. Temperature on the other hand are needed for chemical reaction or processing done on the chip. For instance, polymerase chain reaction (PCR) relies on repetitive heating and cooling cycles for rapid DNA melting and enzymatic replication, during which the temperature fluctuates between 52◦C and 96◦C [31], [172]. Thus, a material of considerable temperature resistance is a requirement. Another important feature is the surface properties which dictates the solid-fluid interface relationship. A good example is the interaction between microchannel surfaces and active fluids (reagent). This interactions can be described physically in terms of surface hardness and roughness which are the main factors that determines hydrophobic or hydrophilic characteristics. When the surface is hydrophilic capillary flow is enhanced, while the opposite applies to hydrophobic surfaces. Although, in recent times innovative methods such as surface modification techniques are being employed to treat specific surface to adhere specific surface requirements. In terms of requirements, hydrophilic patches are required to speedup flow while hydrophobic patches for stopping fluid flow [173]. A common surface modification technique is plasma treatment [174]. Applications involving optical properties is usually associated with fluorescence which is the emission of electromagnetic radiation in this case Ultra Violet (UV) light to aid chemical reaction or DNA detection. This real-time fluorescence detection system [175]–[177] are usually employed lab-on-a-chip applications, thus the degree of material transparency becomes highly significant.

Chemical resistance (inertness), antifouling and disposability are also vital requirements in material selection. Chemical resistance involves material surface reaction to chemicals (organic solvent, water etc.) as shown in table 1. The main interest in this reaction is the whether the contact surface and overall nature of the material is altered or not. This alteration relates to absorption and adsorption of the small molecules of solvents in contact with material surface. Whereas, when the concerned chemicals or reaction are of biological connotations the term biocompatibility is used in reference to the material. For instance, absorption of organic solvents in PDMS fabricated chip causes swelling of the chip, which results to distortion of the microchannels [179], [180]. Therefore the fluid flow within the channels are impaired and might lead to build up of excessive back pressure in the pumping mechanism. Similarly, antifouling otherwise known as Protein fouling is the accumulation of proteins on a surface, especially in

microchannels. Fouling of surfaces in microfluidics devices, predominantly, when protein or enzymatic solutions are used often creates both restriction of flow channels of very small dimensions and also alter the surface chemistry of the channels [181], [182]. For all the above listed chemical material properties surface modification techniques are usually applied to improve their functionalities.

Material Disposability comes in two folds which can be identified as cost and eco-friendliness. Material cost plays a major role in chip prototyping and commercialization because at low cost microfluidic POCT device prototyping research is made easier while commercialization of new design products are aided by affordability. The factors that determine cost are the material availability and cost of synthesis or production. Inexpensive materials tend to be ubiquitously available in the market while at the same time easy and cheaper to synthesize. Since polymers commonly used in microfluidics device fabrication are non- biodegradable, recycling becomes the best effort that helps reduce the high rates of plastic pollution. Then again there have been recent use of biodegradable polymers [183] in microfluidics device in tissue engineering [184], [185].

1.2 Silicon

Considering the wide variety of microfabrication processes for microfluidic and MEMS devices which are largely inherited from microelectronics fabrication; therefore making silicon by far the most prevalent substrate material in use. Before the rapid growth of interest in polymer materials for MEMS, silicon was the most important material for microelectronics because of its semiconductor properties. Although brittle when stressed to the point of fracture, silicon is remarkably effective as a mechanical material [186]. The crystalline structure of silicon inhibits gas permeability; which is one of the necessary characteristic vital for cell culturing in microfluidic systems [134]. It also exhibits linearly elastic behaviour below its yield strength with no hysteresis and suffers no plastic deformation or creep except under very extreme temperatures well beyond relevance to microfluidic applications. As a result, their high material stiffness makes it very difficult for the fabrication of mechanically movable microfluidic structures (diaphragms) required for microvalves and pumps; which fair better under soft and flexible materials. Though, silicon is still a generally utilized material for moulds replication in microfluidics.

Silicon is also prevalent in microfluidics in the form of polysilicon (i.e., polycrystalline silicon) and amorphous silicon. In both cases, the silicon is typically deposited as thin films by vapour deposition, and can be doped for electronic device functionality. Polysilicon is used in many diverse ways for surface micromachined sensors and actuators. For example, in the case of actuation, polysilicon has been used for electrostatic diaphragms [187] and as heating elements for micropumps. Properly doped polysilicon is also effective for sensing elements based on capacitive displacement [188] and piezoresistive strain measurement. Another unique aspect of silicon is that it can be made highly porous with good uniformity by an anodic electrochemical etch process. Porous silicon has extremely high surface-to-volume ratio, which is particularly advantageous for applications with surface reactions involving catalysis, adsorption and/or desorption [189].

1.3 Glass

The term glass usually refers to materials that are predominately amorphous silicon dioxide (SiO2), also known as silica. Varieties of glass are made by including other compounds such as sodium carbonate, calcium oxide, and boron oxide to produce different thermal, mechanical, and optical

characteristics. Like silicon, glass is rigid, dimensionally stable (thickness of 30μm can be handled) and relatively brittle. Many common categories of glass are optically transparent, making glass favourable for applications that require imaging or optical methods of detection for fluids particles. Glass is a very convenient substrate for microfluidic devices because it is readily available in flat form, typically cut into rectangular slides or circular wafers. For applications such as capillary electrophoresis, glass microchannel chips are routinely produced as either commercial off-the-shelf products or even semi-custom layouts. Unless specifically engineered for electrical conductivity, conventional glass exhibits sufficient electrical insulation such that it can serve as a substrate for direct patterning of conductive metal lines and functional electrodes [190], [191].

A common way of creating channels in glass substrates is by wet etching, typically with concentrated hydrofluoric acid. Wet etching of glass occurs isotropically and typically produces rounded profiles with low aspect ratio. Holes and channels in glass substrates can be fabricated by ultrasonic drilling and laser ablation. There are also formulations of photosensitive glass that exhibit spatial etch selectivity when exposed to UV radiation through a mask [192]. Although the majority of glass microfluidic devices use slides or wafers, glass in other forms can also be used to fabricate channel-like structures using spin-on-glass [193] or sputtered films. A good example of commonly used derivative is borosilicate glass. It has an excellent ability to resist strong acids, saline solutions, strong oxidizing and corrosive chemicals. In the same way their chemical inertness exceeds that of most metals and other materials because at temperatures above 100 ˚C they still retain their inertness for a long period of time. Economically, they are easily mass produced and readily available in differs thickness.

1.4 Fused Silica Quartz

Fused silica quartz is dissimilar to quartz which is a crystalline material whereas fused silica quartz is amorphous, just like other glass forms they are that are mostly made up of silica in its non-crystalline form. They can be manufactured using several different processes. Prominent amongst this is vitresous method (splat-quenching or melt-quenching) is used to form the quartz by heating the material to it's melting point and rapidly cooling it. While the fused used Silica is formed by fusing high purity silica in a specially designed furnace. The overall procedure is carried out at extremely high temperatures, over 5000C.

The microfluidic device fabrication processes with this material is similar in precision to the ones used in the electronics industry. For instance the channels for fluid flow are etched into materials by photolithography processes. While in the case of multi-patterned layers can be very accurately aligned and fused together. Recently Engineers at Dolomite can now etch optically smooth features with depths of up to 150microns which is far deeper than most available solutions on the marketplace which can only offer depths in the area of 20microns [231].

In comparison to glass, quartz is much harder with great thermal shock resistance. It also has an excellent chemically inertness; fused silica quartz can handle high concentration of acids except hydrofluoric acid even at low concentrations. They do have superior optical properties (UV transparency) in comparison to glass and can be used for applications such as flow cytometry (cell sorting and cell counting). For example, Institute of Photonic Technology inn Germany in collaboration with the Department of Internal Medicine have develop a Quartz microfluidic chip

that can be used for tumour cell identification using Raman spectroscopy in combination with optical traps [232]. Some other benefits include non-auto-fluorescent and non-porous characteristics making it a preferred material for applications in the POCT.

1.5 Metals

Metals are obviously distinguished by having Metals are obviously distinguished by having significantly higher electrical conductivity than other categories of materials used in microfluidics. Accordingly, metals are frequently used for functional electrical components such as electrodes, conducing lines, or signal interface contacts. As conductors of electricity, metals may also be used to modify electromagnetic fields, which may subsequently be used in novel ways for applications such as biological cell manipulation [196]. Another functional merit for metals is high thermal conductivity. For example, a heat spreader based on micro heat pipe design has been constructed from layers of copper and brass for microprocessor cooling [197], [198]. The relatively high mechanical strength of metals favours their use for high-pressure applications, compared to polymer materials. Some metal alloys that have favourable magnetic properties have been incorporated into functional components such as nickel- iron rotors for active mixing [199], [200]. Magnetic components have also been combined with deformable polymer structures for functionality as micropumps [201] and microvalves. Some microfluidic devices also take advantage of shape memory alloys. Nickel-titanium (NiTi), which changes from its austenite phase to its martensite phase upon cooling and the corresponding shape change, can be used for device actuation.

Gold, nickel, and copper are among the most commonly used metals in microfluidic devices. Gold is often the material of choice for electrical purposes because of superior resistance to corrosion and oxidation, even though other materials such as copper have lower electrical resistivity ($1.7 \times 10{-}6$ Ωcm for copper versus $2.2 \times 10{-}6$ Ωcm for gold). Nickel, copper, and alloys based on nickel or copper are favourable for structures made by electroplating and electroforming. Single nickel electroforming step are good example of commercially viable means of making metal microfluidic structure such as ink-jet print heads [202]. In contrast to gold and copper, the much higher resistivity of platinum ($10.6 \times 10{-}6$ Ωcm) makes it favourable for resistive heating. Other metals such as aluminium and tungsten are prevalent in microelectronics but less common in microfluidic devices.

Another important role of metals in microfluidic device fabrication is tooling. Even if the final device made of a different material, it is sometimes beneficial to have finely patterned tooling to transfer the relevant geometry by hot embossing or other moulding technique. This facilitates more rapid high-volume manufacturing with good repeatability. One approach, for example, is to begin with laser micromachining of patterned tooling in a thin metallic sheet, then to transfer the pattern by hot embossing onto a thermoplastic (PMMA) master, and to complete the process with casting of PDMS atop the PMMA master [207].

1.6 Paper

Paper-based microfluidics" or "lab on paper," provides an innovative system for manipulation and analysis of fluid for a variety of applications. They are typically made up of cellulose or cellulose-polymer that possess excellent compatibility trait with several medical diagnostics applications and can be chemically modified to integrate an extensive range of functional groups that can be covalently bound to DNA or proteins [208], [209]. Just like most papers they are easy to stack, store, transport, depose (burning) and most

especially available in a wide range of thicknesses (0.07-1 mm) [210].

Besides, unlike conventional microfluidics, its preference to fluid flow by capillary driven forces makes it requires little or no ancillary pump which often require external power assistance.

These systems integrate some of the capabilities of conventional microfluidic devices with the simplicity of diagnostic strip tests [211], [212]and can be referred to as micro-pads (μPADs). μPADs are very significant in comparison because they provide bio-analyses that are more rapid, less expensive, and more highly multiplexed than contemporary analyses. They require only minute volumes of fluid and very minimal external supporting equipment or power because fluid movement in μPADs is controlled principally by capillarity and evaporation. Their Features can be identified by a variety of 2D and even 3D microfluidic channels that have been created on paper to confine and manipulate fluid flow within the predesigned pathways on paper [213].unlike orthodox microfluidic devices that have their microchannels fabricated by etching or moulding channels into PMMA, glass, PDMS, or other polymers; instead μPADs make use of patterning sheets of paper into hydrophilic channels constrained by hydro hydrophilic cellulose fibers of paper allowing aqueous fluids to wick along the channels. The flowrate of the wicking is contingent on the the characteristics of the paper, ambient conditions (temperature and relative humidity) and most especially dimensions of the channel. Furthermore, the cellulose matrix can be integrate with conducting carbon or metal fibers [211]. This innovative configuration provides electrically conducting or magnetically responsive patterns on the μPADs. Paper is already used extensively in as point of care device in developing countries where healthcare and disease screening is expensive and not readily available due to low-infrastructure and limited trained medical and health professionals [211], [214].

1.7 Polymer

As a result the growing demands for cheap and disposable POCT devices during the early 1990s, the selection of suitable materials has gradually shifted from the conventional materials such as silicon and glass towards polymers. This gradual change which was eased through by the advent material technological progress can be considered a major innovation in the field of microfluidics POCT which is primarily needed in various biomedical and clinical applications.

Compared to other types of materials, polymers represent a wide variety of material characteristics for microfluidic devices [215], [216]. They have relatively low mechanical strength, low melting point and high electrical resistance. The main advantage that polymers offer is that they can be engineered or synthesized to exhibit certain chemical and physical properties required for targeted functionality such as optical transparency, chemical resistance, stiffness, critical surface tension etc.

1.8 Polymer Chemical Classification

Polymers chemical classification are based on monotonous structural blocks called monomers that are capable of being bonded chemically to other molecules in long chains to form large-sized molecules. These macromolecules or polymers can be used to create diverse material properties from their monomers by polyaddition [217] reaction or polycondensation [218]. The most frequently used monomer chemistries Acrylates and vinyl polymers, Epoxy resins, Thiol–enes, Polyurethanes, Siloxanes.

1.8.1 Epoxy Resins

Epoxy polymers are typical derivatives of glycidyl or oxirane group and can be created from synthesis of Bisphenol A epoxy resin, Bisphenol F epoxy

resin, Bisphenol F Novolac epoxy resin, Aliphatic epoxy resin and Glycidylamine epoxy resin [219]. Further details of the chemistry engineering of epoxy can be found in this textbook [220]. A good example of an epoxy-based polymer is SU8 which is a generally used microfluidic master-mold fabrication photolithography technique. The "8" in SU-8 stands for the 8 epoxy groups in a bisphenol-A novalac glycidyl ether a single moleculecular structure. SU8 photolithography produces a Good adhesion and high aspect ratio negative photoresist that allows for creation of deep channel microfluidic structures and as well as variant depth through multiple UV light exposure [221] (this technique will be discussed in the microfabrication section). In addition, they are also suitable polymers material choice for prototyping techniques such as stereolithography [222], [223].

1.8.2 Thiol–enes

The thiol-ene reaction is acknowledged as a click chemistry reaction given the reactions' maximum yield, fast rate, stereoselectivity and thermodynamic driving force [224]. They are compounds with sulphur hydrogen groups also known as alkene hydrothiolation; which is an organic reaction that forms alkyl sulphide [225]. They are commercially produced from mixing monomers such as trithiol with triene or tetrathiol with triene in varying ratios wich are calculated with respect to the amount of free thiol and allyl(ene) groups in the monomer structure [226]. Subsequently, the mixed ratios can then be cured rapidly under UV light through free-radical polymerization at ambient temperature and pressure [227].

Thiol-ene chemistry are now been seen as PDMS substitutes in soft lithography [228]–[230] for bioanalytical applications because they are not prone to protein fouling [231], [232] to swelling upon contact with organic solvents [233], absorption of hydrophobic small molecules [234] and Most importantly high elastic modulus (PDMS is frequently restricted to comparatively low working pressures of about 1 bar [235].

They are mostly utilized in microfluidics for surface engineering and microchannel patterning [236].

1.8.3 Acrylates and Vinyl Polymers

Acrylate monomers are typically derivatives of acrylic acid [237] which consist of vinyl hydrogen and the carboxylic acid, while vinyl monomers are consist of vinyl group [238] or ethylene. However acrylates are industrially easier to synthesize than pure vinyl polymers which are toxic and difficult to handle. An example of a simple acrylic acid synthesise is the methyl methacrylate which has its vinyl hydrogen and carboxylic acid hydrogen substituted by methyl groups to form poly(methyl methacrylate) (PMMA) [239], typically known for their transparency. On the other hand vinyl chloride can be polymerize [240] with the assistance of a radical a catalyst to form of polyvinyl chloride (PVC) which is widely used material.

1.8.4 Polyurethanes

Polyurethanes (PU) polymers also known as polycarbonates are created by the reaction of two monomers di-isocyanate and a polyol that contains containing hydroxyl groups in the presence of a catalyst or by ultraviolet light stimulation [241]. There are of high relevance in microfluidic prototyping because of their suitability in creation of moulds [242] and as structures [243] in microfluidic devices. This polymers also serves as another alternate to PDMS because they are not prone to protein fouling especially when bio fluids are involved for example blood [244]. However they are relatively expensive and not usually transparent.

Polyurethanes robust reaction mechanism can be tailored to fit two typical forms in microfluidics which include elastomers and surface coatings.

Elastomeric polyurethane (PU) which can be derived from bio-source such as castor oil (CO) [243]. This elastomers can be used to produce microvalves elastomer in microvalves that can be integrated with microfluidic devices [245]. In addition, microchannel formation and sealing (both reversible and non-reversible) is easily attainable in PU components by means of partial curing [243].

One the other hand the coating specification applies to surface modification for good compatibility with a wide range of solvents and chemical resistance.

1.8.5 Siloxanes

Siloxane polymers have mostly been used in microfluidics device prototyping for last two decades. They are chemically a class of polymers that exhibit an interchanging silicon–oxygen polymer with each pair of silicon centres separated by one oxygen atom to form backbone chains that are very elastic. Consequently, this renders most siloxanes as elastomeric materials. A principal example is a polydimethylsiloxane (PDMS) that methyl groups as the main polymer backbone. PDMS are of significant importance due to their low critical surface tension, flexibility, chemical resistance and surface hydrophobicity in nature. This defining features of PDMS comprises of the polymer matrix (often aromatic siloxanes) and a curing agent which activates ring opening polymerization or similar crosslinking.

This process usually involves the use of moulds or a solid master that gives the expected shape of the PDMS when cured. This process is known as casting [247].

A substitute method of curing similar to thiol-ene involves the use of a catalyst (typically a platinum catalyst) on a mixture of SiH and vinyl terminated polysiloxanes. A detailed analysis of the synthesis and characterization of siloxanes are found in this text [220].

1.9 Polymer Physical Properties

The physical and mechanical properties of The physical and mechanical properties of polymers can be categorised into three rudimentary temperature dependent parameters in the form of glass transition temperature (Tg), heat distortion temperature (HDT) and decomposition temperature (TD).

Glass transition temperature (Tg), which is of considerable technological importance has its derivation from the molecular comportment of the polymer material. it's an amorphous change unique to only polymers that involve reversible hardened or softening above or below a threshold temperature. As the polymer absorbs heat, up to a certain temperature the intramolecular friction holding each fragment/monomers in the polymer chain is weakened by the relative motion as a result of absorbed energy.

Table 1. Overview of physical properties for common microfluidic polymers and material [178].

Polymer/Material	*Acronym*	*T_g (°C)*	*T_m (°C)*	*CTE ($10^{-6}°C^{-1}$)*	*Tensile Strength (MPa)*	*Optical Transmissivity*		*Water Absorption (%)*	*Acid/Base Resistance*	*Solvent Resistance*
						Visible	UV[a]			
Cyclic olefin (co)polymer	COC/COP	70-155	190-320	60-80	60	Excellent	Excellent	0.01	Good	Excellent
Polymethylmethacrylate	PMMA	100-122	250-260	70-150	70	Excellent	Good	0.3-0.6	Good	Good
Polycarbonate	PC	145-148	260-270	60-70	70	Excellent	Poor	0.12-0.34	Good	Good
Polystyrene	PS	92-100	240-260	10-150	40	Excellent	Poor	0.02-0.15	Good	Poor
Polypropylene	PP	-20	160	18-185	40	Good	Fair	0.10	Good	Good
Polyoxymethylene	POM	60	190-210	11	73	Poor	Poor	0.22	Good	Good
Polyetheretherketone	PEEK	147-158	340-350	47-54	96	Poor	Poor	0.1-0.5	Good	Excellent
Polyethylene terephthalate	PET	69-78	248-260	48-78	55	Good	Good	0.1-0.3	Excellent	Excellent
Polyethylene	PE	-30	120-130	180-230	15	Fair	Fair	0.01	Excellent	Excellent
Polyvinylidene chloride	PVDC	0	76	190	54	Good	Poor	0.1	Good	Good
Polyvinyl chloride	PVC	80	180-210	50	51	Good	Poor	0.04-0.4	Excellent	Good
Polysulfone	PSU	170-187	180-190	55-60	-	Fair	Poor	0.3-0.4	Good	Fair
Polydimethylsiloxane	PDMS	-125	-40	310	2.24	Excellent	Excellent	0.05	Good	Good
Soda-Lime Glass	Silica	564	1000	9.5	74	Excellent	Excellent	0	Good	Good
Epoxy Resin	SU8	50-200	380	52	34	Excellent	Excellent	0.65	Good	Good

At this point already hard polymers will have larger segments of their polymer chain moving freely, leading to a substantial softening of the material. On the other hand, when already soft polymers cooled below their T_g they become hard and brittle, like glass. The case of heat distortion temperature (HDT) describes the maximum temperature for which a polymer material susceptible to mechanical failure from stress as it would simply give way beyond this temperature. The last important parameter, decomposition temperature (TD), is the point at which the physical characteristics of the polymer is permanently altered as a result of the total breakdown of the polymer chains. At this point in temperature, the polymer is known to decompose.

1.9.1 Thermosets (duroplastic materials)

These materials often called resins and are usually liquid at room temperature. They typically formed from a corresponding monomer that undergoes a crosslinking by a chemical reaction, photoinitiator or thermo-initiator for polymerization. Initiated chemical reaction is done by mixing the monomer with a curing agent. While crosslinking initiated physically by light (photoinitiator) are typically UV irradiation and curing induced at a temperature typically above 200^0C [248], [249] are a good example of thermo-initiator reaction. All these curing (cross-linking) processes involve an irreversible chemical reaction and once taken place the polymer becomes rigid with a significant increase in molecular weight and higher melting point. Furthermore, the crosslinking forms close-fitting and solid three-dimensional network that are usually stable at room temperature. When subjected to unrestrained heating, the cured material results in reaching the decomposition temperature earlier than the melting point which will eventually decompose the polymer. Consequently, a thermoset material cannot be melted and re-modelled after undergoing curing process because their Tg is typically rather high and close to the decomposition temperature (TD) so, therefore, they burn instead of melting. As a result thermosets cannot be recycled therefore less eco-friendly. Well on the brighter side they do possess good dimensional stability, thermal stability, chemical resistance and electrical insulation properties, which makes them suitable for fabrication of microfluidics devices.

Archetypal examples of thermoset polymers in microfabrication are the resist materials for microfluidic applications, especially the photoresist (negative & positive) SU-8 (see Photolithography).

1.9.2 Elastomers

Elastomers typically known as silicone rubber are polymers with glass transition temperatures characteristically lower than the normal operating room temperature. When they are cooled to their Glass Temperature, there is less mobility between the polymer chains that eventually results in the material becoming brittle and less elastic. Just as their name (elastomer/rubber) they are known to undergo elastic deformation as a result of very weak inter-molecular forces with generally low Young's modulus and high failure strain rate in comparison with other materials. They also share similar characteristics with thermoset with regards to TD even though thermoplastic elastomer does exist. Engineered thermoplastic elastomers (TPE's), are one of the most multipurpose polymers available [250] because of the combined performance properties of thermoset rubber with the processing ease of today plastics. As a result, there is versatility of design options and better cost-reduction opportunities. The most commonly used elastomer in microfluidics prototyping is PDMS, and recently, fluorinated elastomers (FKM/FFKM) [251]–[253] have gained significant traction in the

community. These materials are exhibit number of properties that make them excellent materials for microfluidics that include very low critical surface tensions, high biocompatibility and outstanding chemical resistance. As well most of these fluorinated elastomers have their glass transition temperatures well below room temperature.

Since elastomers are usually soft, flexible and able to deform elastically without extensive pressure they are therefore an ideal material for active microfluidic components such as membrane and mechanical valves needed for microvalves or micropumps. Furthermore, they are also suitable for the creation of deflectable channels in regards to TPE material [250], [254].

1.9.3 Thermoplastic materials

Thermoplastics Compared to thermosets is made up of linear molecular chains not cross-linked. This polymer chain configuration supports easy movement within the polymer chains bulk as intermolecular forces weaken rapidly at high temperatures. Most thermoplastics do have high molecular weight and with unrestricted heating at temperatures above their Tg, they melt into a viscous liquid and then solidifies upon cooling [86], unlike thermosets that decompose. Thermoplastics, therefore, can be moulded or reshaped by heating. There two classes of this polymer. First of all, is the amorphous thermoplastic, which has intermingled molecular chains with no crystalline structure present within the material. This polymer Chain disorder leads to intermolecular twisting and coiling since there is no crystalline structure present. Consequently, this means the materials are susceptible to failure above the glass their transition point due to low Heat distortion temperature, HDT. In additional, there are known for mostly their transparent or translucent, low tendency to creep, good dimensional stability, low tendency to warp, brittleness, low chemical resistance sensitive to stress cracking.

On the other hand, Semi-crystalline is denser than amorphous since the degree of crystallinity is proportional to density measurement [87], [88]. This thermoplastics have some macromolecules in the form of crystalline structures dispersed throughout the material. As a result of this crystalline regions, the materials have a tendency to be very hard (resilient intermolecular forces); and capable of withstanding mechanical stress above the glass transition temperature (high Heat distortion temperature). Their material properties are characterized by being translucent or opaque, good fatigue resistance, toughness, and good chemical resistance. Table 2 shows various thermoplastic materials and their corresponding characteristics.

2. Material Bonding Properties

Bonding in microfluidics is a vital process that involves sealing two or more substrate arranged in a specific configuration that forms the internal environment of the Lab-on-a-chip (LOC) devices. This internal environment consists of microfluidic elements such as microchannels, mixer, valves, reaction chambers, fluidic connectors (inlet port and exit port). The Bond strength which is a significant factor in the sealing process can be reversible (relatively weak) but most commonly used applications are irreversible (permanent). Similarly, the bond interface is also another significant factor for consideration because it must provide appropriate chemical or solvent compatibility to avert degradation during usage, without compromising the dimensional integrity of the microchannels as a result of deformation during the bonding process.

The main concerns for the bond interface include surface chemistry, optical properties, material compatibility and uniformity of the channel sidewalls. Likewise, the already bonded substrates

Polymer/Material	Price	Commonly Used Microfluidic Applications
Cyclic olefin (co)polymer	Low	Has been utilized, amongst others, as material for microfluidic devices in liquid chromatography [383] and blood typing [384].
Polymethylmethacrylate	Low	Has been used for the Fabrication of devices for on-chip electrophoresis [385] and for the separation of DNA [386]. PMMA exhibits very low auto fluorescence, making it an excellent material especially suitable for optical applications.[387].
Polycarbonate	Low	has been used, among others, for the creation of microfluidic mixers [126] and devices for DNA amplification [12].
Polystyrene	Low	has been used, among others, as substrate material for cell culture devices [388] and cell growth studies[389]
Polypropylene	Low	has been used expansively as substrate material for optical biosensors in CD format [390] and is generally used as a material for membranes on chip [391].
Polyoxymethylene	Low	mostly used as material for microfluidic moulds [392], [393] and particle separation [394].
Polyetheretherketone	High	has been used for the creation of microfluidic networks for capillary electrophoresis [395] and fluidic pre-concentration of analytes for mass spectroscopy [396].
Polyethylene terephthalate	Low	has been used, amongst others, for the Fabrication of devices for capillary zone electrophoresis [285], [397].
Polyethylene		
Polyvinylidene chloride		has been used, among others, for the creation of microfluidic pumps[398] and for capillary electrophoresis devices[399].
Polyvinyl chloride	Low	
Polysulfone	High	has been used for the encapsulation of droplets in microfluidic devices [400] and as material for filtration [401].

Polydimethylsiloxane	Medium	Mostly used in Microfluidics chip prototyping due to its affordable processing with fast turnaround times and also suitable for the creation of deflectable channels, membranes and mechanical valves [402]–[405].
Soda-Lime Glass (Slides)	Low	Mostly Used in Microfluidics prototyping with PDMS (good bonding substrate), creation of electroosmotic flow chips [406]–[408].
Epoxy Resin (SU8)	High	Used in electroplating moulds, sensors creation, actuators, and most especially, SU-8 can be used to create structures (microchannels) with dimensions ranging from millimetres to hundreds of nanometres [409]–[411].

Table 2. Polymers and other microfluidic materials with their relative commercial viability and general microfluidic use [115].

required to constraining the reagents, solvents and bio-samples in specific volumes while also preventing unrestrained dispersion of liquids along wettable areas. Furthermore, External contaminants (dust, etc.) are prevented from coming into the chip. Likewise the anticipated fluid waste are restricted from going to outside world (biohazard). Finally, evaporation which is the main antagonist of fluid sample and reagents in the chip are brought to a minimal level especially during thermochemical reactions. The Selection of bonding techniques depend mostly on the materials characteristics and type of constraints imposed by the application. Several bonding techniques are available, both past and recent are covered in this review journals [122]–[124].

However, this thesis discusses the commonly used techniques in microfluidics substrate bonding which include adhesive bonding, thermal fusion bonding, solvent-based bonding, localized welding and Surface treatment and modification.

In general microfluidic bonding techniques can be characterised as either indirect or direct. Indirect bonding involves the use of an extra layer apart from the substrates in concerned. This layer is an adhesive that seals the two substrates and their encapsulated internal microfluidic elements together by charge interactions [261], [262]. The charge interactions can be a result of chemical (covalent) bonding or van derWaals forces [262], [263]. In contrast, direct bonding methods mate the substrates by molecular entanglement, which is mechanical interlocking of two surfaces by relative diffusion between them. This process is done without any additional materials added to the interface. It is distinguished by its ability to produce microchannels with homogeneous sidewalls [178].

2.1 Adhesive Bonding

[Most commonly used adhesive are UV curable [264], with the bonding process performed by applying a thin layer of a high viscosity liquid adhesive which is then cured by UV light irradiation. This process is illustrated in Figure 2.18 which shows adhesive layer bonding for PMMA substrates [265]. Another common, inexpensive method for adhesive bonding is the use of lamination films as low as 40 μm [264], [266], since most Commercial laminators are inexpensive and simple to use. The drawback to this system is intermediate adhesive layer mostly produces composite layer chip with inconsistent microchannel sidewalls and clogging of microchannels. Furthermore, the bonded surfaces tend to have different chemical, optical and mechanical properties than the bulk substrate. Although, an extensive range of UV-curable adhesives is accessible, they are typically derived from polyester or acrylate resins.

2.2 Thermal Fusion Bonding

This direct technique involves the simultaneous application of pressure and heat on both substrates surfaces. This bonding process gives a moderately high bonding strength and is mostly applied to thermoplastic materials because the Substrates are heated to temperatures near or above the glass transition temperature (Tg). Although, unrestrained temperatures and pressures application or use of materials with different Tg may lead to microchannel distortion and collapse. Hence, the use of a programmable hot press [265], [267]–[269]such as high throughput roller laminator [270] that can properly regulate temperature, pressure, and time is vital to attaining high bond strength while preventing deformation of the embedded microchannels due to bulk polymer flow. Using this method, consistent stability of channel cross-sections can be attained,

as revealed in Figure2.3.2 that shows the case of laser micromachined channels in PMMA [271].

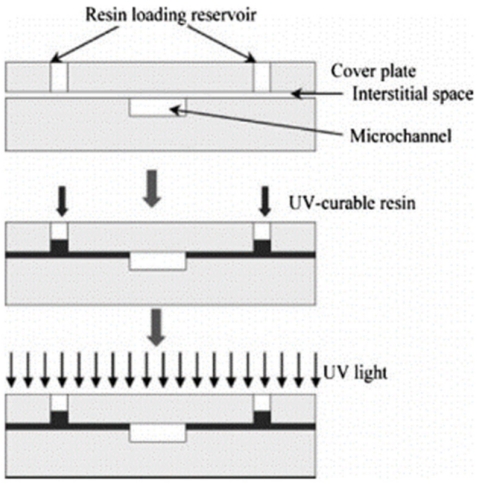

Figure 2.1. Capillarity-mediated resin introduction of UV-curable adhesive [168]. Copyright Wiley-VCH Verlag GmbH & Co. KGaA, copied with permission.

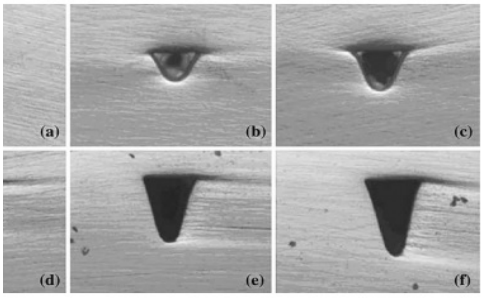

Figure 2.2. Cross-sectional views of enclosed laser micromachined PMMA channels, with increasing depth from a–f, thermally bonded at 180C, well above Tg, using a low bonding pressure below 20 kPa [168]. Copyright IOP Publishing Ltd., reproduced with permission

2.3 Solvent-Based Bonding

This technique is similar to adhesive indirect method because it that it requires a solvent between the merged surfaces. However, in this case the solvent used to bond the substrate together, temporarily soften and dissolves the material. Consequently, the surface molecules of the materials mix together to form a permanent bond as the solvent evaporates [153]. Solvent bonding of thermoplastics makes use of polymer solubility in designated solvent systems to achieve entanglement of polymer chains across the interface. As a result, the polymer chains become mobile and can freely diffuse across the solvated layer, leading to broad interweaving of chains between the surfaces to create exceptionally strong bonds [154].

PMMA substrates immersion in ethanol for at last 10 minutes before joining them together under pressure is a simple illustration is Solvent bonding that has been performed by this research group [139].

2.4 Localized Welding

It's a direct bonding technique that is commonly used on thermoplastic. It involves the use of ultrasonic energy to induce heating and tempering at the interface of the mating parts [275]. Another alternative method is the use of microwave energy to heat embedded metal films located between the desired bond surfaces. An advantage of this technique is selective use of energy to locally target specific regions or uniformly all mating interfaces for bonding [276]. There are commercially viable systems operating at 35 kHz [277] that can be efficiently used on thermoplastic polymers such as PMMA (Poly(methyl methacrylate) and PEEK (polyetheretherketone).

Table 2. Synopsis of general bonding techniques for microfluidic device [178].

Bonding Method	Bonding Strength	Bonding Quality	Process Complexity	Bonding Time	Cost	Advantage	Limitation	Suitable Material	References
Solvent bonding	High	Fair	Low	Low	Low	Simple, fast, low temperature, high bond strength, low cost	Soften polymer surface may collapse channel from un-optimized process	PMMA, PC, COC	[289]–[293]
Solvent Bonding with sacrificial Material	High	Good	High	Medium	Low	High bond strength, low cost, low channel collapse and clogging	Sacrificial material needed to be applied into channel before bonding and removed after bonding	PMMA	[294], [295]
Localized welding	Medium	Fair	Medium-high	Medium	Medium	Low temperature, localized bonding	Energy director (ultrasonic welding) or metal layer (microwave welding) are required	PMMA, PEEK	[296], [297]
Surface Treatment Bonding	Medium-high	Good	Medium	Medium	Medium-high	Low temperature bonding, low channel deformation	Surface chemistry changed after treatment	PMMA, PC, COC, PS, PET	[298]–[300]
Adhesive Printing Bonding	High	Fair	Medium-high	Short-medium	Low-medium	Low temperature, high bond strength, low channel clogging, controllable adhesive thickness	Scarification channel (contact printing) or printing mask (screen printing) required	PMMA. COC	[301], [302]

Adhesive interstitial Bonding	High	Fair	Low	Short	Low	Low temperature, high bond strength, low channel clogging, controllable adhesive thickness	Soften polymer surface may collapse channel from un-optimized process	PMMA	[303], [304]
PDMS-interface bonding	Medium	Fair	Medium	Long	Medium	Simple, fast, low temperature, high bond strength, low channel clogging, low cost	Sacrificial material need applied into channel before bonding and removed after bonding	PMMA	[265]
Lamination film bonding	Medium	Fair	Low	Short	Low	Low temperature, compatible with PDMS microfluidics	Energy director (ultrasonic welding) or metal layer (microwave welding) are required	PMMA, PC, PS, PET	[289], [305], [306]
Thermal fusion bonding	Medium	Fair	Low	Long	Low-medium	Simple, fast, low cost, low temperature, no adhesive clogging	Surface chemistry changed after treatment	PMMA, PC, PS, Nylon, CO, PSU	[307]–[310]

2.5 Surface Treatment and Modification

This form of direct bonding technique that functions by increasing the surface energy of the substrates required to bond. Increased surface energy helps to improve the hydrophilic properties of mating surfaces. As a result, mechanical interlocking and inter-diffusion of polymer chains between the surfaces are enhanced [278]. The substrates are held together by the generation of electrostatic interactions, and also surfaces possessing high specific energy in the form of polar functional groups can create hydrogen or covalent bonds across the interface that are capable of producing bond strengths beyond the cohesive strength of the bulk polymer [279]. Similar to localized welding, selective region use of a mask can be used to apply surface treatment and modification to specific regions. For example, PDMS layer to be bonded is covered with a masking material during corona discharge treatment to protect areas from exposure to the corona plasma so that only the unprotected surfaces are activated. Subsequently, the activated surfaces are hydrophilic, with chemically active functional groups that binds to other activated surfaces, while the masked areas remain unbounded [280], [281]. This example is an illustration of O2 plasma surface treatment done by the aid of corona discharge (fig 2.3.3). Corona discharge used for bonding is a process by which an electrical discharge occurs between an electrically charged conductor (electrode) and the surface of a substrate. This occurrence is as a result of potential gradient (electric field) and ionization of the neutral media fluid, typically air [282]. This fluid ionization process creates a region of plasma around the electrode as free electrons randomly accelerate across the air gap in the presence of a high voltage discharge. Subsequently, when a substrate surface is positioned in the discharge path, high energy electrons create free radicals by colliding with the surface to breakup their molecular bonds. These free radicals form various chemical functional groups [283], [284] required for effectively increasing surface energy and enhancing chemical bonding to another activated surface, in the presence of oxygen (oxidational reaction). Examples of functional groups include carbonyl (-C=O-). Carboxyl (HOOC-), hydroperoxide (HOO-) and hydroxyl (HO-) groups [284], [285].

Ultraviolet light (UV), is a simpler alternative to plasmas for the enhancement of substrate surface energy. The Exposure of UV light to polymer substrates especially thermoplastics results in photodegradation, which is the primary mechanism creates photo-oxidation and breakup of polymer chains on the surface [286]. Typically, light exposure within the range of 300–400 nm is usually sufficient to break chemical bonds within most thermoplastics [287], [288].

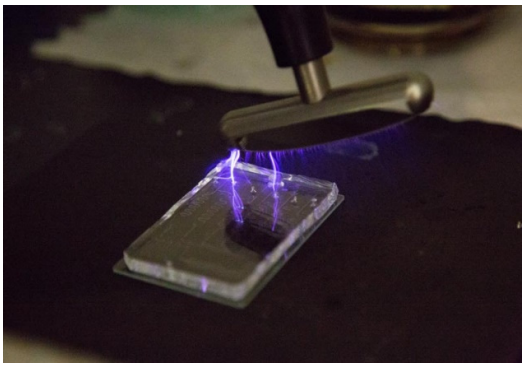

Figure 2.3. Corona discharge used to bond surfaces of PDMS to glass.

3. Prototype Fabrication Technology

The need to manufacture POCT devices at relatively cheap cost brought about rapid development microfabrication technology in the medical field. The earlier years of microfluidics devices were predominantly produced with techniques borrowed from the microelectronics field, and they predominantly involved materials

like glass, quartz or silicon. However, the advent of new technological processes brought into focus the demand for devices which are disposable and inexpensive.

Contemporary techniques can be distinguished by their individual protocols employed to establish efficient channel network or fluid circuit in the chip. The chip functionalities, are largely defined by microchannel aspect ratio, with channel dimensions as low 0.1μm to as large as 500μm. As a result choice of fabrication methods are tied to the anticipated channel dimensions on cost and production time. They can be divided into two areas: material depositing techniques and material removing technique.

3.1 Material Depositing Technology

This represent the successive build of bulk material on a substrate or a Standalone structure which can be used directly or as a mould for replication of microfluidic components. Parts produced can be used directly or bonded to achieve expected functionality. While the case of replication involves indirect use of fabricated parts to create intended components for utilization. In layer-to-layer manufacturing a part is broken down into multi slices that are then created and coupled by means of solvent or heat supported lamination or bonding processes. The materials used are usually wax, resin or powder. A good example of this techniques is 3D printing.

3.2 3D Printing

3D printing that utilize a layering accretion system to build solid structures from either liquid resin or powder from a digital file. This technology offers a broad range of methods to synthesize solid structures of various shapes or geometry that differ in physical characteristics with respect to the method of production.

These methods includes stereolithography (vat Photopolymerisation), ink jetting, binder Jetting, Material Extrusion and Powder Bed.

3.2.1 Stereolithography

Stereolithography (STL) is a conventional additive layer-on-layer manufacturing technique. STL is one of the most significant rapid prototyping methods in the microfluidic research industry today. It can be used to create very fine structures and, more importantly, allows for fast turnaround of functional prototypes used directly or replication molds. The basic process is called Vat Photopolymerization [311], it involves consecutive 'printing' thin layers of a curable material, e.g., a UV curable material, cumulatively on top of another by the use of UV Laser beam. The three-dimensional model (3D CAD design) is divided into thin micro multiple layers before light exposure. Upon exposure to UV light, the surface of the liquid resin solidifies. This hardening process is responsible for forming successive individual layers of the anticipated 3D object and is carried out repeatedly till 3D object is formed [312].

The Parts produced, based on this technique do have the considerable mechanical toughness and are capable of high detail definition. However, they do have some disadvantages such as post production that involves immersion in a chemical bath to eradicate unwanted resin before being cured in an ultraviolet oven. Likewise, the support structures which are interminably present can be difficult and time-consuming to remove. Their dependency on UV light has gradually being reduced as recent improvement of photoinitiators, have afforded several options in the choice of light not restricted to UV. As a result, extensive range of high-intensity light sources of differing visible wavelengths can be used as a choice for polymerization [313], [314].

3.2.2 3D Inkjet Printing

Inkjet 3D printing process is similar to regular inkjet paper printer but in this case light curable resins and wax instead of inks. In this combination,

the wax is expected to create spatially constrained volumes which are to be filled with the light curable resins. The sequence of layer building involves an array of nozzles that create droplets of heated low viscous wax that instantaneously form cavities which are subsequently spotted with resin before cured by light exposure.

Similar to STL this system can be used for an extensive range of microfluidic fabrications involving mold replications. Although their final product finish is not as detailed as STL; they are still relatively close in comparison. Furthermore, the print mixture of UV curable acrylic resins and waxes makes easy post cleaning process because the waxes serve as supporting materials that can be removed easily. The foremost downside of inkjet printing is that most parts produced from this technique cannot be used directly because due to low chemical or biological compatibility [121].

3.2.3 Binder jetting

The technology was originally developed at the Massachusetts Institute of Technology in 1993. The technological process of layering involves the use of glue applied through jet nozzles to bind together powder based particles spread in equal layers using a slider that guarantees a smooth and even surface. The building space is typically a platform onto which a thin layer of powder is spread cumulatively to form the shape of a programmed 3D object. After the consecutive accumulation of layers, the finished part is typically tempered to allow full curing of the glue. Subsequently, the non-bound powder particles are then cleaned off.

This system pales in comparison to STL or 3Dinkjet in product finish but what it lacks in finishing it makes up in cost and faster turnaround. Conversely, this technique does have a major drawback: the dominant chemical and physical properties of the part created is defined by the glue used. In addition, parts created by this process can't be transparent because of the solid particles combination. Likewise, inconsistent binding of particles can result in porosity which makes it highly unsuitable for direct microfluidic use because of potential leakages. Again, this method is mostly suitable for mould creation for microfluidic chip models of bigger aspect ratio because the difficulty of removing powder from long and narrow channels.

3.2.4 Material Extrusion

The Fused deposition modeling (FDM) technology is a commonly used material extrusion technique. The process involves a precise control of heated material through a plastic filament or coiled metal wire. Layers are built by two nozzles; one for the primary material and another for the support structure. The primary nozzle extrudes molten material forcefully out in both horizontal and vertical directions before hardening. The material mostly used are Acrylonitrile Butadiene Styrene (ABS) and Polylactic acid (PLA). Concurrently, secondary nozzle also typically ejects water soluble material for internal structures while low mechanical strength structures for external support. FDM has a unique advantage from other techniques, due to its ability to create multi-materials components without the need of specific polymer modifiers [316]. Thus, materials with different chemical or physical properties can be applied (including stiffness and color) subsequently. Acrylonitrile butadiene styrene (ABS) is a commonly used material in FDM while conventional polymers such as PC, PCL, PP or PS can be used as well in this process. The main weakness of FDM is the inconsistent definitions of the part geometrical structure as a result of the layer deposition characteristics that tend to mirror vivid shapes of the cylindrical wire used for layer formation 269. As a result, the final microchannel surfaces are rough, and sidewall shapes are skewed. This disadvantage disqualifies direct

microfluidic use because the skewed channels can cause flow obstruction, leakages and most especially surface binding issues. Still, FDM can be suitable for mold replication because of fast turnaround, low cost of fabrication and no post curing.

3.2.5 Powder Bed

This process is similar to binder jetting but in this case, a high-powered laser is used to fuse Small particles plastic, metal, ceramic or glass powders into a concise bulk of the anticipated 3D object. Unlike binder jetting, the chemical and biological compatibility of the created parts are defined only by the bulk material properties. The most commonly used technique for this process is Selective laser sintering (SLS) which builds up layers by using a laser beam to scan selectively across the surface of the powder bed. After each cross-section is scanned, the fused powder mass bed is lowered by one layer thickness before a new layer is applied on top and the routine is repeated until the object is completed. In SLS there is no requirement for support structure since all untouched powder remains becomes support for the sintered ones.

As of yet this technique suffers major limitations in either direct use or indirect (mould replication) use in microfluidic research because the created parts are porous thus leading to mechanical toughness and surface finishing impairment.

3.2.6 Lithography

Lithography is a hybrid of both material removing and deposition technology. It is essential to note that lithography can be defined regarding direct use only. In the broad spectrum of prototyping, techniques lithography leans towards material deposition, although it requires material removal techniques as a complementary process to achieve the anticipated functioning POCT chip. The rudimentary process behind is selective lithography imprinting, which involves creating patterns on specific areas while simultaneously protecting areas not preferred untouched. For instance, ink can be used to create patterns on a material while the areas that are expected to be untouched are covered with wax. Good examples of these techniques that can be utilized for microfluidics fabrication are optical and x-ray lithography.

3.2.7 Optical Lithography

Optical lithography makes use of UV light to transfer geometric patterns on top of sensitive materials that are known as photoresist on the surface of a substrate. Commonly used substrate and photoresist are silicon wafer and SU-8. The process starts with the deposition of silicon dioxide (SiO_2) which serves as a barrier layer on the surface of the wafer. Subsequently, a technique is known as spin coating[317], [318] is used to build the required height in micrometers by uniform layer on layer deposition on the wafer surface. Irradiation is then applied through a glass photomask that can cause the exposed resist to either be more soluble (positive resist) or less soluble (negative resist). For positive resists, the dissolution by solubility that occurs due to light exposure is washed away by the developer solvent to leave precise openings surrounded by walls of resist untouched. The exact opposite is the case for negative resists as exposure to light induces polymerization that causes the resist to be insoluble to the developer solution. Whereas the unexposed area are then removed by the developer solution.

The main advantage of this technique above others is the closure of micro-channels which is inclusive in the fabrication method without any additional bonding process. Micro-channel development depends on several key factors which include resisting material, spin rotational speed, the power of exposure and tilting angle of the substrate. On the other hand channel, the closure can be achieved

after the initial light exposure and developer treatment is carried out, a second SU-8 layer is spun on top and processed similarly. As well, the use of SU-8 can also allow on-chip integration to other SU-8 created functional components, like micropumps, microvalves, and complex microfluidic networks [412]. The recent improvement in technology has afforded cheaper, and faster alternative using dry film resist (DFR) [319], [320]. DFR offers numerous advantages over liquid resist (SU8) such as good adaptability, exceptional adhesion to any substrate, decent flatness, no requirement of liquid handling, even resist distribution, low energy exposure, low cost and short processing time. However, the main challenge of this method is the setting up cost which is relatively very high in comparison to other techniques even though DFR have cheaper to setup than SU-8. Furthermore, SU-8 are predisposed to large internal stress and once developed; they are very difficult to be removed from structures. Likewise, both liquid and a DFR require a uniform flat substrate to create precise structures; they also are not effective in create non-flat surface structures, and require an extremely clean room environment for its protocols.

3.2.8 X-ray Lithography

Lately, X-ray lithography has been adapted [321]–[323] for fabricating polymer microchannels using PMMA as substrate. PMMA is a suitable material for this process because of its high sensitivity to X-ray absorption (mild X-rays of 0.7-0.8mm) and degradation. This technique is similar to the positive resist technique of optical lithography. But in this case, the photomask that bears the geometrical patterns is made of gold. Gold is a typical X-ray absorber because of its high atomic number, and the mask thickness depends on of the intensity of the exposure. For example, the gold mask must be approximately 5 to 10 micrometers thick to absorb x-rays with energy in the range of 5 keV to provide corresponding depth into PMMA of several hundred micrometers [324]. As the thick gold layer absorbs X-rays, the sections that are transparent to the X-rays are degraded. On the other hand, the photoresist which is PMMA can be spun as one single layer, multiple layers or joined as a pre-cast commercial sheet. The sheet is joined to the substrate by the liquid monomer, MMA. After the exposure, the degradation of PMMA into soluble oligomer [325] before they are dissolved in a developing solvent comes as a result of X-ray induced scission reactions.

This technique yield better high aspect ratio structures than photolithography because X-ray operates at a much shorter wavelength than UV light, even Deep UV (DUV)[326] light and also provide increased lateral resolution. However their setup cost goes into millions of dollars, and operating cost can run into hundreds of dollars per hour just to recuperate the actual operating expenses. Nevertheless, subsequent duplicates PMMA molds can be made from the master synchrotron made mold reduce cost by injection molding or hot embossing. This method is mostly suited from replication, not direct use.

3.3 Material Removing Technology

Unlike material depositing techniques, material removing techniques creates structures by locally removing material from designated parts of a bulk. In microfluidics techniques such as laser ablation, micromilling or etching are commonly used. These methods typically creates negative spaces that form the microchannels and fluidic elements in substrates. However they are generally not suitable when cost of the substrate is a major concern.

3.3.1 Etching

This technology is one of the earliest fabrication method used in microelectronics or MEMS involving silicon and glass. Likewise, they have mostly being used as a complementary process in techniques as optical lithography and

micromachining. Due to current trend glass, microfluidics components seems to be the preferred choice in the POCT field due to its physical characteristics of transparency. Etching techniques are categorized either as dry or wet etching. When the material is removed from it can do by either process it can either be isotropically (uniformly in all directions) or anisotropic etching (constant surface area and uniformity in depth). The major difference between the two processes is the material removal rate which is faster in wet-etching and can be subjected to varying temperature or the concentration of the wetting agent. Though, both require mask similar to optical lithography so only unmasked areas will be touched. In dry etching, the removal process is done by physical, chemical or both means. Physical dry etching utilizes plasma that generates bombarding ions, electrons or photons with high kinetic energy to knock out the atoms from the substrate surface, which in turns results in material disintegration by evaporation. While, the case of chemical dry etching don't require actual liquid etchants but instead gas etchant such as tetrafluoromethane (CH4), sulfur hexafluoride (SF6), nitrogen trifluoride (NF3), chlorine gas (Cl2), or fluorine (F2) [327] to cause surface ablation. A commonly known combination (physical and chemical) is called reactive ion etching. This process is the most extensively used dry etching technic because it's faster and able to achieved better resolution than both the physical and chemical results. The method of operation involves dissociation of enchanting molecules to more reactive species by high energy collision from plasma ionization reaction.

On the other hand, wet etching involves exposing the substrates to corrosive solvents in liquid form. As the liquid etchant diffuses across the exposed surfaces, a reduction-oxidation reaction occurs between the liquid-solid interfaces causing degradation. Furthermore, the rate degradation determines is determined by the concentration of the etchant. Isotropic wet etching uses a combination of hydrofluoric acid, nitric acid, and acetic acid (HNA) as etchant solvent for silicon. While, potassium hydroxide (KOH), ethylenediamine pyrocatechol (EDP), or tetramethylammonium hydroxide (TMAH) are some of the anisotropic wet etching agents for silicon [328]. The major advantages dry etching is anisotropic etch profile is easily attainable, enchant consumption is relatively small. Whereas, wet etching requires simple equipment and possess high substrate selectivity. For the disadvantages, dry etching requires complex equipment and protocols, while their substrate material selectivity is very low. The major setbacks of wet etching are relatively high cost of etchant and inconsistent precision (prone to undercutting) of small geometries [329], [330]. Overall, it is possible to use this technique for replication mould or direct use in microfluidic chips fabrication.

3.3.2 Laser ablation

This micromachining process involves using a powerful laser to shape or create geometric structures on a substrate. Just as lithography and etching techniques discussed ablation may be achieved by exposure through a mask. The defining difference between the substrate and mask is the significant absorption at the laser wavelength. For the mask, they are expected to have very low absorption, e.g. most metals. A good example of a commonly used substrate is PMMA due to its significant absorption of the emission wavelength of the laser (i.e. 427 °C for PMMA) [331]. Alternatively, direct-write maskless systems can still be used to create channels and other microfluidic structures. In this process, the laser is held at a constant position while the platform that bears the substrate is moveable. This technique has a better turnaround because the design of the

microchannel network can be changed quickly during the prototyping process instead of time spent designing new masks. While the drawback of this method is the inability to mass produce parts since they are made in a sequential manner.

In general, the shape develops by laser ablation are usually square or rectangular with straight edges. Moreover, laser-ablated channels have far worse surface roughness than most material removing techniques. The degree of roughness is highly reliant on the absorption of the polymer at the excimer wavelength. While, the depth of laser-ablated channels is dependent on many parameters including polymer absorption, laser power, pulse rate, and some passes made across the channel. There are varieties of commercially available plastics such as polycarbonate, polystyrene, cellulose acetate, and poly(ethylene terephthalate) [306], [332], [333] that can be used to fabricated microchannels using ArF excimer laser (193 nm)[334].

3.3.3 Micromilling

micromilling process involves micro-cutting that is characterized by the mechanical interaction of a fast spinning piercing tool that causes splintering within specifically defined paths on the substrate. The residue of this process is usually in the form of chips [335] that can be easily blown or washed off. This method is mostly suited to mold replication in microfluidics, and the type of material general used as substrate are metals (e.g. aluminum). Although polymers can also be subjected to this process, they are highly selective due to their comparable mechanical strength to metals. PMMA is a good example of commonly used polymers because of its good mechanical strength, thermal resistance, and dimensional stability. Furthermore, PMMA optical transparency also provides a major advantage. The capability of producing high-quality microchannels and other geometric structures are determined by the material, diameter and sharpness of the cutting tools. The main cutting tools in this miniaturization process are cemented carbide and diamond. Both tools achievable minimum width of the microchannels is proportional to the diameter of the tool. There are commercially available carbide tools down to the size of 5µm while diamond is within the Range of 100µm. However, tools below 100µm are prone to unpredictable failures. In the case of tool sharpness, diamond mills are within the range of 50nm and are capable of surface roughness Ra 10nm with no burrs (channel edge roughness). Whereas, carbide mills have a sharpness around 1µm to 10µm [413], that can create surface roughness of about 0.1µm to 0.3µm Ra [336]with considerable burrs.

The major shortcoming of micromilling is the difficulty in defining small geometric structures consistently due to excessive tool failure. Furthermore, they do have expensive setup cost but are relatively cheaper in comparison to lithography. On the bright side, Micromilling is a capable and cost-effective technique to fabricate PMMA microfluidics for research purposes.

3.3.4 Micro Electrical Discharge Machining

Micro Electrical Discharge Machining (EDM) is quite similar with the principals of macro Electrical Discharge Machining the only difference is the plasma channel diameter. Micro-scale EDM is a thermal process that utilizes electrical discharges to erode electrically conductive materials. Since the materials only applicable are metals, this easily categorizes this method as means for mold making. This process involves two electrodes that are separated by a dielectric medium, then brought together to a specific threshold were the dielectric medium breaks down and becomes conductive. As a result, sparks will be generated between the electrodes that creates a successive surge of thermal energy. When this thermal energy is

released, it causes the material surface to melt and evaporate rapidly, creating voids. The precise control of the energy magnitude regarding voltage and current can help create micro features on any electrically conductive material. Since µEDM is a no-contact and no-force process in comparison to micromilling they can easily be used to cut micro features of complex shapes and thin walled microchannels without distortion. Moreover, the µEDM process leaves no burrs. The major drawbacks are the use of only conductive materials, i.e., (insulators) are out of the process. Moreover, setup cost is more expensive than conventional micromilling.

4. Prototype Replication technology

This technological process is employed for the sole purpose of replicating parts and components that are integral to the entire POCT chip formation at a mass production level. Commercial viability is also key to this process, as a low cost at high quality improves marketability. Consequently, this is targeted towards end users, but some of its methods can also be utilized in research prototyping. A typical process involves selection of precision fabrication technique to create a master mould that bears the intended design to be replicated through a specific process to several parts.

4.1 Injection Moulding

In this replication method, wet or dry etching techniques are employed to create structures with higher aspect ratios [337] and precise geometrical features on a silicon substrate. Subsequently, nickel electroformed [337] is the process used to produce the metal master mold by electroplating a layer of metal, with a thickness within the range of few micrometers to a few millimeters. Metal masters are a lot stronger and longer lasting than masters made of silicon, glass or polymers. They can be utilized to yield hundreds of thousands of injection molded parts with features microfluidic elements. The replication process involves the nickel electroformed being mounted onto a mold insert and the polymer of choice is melted to a viscous liquid when pushed by a mechanical screw through a heated chamber. Afterward, the liquid polymer is injected at high pressure into the mounted mold (with nickel electroforming), and as contact is made with the mold walls, the heated polymers start to cool down, resulting in well-defined solid features [338]. Injection molding technique is very versatile and almost any plastic part, or component can be made efficiently. PMMA [339] and PC [340] are good examples of polymers used in this replication process. The major advantage of this technique is accuracy; it can be used to produce channel sizes ranging from10µm to few hundred micrometers. Their major Limitation is that they are not cost effective for research prototyping since few copies are required with a frequent change of designs.

4.2 Hot Embossing

This method shares a similar process to injection molding in the case of metal master mold preparation. However, this technique involves the use of a hydraulic press to imprint the master mould forcefully on a polymer material after it has been softening to a temperature close to the T_g. The stamp with the mold design is applied at low pressure for a period less than 10 minutes on the plastic. As a result plastic, microchannel features are the exact mirror of the metal stamp. Alternatively, this same process can still be done in plastic at room temperature, but high pressures. Though the turnaround time is a lot shorter, the product finishing is much more dependent on numerous constraints including imprinting pressure, imprinting time and properties of the plastic itself [340]. Moreover, the lifespan of room temperature imprinting is a lot shorter than at elevated temperature.

Hot embossing or room temperature imprinting can be successive done on several types of plastic with excellent device-to-device reproducibility. Good examples of plastics include polystyrene (PS)[341], polyethylene tetra phthalate glycol (PETG)[342], polymethylmethacrylate (PMMA) [343], polyvinylchloride (PVC), and polycarbonate [344]. Just like injection molding their downside is the setup cost and lack of flexibility in design altering needed for prototyping research.

4.3 Soft lithography

Soft lithography is a widely used rapid and efficient way to create microfluidic prototypes. This method is a very cost effective and is used extensively for research for research purposes. As with all other techniques described thus far, a positive relief master may be needed, but not necessary in silicon. As for this technique, since its research inclined the turnaround time is highly dependent on the fabrication method of making the master mold. As of recent 3D printing techniques have been useful in fulfilling this requirement because of the flexibility involved in design changes endemic in rapid prototyping. In the case of material utilized, an elastomeric polymer that is liquid at room temperature is required to be cast onto the master mold and allowed to cure at a high temperature. Subsequently, the cured material with the micropatterns is bonded to another substrate more likely glass, before they are functional. A commonly used material for this process is PDMS because of its favorable mechanical and optical properties. PDMS is a mixture ratio of a prepolymer and curing agent. A standard mix ratio is 10:1 (i.e. 10g of prepolymer to 1g of curing agent) [246]. As a result, the mechanical properties of PDMS can be narrowly altered by either increasing the prepolymer to reduce elastic modulus or increasing curing agent to increase elastic modulus. The curing process of PDMS can occur slowly at room temperature or speedily at a slightly elevated temperature (generally 40–70 °C for PDMS) before they are peeled off the mold. Polyurethane elastomer is a very good alternative to PDMS as it has better comparative mechanical strength [345] with optical transparency. However, the protocols involved in casting are very stringent and do have potential health [346] concerns.

The major drawback in soft lithography is the design limitation since most moulds are created as either positive or negative the outcome of the cast is a 2.5 Dimensional (2.5-D) object that requires another layer substrate (glass or similar material) to complete it. Although, the fabrication of 3-D is not somewhat impossible but will require several designs of molds, that are individually representative of different layers in a multi-layer three-dimensional structure [347]

5. Conclusion

In this paper, material properties such as mechanical resilience, transparency and high-temperature tolerance and biocompatibility form the major characteristics needed in POCT substrates. Amongst the various material discussed polymers as substrate have shown better significance due to their wide range of material characteristics suitable for microfluidic applications. Good examples are the combination of both good optical and thermal characteristics needed in primary chip functions such as DNA amplification and detection. PDMS, PMMA, PC and COC tend to be most widely used polymers due to their low cost, ease of fabrication and market availability. However, other materials that pale in comparison to polymers such as metals, silicon, etc. which don't account for the bulk parts of the POCT chip, do contribute to other microfluidic elements creation or enhancement. For instance, silicon can be used for electromechanical components such as electrostatic diaphragms for valves or pumps. While gold can be used as alternate means of optical high-sensitivity

detection by in microfluidic channels by Resonant light scattering spectroscopy.

On the other hand, fabrication techniques mainly revolve around setup cost, production cost, surface roughness, the simplicity of operation and aspect ratio definition. Of all the above attributes mentioned, none of the fabrication technique discussed offers a total solution. Moreover, it can be deduced that as the surface finish and aspect ratio improves there is a significant correspondence in the product and setup cost. Besides, prevalent technology makes some of these techniques not yet appropriate for POCT device creation because of the unsatisfactory surface finishing or the limited choice of materials that can be processed with their respective protocols. Nonetheless, 3D print offers a reasonable solution in academic or research environment as a result of the recent improvement and economic availability of printers in the marketplace. While for the commercial aspect, hot embossing, and injection moulding are the still the best available option as of yet.

APPENDIX B

Sensors & Transducers

http://www.sensorsportal.com are

Testing

[1] Luck EREKU, [1] Ruth MACKAY, [1] Wamadeva BALACHANDRAN, [2] Kolawole AJAYI

[1] School of Engineering and Design, Brunel University, Kingston Lane, Uxbridge, UK

[2] University of Lagos, Akoka, Lagos, Nigeria

[1] Tel.: +441895267378, fax: +441895258728

[1] E-mail:luck.ereku@brunel.ac.uk

Abstract: The recent advent of the miniaturization technology witnessed over the last decades has led to development and creation of several conventional microfluidic techniques. A microfluidic platform can be broken down into a set of fluidic unit operations which are miniaturised versions of orthodox large scale (bio-chemical) laboratory operations. These miniaturised operations are designed for easy integration and automation within a well-defined fabrication technology; which permits simple, easy, fast, and cost-efficient implementation of different application-specific bio-chemical processes for point care diagnostics. Processes that can be automated at this scale include nucleic acid extraction, amplification and detection. The improvement in technology within the previous decades has led to significant developments of techniques used in implementing several microfluidic processes. The auspicious developments that have greatly impacted areas in medical research, therapeutics and POCT applications are brought into focus by this research on a continuous flow configuration. Through these visualization platforms such as pressure driven flow, magneto-hydrodynamics dielectrophoresis, large-scale integration are analysed under continuous flow characteristics. Finally, this review also provides adequate examples whilst investigating the strengths and limitations of every technique. *Copyright © 2014 IFSA Publishing, S. L.*

Keywords: Continuous Flow, Pressure Driven, Microfluidics, Point of Care Testing, Lab-on- a- Chip.

1. Microfluidics Technology

In the latter period of the 20th Century, the interest in the innovative use of microfluidic technology for expedient clinical application especially in the case of “point-of-care” diagnosis of diseases grew propitiously [1], [2]. This growing trend brought about the inception of the device known as “lab-on-a-chip” i.e. the miniaturisation of laboratory processes within a microfluidic device. This technology is a multidisciplinary field intersecting engineering, physics, chemistry, micro-technology and biotechnology, with practical applications to the design of systems in which small volumes of fluids are required. The systems developed by microfluidic technology can be used to automate biological experiments by manipulating geometrically constrained small quantities of fluid, typically within the sub-millimetre scale. This conventional technology depends on the behaviour of continuous liquid flow through micro fabricated channels. However, actuation of flow is implemented with external assistance of micro-pumps and micro-valves which are complex and cumbersome. The physical properties of fluids at the micro-scale differ from the generic behaviour of macro-scale quantity in factors such as surface tension, energy dissipation and fluidic resistance. Microfluidics analyse how these properties can change, and how they can be exploited for specific design requirements.

The microfluidic lab-on-chip device is a subset of micro-electromechanical systems (MEMS) for biological application which is collectively known as (BioMEMS). MEMS technology involves integration of electrical and mechanical components which is inclusive of micro sensors, micro pumps and micro actuators in the same platform using standard fabrication techniques of the semiconductor industry with similar equipment and materials [4]. The advent of this technological breakthrough has led to the development of micro-total-analysis-systems (μ-TAS) which is similar to lab-on-a-chip platforms (LOC). LOC technology involves the scaling of single or multiple lab processes down to chip-format, whereas "μTAS" is dedicated to the integration of the total sequence of lab processes to perform chemical analysis and can also be used in diverse application for other analysis including chromatography (Vilker et al., 2002). Rapid development of miniaturised laboratory diagnostic devices could provide a great impact on modern society’s health by allowing rapid and low cost diagnosis of diseases. In recent years there has been tremendous interest in harnessing the full potential of this approach and, consequently the development of countless microfluidic devices and fabrication methods. Materials such as poly-dimethyl siloxane (PDMS) and Poly-methyl methacrylate (PMMA) have emerged recently as excellent alternatives to the silicon and glass used in early devices fabricated by MEMS processes [414]–[416]. Increase in popularity of their use in the manufacturing of microfluidic devices stems from low cost, excellent optical transparency, attractive mechanical/chemical properties and simple fabrication procedures.

The revolutionary idea of fitting an entire laboratory on a chip was motivated by the electronic industry fitting an entire computer on a microelectronic circuit chip. In a typical diagnostic scenario, the sample is collected from the site and sent to centralised laboratories for analysis, which is a cost intensive and time consuming process. Miniaturised laboratory analysis techniques offer many advantages over standard bench-top procedures: small volume requirement which means only small quantities of reagents are needed reducing costs and waste, contamination is reduced by removing pipetting stages and lab on a chip is conducive to automation, analysis times are also effectively shortened since efficiencies are usually

higher when working on a smaller scale with operational simplicity. Benefits include fast analysis time, portability, cost reduction, disposability, reduced consumption of reagents and efficiency, all of which are revolutionizing clinical diagnostics and many biochemical laboratory procedures by these means making the lab-on-a-chip technology ideal for near-patient and point-of-care testing. Simplified device fabrication and the possibility of incorporating densely integrated microvalves into designs [416] have helped microfluidics to explode as ubiquitous technology that has found applications in many diverse fields, however complete 'sample-in to answer-out' solutions have delayed LOC devices reaching the market. Whilst amplification [417] and detection methods have been well developed for individual systems with low limits of detection; sample preparation has had little development and is impeding development of true POC devices which are simple, rapid, sensitive, specific and affordable [9], [165], [417]

2. Point Of Care Diagonistics (Poct)

POCT is peripheral laboratory testing or Near Patient Testing (NPT) that involves any analytical test performed for or by a patient outside the conventional medical laboratory setting [418], [419]. The principal concept behind POCT is to provide quick identification of diseases at the time the test is carried out [165]. This innovation improves the likelihood that the patient, physician, and care team will receive the results faster thus making room for instantaneous clinical management decisions to be made. Examples of POCT include blood glucose testing, blood gas and electrolytes analysis, infectious disease testing, urine strip testing and pregnancy testing. Commercialisation of this medical diagnostic innovation involves the combination of the POCT concept with microfluidic technology. This combination has led to production of handheld and portable diagnostic kits that come either in multiple parts or a compact integrated piece (all in one kit). Figure2.10 provides an illustration of the multiple parts diagnostic kit that includes the sample collection platform (LOAC) and an electronic identification component. On the other hand the integrated diagnostic kit has both the sample and detection platforms in a compact piece, leading to possible trade-offs in reusability over compatibility. The use of one device to test multiple predisposed disease symptoms has led to POCT industries investigating reusable devices. This approach encourages sound economic advantages in cost reduction and material wastage. Top amongst various design initiatives are the disposable LOC platforms that can provide these POCT production companies a convenient means to achieve this economic and versatility advantages. Furthermore the user friendliness approach of diagnostic testing kits operation adds another dimension to the overall system, such that a semi-skilled operator or patient self-test can be carried out conveniently to achieve reliable results. With these qualities public acceptance and adoption becomes easier which improves marketability. Besides the diverse fields of applications that are associated with a number of POCT devices, there some important requirements of the different market segments that include [131]:

- Portability: miniaturized, hand-held device with low energy consumption
- Output: number of samples/assays per day
- Cost of instrument: investment costs of the instrument (reading device)
- Cost of disposables: defining the costs per assay (together with reagent consumption)

- Number of parameters per sample: number of different parameters to be analysed per sample
- Low reagent consumption: amount of sample and/or reagents required per assay
- Diversity of unit operations: the variety/comprehensiveness of laboratory operations that can be adopted.
- Precision: the volume and time resolution that is applicable.
- Programmability: the flexibility to adapt liquid manipulating protocols without fabricating a new chip.

Figure2.1. Pictures of a disposable chip and automation control device.

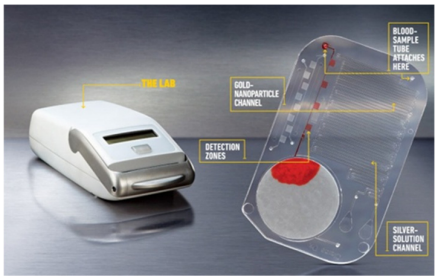

Figure2.2. Picture of lab-on-a-chip with external automation [115]

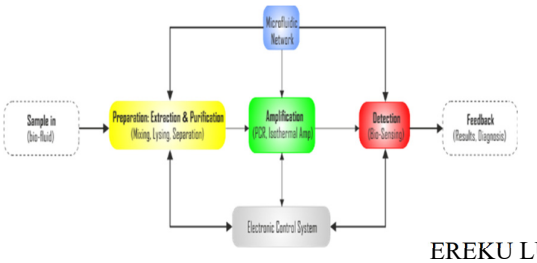

Figure2.3. illustrates a block diagram of a LOAC diagnostic chip. A POCT diagnostic device has three fundamental **Figure2.3.** illustrates a block diagram of a LOAC diagnostic chip. A POCT diagnostic device has three fundamental functionalities: sample preparation, amplification (only for DNA) and sample analysis or detection. However, an additional step might be needed for pre-processing of the sample to increase the concentration of the target molecules such as filtering and pre-mixing (i.e. urine sample).

Microhydrodynamics

Since most microfluidic systems operate at low Reynolds numbers the physical properties of fluids at the micro-scale can differ from the generic behaviour of macro-scale quantities in factors such as surface tension, energy dissipation and fluidic resistance. The field of micro-hydrodynamics analyses how these properties can change, and how they can be worked around, or exploited for specific design requirements. In microfluidic systems, liquid movement can be categorised under two means of fluid transportation; which are continuous flow and discrete flow.

Continuous flow is defined by incessant and seamless flow of fluid/fluids (miscible or immiscible) which are composed of molecules that collide with one another within a confined boundary (microfabricated channels). Moreover, these molecules are assumed to obey the continuum assumption [51], which considers fluid being made up of molecules in a continuous phase rather than in a discrete phase. As a result, physical properties such as pressure, density, temperature, and velocity of infinitesimally small fluid particles are assumed to vary continuously with reference to one another [52]. Most pressure driven flow POCT

devices operate under these means of fluid transportation. Some examples of pressure driven flow which makes use of micropumps, plungers or mechanical blisters utilize this means of fluid transportation. Furthermore non-mechanical techniques such as sound waves or a combination of capillary forces with electrokinetic mechanisms (e.g. electro-osmotic flow) [53], [54] also utilize this means.

On the other hand, discrete microfluidics commonly known as droplet microfluidics, utilizes minute or discrete volume of fluid in the form of droplets contained within an immiscible continuous phase as means of transportation (Zengerle & Ducrée, 2004; Liu, Deng, Qin, et al., 2011). The small volumes of fluid are isolated from each other in continuous motion offer the opportunity of novel solutions to today's biomedical engineering challenges for innovative POCT protocols and therapeutics. For instance, droplets allow significant reduction in sample volumes to be analysed, leading to corresponding reduction in cost. Furthermore, compartmentalization in droplets improves assay sensitivity by increasing the effective concentration of rare species and reducing the time needed to reach the detection threshold [57], [58]. In addition, the platform dimensional scaling advantage encourages controlled and rapid mixing of fluids in the droplet reactors, resulting in significantly reduced reaction time, accurate generation and repeatability of droplet operations. Droplet microfluidics incorporates two distinct methods which are digital microfluidics and segmented flow microfluidics [59], [60].

One of the significant properties shared by both types of fluid flow is viscosity (μ); which can be described as the ratio of shear stress to velocity gradient. Viscosity describes the resistance of a fluid to any deformation caused by either external body immersed in fluid or between different layers inside the fluid [61]. In addition, the higher surface to volume ratio, higher mass-heat transfer ratio and low Reynolds number are other characteristic properties of fluids in micro-systems.

Another major characteristic endemic at the micro-scale is the flow disposition which is practically defined as laminar flow. Laminar flow or steady flow occurs when fluids move in parallel layers, exhibiting no disorder between their repetitive layers [62], [63]. In fluid dynamics, the velocity of flow varies from zero at the walls to a maximum along the centreline with the flow regime characterized by high momentum diffusion and low momentum convection since there are no cross currents perpendicular to the direction of flow, nor eddies [64], [65]. At low velocities the particles of these fluids are very organized, enabling them to move in straight lines parallel to the pipe walls which in turn inhibit lateral mixing as a result of the adjacent layers sliding past each other effortlessly. When taking into consideration scientific and empirical observations of fluid flows in microchannels of a microfluidic device, Reynolds number of much less than 1 is observed [63], [64], [66]. This type of flow is also known as creeping motion or Stokes flow and it is an extreme case of laminar flow where viscous (friction) effects are much greater than inertial forces [67]–[69]. This relationship is defined as Reynolds number as a dimensionless parameter and is given by the ratio of inertial force (ρV^2L^2) to viscous force (μVL) as follows.

$$\boldsymbol{Re} = \frac{\boldsymbol{inertial\ force}}{\boldsymbol{viscous\ force}} = \frac{\boldsymbol{\rho V^2 L^2}}{\boldsymbol{\mu VL}} = \frac{\boldsymbol{VL}}{\boldsymbol{v}} \qquad (3.\ 10)$$

$$\boldsymbol{v} = \frac{\boldsymbol{\mu}}{\boldsymbol{p}} \left(\frac{\boldsymbol{m^2}}{\boldsymbol{s}} \right)$$

Where, **V** is the characteristic velocity of fluid, **L** is characteristic length of the geometry, $\boldsymbol{\rho}$ is the

fluid density, **μ** is the dynamic fluid viscosity and ***v*** is the kinematic viscosity of the fluid.

In microfluidics, it is usually assumed no gravity, incompressibility and dominant viscous forces. The flow of a fluid through a microfluidic channel can be characterized by the Reynolds number, similar to equation 3.10:

$$\boldsymbol{Re} = \frac{\boldsymbol{LV_{avg}\rho}}{\boldsymbol{\mu}} \qquad (3.\ 11)$$

Where, $\boldsymbol{V_{avg}}$ is the average velocity of the flow, $\boldsymbol{L}$ is the most relevant length scale, $\boldsymbol{\rho}$ is the fluid density and μ is the dynamic fluid viscosity.

Fluid flow through a control volume can be described by the complete Navier-Stokes (N-S) equations. These equations can be derived from the principles of conservation of mass, momentum and energy. Navier-stokes equations are a non-linear set of differential equations which explain the motion of fluid in general. This equation is defined by applying Newton's second law to fluid motion by assumption of continuum fluid and small fluid velocity compared to the speed of light. The general form of these equations has no solution and is used in computational fluid dynamics. Also the equations do not dictate position but rather velocity. A solution of the Navier–Stokes (N-S) equations is called a velocity field or flow field, which is a description of the velocity of the fluid at a given point in space and time. Once the velocity field is solved for, other quantities of interest (such as flow rate or drag force) may be found. The complete equation is shown below [70]:

$$\rho\left[\frac{\partial y}{\partial t} + v \cdot \nabla v\right] = -\nabla p + \nabla\mathbb{T} + f \qquad (3.12)$$

Where v is the flow velocity, ρ is the fluid density, p is the pressure, is the (deviatoric) stress tensor, and f represents body forces (per unit volume) acting on the fluid and ∇ is the Del operator.

The general form of N-S equations can be simplified by assumption of incompressible flow which is common in microfluidics [71]. This assumption simplifies the form of N-S equations and can be written as the following:

$$\rho\left[\frac{\partial v}{\partial t} + v \cdot \nabla v\right] = f_{pressure} + f_{friction} + f_{volume} \qquad (3.\ 13)$$

Where, $\boldsymbol{\partial v/\partial t}$ is the unsteady acceleration, $\boldsymbol{v\cdot\nabla v}$ is the convective acceleration, $\boldsymbol{\rho}$ is the density, $\boldsymbol{f_{pressure}}$ ($-\nabla p$) is the pressure gradient, $\boldsymbol{f_{friction}}$ ($\mu\nabla^2 v$) is the viscosity of fluid, $\boldsymbol{f_{volume}}$ ($-\rho g$) is the body force of fluid.

In microfluidics, the fluid flow is mostly described by Poisson equation. This equation can be derived from N-S equations by applying boundary conditions in micro-channels. When a fluid is bounded by solid walls, the fluid velocity is assumed zero at liquid-solid interface. This is because of molecular interactions between two phases which forces the fluid molecules to seek the momentum and energy equilibrium of solid surface. This phenomenon is called no-slip condition and will be used as boundary condition at interface between fluid and solid surfaces. Therefore the simplification of N-S applies the following conditions for two dimensional flows [71], [72]:

- No slip at the wall
- Infinitesimal gravity, $\boldsymbol{\rho g} = 0$
- Convection effect is negligible, $\boldsymbol{v\cdot\nabla} = 0$
- Laminar flow (steady flow), $\boldsymbol{\partial v/\partial t = 0}$

Therefore Poisson equation for a pressure driven flow is given as:

$-f_{pressure}$ ($-\nabla p$) is the pressure gradient = $f_{friction}$ ($\mu\nabla^2 v$) is the viscosity of fluid:

$$\nabla p = \mu\nabla^2 v \tag{3.14}$$

The two dimensional Cartesian co-ordinates of equation 2.42 are expressed as (White, 1991);

$$\frac{dp}{dx} = \mu\frac{\partial^2 u}{\partial y^2} \tag{3.15}$$

3.1. Viscosity effect

In general, viscosity is the quantity that describes a fluid's resistance to flow. Fluids resist the relative motion of immersed objects through or besides them as well as the motion of layers with differing velocities within them in any flow [73]–[75]. These layers move at different velocities and the fluid's viscosity arises from the shear stress between the layers that ultimately oppose any applied force. Viscosity is important because it acts as an opposing force in mixing of two liquids [74]. Viscosity of a fluid might change by changing the temperature or pressure but if the viscosity of a fluid is constant at all shear rates at constant temperature and pressure; the fluid is known as Newtonian. The relationship between the shear stress and viscosity and velocity in Newtonian fluid can be described as follows [76]:

$$\tau = \mu\frac{\partial u}{\partial y} \tag{3.16}$$

In which, τ is the shear stress, μ is the fluid dynamic viscosity coefficient (***du/dy***) is velocity gradient.

Basically, the viscosities of most liquids (Newtonian) decrease with increasing temperature, and vice versa [76]. As the temperature increases, the average velocity of the molecules in a liquid increases and the amount of time they expend "in contact" with their nearest neighbours decreases. Thus, as temperature increases, the average intermolecular forces decrease [74], [77]. Another factor is pressure, viscosity is normally independent of pressure, but liquids under extreme pressure often experience an increase in viscosity. Since liquids are normally incompressible, an increase in pressure doesn't actually result in bringing the molecules significantly closer together i.e. increase in pressure doesn't register a significant change in viscosity of an incompressible fluid [61], [71].

In the case of non-Newtonian fluids the viscosity is a function of mechanical variables such as shear stress or time. These fluids are also directly affected by temperature and are classified as shear-thinning and shear-thickening [76]. Materials that thicken when worked on or agitated are called shear-thickening fluids. While materials that experience decrease in viscosity under shear stress are described as shear-thinning fluids. Blood falls under this category and is also known as a Bingham plastic [76] because it requires a threshold shear stress for it to make a transition from a high viscosity to a low viscosity fluid. The blood fluid must reach a shear rate of about 100 (1/sec) to be assumed Newtonian and after this shear rate is reached the viscosity is about five times as great as the viscosity of water [78]. Urine at room temperature can be categorised as a Newtonian fluid due to the fact that it contains about 95% of water [78].

3.2. Surface Tension Effect and Capillarity Phenomenon

The cohesive forces between the liquid molecules are responsible for this phenomenon of surface tension which allows the surface of a liquid to resist an external force as a result of imbalance molecular

attractive forces at the interface [70], [79]. In a bulk solution, each molecule is pulled equally in every direction by neighbouring liquid molecules, resulting in a net force of zero. The molecules at the surface do not have other molecules on all sides of them and therefore are pulled inwards. This creates some internal pressure and forces liquid surfaces to contract to the minimal area [80].

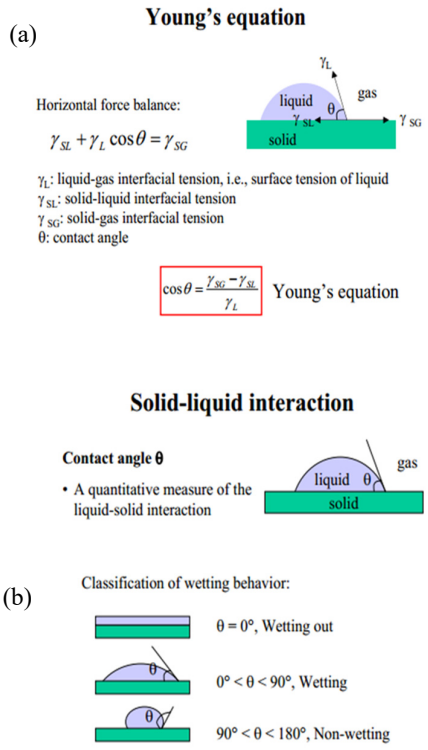

Figure3.1. Young equation depiction of solid-liquid interaction in ambience air, this schematic shows the surface tension forces at the contact line. (a) Liquid drops placed on a flat surface try to adopt spherical cap shape in other to minimize the surface energy. (b) describes the surface wettability in relationship to liquid-surface angle [79].

The surface tension depicted in Figure3.1 is the excess energy per unit area of the fluid surface when it is in contact with another material) or phase (solid or fluid) [81]. This largely determines the spherical shape of the fluid droplet placed on a solid surface. Young's equation shows a liquid droplet in contact with a solid surface and ambient air (Figure3.1a), the equilibrium forces due to the surface tensions at the liquid-gas (γ), solid-liquid (γ_{SL}) and solid-gas (γ_{SG}) interface dictate the contact angle, $\theta_Y = (\gamma_{SG} - \gamma_{SL})/\gamma$ of the liquid on the solid [79]. On the other hand Figure3.1b describes the wettability of the internal surface which is a major criterion in micro-hydrodynamics for controlling in flow. This is solely based on the contact angle of water on the solid surface, the surface can either be classified as hydrophilic (water loving, $\theta_Y < 90^o$) or hydrophobic (water hating, $\theta_Y > 90^o$) [82]. One of the major side effects of high surface tension in fluid flowing through a conduit is that is friction resistance between the solid-fluid interfaces. Due to this surface tension, a stream of fluid splits to form several small droplets in order to minimize the total surface energy [79]. This is known as "Rayleigh-Plateau instability" as a result of the surface tension going to zero. In general, increasing the temperature of a liquid will decrease its surface tension. Likewise Surfactants can also be used to lower the surface tension of a liquid [75], [83]. Besides, this procedure can also be applied to interfacial tension between two liquids or that between a liquid and a gas.

In micro-scaling, surface tension at the interface between the liquid surface and the micro-channel surface is significant to the design because with dimensions in the order of microns, the lengths liquids will travel easily using the capillary force [82]. At a microscopic scale, with gravitational effects minimal, the surface-to-volume ratio increases due to the exceedingly small volumes employed. This characteristic improves the surface tension effect which shares a direct relationship with capillarity [81], [82].

The phenomenon known as capillary action, or capillarity, is the ability of a liquid to flow against gravity, inertia or basically flow spontaneously without the aid of an external force through a

narrow space such as a thin tube, microchannels, porous materials such as paper or non-porous materials such as liquefied carbon fibre [76], [82] and it occurs because of inter-molecular attractive forces between the liquid and solid surrounding surfaces. Subsequently at microscale the gravity effect is infinitesimal, so the diameter of the tube or cross section of a channel has to suffice for the process to be sustainable. So since the energy stored in surface tension is equivalent to the multiplication of the surface tension and surface area; therefore reduction in conduit surface area of any microfluidic system will naturally minimize surface energy which significantly eases fluid flow [81].

Putting this phenomenon in perspective with regards to microfluidics that deal with very narrow channels with liquids under infinitesimal gravitation and high viscous forces with amplified fluid-solid surface tension; capillarity consequently behaves as a medium through which fluid flow can be alleviated. Similarly fluid flow velocity can also be controlled by altering the capillary surface energy. Capillarity therefore plays a major role in aiding fluid flow within the LOAC platform by requiring less external pressure or energy input needed to actuate the flow [71], [75].

4. Microfluidic Large Scale Integration

Microfluidic large scale integration shares semblance to an electronic circuit that has diverse patterns of wiring circuitry responsible for taking current from one point to another [98]–[100]. However, this is a microfluidic tool that entails microfluidic channel networks integrated with thousands of micromechanical valves and hundreds of individually accessible reservoirs [101] organised systematically to carry out complex POCT, medical or bio-chemical applications. These plumbing networks have microvalves that open or close with respect to the pneumatic pressure applied due to elastic membranes that is situated between a liquid-guiding layer and pneumatic control-channels [102]. The overall configuration involves combining several microvalves more multifaceted units like micropumps, mixers, multiplexers, etc. having hundreds of units on one single chip [60].

4.1. Microfluidic Multiplexer

The fluidic multiplexer is a key component of microfluidic large scale integration networks because it contains a blended arrangement of binary valve in patterns that significantly allow specific addressing of large number of independent chambers, increase the processing power of fluidic network exponentially and enabling complex fluid manipulations with a minimal number of controlled inputs [101], [104]–[106].

4.2. Micromixer

Micromixing in microfluidic devices is generally achieved due to the significant small length which is an endemic factor in miniaturization. This length advantage drastically increases the effect of diffusion and advection necessary for diffusion to occur [104]. Correspondingly the channel geometries of micromixers are also designed to decrease the mixing path and increase the contact surface area [104], [107]. Induced mixing at the microscale is generally classified as being passive or active. Passive mixers depend solely on pumping energy, while active mixers make use of an external energy source to achieve mixing.

4.2.1. Diffusion and Advection

Diffusion and advection are both relevant in the study of transport phenomena in fluid flows. The term advection with reference to microfluidics refers to the transport of substance (biological species) from one region to another [104], [107].

While diffusion is the process by which a concentrated group of particles in a volume will by Brownian motion spread out over time so that the average concentration of particles throughout the volume is constant [104]. In this distribution, the given entity moves from regions of higher chemical potential towards lower chemical potentials as shown in Figure4.1. In physics, diffusion can be realised as heat diffusion and molecular diffusion or Brownian motion.

Advection and diffusion in micromixers are also generally characterized accordingly to three nondimensional fluid parameters: Reynolds number Re, Pecle´t number Pe, and Strouhal number St. Pecle´t number is defined as:

$$\boldsymbol{P_e = \frac{uL}{D}} \qquad (4.\ 10)$$

This is a measure of the relative importance of advection and diffusion in providing the mass transport associated with the mixing. Advection is dominant at high Pe [63].

The Strouhal number is defined as:

$$\boldsymbol{St = \frac{fD_h}{u}} \qquad (4.\ 11)$$

where f is the frequency of the disturbance action, is generally associated with active micromixers, and represents the ratio between the residence time of a species and the time period of disturbance [120], [420], [421].

Brownian motion acts in the presence of non-uniform distribution of molecules or particles inside a fluid. Diffusion can be described mathematically in one dimension by the equation below:

$$\boldsymbol{d^2 = 2DT} \qquad (4.\ 12)$$

Where *d* is the distance a particle moves in a time *t*, and *D* is the diffusion coefficient of the particle. Because distance varies to the square power, diffusion becomes very important on the microscale [422].

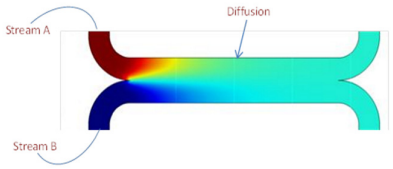

Figure4.1. Illustration of stoke flow diffusion occurrence between two different streams at relatively equal velocity.

4.2.2 Active Mixing

Active mixing uses external excitation to initiate time-dependent perturbations that stir and agitate the streamlines within the fluid for the sole purpose of accelerating the mixing process [108]. They are categorized with respect to the type of external perturbation energy such as acoustic (ultrasonic)-driven [109], thermal-induced [110], pressure field-driven [111], magneto-hydrodynamic [112], electrokinetic [113], dielectrophoretic [114], [115] or electro-wetting [116]. The prominent advantage age of active micromixers is better mixer efficiency in comparison to passive mixers [117]. However, they suffer from the inconvenience cumbersome integration encumbrance from their peripheral devices e.g. actuators, which in the end lead to complex and expensive fabrication process [104]. Furthermore, the use of ultrasonic waves, high temperature gradients lead to extensive damage biological fluids or matrices. A number of groups have used silica particles impregnated with Fe_3O_4 to actively mix fluids in a microchamber using a magnetic field from either a permanent rotating magnet or an electromagnet [118]. Figure below shows the use of 5 mm neodymium-iron-boron magnetic particles (MQP-15-7, Magnequench

International, Inc, Singapore) for optimum active mixing performance at an optional upper frequency limit of 100 Hz [119]. This time-dependent microfluidic operations utilizes flow mixing patterns of two dye streams (black and white) in the presence of ciliated structures as depicted Figure4.1. In general, active mixers are not a popular choice when applying microfluidics to chemical and biological applications [120]. Overall, implementation of such devices in practical applications is limited.

.

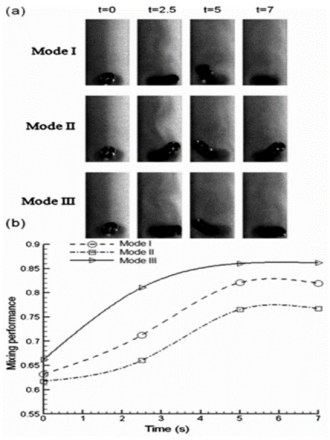

Figure4.1. Time-dependent flow mixing behaviour in three different beating modes (a) and the 2D graphical corresponding mixing performance (b) [119].

4.2.3. Passive Mixing

Passive mixing devices depend exclusively on the energy from fluid pumping and judicious use unique channel designs to constrain the flow configuration therefore increase mixing velocity by reducing the diffusion length and optimising the contact surface area between the different fluids [66], [104]. A good example is the use of a serpentine microchannel structure to coerce the fluid in mixing; as depicted in Figure4.2. Molecular diffusion and chaotic advection are the main reason this mass transport phenomena is possible. Moreover, the design modifications carried out to aid the influence of the laminar flow inside and mixing time reduction is generally achieved by splitting the fluid stream using serial or parallel lamination [121], [122], hydrodynamically focusing mixing streams [123], injecting bubbles of gas (slug) or liquid (droplet) into the flow [124], [125] or improving chaotic advection using ribs and grooves fabricated on the channel walls [126], [127].

Unlike active mixers, passive mixers are generally less costly and involve simpler fabrication methods; they are far better to integrate into more complex LOC platforms [104].

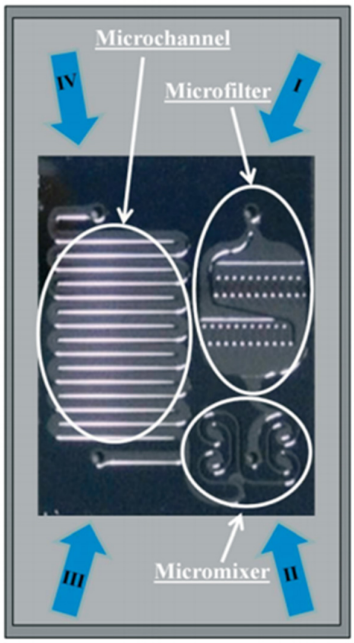

Figure4.2. A picture of a microfluidic chip consisting of microfilter, micromixer and microchannel. (I–III) Inlets for additional samples, lysis buffer, washing and elution buffer. (IV) Outlet for gathering of the extracted DNA [116].

4.3. Micropumps

Since the Reynolds number is typically low in microsystems, several different means of achieving fluid flow control in microfluidics have been developed. The selection of a pump is mostly

biased to mostly moderate performance and low-cost applications, provided that other requirements, like reproducibility and operational stability, can be satisfied.

The majority of these miniaturized pumps come under the classification of electric/electronic(Figure5.30), magnetic, external pressure generators, manual and passive pump systems [128]. Examples of electric/electronic pumps are the piezo actuator, electro-osmotic and peristaltic pumps, while the case of magnetic systems is represented in the form of magneto-hydrodynamic pumps and ferrofluidic pump. Piezo-electric, electro-osmotic and peristaltic pumps can be used for complex microfluidic operations and can be fabricated cheaply. The case of piezo-electric pumps which are the most compact pumps can be used for intermediate flow rates (µL) while electro-osmotic pumps due to their simplicity can be easily integrated into a microsystem. These integrated pumps are mostly the preferred choice for contemporary applications which requires multiple and complex fluidic operations, although the pressure produced for fluid motion cannot be necessarily considered independent of scale (miniaturisation).

Commonly used manual pumps are syringes and blisters, while passive pumps makes use of surface tension or capillary effect to drive fluid flow. The main benefit of these low cost syringe pumps and blisters is their ability of initiating flow rate across microchannels irrespective of the fluidic resistance. This is due to the fact that the fluid traffic is largely dependent on the force displacement of the plunger or finger (blister) which in this case is sufficient (mechanical advantage). On the other hand, the main drawback of manual pumps is the development of pulsatile flows at low flow rates and lack of adequate flow control required for complicated fluid flow sequence.

Finally, the external pressure generators are mostly mechanical computer controlled mechanical devices that can excite pressure when connected to the microfluidic chip. They can also exist as hydrostatic generators which depend on gravity to cause pressure difference for fluid flow. Most of these devices are expensive and are not easy to integrate into standalone microfluidic platforms. However, these simple and low cost pumps generate the required pressure difference needed for fluid flow by varying the altitude of the liquid to air (atmosphere) interface within different reservoirs. This technique makes it impossible for applications in closed fluid flow systems. In all cases, whether the pump is external or integrated, pressure differences within the system are generally inferior to those produced by external sources.

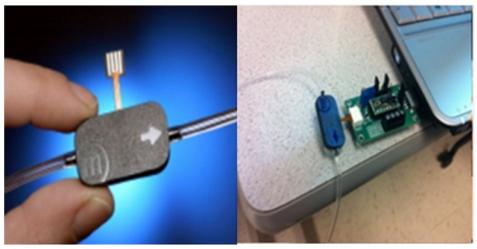

Figure4.3. Disposable microfluidic pump (Bartels Mikrotechnik mp6 Micropump) capable of pumping both air maximum flow: 18 ml/min (300 Hz) and water maximum flow: 7 ml/min (100 Hz). It is made up of a heat and chemical resistant plastic covering (30 x 15 x 3.8 mm^3), weigh 2grams, 2 piezo actuators, 0 - 70 °C operating temperature and an estimataed 5000 hours live time [129]

4.3. Microvalves

The capacity to manipulate fluid flow using valves is indispensable in many microfluidic applications [137]. There are two types of valves: passive valves that require no energy and active valves that use energy for operation. The type of valve used in a

device depends on the amount and type of control needed for the application [128], [138].

Active valves often use external macroscale devices that control the actuation and provide energy. Some recent designs include an electromagnetically actuated microvalve [145] and an air-driven pressure valve [142]. Other active valve designs use energy from the driving fluid, eliminating the need for external power or energy from direct chemical to mechanical conversions.

Passive valves can be used to limit flow to one direction, to remove air, or to provide a temporary flow stop. Passive are one way that control flow through the resistance of the fluid flow along the channel (Figure4.5). By changing the fluid resistance (i.e., the geometry) the passive pressure theory applies [8]. The passive valve theory is a fundamental building block of the structurally programmable microfluidic system (sPROMs) system and much research effort has been directed toward the development of efficient passive valves [148]. The passive valve as described in this work is a device that utilizes the surface properties of a hydrophobic substrate and a geometrical feature control to regulate fluid flow [423].

If the fluid is flowing at a very low velocity, such that the surface tension effects are dominant in controlling the flow characteristics, this abrupt change in width results in a significant increase in the pressure required to move the liquid further as shown in Figure4.4. The required pressure, to push the liquid into the narrow channel, for this geometry can be derived from the principle of virtual work (Hosokawa et al., 1999). Since the fluid entering the narrow channel would experience a higher surface-area-to-volume ratio, there would be an increase in the surface energy of the system. This can be used to derive the expression for pressure needed to overcome the passive valve as [148], [150], [424]:

$$\Delta P = 2\sigma \cos(\theta_C)\left[\left(\frac{1}{w_1}+\frac{1}{h_1}\right)-\left(\frac{1}{w_2}+\frac{1}{h_2}\right)\right] \quad (4.13)$$

Where, W_1 is the width of inlet channel, h_1 is the channel depth, h_1 is the channel depth, σ is the surface tension, θ_c is the fluid contact angle.

The most common channel geometry, have equal depth along the microchannel. Hence, setting $h_1=h_2$ simplifies equation 2.44 to:

$$\Delta P = 2\sigma \cos(\theta_C)\left[\left(\frac{1}{w_1}\right)-\left(\frac{1}{w_2}\right)\right] \quad (4.14)$$

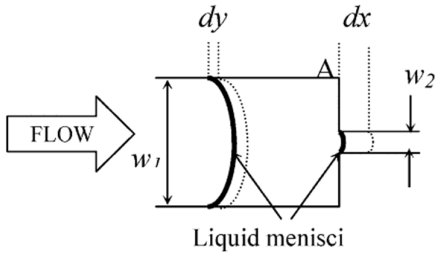

Figure4.4. A schematic of fluid flow through an abrupt junction passive microvalve.

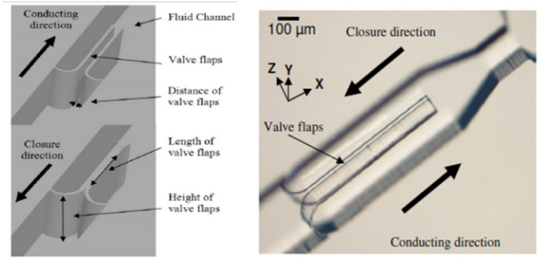

Figure4.5. The passive design is based on two extruded symmetric flexible PDMS-based cantilever bars which act as valve flaps). The distance of the valve flaps is 20µm, the height of the valve flaps is 70µm and the length of the valve flaps is 300, 550, 700, and 1000µm, respectively[151]

5. Pressure Driven Flow

This phenomenon is also known as Poiseuille flow and it exhibits a parabolic flow profile which is basically characterised by liquid movement as a result of pressure gradient between two or multiple points within the system. The liquid control is mostly constrained to a one-dimensional liquid flow in a straight, curved or circular microchannel (Figure5.1) [71], [76], [77]. The nature of process entails the flow

of fluid from a region of high pressure to a region of low pressure.

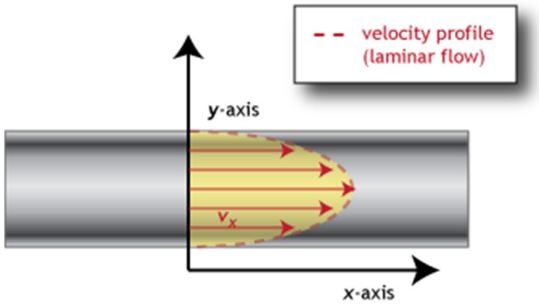

Figure5.1. Schematic representation of the parabolic path way of liquid in a cylindrical conduit [84]

.

Fluid operations carried out on this platform are either capillary driven or linearly actuated. Capillary driven flow involves the high dependence on capillary forces which in turn rely on the channel geometry design (i.e. width, length and height) and surface properties (hydrophobic or hydrophilic) [82]. On the other hand linear actuated devices propel flow by mechanical displacement of liquid through application of force. For instance fluid stored in a reagent reservoir can be propelled by the aid of a plunger into a micro-conduit of negative pressure (Figure5.2). The common denominator that makes all these methods of fluid actuation significant is the presence of the generated pressure gradient. Furthermore novel methods such as electro-osmotic force can also be used to induce pressure driven flow through insertion of in-channel electrodes of relatively small electric potentials [85], [86].

Simplified Navier Stokes equations for pressure driven micro-flows characterized by the significantly reduced Reynolds number (Re<<1)

$$\mathbf{0} = -\boldsymbol{\nabla p} + \boldsymbol{\eta \nabla^2 \vec{u}} \qquad (5.10)$$

Where, p is the pressure, u is the fluid velocity and η is the dynamic viscosity of the liquid.

The relation between pressure and flow rate is described by the Hagen-Poiseuille equation, In the case of cylindrical microchannels experiencing a parabolic flow is given below [87]:

$$\mathbf{\Delta P} = \frac{\mathbf{8\eta LQ}}{\mathbf{\pi r^4}} \qquad (5.11)$$

Where ΔP is the pressure drop between the two ends of the cylindrical conduit, L is the total length of channel, r is the radius, Q is the volumetric flow rate of the channel and v is the average flow velocity across the section.

In the case of planar channels with a height, h, which is much less than the width w (h<<w,) the solution of the Poiseuille flow gives [88], [89]:

$$\boldsymbol{\Delta P} = \frac{\mathbf{12\eta LQ}}{\boldsymbol{wh^3}\left(\mathbf{1}-\frac{\boldsymbol{h}}{\boldsymbol{w}}\left(\frac{\mathbf{192}}{\boldsymbol{\pi^5}}\sum_{\boldsymbol{n=1,3,5}}^{\boldsymbol{\infty}}\frac{\mathbf{1}}{\boldsymbol{n^5}}\tanh\left(\frac{\boldsymbol{n\pi w}}{\mathbf{2}\boldsymbol{h}}\right)\right)\right)} \qquad (5.12)$$

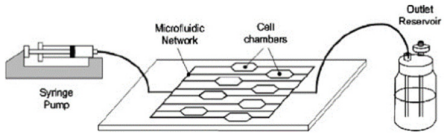

Figure5.2. Schematic representation of external syringe pump used to supply typical pressure-

driven microfluidic platform for living cell analysis [90].

5.1. Electric Circuit Analogy Concept of Fluidic Resistance

The concept of Hagen-Poiseuille equation rewritten as Ohm's law clearly depicts the average flow rate of a liquid within a microfluidic channel as proportional to the pressure gradient imposed on both ends of the channel (fig.5.3) [91], [92].

$$\Delta \boldsymbol{P} = \boldsymbol{R_H Q} \qquad (5.13)$$

The fluidic resistance R_H will depend on the geometry of the cross section (e.g. cylindrical and planar). For instance equation 5.11 and equation 5.12 are the cylindrical and planar Hagen-Poiseuille circuit analogy representation of equation 5.14 and 5.15

$$\boldsymbol{R_H} = \frac{\boldsymbol{8\eta L}}{\boldsymbol{\pi r^4}} \qquad (5.14)$$

$$\boldsymbol{R_H} = \frac{\boldsymbol{12\eta L}}{\boldsymbol{wh^3}\left(\boldsymbol{1-\frac{h}{w}\left(\frac{192}{\pi^5}\sum_{n=1,3,5}^{\infty}\frac{1}{n^5}\tanh\left(\frac{n\pi w}{2h}\right)\right)}\right)} \qquad (6.15)$$

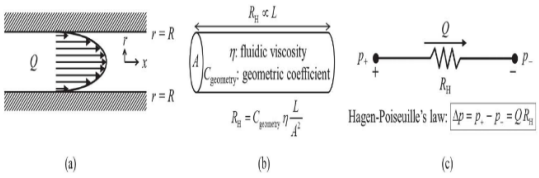

Figure5.2. The physical similarities between the flow of a fluid and the flow of electricity: (a) Poiseuille flow in a circular channel, (b) the hydraulic resistance of the circular channel (Cgeometry¼ 8p for the circular channel), (c) equivalent circuit symbol of a fluidic resistor for the hydraulic resistance and Hagen–Poiseuille's law analogous to a resistor for the electric resistance and Ohm's law [92].

This fluidic resistance is also known as hydraulic resistance and can be used to analyse the flow or pressure relationship within complex microfluidic networks. The validity of this concept relies on some basic assumptions. First of all the flow is considered viscous, incompressible and homogeneous with no presence of convective mixing. Secondly, the steady-state and laminar flow nature of the flow exhibits a parabolic shape profile. Finally, the flow is considered to have a uniform pressure gradient across the microchannel length. By this means estimation of the laminar flow within circular or non-circular channels that are either infinite or finite in length can be with simple mathematical calculation. For instance channels connected in series will be resolved by using "$R_H=R_{H1}+R_{H1}+R_{H2}+...R_{Hn}$ " which will provide the estimated total fluidic resistance of the network. Whereas parallel channels network will have a total resistance of "$1/R_H=1/R_{H1}+1/R_{H1}+1/R_{H2}+...1/R_{Hn}$" [92].

There is an extensive range of diverse applications of these pressure driven systems in the microfluidic platforms. These include the use of plungers, syringes, micropumps (peristaltic and piezo-electric), gas expansion principles, pneumatic displacement of membranes, blisters etc. The advantage they share is the simplicity in design and fabrication processes. They are also economical and affordable but suffer the disadvantages of reproducibility and limited ability to support very complicated microfluidic processes [93].

6. Magneto-hydrodynamics

Magneto-hydrodynamics (MHD) involves the interaction between the flow of an electrically conducting fluid and magnetic fields. This interaction between the electric currents and

magnetic fields results in an indigenous pressure known as Lorentz body forces on conductive fluids (fig.6.10)(ferrofluid, buffer solution or cell media) [152]–[154]. This generated force can then be used to propel, stir and manipulate the fluids; since most applications use buffers and solutions that are often electrically conductive i.e. capable of transmitting electric currents through the solutions [152].

$$F = \boldsymbol{JxB} \tag{6.10}$$

The MHD force is represented by F, while J and B are depicted as the electric current density and magnetic field.

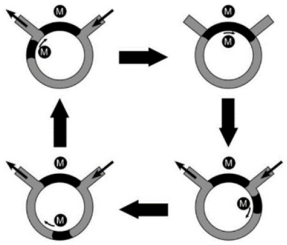

Figure6.1. The principle operation of a circular ferrofluid pump used to manipulate fluids with ferrofluid plugs in circular microchannels [98]

In the domain of microfluidics miniature devices are needed to carry out a large number of operations, MHD offers a sophisticated means to manipulate fluid flow in micro-devices without a need for mechanical components. For example many MHD pumps can be integrated on a lab-on-chip device to enable complex fluidic operations that can be done automatically on a single platform as shown in fig.6.10 [153], [155]. MHD micropumps [156]can be used to pump several conducting liquids especially high-conductivity fluids. These fluids are sometimes present in the aqueous solutions used in medical/biological applications; hence MHD pumps are suitable for POCT. Lab-on-chip applications typically require the use of pumps and valves which are usually cumbersome to implement. In a MHD setting most of the network's channels are equipped with individual electrodes which can be intelligently controlled in the presence of a magnetic field to direct fluid flow along any desired path without a need for mechanical valves [157]. This operation can be used to generate higher flow rates at relatively small electrode potentials, typically below 1V [157]. This gives it an advantage over electroosmosis as liquid flow does not depend on the chemical nature of the capillary surface [158]. One of the major main disadvantages of this technique is that of the generated Lorentz body forces which scales unfavourably as the conduit's dimensions are reduced. Thus, constraining MHD most applications to channel sizes with characteristic dimensions on the order of 100μm or larger [157]. Besides, ionization effect causes the bubbles generation which greatly inhibits the flow rate. The effect of Bubble generation is minimized by reversing the direction of the applied voltage which can be done by using an alternating current driving mechanism to improve their performance [156].

7. Dielectrophoresis

Dielectrophoresis (DEP) technique can be used to manipulate, transport, separate and sort diverse categories of bio-particles in microfluidics although DEP is mostly used as a particle separation technique[159]–[161]. DEP is a tool that can be effectively used for nucleic acid hybridisation, purification and characterisation in POCT devices [162]. Whilst other areas such as manipulation and transportation still require extensive research. As a good separation technique it makes use of a polarization effect that occurs when a non-conductive/dielectric liquid is place in the presence of a non-uniform electric field [53], [87], [163]–[165]. If the polarization effect of the particle supersede that of the suspending medium,

the particle movement will tend towards the region of higher field strength (positive DEP); while, the reverse case will cause the particle to move towards the low potential area (negative DEP). The particles in question maintain an overall net charge of zero regardless of their original randomly oriented state or polarised state. A time-average DEP force applied on a spherical particle can be represented as the equation below [166], [167]

$$\langle \boldsymbol{f} \rangle = [2\pi r^3 \varepsilon_0 \varepsilon_m Re|f_{CM}|\nabla E_{rms}^2] + \left[4\pi r^3\, \varepsilon_0\, \varepsilon_m\, Im|f_{CM}| \sum_{x,y,z} E_{rms}^2\, \nabla\varphi\right] \quad (7.10)$$

$$f_{DEP} = 2\pi r^3 \varepsilon_0 \varepsilon_m Re|f_{CM}|\nabla E_{rms}^2 \quad (7.10a)$$

$$f_{TW-DEP} = 4\pi r^3\, \varepsilon_0\, \varepsilon_m\, Im|f_{CM}|\, \textstyle\sum_{x,y,z} E_{rms}^2\, \nabla\varphi \quad (7.10b)$$

where **r** is the radius of the particle, ε_0= 8.854×10−12 F/m is the permittivity of the vacuum, ε_m is the dielectric constant of the medium, f_{CM} is a complex variable known as Clausius–Mossotti factor, E_{rms} is the root-mean-square value of the applied electric field, and ϕ is the phase component of the electric field. The first part (a) of equation (7.10) can be referred to as 'classical DEP force'. This is the force responsible for pushing the particles towards or away from the regions of strong electric field, i.e. microelectrode tips, with respect to the polarity of Re[f_{CM}]. For example, If Re[$_{fCM}$] > 0 the particle is pushed towards the regions of strong electric field and such a motion is termed positive DEP response. On the other hand, if Re[fCM]<0 the particle is driven away from the regions of strong electric field and exhibits a negative DEP response (Figure7.1a) [168].

Subsequently, the second part (b) is called 'travelling wave (TW) DEP force'. In this case the force causes particles to move towards or away from the direction of the wave propagation, according to the polarity of Im (imaginary) [fCM]. For instance if Im[fCM] > 0 the particle travels towards the smaller phase regions and such a motion is designated a co-field TW response. Alternatively, if Im[fCM] < 0 the particle tends to move towards the larger phase regions and such a motion is called an anti-field TW response (Figure7.1b).

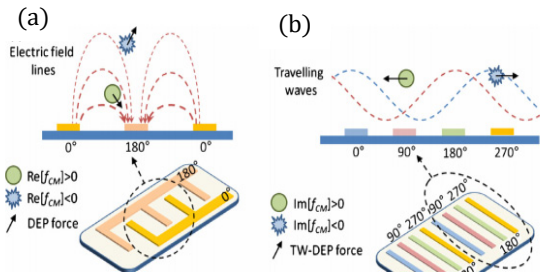

Figure7.1. Non-uniform electric field can be created by metallic microelectrodes patterned on a substrate: (a) the spatial non-uniformity of electric field magnitude induces classical DEP force, while (a) the spatial non-uniformity of the phase component induces TW-DEP force [121].hydraulic resistance and Hagen–Poiseuille's law analogous to a resistor for the electric resistance and Ohm's law [92].

$$f_{CM}(\varepsilon_P^*, \varepsilon_m^*, \omega) = \frac{\varepsilon_P^*(\omega) - \varepsilon_m^*(\omega)}{\varepsilon_P^*(\omega) + 2\varepsilon_m^*(\omega)} \quad (7.11)$$

f_{CM} is the dipolar Clausius-Mosotti factor which is the characterizing parameter of a Dielectrophoretic particle [54].

ε_p, ε_m are the complex permittivities of the particle and the medium respectively.

In turn, the complex permittivity is given by:

$$\varepsilon = \varepsilon_r - i\frac{\sigma}{\omega} \qquad (7.12)$$

$\sqrt{-1}$Where, ε_r is the dielectric constant; σ is the conductivity; ω is the frequency of the applied Electric Field and i is

Furthermore, since they all exhibit substantial amount of di-electrophoretic activity in the presence of non-uniform electric fields, the requirement for pre-charged particles in the system is not a prerequisite condition [168]. The strength of the force exerted by this electric field is directly proportional to the electrical properties of the particles' shape, size and operational frequency of the field. As a result, particles with great sensitivity can be manipulated by a designated electric field. Electric field generation requires fabrication of precise electrodes for the particles attraction; likewise these particles may also require formation of intricate channels for effective separation. It may have certain disadvantages for use with some particles, if their response to the field is not strong enough to be detected. In general dielectrophoresis is a good technique for use in

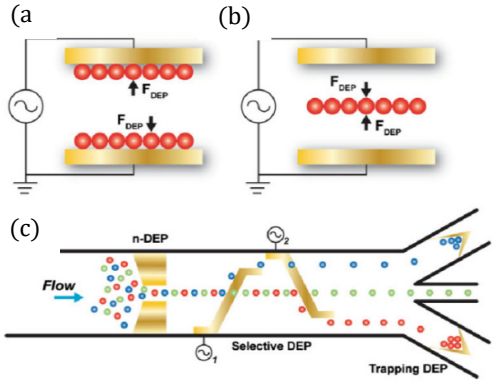

Figure7.2. Dielectrophoretic (DEP) separations can be positive (pDEP) as shown in **(a)** or **(b)** negative (nDEP) which affects where cells are positioned within a field. **(c):** gives a basic depiction of DEP been utilized in a variety of different microfluidic systems [160].

microfluidic devices as the principle of operation is simple and requires less hardware and can also be applied to non-conductive liquids (fig.7.2). Conversely, it covers a wide-span of potential application when compared to standard electrophoresis which requires spatially uniform electric field to pull a charged particle towards the electrode with opposite charge.

Novel methods like binary separation [169], travelling wave DEP [170] and light induced DEP [171] have been performed. In the case of light induced DEP, light-induced dielectrophoretic forces are used to manipulate aqueous droplets immersed in electrically nonconductive liquid such as oil with a light intensity as low as 400 µW/cm2 [171]. Of recent researchers have found ways to use dielectrophoresis based continuous-flow technique for gene vaccination production. This innovative technique [161] demonstrates the quick and efficient separation of parental plasmid, miniplasmid, and minicircle DNA as shown in Figure7.3.

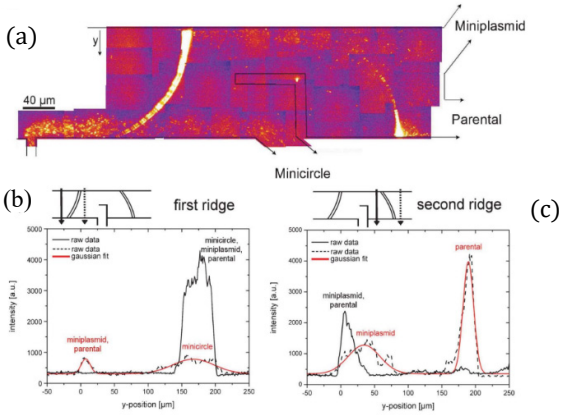

Figure7.3. Separation of the parental plasmid, miniplasmid and minicircle DNA. (a) Combination of the fluorescence microscopy images. A mixture of the parental plasmid, miniplasmid and minicircle DNA is inserted towards the ridges from a side channel (each yellow spot represents one distinct DNA molecule). At the first ridge, the minicircle DNA is separated out of the mixture and

directed into a separate channel. The parental plasmid and miniplasmid DNA are deflected and drift towards the second ridge, where only the parental plasmid DNA is deflected. Thus, all three species are retrieved in separate channels. (b) and (c) Fluorescence intensities up- and downstream of the two ridges. The scan paths are portrayed over the graphs. The black lines signify the scans upstream of the ridge; the dashed lines symbolize the scans downstream of the ridge. The red lines are Gaussian fits. (b) At the first ridge the resolution was Res = 1.10. (c) At the second ridge the resolution was Res = 1.25. Consequently, a complete separation of the three species was achieved with very high separation efficiency [104].

8. Conclusion

This paper gives a polarized view of the techniques used in development and design of POCT Microfluidics devices by categorising them within the broad spectra of continuous flow mechanics. Continuous flow technology is based on the manipulation of continuous liquid flow through microfabricated channels. Researchers in the field are therefore presented with a microfluidic 'toolbox' of techniques and manufacturing methods.

Generally, continuous phase are less complicated and possess simple mode of operation in comparison to discrete. Moreover, they mostly reside in the region of low cost of production or cost-efficient fabrication processes. However, they are more cumbersome; which makes integration of their various techniques more difficult. This is mostly as a result of the dependencies of external sources needed for implementation. For example, the use of plungers, pressure generators and piezo-electric pump in pressure driven flow can be complicated and cumbrous which can significantly affect repeatability.

In summary, selection criteria of each individual technique regardless of the continuous or discrete flow depend heavily on the disadvantage and advantages they present with respect to the intended use, with cost a dominant factor. Within classical microfluidics cost depends on the selected method and fabrication techniques, fluid actuation is required using an external pump or an electric field, thus increasing power requirements; therefore, all point of care devices for molecular diagnostics currently require some form of desktop or handheld device to conduct the control of the fluid and read the results. Paper microfluidics is a new field that has the potential to revolutionise diagnostics and significantly reduce the associated manufacturing and material costs. No external actuation of fluid is required which will allow standalone systems to be created that could use consumer electronic products such as a smartphone to act as a sensing device.